[Frontiers in Bioscience 16, 2812-2902, June 1, 2011]

Matrix vesicles: structure, composition, formation and function in calcification

Roy E. Wuthier

Department of Chemistry and Biochemistry, University of South Carolina, Columbia, SC 29208

TABLE OF CONTENTS

1. Abstract
2. Introduction
3. Morphology of matrix vesicles (MVs)
- *3.1. Conventional transmission electron microscopy*
- *3.2. Cryofixation, freeze-substitution electron microscopy*
- *3.3. Freeze-fracture studies*

4. Isolation of MVs
- *4.1. Crude collagenase digestion methods*
- *4.2. Non-collagenase dependent methods*
- *4.3. Cell culture methods*
- *4.4. Modified collagenase digestion methods*
- *4.5. Other isolation methods*

5. MV proteins
- *5.1. Early SDS-PAGE studies*
- *5.2. Isolation and identification of major MV proteins*
- *5.3. Sequential extraction, separation and characterization of major MV proteins*
- *5.4. Proteomic characterization of MV proteins*

6. MV-associated extracellular matrix proteins
- *6.1. Type VI collagen*
- *6.2. Type X collagen*
- *6.3. Proteoglycan link protein and aggrecan core protein*
- *6.4. Fibrillin-1 and fibrillin-2*

7. MV annexins – acidic phospholipid-dependent ca^{2+}-binding proteins
- *7.1. Annexin A5*
- *7.2. Annexin A6*
- *7.3. Annexin A2*
- *7.4. Annexin A1*
- *7.5. Annexin A11 and Annexin A4*

8. MV enzymes
- *8.1. Tissue-nonspecific alkaline phosphatase(TNAP)*
  - *8.1.1. Molecular structure*
  - *8.1.2. Amino acid sequence*
  - *8.1.3. 3-D structure*
  - *8.1.4. Disposition in the MV membrane*
  - *8.1.5. Catalytic properties*
  - *8.1.6. Collagen-binding properties*
- *8.2. Nucleotide pyrophosphate phosphodiesterase (NPP1, PC1)*
- *8.3. PHOSPHO-1 (Phosphoethanolamine/Phosphocholine phosphatase*
- *8.4. Acid phosphatase*
- *8.5. Proteases and peptidases*
- *8.6. Lactate dehydrogenase and other glycolytic enzymes*
- *8.7. Carbonic anhydrase*
- *8.8. Phospholipases*
  - *8.8.1. Phospholipase A (PLA)*
  - *8.8.2. Phospholipase C (PLC)*
  - *8.8.3. Lysophospholipase C (LPLC)*
  - *8.8.4. Sphingomyelinase (Smase)*
  - *8.8.5. Other MV phospholipases*
- *8.9. Phosphatidylserine synthases*
- *8.10. Phospholipid flippases and scramblases*

9. MV transporters and surface receptors
- *9.1. Cell-surface receptors*
- *9.2. ATP-driven ion pumps and transporters*
- *9.3. Channel proteins and solute-carrier transporters*
- *9.4. Ca^{2+} channel proteins*

9.4.1. L-type Ca^{2+} channels in growth plate chondrocytes
9.4.2. Annexins as Ca^{2+} channels
9.5. Inorganic P (Pi) transporters
9.5.1. Na^{+}-dependent Pi transporters
9.5.2. Na^{+}-independent Pi transporters
10. MV regulatory proteins
10.1. Syntenin
10.2. G_i Protein, alpha-2
10.3. Trp/Trp mono-oxygenase activation protein, etc.
11. MV cytoskeletal proteins
11.1. Actin
11.2. Filamen B, beta
11.3. Actinin
11.4. Tubulin
11.5. Radixin
11.6. Gelsolin and proteins with gelsolin/villin domains
11.7. Plastins
12. MV lipids
12.1. Phospholipids
12.1.1. Fatty acid composition
12.1.2. Physical form of MV phospholipids
12.1.3. Topological distribution of MV phospholipids
12.1.4. Ca^{2+}-binding properties of MV phospholipids
12.2. Nonpolar lipids
12.3. Glycolipids
13. MV electrolytes
13.1. Chemical analyses of intracellular electrolytes in growth plate chondrocytes
13.2. Chemical analyses of electrolytes in isolated MVs
13.3. Chemical analyses of electrolytes in the extracellular fluid and blood plasma
13.4. Ultrastructural analyses of Ca^{2+} and P in cells and MVs
13.5. Chemical analyses of micro-electrolytes in MVs
13.6. Physico-chemical properties of MV mineral forms
13.6.1. X-ray diffraction
13.6.2. FT-IR and FT-Raman analyses
13.7. Solubility properties of nascent MV mineral
14. Formation of MVs
14.1. Electron microscopic studies
14.2. Biochemical studies
14.2.1. Phospholipid metabolic studies
14.2.2. Cell culture studies
14.3. Role of cellular Ca^{2+} and Pi metabolism in MV formation
14.3.1. Histology of cellular Ca^{2+} metabolism during MV formation
14.3.2. Confocal imaging of Ca^{2+} in living growth plate chondrocytes
14.3.3. Biochemistry of mitochondrial Ca^{2+} metabolism
14.4. Growth plate cellular Pi metabolism
14.4.1. Chondrocyte mitochondrial PIC Pi-transporter
14.4.2. Chondrocyte plasma membrane Pi transporters
14.4.3. Chondrocyte mitochondrial permeability transition (MPT) pore
14.5. Growth plate cellular H^{+} (pH) metabolism
14.5.1. Confocal imaging of H^{+} (pH) in living growth plate chondrocytes
15. Kinetics of mineral formation by MVs
15.1. Differing views of MV mineral formation
15.2. Radio-isotope analyses of the kinetics of MV Ca^{2+} and Pi accumulation
15.2.1. Stage 1 – Initial exchange
15.2.2. Stage 2 – Lag period
15.2.3. Stage 3 – Induction period
15.2.4. Stage 4 – Rapid acquisition period
15.2.5. Stage 5 – Plateau period
16. The nucleation core: The driving force in MV Ca^{2+} and Pi accumulation
16.1. Discovery of the nucleation core (NC)
16.2. Isolation of the NC
16.3. Chemical characterization of the NC

16.3.1. Electrophoretic analysis of proteins
16.3.2. Chromatographic analysis of lipids
16.4. Physical characterization of the NC
16.4.1. Transmission electron microscopy (TEM)
16.4.2. FT-IR analysis
16.4.3. ^{31}P-NMR analysis
16.4.4. pH sensitivity
16.5. Summary of NC structure and composition
17. Reconstitution of the NC: role of PS-Ca^{2+}-Pi complex (PS-CPLX) in MV crystal nucleation
17.1. Reconstitution of the nucleational core
17.2. Mathematical analysis of the kinetics of mineral formation
17.3. The physical and nucleational properties of pure PS-CPLX
17.4. Requirements for PS-CPLX formation: pH tolerance
17.5. Molecular rearrangements during PS-CPLX formation
17.6. Effect of Mg^{2+} incorporation on nucleation activity of PS-CPLX
17.7. Role of AnxA5 in MV crystal nucleation
17.8. Mechanism of MV nucleation of OCP
18. Modeling of MV using synthetic unilamellar liposomes
18.1. Effects of Ca^{2+} ionophores on Ca^{2+} uptake
18.2. Minimal effects of AnxA5 on $^{45}Ca^{2+}$ uptake
18.3. Effects of detergents and phospholipase A_2
18.4. Proteoliposomal MV models by other groups
19. Regulation of MV Calcification
19.1. Factors that primarily effect nucleation
19.2. Effects of phospholipid composition
19.3. Stimulatory effects of AnxA5 on MV nucleation
19.4. Effect of non-apatitic electrolytes
19.4.1. Effects of Mg^{2+}
19.4.2. Effects of Zn^{2+}
19.4.3. Effects of PPi
19.5. Inhibitory effects of proteoglycans
19.6. Stimulatory effects of type II and X collagens
19.7. Effects of non-collagenous bone-related proteins
20. Further evaluation of the roles of key MV proteins
20.1. Tissue-nonspecific alkaline phosphatase (TNAP)
20.1.1. Role of TNAP in PPi hydrolysis
20.1.2. Additional roles of TNAP
20.1.3. Improperly assigned roles of TNAP
20.2. Annexin A5 (AnxA5)
20.2.1. Questionable role in Ca^{2+} entrance into MVs
20.2.2. Activation of the nucleational core
20.2.3. Does AnxA5 have a physiological function?
20.2.4. Effects of double knockout of AnxA5 and AnxA6 on expression of other genes
20.2.5. Possible substitution of PS-receptor (Ptdsr) for AnxA5
20.2.6. What would be the effects of expression of defective AnxA5 mutants?
20.2.7. Is the need for AnxA5 stress-dependent?
20.3. PS Synthase
20.3.1. PS synthesis is not high-energy dependent, but requires Ca^{2+}
20.3.2. PSS1 and PSS2 gene knockouts
20.4. Phospholipase A and C activities
20.4.1. Membrane lysis and Ca^{2+} access to nucleational core
20.4.2. Role in the egress of mineral from the vesicle lumen
20.4.3. Salvage of phospholipid P for mineral formation
20.5. PHOSPHO-1
20.5.1. Salvage of Pi and choline^{+} from phospholipid breakdown
20.5.2. Inhibition of PHOSPHO1 activity
20.5.3. PHOSPHO1 gene knockout
20.5.4. Co-modulation of TNAP and PHOSPHO1 gene expression
20.5.5. Effect on MV mineral formation
21. Perspectives
22. Acknowledgements
23. References

1. ABSTRACT

Matrix vesicles (MVs) induce calcification during endochondral bone formation. Experimental methods for structural, compositional, and functional analysis of MVs are reviewed. MV proteins, enzymes, receptors, transporters, regulators, lipids and electrolytes are detailed. MV formation is considered from both structural and biochemical perspectives. Confocal imaging of Ca^{2+} and H^{+} were used to depict how living chondrocytes form MVs. Biochemical studies revealed that coordinated mitochondrial Ca^{2+} and Pi metabolism produce MVs containing a nucleational complex (NC) of amorphous calcium phosphate, phosphatidylserine and annexin A5 – all critical to the mechanism of mineral nucleation. Reconstitution of the NC and modeling with unilamellar vesicles reveal how the NC transforms into octacalcium phosphate, regulated by Mg^{2+}, Zn^{2+} and annexin A5. Extravasation of intravesicular mineral is mediated by phospholipases and tissue-nonspecific alkaline phosphatase (TNAP). In the extravesicular matrix, hydroxyapatite crystal propagation is enhanced by cartilage collagens and TNAP, which destroys inhibitory PPi, and by metalloproteases that degrade proteoglycans. Other proteins also modulate mineral formation. Recent findings from single and multiple gene knockouts of TNAP, NPP1, ANK, PHOSPHO1, and Annexin A5 are reviewed.

2. INTRODUCTION

Skeletal formation is a highly complex process that involves cellular proliferation and differentiation – like development of all tissues – but superimposed on this is the need for mineralization to enable bone to physically support bodily functions. There are two major types of bone formation: endochondral and intramembranous. Endochondral bone formation begins as a cartilaginous anlage and is observed during formation of long bones such as those of the limbs and ribs. Intramembranous bone formation is characteristic of "flat" bones such as the skull and vertebra. Within each type of bone formation there are variations depending on the species and the nature of the bone being considered. Skeletal development involves growth, expansion and remodeling of the bony structure. Specialized types of cells are involved at each stage.

While there are many commonalities in the mechanism of mineral deposition in various species and genera within the vertebrate order, there are also significant variations depending on size and rate of skeletal formation. Recently, for assessment of the roles of the various proteins and enzymes involved, skeletal research has focused increasingly on the use of gene deletions of putative key targets in highly-inbred laboratory mice. Of necessity, many heterozygous characteristics of native wildtype animals have had to be eliminated to produce the genetic homogeneity required for knockout studies. To ensure reproducible results, these laboratory animals must be reared in a highly protective environment with optimal nutrition, temperature and cleanliness, and with minimal stress. For direct biochemical analyses of growth plate mineralization, fetal bovine tissues were initially used; however, much of the subsequent research utilized developing bones of hybrid, broiler-strain chickens because of the exceptional amounts of material readily available at very low cost. This has enabled direct biochemical analysis of key components critical for elucidation of this highly complex system. Others, in order to overcome the problem of insufficient tissue mass, have resorted to the use of rachitic rats. However, none of these experimental approaches is necessarily ideal. In comparison to the mouse, the human skeleton is massive, over one-thousand times larger, and it lasts over one-hundred times longer. Thus, it is doubtful that mineral formation in a diminutive vertebrate like the mouse is entirely analogous to that in humans. On the other hand, the extreme demands for rapid growth and mineralization of bone in the broiler-strain chicken may well require specialized features that are not required for skeletal development of the mouse – or the human – except perhaps during the pubertal growth spurt. Finally, the use of rachitic rat growth plate tissue, while expedient, is problematic because of the fact that the the tissue, by definition, is abnormal.

It is also important to understand that in endochondral calcification, induction of calcium deposition is not directly analogous to that in true bone formation. Endochondral calcification is a primary, but provisional process; its end product, calcified cartilage, is more heavily calcified, but is mechanically weaker than true bone. It is destined to be largely replaced by cancellous bone. Endochondral calcification is mediated by growth plate chondrocytes; it is a rapid *de novo* process that begins with Ca^{2+} and Pi ions in solution. It involves overcoming of a sizeable nucleation barrier that requires the direct mediation of cellular metabolic activity. It utilizes extracellular vesicles and ends with formation of large amounts of microcrystalline, Ca^{2+}-deficient, acid-phosphate-rich apatite deposits embedded in a proteoglycan and cartilage-specific collage-rich matrix. In contrast, true bone formation is mediated by osteoblasts; it is a secondary process that typically requires the presence of pre-existing mineral. During initial cancellous bone formation, osteoblasts deposit mineral upon a calcified cartilage scaffold; they guide formation of biological apatite into a predominantly type I collagen matrix. This leads to formation of the mechanically robust composite structure characteristic of bone. During embryonic intramembranous and subsequent periosteal bone formation, osteoblasts – not chondrocytes – facilitate and guide mineral formation.

The discovery that discrete extracellular nanostructures are the site of initial mineral deposition in growth plate cartilage of long bones was made independently over 40 years ago in the late 1960's by Anderson (1, 2) and Bonucci (3, 4). While there was some initial controversy, it soon became apparent that these structures are typically invested by a trilaminar membrane; thus the name, "matrix vesicles – MVs", became their accepted title. Since their initial discovery in growth plate cartilage, MVs have been found to be the locus of the first mineral deposits in intramembranous bone formation (5), in fracture callus (6-8), in developing dentin (5, 9), in developing deer antler (10), in pathological calcifications in

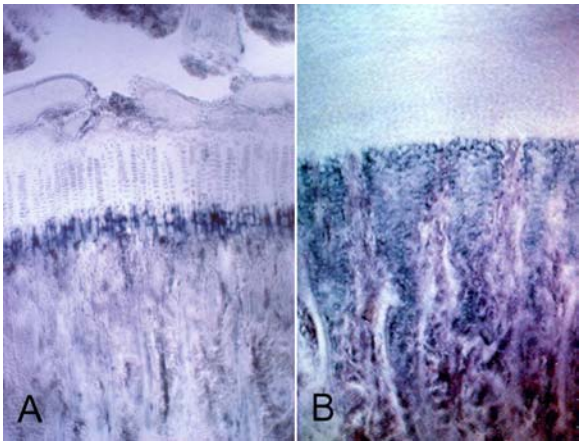

Figure 1. Sudan Black B Staining of Growth Plate Cartilage. **A** – Rat Tibia; **B** – Chick Tibia – Tissues were fixed in formalin-saline solution; after fixation they were extracted with pyridine at 60°C for 8 h. Following rehydration through a series of alcohol solutions, the tissue was decalcified with formic acid-sodium citrate (577). After embedding in gelatin, sectioning was done on a freezing microtome. The sections were stained with a saturated solution of Sudan black B in 70% ethanol for 3 minutes. After a brief rinse with 70% ethanol, sections were brought to water and mounted in glycerin-jelly (16-18). 1A – In the rat epiphysis vascular penetration occurs at the base of each column of differentiating chondrocytes; note the intense blue-black stain in the extracellular matrix around the hypertrophic chondrocytes where mineral formation is in progress (16). 1B – In the chick epiphysis vascular penetration occurs only at intervals, leaving zones of hypertrophic chondrocytes projecting as 'tongues' into the underlying marrow space. Note the same blue-black stain in the extracellular matrix around the hypertrophic chondrocytes. Subsequent studies have demonstrated the lipid nature of the Sudan black B-staining material, which is complexed with the newly forming mineral at these sites. (Figure 1A, color slide published in black and white by Irving (16); Figure 1B, color slide previously unpublished.)

aortic valves (11) and in osteosarcoma (12, 13). In addition, in other studies (14, 15) the initial site of mineral deposition in calcifying turkey leg tendon was also shown to begin within MVs and spread to the adjacent type I collagen fibrils.

The primary focus of this review is on *de novo* mineral formation in the epiphyseal growth plate of vertebrates. This is a cell-mediated process, discovered in the rat to be initiated by MVs (1, 3). However, this discovery was antedated by almost a decade by Irving *et al.* who found intensely staining Sudanophilic material in the extracellular matrix at the calcification front of the tibial growth plate of the rat and chicken, respectively (Figure 1A–B). This unusual lipid staining pattern was subsequently observed at the calcification front in all vertebrate species investigated (16-18). As will be described later, the Sudanophilic material is mineral-associated lipid, shown to be primarily acidic phospholipids – particularly phosphatidylserine (PS) (19-23). Although initially regarded as an artifact caused by the affinity of Ca^{2+} for PS (24-27), subsequent *in vivo* studies by Eisenberg *et al.* (28) established that this association was of biological origin. The ensuing finding that MVs have high levels of phospholipids enriched in PS (29-31), corroborated the finding of Sudanophilia at the calcification front, linking it to the presence of MVs.

It is important to point out that MVs are *not* typically associated with mineral deposition beyond the early inductive phase of calcification. Thus, MVs are not associated with the massive mineralization that occurs later in bone, dentin or cementum, nor are they association with mineralization events occurring during enamel formation. Thus their biological role appears confined to that of induction of solid mineral formation in tissues where no mineral phase previously existed. Despite a general acceptance of this role for MVs, they may not be responsible for the induction of mineral deposition in all vertebrate calcifying tissues. It is quite likely that some types of pathological calcification are brought about by other means.

3. MORPHOLOGY OF MATRIX VESICLES

Since their discovery over four decades ago, a great deal of work has been focused on MVs in an attempt to characterize their basic structural and chemical features. Much attention also has been focused on the mechanism of MV formation and their mode of action. First, to be discussed will be two sections on morphological and biochemical characterization. Later sections will deal with MV formation and the mechanism and regulation of MV-induced calcification.

3.1. Conventional transmission electron microscopy

Studies that led to the discovery of MVs were morphological in nature and the first observations made of MVs were of conventionally fixed and stained transmission electron microscopy (TEM) preparations (1-4). In general, these methods revealed MVs to be somewhat heterogeneous structures ranging from about 100 to 300 nm in diameter, typically enclosed by a trilaminar membrane, containing varying amounts of relatively amorphous osmiophilic material. Some, but by no means all of these vesicles were found to contain electron-dense crystalline structures. These mineral crystals were frequently associated with the inner surface of the lipid bilayer. Some studies have utilized La^{3+} as a probe for Ca^{2+} binding sites associated with MV mineral deposition (32, 33). La^{3+} is a rare-earth cation with an ionic radius similar to Ca^{2+}; it binds with high affinity to Ca^{2+}-binding sites such as acidic phospholipids of the MV membrane as well as focal proteoglycan aggregates. However, its charge-density and coordination chemistry are quite different from those of Ca^{2+} (34, 35). La^{3+} has no biological ion porter and thus does not penetrate intact membranes or enter living cells; in fact, submicromolar levels of La^{3+} block Ca^{2+}-release-activated channels (36). While La^{3+} binds tenaciously to Ca^{2+}-binding sites in the extracellular matrix and displaces Ca^{2+} (33), it apparently does not displace Ca^{2+} in

microcrystalline apatitic deposits. In these studies it was noted that there were two types of MVs; some were dense and stained heavily with La^{3+}; others were "light" and unstained. Thyberg and Friberg (37, 38) also made note of the heterogeneity of MVs and concluded that there were two types of vesicles, one of which derived from lysosomes. While many have noted heterogeneity in MV structures, there is now a much clearer understanding of their origin.

3.2. Cryofixation, freeze-substitution electron microscopy

Conventional tissue processing for TEM observation typically involves fixation with glutaraldehyde, post-fixing with osmium tetroxide, dehydration steps in alcohols, embedding in plastic, ultra-thin sectioning, flotation of the sections on aqueous medium, and frequently post-staining with uranyl acetate or lead acetate to increase electron density. It is now evident that these steps can cause major alteration in the native structure of the vesicles and their enclosed mineral, as well as in the surrounding tissue. To avoid these problems, several alternative approaches have been employed to reduce artifacts. Hunziker and others (39-41) reported the use of cryofixation and freeze-substitution for the preservation of details of MV structure. In their methods, rapid (40 msec) high-pressure freezing at liquid N temperature was used to prevent ice crystal formation. This was followed by dehydration at –90^{o}C with anhydrous methanol containing uranyl acetate (0.05%) and glutaraldehyde (2%), with gradual warming steps to –60^{o}C and –30^{o}C, replacement of methanol with acetone and infiltration with resin at +4°C. Such techniques prevented collapse of the proteoglycan network in the extracellular areas and the shrinkage of chondrocytes seen in conventional methods. MVs appeared to be attached to the surrounding matrix proteins (both proteoglycans and collagen fibrils); the trilaminar membrane was clearly evident. Similar cryofixation methods have been used by Arsenault *et al.* (42, 43), but with the use of "slam-freezing" in which freshly excised tissue was rapidly brought into contact with a copper block prechilled to <25°K with liquid helium. In addition, high resolution elemental mapping of the resultant preparations was performed using the electron spectroscopic imaging (ESI) technique of Ottensmeyer and Andrew (44). MVs again showed intimate association with matrix proteoglycans and collagen, and frequently contained what appeared to be mineral deposits (Figure 2A). Elemental mapping showed the presence of both Ca and P in electron-dense material in the vesicle lumen; however the intensity and localization of the two elements did not precisely coincide (Figure 2B) (40, 42).

Another problem attendant with tissue preservation using cryofixation and freeze substitution techniques concerns the handling of tissue sections. Typically these are floated on aqueous medium before being picked up by the coated grids. While macromolecules trapped in the plastic resin are well preserved, this step permits the loss of soluble electrolytes and small molecules from tissue specimens. To avoid this aqueous step, both ethylene glycol and glycerol have been used as flotation media. In a detailed study of these different anhydrous methods, Morris *et al.* (45) showed that with either freeze substitution, cryo-ultramicrotomy, or anhydrous ethylene glycol tissue processing, MVs were the locus of the first mineral crystallites seen in calcifying growth plate cartilage. The vesicles were shown to contain both Ca and P by energy-dispersive X-ray analysis. It should be mentioned here that one of the problems with the use of ethylene glycol processing after cryo-ultramicrotomy is that of poor membrane preservation. Subsequently, papers by Arsenault and Hunziker (40, 41), and Akisaka *et al.* (46) exploited the rapid cryofixation, freeze-substitution method, avoiding the use of post-staining and aqueous flotation methods. With these methods it became clear that much of the apparent heterogeneity seen in MVs with the various staining methods arises from artifacts directly attributable to the stain itself. Although the contrast was weak, the appearance of the unfixed, unstained MVs handled anhydrously after cryofixation and freeze-substitution was relatively uniform (46). Many contained uniform amorphous electron-dense material, with some vesicles containing small crystallites. These were best seen using selected-area dark field imaging (40). Perhaps of greatest importance, staining was shown by EDAX X-ray microanalysis to totally displace both Ca and P from the vesicles (40). In light of these findings, interpretation of conventionally prepared transmission electron micrographs showing MVs in tissue sections of mineralizing tissues must be done with great caution.

3.3. Freeze-fracture studies

Another technique that has yielded important information about MV structure is freeze-fracture. The first studies on MVs using this technique were reported in 1978 by Cecil and Anderson (47) and Borg *et al.* (48) at the Second Conference on Matrix Vesicles. These, and subsequent studies (49-51) have consistently revealed the presence of abundant MVs in the extracellular matrix of growth plate cartilage. The observed MVs fractured in a manner consistent with a lipid bilayer-enclosed structure. They possess well-defined intramembranous particles distributed more abundantly on the outer convex protoplasmic (PF) face than on the concave inner exoplasmic face (EF) of the vesicle membrane (Figure 3). The distribution of intramembranous particles in MVs was similar to that seen on the plasma membrane of the microvilli from which the vesicles appear to derive. The importance of this observation is that it reveals that the MV membrane retains the normal inside-outside orientation during the vesiculation process. This finding has major bearing on the role of Ca^{2+}-dependent ATPase in Ca^{2+} loading by MVs.

Freeze-fracture studies also suggest that MVs derive not only by budding from cellular processes, and from cell disintegration (as indicated by some electron microscopic methods), but also from protrusions at smooth surfaces (46). Further, freeze-fracture studies revealed a close association between MVs and collagen fibers (47, 48). Remnants of MVs can be detected within islets of developing mineral deposits (50). Finally, freeze-fracture studies by Akisaka *et al.* (46) suggest that MVs can be

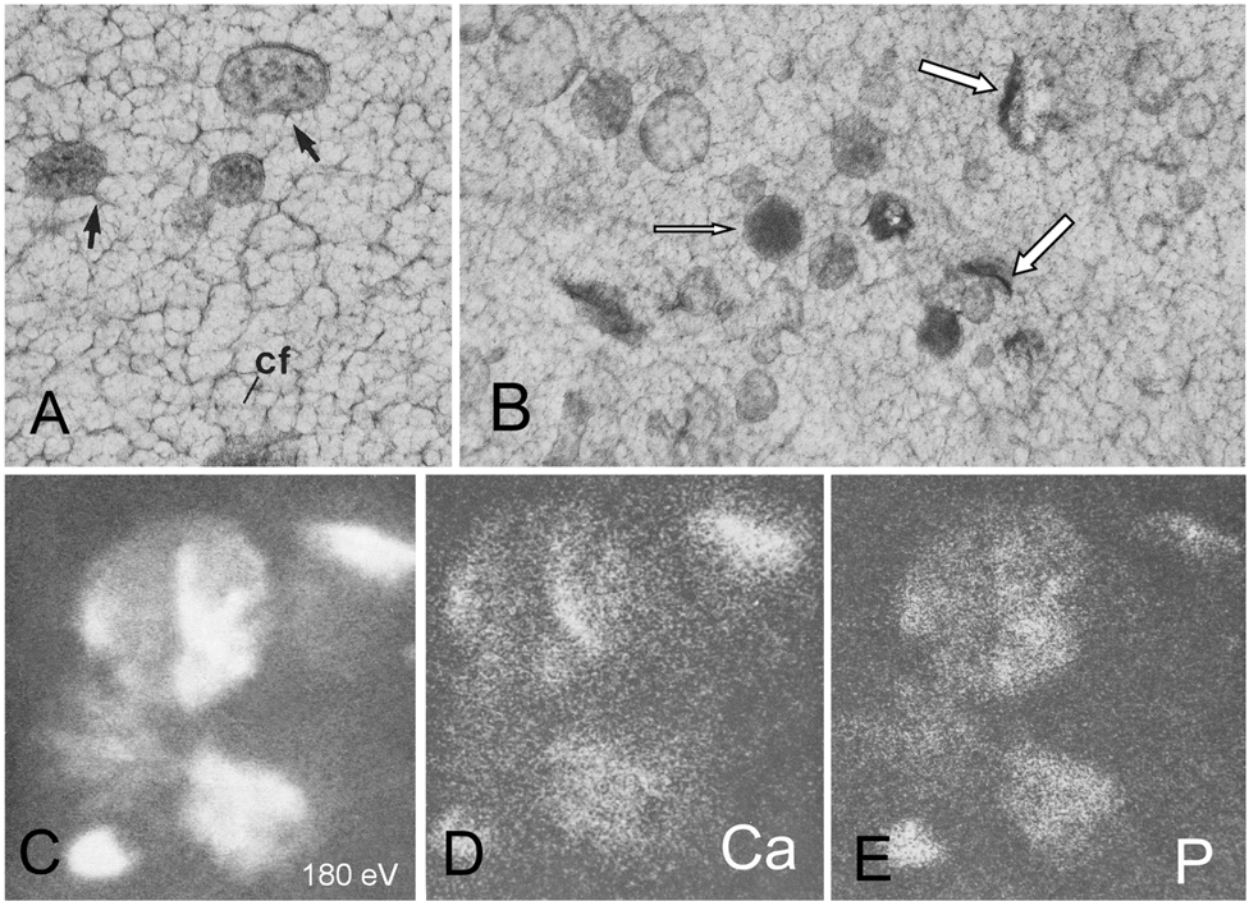

Figure 2. Matrix Vesicles Visualized by Slam Freezing, Freeze-Substitution and Electron Spectroscopic Imaging (ESI). Freshly excised femoral heads from 2-day-old mice were cut longitudinally and transferred to a slam-freezing device and slammed onto a copper block cooled to <25°K with liquid helium. The tissues were then stored in liquid N_2, transferred to 2.5% OsO_4 in acetone, and substituted for 40 h at –85°C, warmed to –20°C for 1 h, 0°C for 1 h, and to RT with 3 changes of acetone. Specimens were embedded in Spurr resin, and sectioned. **2A** – MVs of the proliferative zone showing attachment of the surface of the vesicles to proteoglycans (arrows) and collagen fibrils (cf). **2B** – MVs hypertrophic zone showing variable size and content density; note mineral deposits (open arrows). **2C-E** – Digitized ESI of MVs showing electron density (C), Ca (D) and P (E), respectively. Note that the intensities of Ca and P do not completely overlap indicating that they are not all in combined form. The MV in these images ranged in size from 70-160 nm in diameter. (Adapted from (578) with permission from William T. Butler, Ed..)

categorized with respect to intramembranous particle distribution. MVs in the reserve and proliferative regions tended to be more uniform and had a random distribution of intramembranous particles on the EF and PF faces. In the hypertrophic region, MVs tended to be of two types: those with no intramembranous particles and those in which they were aggregated. MVs with aggregated intramembranous particles were associated with mineralization; those free of intramembranous particles were not. These data suggest that the intramembranous particles may be involved in mineralization and raise the important question as to which proteins are present in these particles. This question has not been addressed.

4. ISOLATION OF MATRIX VESICLES

One of the early obstacles to biochemical characterization of MVs was the lack of reliable methods for isolation of pure, chemically intact, biologically functional structures. This problem stemmed from the fact that MVs, as their name implies, are embedded among extracellular matrix connective tissue macromolecules such as proteoglycans and collagens. Further, MVs comprise only a minor fraction of the total mass of the tissue. Initially, the general approach used to obtain MVs from tissues involved use of crude collagenase, plus or minus other enzymes to digest the tissue slices, followed by differential centrifugation (52-54), with or without further subfractionation. To avoid the use of proteases, others used tissue homogenization followed by differential centrifugation and further subfractionation using either sucrose gradient methods (55, 56) or Percoll gradients (57) to produce MV-enriched microsomes (MVEM). Another method involved simple centrifugation of the spent medium from primary cultures of growth plate chondrocytes to produce "media vesicles" (MeV) (58). A major problem

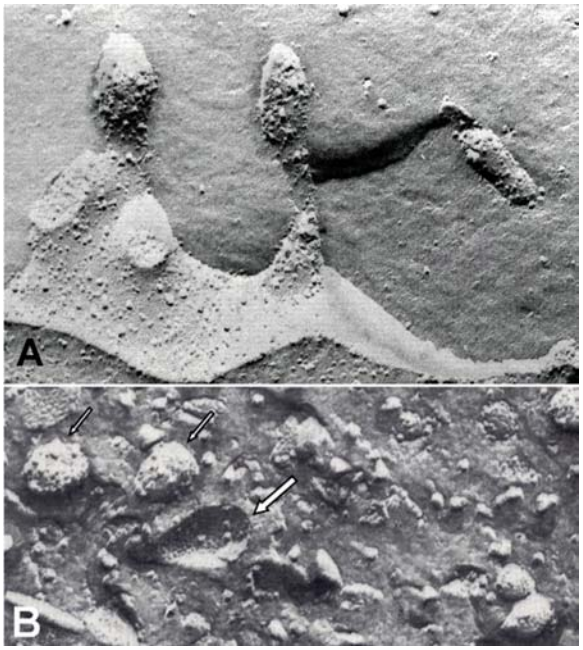

Figure 3. Freeze-Fracture Analysis of Chicken Epiphyseal Growth Plate Cartilage. For freeze-fracture, the epiphyseal cartilage tissues were dissected and placed in 25% buffered isotonic glycerol. They were then quick-frozen in Freon 22, transferred to liquid N_2, and fractured using a Baltzer 301 Freeze-Fracture apparatus at –130 ºC. Following coating with platinum and carbon, the replicas were freed of adhering organic matter with sodium hypochlorite, rinsed with distilled water, and examined by TEM. (Note that using this shadowing technique, upward projecting surfaces are coated black, while downward projecting surfaces appear white.) **3A** – Cell processes of a hypertrophic chondrocyte. Shown is the external convex (*p*) surface of two cytoplasmic projections, 0.11–0.15 microns in diameter, showing numerous membrane-associated particles (MAPS), 95–180 Angstroms in diameter. Note on the lower left that two of the projections have been fractured in cross section. **3B** – Matrix vesicles in the extraterritorial matrix near the hypertrophic chondrocyte. The diameter of the vesicles (0.09 – 0.13 microns) is very similar to that of the cell processes in A. Note that the topographical distributions of MAPS on the external surface of the MVs, *e.g.* two on left (narrow arrows) are essentially identical to those seen on the external (*p*) surfaces of the cytoplasmic projections of the hypertrophic chondrocyte shown in A, above. Also note one slightly larger ovate MV (broad arrow) is fractured so that the inner concave (*e*) surface is presented. Here, it is evident that the distribution of MAPS on the inner *e*-surface of MVs is much sparser than on the external *p*-surface. These findings reveal that inversion of the plasma membrane did not occur upon vesiculation. (Figure 3A, adapted from (48) with permission from Springer. Figure 3B adapted from (55) with permission from Elsevier.)

with MVs isolated with crude collagenase, as originally described by Ali *et al.* (52) was that they showed evidence of substantial damage to most of the resident proteins, even though their lipid and electrolyte content appeared to be less seriously affected. Significantly, this protease digestion method did not significantly damage the activity of alkaline phosphatase, which apparently was protected by its large 18–22 kDa glycan "umbrella" (59). In order to initiate mineral deposition, these MVs required the addition of high levels of organic phosphate substrates, typically 10 mM beta-glycerophosphate. On the other hand, the non-enzymatically released MVEMs, while very active in their ability to induce mineral formation without use of organic phosphate substrates, suffered from the presence of significant contamination of subcellular membrane fragments (55). Attempts to purify MVEM by a variety of methods met with limited success. Some success was achieved through use of Percoll gradients that do not cause the osmotic effects of sucrose, but there was difficulty with contaminating Percoll in the MVEM fraction (57). Subsequent work using much milder tissue digestion methods have enabled the isolation of MV that retain their complement of normal proteins (60-62), as well as the ability to rapidly initiate mineral formation. They also appear to have minimal contamination with intracellular membrane fragments.

4.1. Crude collagenase digestion methods

While there has been considerable controversy as to which is the best method of MV isolation, there probably is no 'best' method; each can serve some useful purpose. For example, the original crude collagenase digestion method of Ali *et al.* (52), while yielding vesicles that appeared quite homogeneous by conventional electron microscopy, caused major damage to external vesicle proteins. Nevertheless, the method was of value for analysis of MV lipids (29-31) and electrolytes (63, 64), and for certain MV enzymes (e.g. tissue-nonspecific alkaline phosphatase, TNAP) that are resistant to the nonspecific proteases present in crude collagenase (54). While collagenase-released MVs (CRMVs) have continued to be used by several groups for metabolic studies on the induction of mineralization, the damage caused to the external proteins and ion porters by crude collagenase undoubtedly alter their ability to induce mineralization and must be interpreted with caution.

4.2. Non-collagenase-dependent methods

To avoid problems arising from damage caused by the nonspecific proteases present in crude collagenase, MVEM were isolated by tissue homogenization and differential centrifugation. Such preparations very actively accumulated Ca^{2+} and inorganic phosphate (Pi), and rapidly induced mineral formation from synthetic lymph without the addition of organic phosphate substrates (55, 56). However, they contained intracellular membrane fragments, and could have entrapped extravesicular mineral during the homogenization process. Such MVEM were studied extensively. Preparations from the proliferating zone of growth plate cartilage neither accumulated significant Ca^{2+}, nor Pi, nor induced calcification (55); MVEM from the hypertrophic zone readily induced mineralization. This showed that the ability to induce mineralization was not a general property of microsomes. Further, Ca^{2+} uptake by active MVEM could be inactivated

simply by exposure to proteases (65). This revealed that induction of mineralization by MVEM did not result from contaminating mineral; otherwise the proteases would have exposed it and enabled even more rapid mineralization. However, these preparations were not homogeneous. Attempts to purify them using sucrose gradients, while eliminating many subcellular fragments, destroyed their ability to mineralize. The osmotic effects of the high sucrose concentrations caused major loss of Ca^{2+} and Pi from the vesicles (65-67). This revealed that the Ca^{2+} and Pi present were not stable; otherwise they would have survived this gradient procedure. Thus, although sucrose step-gradients enabled the preparation of fractions essentially identical by TEM to CRMV and had similar TNAP activity, they lacked the original ability of MVEM to induce mineral deposition (55, 56). In contrast, isosmotic Percoll gradients enabled the fractionation of MVEM into two major subpopulations, one of which readily induced mineralization, the other not (57). While this fractionation procedure improved the purity of the isolated MV fractions, Percoll contaminated the samples.

4.3. Cell culture methods

The use of growth plate chondrocyte cultures that release vesicles into the culture medium was also used to gain some insight into the protein and lipid composition of cell-released vesicles and in the mechanism of MV formation (68-72). However, a significant problem was that vesicles released into the culture medium (MeV) are not identical to those trapped in the matrix (71, 73-75). One significant difference is that these released vesicles differ in their lipid composition (73), as well as their ability to accumulate mineral ions. Another is that they had no detectable annexins, lipid-dependent Ca^{2+}-binding proteins characteristic of MV isolated from native tissue, or the matrix of cultured chondrocytes (76).

4.4. Modified collagenase digestion methods

Progressive refinements in the original collagenase digestion method have been made that have significantly reduced the deleterious effects of the nonspecific proteases present in crude bacterial collagenases (61, 62). These entail reduction in the concentration of collagenase and the length of exposure, as well as certain post-digestion manipulations that facilitate the release of MV entrapped in the partially digested matrix. Such preparations rapidly mineralize when incubated in synthetic cartilage lymph in the absence of organic phosphate substrates. Protein patterns of these MVs are reproducible, showing numerous characteristic major bands. Mineralization of these MVs is highly sensitive to protease treatment; low levels of chymotrypsin or trypsin rapidly ablate their ability to mineralize (60, 61). And like MVEM, these vesicles are highly sensitive to pH; exposure to pH 6 buffers for only a few minutes almost totally destroys their ability to induce mineralization, even when subsequently supplied with organic phosphate substrates (77). Despite these improvements, there is some protease damage to these MV preparations, albeit not to such an extent as to destroy their ability to induce mineral deposition. This modified procedure for MV isolation has been used successfully by Balcerzak *et al.* (78) for proteomic analysis of MV proteins.

4.5. Other isolation methods

Various other approaches have been reported in the past for the purification of CRMVs. Anderson's group has utilized rachitic rat epiphyseal growth plate cartilage as a tissue source for isolation of CRMVs (79-82). Shapiro *et al.* have employed isoelectric focusing of CRMV (83). Vaananen and Korhonen used Percoll gradients to purify CRMV from lysosomal contaminants (84). Slavkin *et al.* (85) used Bio-Gel A-15m size-exclusion chromatography to purify CRMV released from predentine; and Deutsch and Sela *et al.* (86) used a combination of collagenase digestion, differential centrifugation and sucrose step-gradient fractionation to isolate MVs from alveolar bone. Very recently, Xiao *et al.* isolated MV from mineralizing osteoblasts for proteomic analysis (87). Thus, many different techniques have been used to isolate MV from various mineralizing tissues. Keeping this in mind, the proteins, enzymes, lipids, and electrolytes found in various MV preparations will now be explored. For most biochemical characterizations reported in this review, the MVs were isolated from normal, 6–8 week old, rapidly growing broiler-strain chickens.

5. MATRIX VESICLE PROTEINS

A major impediment to the analysis of MV proteins was the difficulty of isolating pure vesicles from the tissue without concomitant damage to the constitutive proteins. Through modifications in the isolation procedures for MV isolation – as was just discussed – significant progress in the characterization of MV proteins has been made. Very recently proteomic analysis of MVs has greatly expanded our perception of the complexity of the patterns of proteins expressed. This methodology has revealed the large number of proteins present, which now can be categorized into subclasses with implications as to their importance to MV formation and function. While proteomic analysis of MV proteins has become of great value in assessing the panoply of proteins present, certain important proteins are nevertheless missed. Therefore, in this review, biochemical, enzymatic, and proteomic analytical data will be used to present an integrated view of the nature and importance of the proteins detected.

5.1. Early SDS-PAGE Studies

Several early studies explored the sodium dodecyl sulfate – polyacrylamide gel electrophoresis (SDS-PAGE) patterns of proteins present in MV using crude collagenase digestion (88-90), as well as MVEM (55-57, 65, 68) and culture media vesicles(58, 69, 70, 91). While there was considerable variability in the patterns of MV proteins from the various tissues, animal species, and MV preparations, certain protein bands nevertheless were consistently observed; these include two or three intensely staining bands in the 30-38 kDa range, two strongly staining bands at 40-48 kDa, and bands frequently appearing in the 55 kDa, 90-100 kDa and 130-150 kDa range. Initially little effort was made to identify these proteins, although there were some estimates based on the apparent size of the proteins. Work by Muhlrad *et al.* (92)

provided evidence for the presence of actin in MV isolated from rat alveolar bone, but beyond assessment of enzyme activity, limited attempt was made to assign a function to the proteins identified in MVs.

5.2. Isolation and Identification of Major MV Proteins

It should be mentioned here that early studies with MVEM showed that trypsin treatment reduced uptake of Ca^{2+} much more than uptake of Pi (57, 65)). When later studies again showed that protease treatment of actively calcifying MV fractions markedly impaired their ability to mineralize and that the effect of protease treatment was not due to damage to alkaline phosphatase activity (66), effort was begun in earnest to isolate, identify and characterize proteins critical to MV ion accumulation (76). The approach used was based on improved methods of isolation (See 4.4. above) that resulted in mineralization-competent MV; it compared several types of biologically active MV preparations (58, 66, 71, 76, 91). Proteins isolated from intact, but non-homogeneous MVEM prepared by non-protease-dependent methods, were compared with those from pure, but partially damaged CRMV. Highly purified proteins from both types of MV preparations were used to raise monospecific polyclonal antibodies (59-61, 93). These antibodies, and well-characterized antibodies directed toward known proteins, were then used to identify cross-reactive proteins in each type of MV preparation. In this manner, intact samples of MV proteins were isolated from MVEM preparations; incomplete but pure MV proteins were isolated from the partially damaged collagenase-released MV (61). This technique was used successfully to identify several major groups of MV proteins.

5.3. Sequential extraction, separation, and characterization of major MV proteins

Using sequential extractions with buffered salt, non-ionic detergent and ethylene glycol tetra-acetate (EGTA) solutions, Genge *et al.* and Wu *et al.* (61, 94) developed methods that enabled the proteins of the isolated MV to be selectively extracted in a step-wise fashion. For example, treatment of isolated CRMV with hypertonic salt solutions selectively released bands migrating on SDS-PAGE at an apparent MW of 130-150 kDa (95). These released proteins were identified using both monoclonal and polyclonal antibodies to be type II collagen and its fragments. Subsequent extraction of the vesicle pellet with low ionic strength solutions released two major MV proteins migrating on SDS-PAGE at apparent MW of 40-48 kDa (96). These water-extractable proteins were identified to be proteoglycan link and hyaluronic acid binding region protein using both monoclonal antibodies and N-terminal amino acid sequencing of the proteins. Further extraction of the residual MV pellet with Triton X-100 detergent-containing buffers released TNAP and a variety of other quantitatively minor uncharacterized proteins. Next, extraction of the residual pellet with EGTA under specific pH and ionic strength conditions selectively released two classes of phospholipid-dependent Ca^{2+}-binding proteins (61, 94, 97) (Figures 4A–C). Variations on this extraction scheme also enabled the selective extraction of TNAP largely free of other MV proteins (59).

5.4. Proteomic characterization of matrix vesicle proteins

The chemical dissection just delineated led to identification and characterization of many major MV proteins. The development of a proteomic approach proved to be of great value in more completely identifying the array of proteins present in authentic MVs. However, it is critically important in any proteomic study to utilize carefully purified, homogenous, functionally active MVs capable of inducing rapid mineralization. Two very recent studies on the MV proteome come to mind: the Xiao *et al.* studies (87, 98, 99) using vesicles isolated from cultured mouse cranial osteoblasts (both collagenase-released and culture media MV), and the 2008 Balcerzak *et al.* study (78) using MVs isolated from femurs of chicken embryos. While a huge number of proteins (>1000) were implicated by the Xiao *et al.* studies, the purity and functional activity of the vesicles analyzed were not clearly established. Neither was there any clear analysis of the probability that these proteins were from bona fide MVs. Also, there was no indication of whether these vesicles were capable of inducing mineralization – a critical feature of their known biological activity. Regrettably, there is ample reason to believe that these vesicle fractions were seriously contaminated with cell and matrix debris. In contrast, the purity of the MVs isolated by Balcerzak et al. from chick embryo femurs was much better documented; the vesicles were clearly shown to induce mineral formation, and the SDS-PAGE profiles were very similar to those of previously published reports on protein patterns of functional MVs (60, 61). The number of proteins identified by Balcerzak et al. was still large (126 gene products); but, these were each presented with an indication of their abundance, the reliability of their identification, and their likely function.

Nevertheless, it is important to note that despite the plethora of proteins reported in these studies, several key enzymes and proteins known be present in MVs from their biological activities were not detected. For example, two known Pi transporters, an L-type Ca^{2+} channel, and a variety of phospholipases and growth factors known to be present in growth plate chondrocytes and MVs were not detected by these proteomic analyses. Their absence therefore raises a significant note of caution. Possible reasons for failing to detect these proteins are: 1) that ion transporters are relatively large multi-transmembrane integral proteins that may not have been properly dissolved in the detergents used; and 2) that very small proteins like the phospholipases and growth factors may have been lost during preparation of the vesicles for analysis. With these caveats, the array of proteins identified in the chick embryo femur MV by Balcerzak *et al.* will be presented, along with their Mascot Scores (100). The Mascot Score (MS) = –10*Log(P), where P is the probability that the observed match is a random event (101) A big score means that the probability for a given protein to be in MVs is high. Thus, the MS is shown in brackets next to each protein identified by the proteomic analysis.

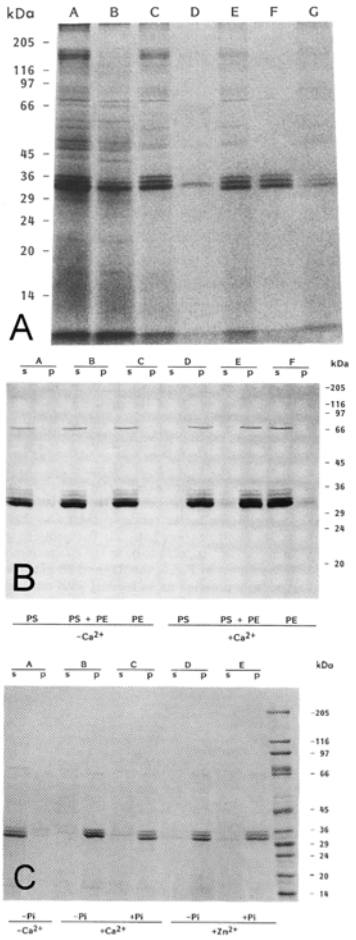

Figure 4. Fractionation of Collagenase-Released Matrix Vesicle Proteins Revealing the Presence of Several Acidic Phosholipid-Dependent-Ca^{2+} Binding Proteins (Annexins). 4A – SDS-PAGE gradient gel of collagenase-released MVs (CRMV) and subfractions – CRMV (*lane A)* were incubated at 25 ºC for 20 min in 1% Triton X-100 buffer (100 mM NaCl, 10 mM Tris-HCl, 5 mM $CaCl_2$, 2,5 mM $MgCl_2$, 1 mM NaN_3, pH 7.4) at a final protein concentration of 4 mg/ml. After centrifugation for 20 min at 130,000 x g, the supernatant (*lane B*) was removed and the pellet (*lane C*) washed with SCL, recentrifuged, and the supernatant (*lane D*) and the pellet were collected. The pellet (*lane E*) was then extracted by homogenization in an EGTA-containing buffer (10 mM Tris-HCl, 100 mM NaCl, 5.0 mM EGTA, 2.5 mM $MgCl_2$, 1 mM dithiothreitol, 1 mM NaN_3 , pH 7.4), incubated at room temperature for 15 min, and centrifuged as above. The supernatant fraction (*lane F*) and the insoluble residue (*lane* G), as well as the other fractions, were analyzed by SDS-PAGE (7.5–15.0% gel). Molecular mass markers, expressed in kDa, are shown on the left. Note that EGTA removed a highly select group of proteins (the annexins) from MVs following the preliminary extraction with nonionic detergent. Three major bands of ~30-, 33-, and 36-kDa, and a lesser 68-kDa protein, based on Coomassie Blue staining, account for ~one-third of the total MV proteins. The 30- and 33-kDa proteins are now known to be annexin A5 (AnxA5); the 36-kDa protein is annexin A2 (AnxA2); and the 68-kDa protein is annexin A6 (AnxA6). 4B – Lipid specificity of Ca^{2+}-binding to MV annexins – The MV annexins were mixed with either pure PS, pure PE, or a 1:1 mixture of PS and PE (400 micrograms/ml) in a buffer composed of Tris-HCl (10 mM, pH 7.5), KCl (100 mM), $MgCl_2$ (2.5 mM), DTT (0.5 mM), and EGTA (5.0 mM), without (*A, B, C*) or with (*D,E,F*) 5.0 mM $CaCl_2$, <1 microM *free* Ca^{2+} (579). After 20 min incubation at RT, the liposomes were sedimented at 130,000 x *g*. Equivalent portions of the supernatant (s) or pellet (p) fractions were analyzed by SDS-PAGE (10% gel) and stained with Coomassie Blue. Note that in the presence of Ca^{2+}, the MV annexins sediment with pure PS (*D*) or a 1:1 mixture of PS and PE (*E*), but minimally with pure PE (*F*) at this Ca^{2+} ion activity level. (When PC and PI were similarly tested, the MV annexins did not show bind to PC, but did bind to PI, in the presence of Ca^{2+}). Also note that in the presence of 2.5 mM Mg^{2+}, but absence of Ca^{2+}, that the annexins have NO affinity for PS or PE (*lanes A, B, C)*. 4C – Effects of Pi on Ca^{2+}- or Zn^{2+}-dependent binding of annexins to PS – Procedures were as with B except that Pi (10 mM) was added to the PS liposome/annexin mixture prior to addition of 5 mM Ca^{2+} (<1 microM *free* Ca^{2+}) or 5 mM Zn^{2+} (<1 microM *free* Zn^{2+}). 4A, interaction of annexins with PS alone; 4B, PS + Ca^{2+}; 4C, PS + Pi + Ca^{2+}; 4D, PS + Zn^{2+}; or *E*, PS + Pi + Zn^{2+}. Supernatant (s) and pellet (p) fractions on 7.5–15% SDS-PAGE are shown. Note that in the presence of either Ca^{2+} or Zn^{2+}, the annexins sedimented with PS. Also note that Pi did not interfere with this interaction. (These figures were originally published in (60) by the American Society for Biochemistry and Molecular Biology.)

6. MATRIX VESICLE-ASSOCIATED EXTRACELLULAR MATRIX PROTEINS

Surprisingly, extracellular matrix proteins represent some of the major MV proteins identified by proteomic analysis. They appear to be proteins attached to MVs *via* various linkages. However, their presence in isolated MV fractions is in close agreement with previous studies that documented the strong binding between MVs and certain matrix proteins present in growth plate cartilage (95, 96, 102, 103).

6.1. Type VI collagen

The proteomic discovery of the abundance of Type VI collagen in the MV fraction is the first indication of its close relationship with MVs (78). This analysis revealed the presence of each of the three collagen chains: alpha-1 [Mascot Score, 1621], alpha-2 [1556], and alpha-3 [1023] in the MV fraction, indicative that a substantial amount of Type VI collagen is associated with MVs. Type VI collagen is a major component of microfibrils present in the capsule that defines the pericellular matrix surrounding individual chondrons (104). Mutant forms of type VI collagen appear to be causally involved in various classes of muscular dystrophy (105-108). Of special interest to growth plate mineralization, Type VI collagen receptors on the chondrocyte surface (NG2-proteoglycan) (109, 110) act as transducers to mitochondria within the cells, affecting their permeation transition pore for Ca^{2+} (111). As will be discussed later, this appears to have an important influence on mitochondrial Ca^{2+} release (112).

6.2. Type X collagen

Type X collagen has long been associated with the hypertrophic region of growth plate chondrocytes, and was assumed to be involved either in the onset or regulation of mineral formation (113-115). Recent studies by Genge *et al.* using synthetic MV nucleational complexes found that Type X collagen had a small inhibitory effect on the onset and rate of mineral formation; however it significantly extended the length of the "rapid formation" period, thereby altering the kinetics of the overall amount of mineral formation (116). Only one representative of type X collagen: alpha-1 was observed in the MV proteome; it's Mascot score [142] was weak and indicated that only minimal amounts of Type X collagen were present in the MV fraction (78). In light of the documented tight binding of Type X collagen to MV (95, 102, 103) it is likely that the use of bacterial collagenases during isolation of MV caused the Type X collagen to become largely degraded. More will be said about type X collagen later.

6.3. Proteoglycan link protein and aggrecan core protein

Proteoglycan link protein and aggrecan core protein were first shown to be tightly associated with MVs by Wu *et al.* in 1991 (96). Both proteins were found to be major components of isolated functionally active MVs and could be dissociated by exposure to low ionic strength buffer. These early findings were confirmed by the recent proteomic analyses of avian MVs (78). Their Mascot Scores, [1040] for proteoglycan link protein, and [966] for aggrecan core protein, indicate a strong presence in the isolated MV fraction. Proteoglycan link protein is known to stabilize aggregates of proteoglycan monomers with hyaluronic acid in the extracellular cartilage matrix. Similarly, aggrecan core protein serves as the attachment site of chondroitin sulfate and keratin sulfate chains in the large proteoglycan macromolecule. MVs are known to be embedded in the extracellular matrix around hypertrophic chondrocytes; freeze-clamp ultrastructural studies have confirmed the filamentous attachments between the MV and the extracellular matrix (43). Thus, it was not surprising that proteoglycan-related proteins would be observed in the MV proteome. Small amounts of additional proteoglycan-related proteins were also identified by proteomic analysis (78).

6.4. Fibrillin-1 and Fibrillin-2

The fibrillins have also been observed by proteome analysis of isolated MVs; the Mascot Scores of Fibrillin-1 [549] and Fibrillin-2, [672] indicate a significant presence in MVs. Fibrillins are present in the extracellular matrix of growth plate cartilage (115, 117-119). Mutations in the fibrillin gene have been linked to the Marfan syndrome (120). Flash-frozen ultrastructural examination of growth plate cartilage has revealed that MVs are attached to microfibrils in the extracellular matrix (41, 44). Although not established morphologically, it is probable that the fibrillins are present in combination with type VI collagen in the pericellular domain and are attached to MVs in the extracellular matrix.

7. THE ANNEXINS – ACIDIC-PHOSPHOLIPID-DEPENDENT Ca^{2+}-BINDING PROTEINS

The dominant, most abundant proteins detected by the proteomic assay were the annexins; they compromise a large family of acidic phospholipid-dependent Ca^{2+}-binding proteins. The Mascot Score [2877] of annexin A5 (AnxA5) was the highest score for any MV protein; however, annexin A6 (AnxA6) [1798] and annexin A2 (AnxA2) [956] were also high-ranking (78). These findings are in close agreement with earlier analyses of proteins present in nucleationally-active MVs made by Genge *et al.* in 1989 showing that the annexins were major proteins and that they bound tightly to PS in a Ca^{2+}-dependent manner (Figure 4A-C, Figure 5) (60). However, proteomic analyses have also identified three additional annexins not evident from the earlier studies: annexin A1 (AnxA1) [1197], annexin A11 (AnxA11) [846], and annexin A4 (AnxA4) [327].

7.1. Annexin A5

AnxA5 is a ~33 kDa protein that has been extensively studied during the past 20 years. Its 3-D crystalline structure was established already 20 years ago and revealed a predominant cluster of alpha-helices that define a hydrophilic pore through the center of the protein (121, 122). This pore was thought to serve as a Ca^{2+} channel in the MV membrane, even though it exhibited no transmembrane domains (123-125). AnxA5 is known to form triskelion arrayed trimers that bind to the surface of acidic phospholipid-containing bilayers (126-130). There

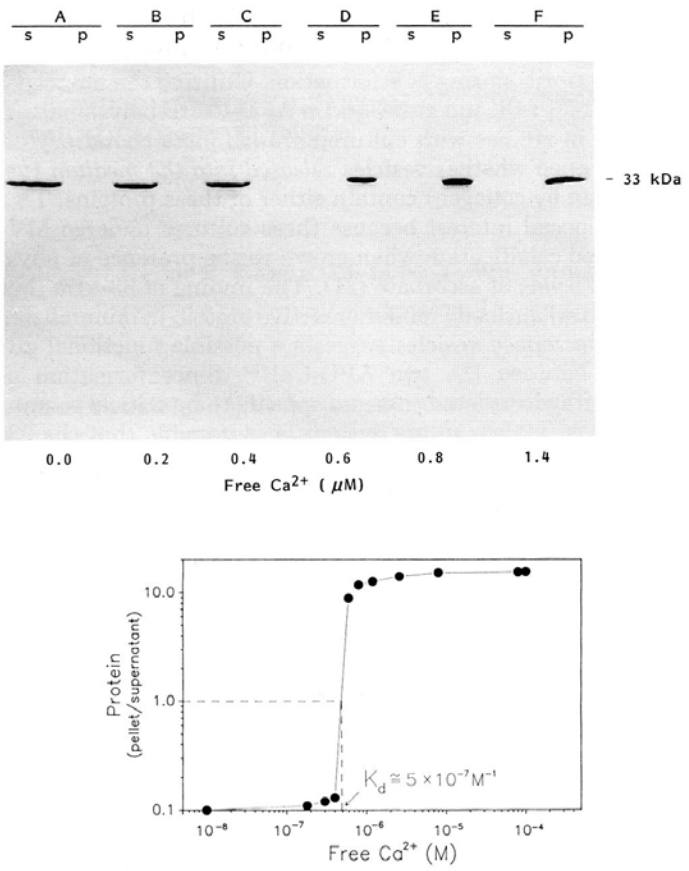

Figure 5. SDS-PAGE Gel Showing PS-Dependent Ca^{2+}-Binding Affinity of Annexin A5. Pure 33-kDa AnxA5 protein (70 micrograms/ml) was incubated for 20 min at 25 ºC in a mixture containing 10 mM Tris-HCl (pH 6.8), 140 mM NaCl, 4 mM EGTA, 1 mM DTT, 400 micrograms/ml PS, yielding 0–1.4 microM, *free* Ca^{2+}. After centrifugation at 130,000 x *g*, equivalent samples of each supernatant (s) and pellet (p) fraction were analyzed by SDS-PAGE (13% gel) and visualized using Coomassie Blue (upper panel). After destaining, gels were scanned using a Zeineh densitometer, the area under each peak being quantitated by integration (lower panel). Note that half-maximal binding of AnxA5 to PS occurred at a Ca^{2+} ion activity of 5 x 10^{-7} M. (This figure was originally published in (60) by the American Society for Biochemistry and Molecular Biology.)

is evidence that these trimers may be involved in the nucleational core of MVs and contribute to the ability of MVs to induce mineral formation (131). AnxA5 becomes exposed to the external surface of cells undergoing apoptosis (132-135), and as such has been used to monitor programmed cell death. More than any other protein so far studied, AnxA5 greatly accelerates the nucleational activity of the acidic phospholipid-Ca^{2+}-Pi complexes present in the nucleational core that triggers *de novo* calcium phosphate mineral formation in MVs (116, 131, 136). AnxA5 specifically overcomes the inhibitory effects of Mg^{2+} that otherwise greatly slow the induction of mineral formation (137). The key roles of AnxA5 in growth plate mineralization will be discussed later.

7.2. Annexin A6

AnxA6 is a genetically-fused double version of an ancient annexin with eight instead of four domains; it has a MW of ~68 kDa (138, 139). The crystal structure of AnxA6 has been determined (140) and reveals six Ca^{2+}-binding sites in AB loops analogous to the three present in AnxA5 (141). AnxA6 has been implicated in mediating endosome aggregation and vesicle fusion during exocytosis (142). Expression of AnxA6 in cells reduces cell proliferation (143) and thus may play that role in growth plate cartilage in the zones of maturation and hypertrophy where cell division ceases. Recent studies on calcification in vascular smooth muscle cells have shown that their MVs are rich in AnxA6 and AnxA2; they stimulate mineralization when associated with type I, but not type II collagen (144). Curiously, these vascular smooth muscle MVs had no AnxA5 present – in stark contrast to cartilage MVs. This recent study indicates that AnxA6 (and possibly AnxA2) may be important for adherence to type I collagen in smooth muscle calcification.

7.3. Annexin A2

Like other annexins, AnxA2 is a ~36 kDa Ca^{2+}-dependent phospholipid-binding protein abundantly present in MVs (94, 145). AnxA2 has been implicated in diverse cellular processes involving linkage of membrane-associated protein complexes to the actin cytoskeleton, *e.g.*

ion channel formation, and cell-matrix interactions (146). Another of its functions appears to be facilitating exocytosis of intracellular proteins to the extracellular domain (147). Studies by Hale *et al.* (69) reveal that dissociation of actin microfibrils from the cell membrane stimulates MV formation; AnxA2 has been implicated in the detachment of membrane plaques from actin filaments, leading to the formation of cell-surface blebs (148). The available data strongly suggest that AnxA2 is directly involved in the formation of MVs. Studies to date do not indicate that AnxA2 enhances cartilage MV mineralization (136, 145), although it is possible that it may enhance mineralization of MVs formed by vascular smooth muscle (144).

7.4. Annexin A1

AnxA1, also known as Lipocortin I, was found to be abundant in MVs by proteomic analysis (78). It has a molecular weight of approximately 40 kDa and preferentially localizes to the cytosolic face of the plasma membrane upon elevation of intracellular Ca^{2+} (149, 150). AnxA1 has inhibitory activity toward phospholipase A_2 (151, 152). Since phospholipase A_2 is required for the biosynthesis of the eicosanoid mediators of inflammation, prostaglandins and leukotrienes, AnxA1 has potential anti-inflammatory activity (151, 153). Glucocorticoids are known to stimulate production of lipocortin (153). Prostaglandins are known to be synthesized by growth plate chondrocytes (154). It is apparent that the presence of lipocortin (AnxA1) in MVs, and the cells that produce them, serves as a regulatory mechanism controlling the inflammatory process during growth plate development (155) – perhaps also being involved in regulation of angiogenesis and vascular invasion (156) after mineralization of the cartilage matrix.

7.5. Annexin A11 and Annexin A4

AnxA11 and AnxA4 are other members of the annexin family found by proteomic analysis to be a significant presence in MV (78). AnxA11 is a 56-kD protein that has been shown to interact with PDCD6 (Programmed Cell Death Protein 6), a Ca^{2+}-binding protein belonging to the penta-EF-hand protein family that participates in glucocorticoid-induced programmed cell death (157). Thus, AnxA11 appears to work in synergism with AnxA5 during the process of programmed cell death that appears to accompany MV formation. AnxA4 was also detected at low levels in the MV proteome. Its role in MV function is uncertain. The involvement of specific annexins in MV-mediated mineral formation will be discussed in more detail later in this review.

8. MATRIX VESICLE ENZYMES

A wide variety of enzyme *activities* have been found in MV; these fall into several general classes: phosphatases, nucleotide triphosphate pyrophospho-hydrolase, phospholipases, esterases, proteases and peptidases, and a wide variety of others. Forty years ago Ali *et al.* (52) upon successful isolation of MVs made a study of their constituent enzymes (53). This work indicated that MVs were highly enriched in TNAP, ATPase and pyrophosphatase activities. (However, it is important to note here that any enzyme that can hydrolyze ATP can be considered to be an "ATPase"; similarly any enzyme capable of hydrolyzing PPi is by definition a "pyrophosphatase". As will discussed later, these activities appear to result from only one enzyme – TNAP). MVs also exhibited several other phosphatase activities, but not acid phosphatase. Subsequent broader screening of MV enzyme activities in two independent studies using both collagenase-released (158) and non-collagenase-released, sucrose gradient-purified MV (56) observed that MVs did not exhibit significant activities of intracellular organelle-related enzymes such as NADPH-cytochrome c reductase (endoplasmic reticulum), succinate dehydrogenase, NADH-cytochrome c reductase and cytochrome oxidase (mitochondria), cathepsin D and β-glucuronidase (lysosomes). Additional studies described the activities of two ubiquitous enzymes, lactate dehydrogenase (159) and carbonic anhydrase (160) in isolated MV. On the other hand, very recent proteomic studies on MVs have detected the *physical presence* of a large array of enzymes, including small amounts of many cytosolic enzymes, as well as significant amounts of peptidases and amino transferases (78).

8.1. MV alkaline phosphatase

Special interest in alkaline phosphatase stems from the fact that as early as 1923 its activity was found to be associated with the mineralization process (161). Much later when MVs were established as sites of *de novo* mineralization, they were found to possess intense TNAP activity (52, 53). Recent proteomic analysis has shown that TNAP has by far the most dominant physical presence of any enzyme in MV [MS = 2549] (78). TNAP is one of four AP isozymes typically found in mammals. Unequivocal evidence that TNAP is directly involved in mineralization during skeletal development *in vivo* has come from recent gene knockout studies in mice (162, 163). Some have concluded that the primary function of TNAP is due to its pyrophosphohydrolase activity (164, 165); however, there is evidence that other aspects of its activity may contribute significantly to mineral formation.

8.1.1. Molecular structure

Like other vertebrate alkaline phosphatases, TNAP is a homodimer with a core protein molecular mass of ~57 kDa. It is now well established from genetic data that the human form contains 534 amino acids (166); and like other AP isozymes, TNAP is covalently attached to the outer membrane of cells and MVs by a glycosyl-phosphatidylinositol tether near the C-terminal end of the enzyme (167). TNAP is post-transcriptionally glycosylated at several sites with substantial levels of N-linked oligosaccharides to yield a glycoprotein with total molecular mass of ~80 kDa. The avian MV enzyme occurs in two different membrane-bound glycosylated forms of 77 and 81.5 kDa; these represent the 59 kDa protein core to which are attached either four or five 4.5 kDa N-linked oligosaccharides, respectively (59). These oligosaccharides form a shield that largely protects TNAP from proteolytic inactivation during MV isolation. These findings are consistent with earlier studies by Wu *et al.*

(59) and Hsu *et al.* (168, 169).

8.1.2. Amino acid sequence

MV-TNAP has not been directly sequenced; but the sequences of TNAP isozymes from various vertebrate species have been deduced from cDNAs. There is significant homology between *E. coli,* rat, human, and chicken TNAP, especially in the catalytic, metal-binding regions. There are differences in other regions of the enzyme. Between mammalian species, the sequences of TNAP have shown a high degree of identity (>90%); however differences between chicken cartilage and mammalian TNAP are such that antibodies to the mammalian TNAP only weakly cross-reacted with chicken cartilage isozyme; similarly, mammalian cDNA probes do not hybridize well with the avian cartilage form (59).

8.1.3. Three-Dimensional (3-D) structure

To date, this has not been determined; however, structures have been solved for the *E. coli* enzyme (170, 171), for human placental AP (172, 173) and some other APs. These studies reveal a compact, dimeric enzyme with four metal-binding sites in or near the catalytic region of each subunit. There are two Zn^{2+} ions and one Mg^{2+} at the catalytic site of each subunit, and a stabilizing Ca^{2+} ion located 10 angstroms from the active site (172). This Ca^{2+}-binding property of TNAP was foreshadowed by the much earlier observations of Stagni (174) and de Bernard *et al.* (175) who implicated this in the mineralization mechanism. Because of the heavy glycosylation of the vertebrate APs, no diffraction-quality crystals of the intact enzyme have been obtained. However, the intimacy between TNAP and the developing mineral phase during MV mineralization (76) underlines the importance of establishing the 3-D structure of the enzyme.

8.1.4. Disposition in MV membrane

Disposition of TNAP in membranes is key to understanding its function. Studies by Low *et al.* (167) revealed that AP is an ectoenzyme, covalently anchored to the plasma membrane by a glycosylphosphatidylinositol (GPI) linkage to the external lipid bilayer. TNAP can be selectively removed from the MV membrane by the action of a highly specific bacterial phospholipase C which attacks only this GPI link (66). Despite its external localization, AP is remarkably insensitive to protease attack because of the glycan "umbrella" previously described. Further, attachment of TNAP *via* its GPI-based anchor appears to facilitate mineral formation to an apatitic form indistinguishable from that produced by intact MVs (176). These findings are consistent with earlier work showing that activity of TNAP dies off in direct proportion to the extent of MV mineralization (76). This finding indicates an intimate, self-destructive physical association occurs between membrane-bound MV-TNAP and the mineral that is being formed.

8.1.5. Catalytic properties

The broad spectrum of phosphatase activity in MV, including pyrophosphohydrolase, is due primarily to that of TNAP (54, 177). These findings are in accord with earlier work by Moss *et al.* (178, 179) who found that TNAP possessed both pyrophosphatase as well as general phosphoesterase activity. MV TNAP has significant catalytic activity toward PPi and other phosphorylated substrates under extracellular conditions, as has been often demonstrated by studies that show enhancement of MV calcification when supplied with organic phosphate substrates (82, 180). Moreover, the finding that knockout of TNAP in mice gives rise to a distinct form of osteomalacia (181-183) directly confirms its physiological significance. However it is important to note that despite the lack of TNAP, normal mineral formation nevertheless occurred within the MVs – but it did not spread to the surrounding matrix (163). Coupled with the observation of the self-destructive physical association between TNAP and MV mineral formation (76), it is evident that TNAP is required for the progression of mineral from the MV lumen to the extracellular matrix.

8.1.6. Collagen-binding properties

MV-TNAP has been shown to bind with high-affinity to types II and X collagen (69, 95, 184). This is consistent with evidence that TNAP is localized on the external face of the MV membrane (66). Licia Wu found that when either type II or X collagen was incubated with intact MVs, each co-sedimented with the vesicles (75). Further, TNAP in detergent extracts of collagenase-released MV was found to bind tightly to columns of immobilized native type II or X collagen (95). A collagen-binding loop evident in 3-D TNAP structure appears to be responsible (185). Several other MV proteins also bind to type II and X collagens, but not to type I collagen – findings that help explain how MVs are attached to the cartilage extracellular matrix and facilitate the spread of mineral formation into the extravesicular matrix. Electron microscopic studies using freeze-quenching methods show that MVs are attached to the matrix by filamentous protein strands (40-42, 46).

8.2. Nucleotide pyrophosphatase/phosphodiesterase (NPP1, PC1)

Many studies have revealed the presence of NPP1 activity in MVs (165, 186-193). In fact, recent data indicate that the ATPase activity found in MVs can be largely attributed to TNAP and NPP1 (190,193). Recent proteomic analyses of MVs isolated from chicken embryo femurs have confirmed the presence of NPP1 [Mascot Score, 684], however, at only about one-fourth the level of TNAP (78). This ecto-enzyme hydrolyzes nucleotide triphosphates to produce nucleotide monophosphates + PPi *extracellularly*. There the released PPi would act as a HAP crystal growth inhibitor (194); however, being a substrate for TNAP it would be rapidly hydrolyzed (189). NPP1 accounts for nearly all the ecto-pyrophosphatase activity of chondrocytes (195) and the release of PPi is thought to provide a means for regulating apatitic mineral formation (194). More will be made of this in the discussion of the role of PPi in regulation of mineral formation. NPP1 is a type 2 membrane glycoprotein, a member of a small multigene family of nucleotide pyrophosphatase-/phosphodiesterases (196). It is a 240 kDa homodimer comprised of 2 disulfide-bonded 120 kDa subunits (197-198). NPP1 is expressed strongly in bone and cartilage,

but most notably in chondrocytes (165). It has been shown to possess both alkaline phosphodiesterase I (EC 3.1.4.1) and nucleotide pyrophosphatase (EC 3.6.1.9) activities (199). NPP1 also has been found to exhibit auto-phosphorylation activity, which inactivates its other two enzymatic activities (200, 201). It has been suggested that auto-phosphorylation, which occurs at low level ATP concentrations, is a regulatory mechanism preventing depletion of nucleotides when they are scarce.

8.3. PHOSPHO-1 (phosphoethanolamine/phospho-choline phosphatase)

PHOSPHO-1 is a recently identified phosphatase that exhibits enzymatic activity in MVs (202) and represents a significant amount of the protein present. Deduced by proteomic analysis, PHOSPHO-1 has a Mascot Score of [420], about one-sixth the level of TNAP (78). PHOSPHO-1 is a 267 amino acid, 29.7 kDa member of the haloacid dehalogenase (HAD) super family of Mg^{2+}-dependent hydrolases (203). The active site of PHOSPHO-1 has been shown by crystallographic and mutation analysis to consist of three aspartate residues at positions 32, 34 and 203 coordinated with Mg^{2+} (203). Because gene expression of PHOSPHO-1 is upregulated as much as 120-fold in mineralizing cells as compared to soft tissue cells, the enzyme is now thought to generate Pi within MV (204). Very recent (2010) studies suggest that inhibitors of PHOSPHO-1 can block mineralization of embryonic long bones of chicks, as assessed by alcian blue/alizarin red staining (205). This finding, coupled with the recent study indicating that inhibition of PHOSPHO-1 can block MV mineralization (203), suggest that PHOSPHO-1 is involved in long bone mineralization *in vivo*. It is therefore of interest to understand how this enzyme contributes, given the predominant activity of TNAP. The main substrates for PHOSPHO-1, phosphoethanolamine (PEA) and phosphocholine (PCho) are products of the action of phospholipase C on membrane phospholipids, phosphatidylcholine (PC) and phosphatidylethanolamine (PE) (206). Recent studies by Wu *et al.* have shown that the PE and PC content of MVs decreases rapidly during MV-mediated mineral formation, accompanied by an accumulation of 1,2-diacylglycerol and 1-monoacylglycerol (207). These findings present clear evidence that phospholipase C-dependent breakdown in MV phospholipids accompanies MV mineralization. Taken together, these findings reveal that combined actions of phospholipase C and PHOSPHO-1 release Pi (as well as ethanolamine and choline) from membrane phospholipids, making them available for use in biomineralization. Further, recent studies show that Pi uptake by mineralizing MVs is not strictly Na^{+}-dependent; Pi uptake is enhanced when $choline^{+}$ is substituted for Na^{+} (208). This will be covered in more detail in the section dealing with Pi uptake during MV formation.

8.4. Acid phosphatase

Several other MV phosphatases also have received significant attention in the past. In a 1995 review, Anderson cited studies that indicate several types of phosphatases: pyrophosphatase (PPiase), 5'-AMPase, nucleotide triphosphate phosphatase (NTPPase), as well as Ca^{2+}-ATPase (209) are present in MVs. While it is probable that PPiase and 5'-AMPase simply represent manifestations of TNAP, the activity of acid phosphatase is clearly separate. Early studies by Thyberg and Friberg (37) revealed the presence of acid phosphatase histochemically in MV. Subsequent biochemical studies by Ali (158),Watkins *et al.* (56) and Deutsch *et al.* (86) have detected modest levels in MVs. On the other hand, using Percoll fractionation, Vaananen separated acid phosphatase-containing from other MV (84). Thus some MVs contain acid phosphatase; it is perhaps those derived from lysosomal extrusion (46) as suggested by Thyberg and Friberg (37). The fact that proteomic analysis failed to detect acid phosphatase in mineralizing MVs from chicken cartilage (78) makes it doubtful that MVs containing acid phosphatase activity function in the induction of mineral formation.

8.5. Proteases and peptidases

The presence of peptidase (210) and protease (211) activities associated with MV have been confirmed by proteomic studies on MVs isolated from actively mineralizing chicken bones, showing a significant [MS = 1476] total level (78). This supports the concept that enzymatic degradation of the proteoglycan matrix of growth plate cartilage is important in facilitating mineral formation, an idea raised over 40 years ago (212, 213) prior to their discovery in MVs (214). These aminopeptidases, which exhibit activity toward a variety of synthetic peptides and amino acyl esters (210), are blocked by N-carbobenzoxylation. Such enzymes are commonly detected in plasma membrane fractions. In studies by Katsura *et al.* a neutral metalloprotease isolated from growth plate MVs readily degraded proteoglycans (211). It had a molecular mass of 33 kDa, a pH optimum of 7.2, and was latent within MVs until activated by detergents. The fact that the activity is latent has important physiological implications. It is probable that it becomes activated when the vesicle membrane ruptures after onset of apatite crystal formation. Thus, initiation of MV-induced mineralization becomes coupled with degradation of the inhibitory proteoglycan matrix. This concept will be developed further when the regulatory role of proteoglycans is discussed.

8.6. Lactate dehydrogenase and other glycolytic enzymes

Nearly 20 years ago studies by Hosokawa *et al.* (159, 215) documented the presence of lactate dehydrogenase (LDH) in isolated MV. While no other glycolytic enzymes were detected at the time, very recent proteomic studies have not only detected significant levels of LDH [Mascot Score = 855], but seven of the eleven glycolytic enzymes normally present in cells were also observed (78). In addition, several enzymes were found that pertain to the synthesis of the proteoglycans that are abundant in cartilage. These enzymes appear to be adventitious carryovers that occur during MV formation; thus, the abundant presence of LDH speaks of the relatively hypoxic state of growth plate chondrocytes prior to the time of MV formation (216).

8.7. Carbonic anhydrase

Carbonic anhydrase (CA) was first implicated in endochondral calcification by Cuervo in Howell's group nearly 40 years ago (217) in conjunction with studies on the pH and pCO_2 of the extracellular fluid. CA has since been observed in growth plate cartilage in two isozymic forms (218-220). CA isozyme II was notably present in the extracellular matrix of hypertrophic and calcifying cartilage, the locus of MVs. Sauer *et al.* (160) were the first to document CA activity in isolated MVs, observing levels comparable to those reported earlier for avian growth plate cartilage. Treatment of the isolated vesicles with acetazolamide, a CA inhibitor, delayed but did not prevent MV mineralization. Thus it is probable that CA modulates the activity of MVs, but may not to be absolutely essential for MV function.

8.8. Phospholipases

Observations on the lipid composition of growth plate cartilage (20) and MVs (30, 221) have provided evidence for the presence of significant phospholipase activity, even though none of these enzymes has been isolated physically. In MVs obtained from chicken growth plate cartilage, 10–15% of the total phospholipids are lysophospholipids, indicative of the presence of significant phospholipase A activity (29-31, 222). Clues regarding the nature of phospholipases in MVs come from studies on changes in lipid composition of growth plate chondrocytes during MV formation – as well as during induction of mineral formation by MVs. For example, depletion in PC and increase in lysophospholipids characteristic of MVs are already evident in microvilli from which MVs derive (73). Further, induction of mineral formation by MVs causes a progressive decline in phospholipid levels (207). This marked reduction is accompanied by the buildup of free fatty acids (FFA), 1,2-diacylglycerols (1,2-DAG) and 1-monoacylglycerols (1-MAG). The two phospholipids undergoing the most extensive hydrolysis during mineral formation were phosphatidylinositol (PI) and sphingomyelin (SM). PE and PC also were extensively degraded, but not as rapidly. These findings parallel those made with frozen-thawed slices of calcifying epiphyseal cartilage (223).

These studies lead to several conclusions. 1) The high levels of lysophospholipids present in growth plate cartilage and MVs provide direct evidence for the presence of phospholipase A (PLA) activity. 2) The progressive decline in PC and PE, coupled with the buildup of 1,2-DAG, provides evidence for the presence of phospholipase C (PLC) activity in MV (207). 3) The lack of accumulation of lysophosphatidylcholine (LPC) and lysophosphatidylethanolamine (LPE) during induction of mineral formation by MVs, coupled with the increase in 1-MAG, is evidence for the presence of lysophospholipase C (LPLC) activity. 4) The very rapid decline in SM reveals the presence of sphingomyelinase activity. 5) The extremely rapid decrease in the level of PI, without buildup of lysophosphatidylinositol (LPI), suggests degradation by PI-specific PLC activity. 6) The unique pattern of PS and lysophosphatidylserine (LPS) metabolism in which buildup occurs during MV mineralization points to active base-exchange PS synthase enzymes that transfer serine to LPE or PE to form LPS or PS. 7) Levels of phosphatidic acid (PA) in MVs are generally low, indicating low phospholipase D (PLD) activity (207); however, Balcerzak *et al.* recently describe phosphorylation-dependent PLD activity in MVs (224).

8.8.1. Phospholipase A (PLA)

PLAs represents a large class of typically small (13-14 kDa) Ca^{2+}-dependent enzymes that hydrolyze the *sn-1* or *sn-2* ester of glycerophospholipids to produce a fatty acid and a lysophospholipid (monoacyl phosphoglyceride) (225-226). PLA_1 causes the release of a free fatty acid from the *sn*-1 position of glycerol to produce 2-monoacyl phosphoglycerides; PLA_2 causes release of fatty acid from the *sn*-2 position of glycerol to produce 1-monoacyl phosphoglycerides. (Typically the fatty acid present in the *sn*-2 position is polyunsaturated and serves as a substrate for eicosanoid biosynthesis). Attempts to physically isolate the PLA enzyme present in growth plate cartilage have so far failed. However, characterization of its activity has met with limited success. MV-PLA activity is Ca^{2+}-dependent and is highly selective for intramembranous, as opposed to externally added phospholipid substrates – implying that it was an integral membrane protein (227). The enzyme had optimal activity at pH 8, displayed A_2 specificity, and hydrolyzed PC in preference to PE or other membrane phospholipids. Its properties resemble activities reported for PLA_2 activity isolated from human rheumatoid synovial fluid (229-230). Schwartz and Boyan (231-232) explored the effect of two vitamin D metabolites, 1,25-dihydroxyvitamin D_3 (1,25-$(OH)D_3$) and 24,25-dihydroxyvitamin D_3 (24,25-$(OH)D_3$) on the activity of PLA_2 in cultured chondrocytes. They found a marked enrichment in PLA_2 activity in MV, compared to the plasma membrane. Further, 1,25-$(OH)D_3$ at levels of 10^{-8} and 10^{-9} M significantly increased PLA_2 activity in MV, but not in the plasma membrane. Thus, vitamin D metabolites influence the activity of PLA_2 in growth plate chondrocytes. It is of further interest that the annexins act as PLA_2 inhibitors (233), protecting PS from degradation during MV formation by interfering with PLA_2 binding to PS (60, 151).

8.8.2. Phospholipase C (PLC)

PLC acts on glycerophospholipids to release 1,2-DAG and the phosphorylated polar head group of the parent phospholipid. There are two broad classes of PLC. One type rapidly hydrolyzes phosphatidylinositol 4,5 bis-phosphate (PIP_2) to produce 1,2-DAG and 1,4,5-inositol trisphosphate (IP_3) – products that are involved in transient receptor-mediated PI-cycle cell signaling (234-239). A slower acting PC-specific PLC has been shown to be involved in regulation of the cell cycle, cell division and apoptosis (240-245). PC-PLC acts on PC to produce 1,2-DAG and PCho. PC-PLCs from both rat (246) and human (247) fibroblast-like cell lines have been characterized. The human homolog is a 66 kDa enzyme that is directly involved in regulating the cell cycle in fibroblasts. It is upregulated by mitogens such as platelet-derived growth factor (PDGF). Although the action of PIP_2-specific PLC has been studied in chondrocytes (239, 248), there have

been no studies on PLC activity toward PC or PE, two far more abundant lipids in growth plate cells and MV. Breakdown of MV lipids during *in vitro* calcification causes progressive buildup of both 1,2-DAG and 1-MAG, findings indicative of the presence of PLC and lysophospholipase C (LPLC) activity, respectively (207). While neither enzyme has been characterized in growth plate chondrocytes, PC-PLC and PE-PLC have been extensively studied in other tissues where they appear to be involved in cellular proliferation (249-250). In view of the rapid cell division that occurs in the proliferative zone of growth plate cartilage, it is not surprising to see evidence of PLC activity in MVs. The recent finding that PHOSPHO1 targets hydrolysis of PEA and PCho, two specific products of PLC action on PE and PC, respectively, reveals a direct connection that appears to contribute to the function of MV in inducing mineral formation.

8.8.3. Lysophospholipase C (LPLC)

One of the enigmas observed during incubation of growth plate cartilage slices, or of MVs during induction of mineral formation, was the finding that despite the significant loss of PC and PE, there was little concomitant *accumulation* of LPC or LPE (207). While this might be explained by the presence of the alternative PC-PLC or PE-PLC pathway, the extent of accumulation of 1,2-DAG was not sufficient to explain the loss of these lipids. On the other hand, the obvious accumulation of 1-MAG during MV mineralization provides a more plausible alternative explanation – namely the presence of LPLC activity. Recently, a study of the ubiquitous NPP family of ectoenzymes, of which the previously described PC-1 (NPP1) is a member, reported the presence of additional family members, NPP2, NPP6 and NPP7 (251). These family members, rather than attacking nucleotide phospho-diesters, attacked lysophospholipids. NPP6 had activity toward LPC with polyunsaturated acyl chains. It also hydrolyzed sphingosylphosphocholine (SPC), the lyso form of sphingomyelin (SM) (251). The products of PC-LPLC (NPP6) action on LPC are PCho + 1-MAG; those on SPC are PCho + sphingosine; action on GPC yielded PCho + glycerol. Thus, NPP6 specifically cleaves the P–O bond opposite the choline residue. The significance of NPP6 to MV lipid metabolism is that it would provide a mechanism for further degradation of PCho resulting from breakdown of both PC and SM present in MVs. And as noted before, PCho is a preferred substrate for PHOSPHO1 and would release Pi needed for supporting mineral formation.

8.8.4. Sphingomyelinase (SMase)

SM is specifically enriched in MVs compared to the plasma membrane of growth plate chondrocytes from which they derive (73). However, SM is also one of the lipids most rapidly degraded when MVs are incubated in synthetic cartilage lymph and allowed to mineralize (207). This indicates that a highly active SMase must be operative during MV mineralization. SMases hydrolyze SM to ceramide (N-acyl sphingosine) and PCho. Since the pH of the MV incubation was 7.5, it can be assumed that the activity observed is from one of the neutral SMases (nSMase). In fact three distinct nSMase isoforms have been identified: nSMase-1, -2, and -3; they differ in subcellular localization, tissue specificity, and enzymatic properties (252-253). A likely candidate for the MV enzyme is nSMase-2, a Mg^{2+}-dependent isozyme, localized to the plasma membrane (254-257). Its activity is enhanced by phosphatidylserine (PS) (258), a lipid specifically enriched in the MV inner leaflet (259). nSMase-2 is also known to be localized to the inner leaflet of the plasma membrane (260-261). Upregulation of nSMase-2 has been shown to cause arrest of the cell cycle in the G0/G1 phase (262); upregulation of nSMase-2 is also associated with programmed cell death (263). Based on gene sequencing, nSMase-2 is now known to be identical with sphingomyelin phosphodiesterase-3 (SMPD3). Two independent studies have shown that knockout of the SMPD3 gene in mice causes skeletal defects: chondrodysplasia and dwarfism (264) or osteogenesis and dentinogenesis imperfecta (265). These findings may relate to the role of nSMase-2 in MVs. Features most directly relevant to MV mineralization are: 1) its product, PCho, is a key substrate for PHOSPHO1, a MV enzyme that releases Pi into the vesicle lumen; and 2) that breakdown of SM would help destabilize the MV membrane and facilitate outgrowth of mineral from the vesicle lumen into the extracellular matrix.

8.8.5. Other MV phospholipases

As noted above, PI is very rapidly degraded during the onset of MV mineralization (207); after only 4 h incubation 80% of the PI is lost. This loss is not accompanied by any increase in LPI, suggesting that PI may be degraded by a PI-specific PLC activity.

8.9. Phosphatidylserine synthases

Based on changes that occur in the levels of phosphatidylserine (PS) during MV mineral formation, there must be unique pathways for metabolizing this important lipid. PS binds to Ca^{2+} and Pi to form lipid-Ca^{2+}-Pi complexes (266) with the ability to rapidly nucleate hydroxyapatite (HA) mineral formation when incubated in synthetic cartilage lymph (SCL) (137). During MV mineralization, after initial rapid and almost total loss of non-complexed PS, the levels of PS, and its LPS form, progressively increased during the remainder of the incubation period and were largely complexed with the newly forming mineral (207). These are remarkable findings. The only plausible explanation for this increase is the presence of the non-energy-dependent, Ca^{2+}-dependent, base-exchange mechanism of PS-synthase previously noted in growth plate cartilage (267) and MVs (268). The free amino acid, serine, undergoes Ca^{2+}-dependent exchange with either the ethanolamine group of PE, or the choline group of PC, to form PS (269). ATP is not required for this reaction. Normally, PS is synthesized in mitochondria-associated membranes by action of either of two PS synthases that cause exchange of serine for choline (PS synthase-1) or for ethanolamine (PS synthase-2) (270). It is probable these PS synthases become incorporated into the plasma membrane upon transfer of Ca^{2+} (and Pi) during MV formation (8, 271-275). PS synthases are ~56 kDa, multi-pass integral membrane proteins (276-279) that could be transferred directly to the MVs. That this actually occurs is evident from the fact that

[^{3}H]serine is incorporated into PS of isolated MVs; it occurs by a mechanism that requires Ca^{2+}, but not nucleotide triphosphates (268). This provides a plausible explanation for the ~5-fold enrichment of PS in MVs compared to the cells from which they derive (29, 30). Intraorganelle transport of PS, known to occur in all cells (280), also helps explain how PS synthesized in mitochondria-associated membranes becomes transferred to the plasma membrane and ultimately to MVs.

8.10. Phospholipid flippases and scramblases

Flippases are P-type ATPases that mediate the unidirectional "flipping" of PS from the outer leaflet of the plasma membrane to maintain the asymmetric transbilayer distribution of PS (281). On the other hand, scramblases are enzymes responsible for the bidirectional translocation of phospholipids between the two leaflets of the lipid bilayer of cell membranes (282-284). Scramblases are activated by Ca^{2+}, do not require ATP for activity, and tend to randomize the distribution of PS in the bilayer (285). In humans, phospholipid scramblases constitute a family of five homologous proteins. In normal cells, the inner-leaflet facing the inside of the cell contains negatively-charged PS and neutral PE; the outer-leaflet, facing the extracellular environment, contains PC and SM. Scramblases transport negatively-charged phospholipids from the inner-leaflet to the outer-leaflet, and vice versa; thus, they have the capacity to randomize the sidedness of phospholipids in membrane bilayers (286). A recent report describes phospholipid scramblase activity in growth plate chondrocytes indicating its association with TNAP-containing lipid rafts during MV formation (287). Since PS is an integral component of the nucleational complex that triggers mineral formation by MVs (288), exposure to the extravesicular fluid could be a key event that enables the newly formed crystalline mineral to propagate into the extracellular matrix. Failure to do this is an apparent feature in the TNAP knockout mouse; the paradoxical finding is that while mineral forms normally within the MVs, it does not become externalized (289). Taken with the finding that scramblase is associated with TNAP in the cell membrane, externalization of newly forming mineral in MVs must require the presence of TNAP – as well as scramblase activity. The only study in which the sidedness of the two key amine-containing phospholipids, PS and PE, has been analyzed in the MV membrane revealed that *ca.* 80% of the PS remains localized within the MVs, whereas 50% of the PE was external (259). The fact that PS in MVs remains largely internal is significant because one of the signal features of cellular apoptosis is the externalization of PS to the outer leaflet (132, 290). Hence, MVs are not typical apoptotic bodies. The PS-Ca^{2+}-Pi complexes formed during MV construction resist scramblase activity because the complexed calcium phosphate stabilizes the membrane.

9. MATRIX VESICLE MEMBRANE SURFACE RECEPTORS AND TRANSPORTERS

9.1. Cell Surface receptors

Proteomic analysis of isolated MVs also revealed the presence of numerous cell surface receptors, but none would be considered to be quantitatively major proteins (78). The most abundant receptor was CSG-HT7 [Mascot Score = 521], a cell surface glycoprotein known to be associated with the ingrowth of vascular endothelial cells (291-292). It is probable that the presence of this MV protein serves as part of an angiogenesis signal, once mineralization of the cartilage matrix has occurred. The next most abundant cell surface protein [Mascot Score = 433] was CDON, a cell surface receptor of the immuno-globulin (Ig)/fibronectin type III repeat family; however, its specific function has not been elucidated (293-294). Numerically, the most well represented receptors in avian MVs were the four integrins: alpha-5, beta-1, alpha-3, and beta-5, which were detected at [Mascot Scores] of 369, 337, 169, and 71, respectively. These integrins undoubtedly facilitate anchoring of the MVs to the extracellular matrix collagens (295-300). Another receptor, CD36, [Mascot Score 131], is an integral membrane protein found on the surface of many vertebrate cell types. It is a member of the class B scavenger receptor family of cell surface proteins that bind to many ligands including collagen. It has been shown very recently to be a pattern recognition receptor in hypertrophic chondrocytes (301). CD36 may function in opsinization of MV remnants during chondroclastic resorption of calcified cartilage at the time of replacement by cancellous bone. All of these receptors appear to be vestiges of the plasma membrane of the hypertrophic chondrocytes; they appear to function in growth plate development rather than in MV mineralization *per se*.

9.2. ATP-driven ion pumps and transporters

Many different transporters were detected in the proteome of MVs. They ranged in abundance from Mascot Scores [MS] of 619 down to 68. All appear to represent porters present in the plasma membrane of the chondrocytes from which the MVs derived. Of the 23 transporters detected, the most abundant, quantitatively, were five **Na^+/K^+ ATPases** (alpha-1, [MS – 619], alpha-2, [MS – 397], beta-3, [MS – 193], beta-1, [MS – 127], and beta-2, [MS – 96]), and three **H^+-ATPases** (subunit B, [MS – 248], subunit A, [MS – 271], and subunit S1, [MS – 94]). To be active in MVs, these ion pump ATPases would require the presence of ATP, which could arise only from synthesis by the parent chondrocytes. However, the levels of ATP in MVs are very low (302) and are insufficient to drive Na^+ extrusion and K^+ uptake. This is borne out by direct analysis of the electrolytes of MVs, which were found to be much richer in Na^+ than K^+ – the opposite of what occurs in the cells from which they derive (63). Thus, although abundant, it is apparent that these ATP-driven ion pumps do not support ion transport activity in MVs. Also notably abundant was a **choline transporter** [MS – 409], which may have important activity in conjunction with the product of the PHOSPHO-1 enzyme that hydrolyzes P-choline and P-ethanolamine to Pi and their respective bases (193, 202). It is noteworthy that choline has been found to be a better co-substrate for Pi uptake by MVs than was Na^+ (208, 303).

9.3. Channel proteins and solute-carrier transporters

Three significantly abundant ion channels were detected by proteomic analysis of MVs. Of special interest

was TRPV4 [MS – 350], a transient potential cation channel that appears to be important in regulation of osmotic pressure (304-305). In the maturing growth plate chondrocytes, the presence of TRPV4 very likely has an important function in the major osmotic swelling that occurs upon hypertrophy when cell volume expands over 9-fold going from the proliferating to the hypertrophic state (306). Also of interest are CLIC4 [MS – 359] – the Channel 4 intracellular Cl^- transporter (307-309); this channel protein transports Cl^- in exchange for HCO_3^- (310-311), and appears to be important in buffering the internal pH of MVs. The third is VDAC-2, [MS – 381] – the Channel 2 voltage-dependent anion-selective channel present in the mitochondrial outer membrane (312-313). This channel may play a part in the mitochondrial permeability transition pore that becomes activated prior to formation of MVs by hypertrophic chondrocytes (314). Although the Mascot Score of VDAC-2 is not large, it may represent a mitochondrial outer membrane protein incorporated into MVs. The most numerous of all the transporters detected by proteomic analysis of isolated avian growth plate MVs were the solute-carrier family (SLC-family). In total nine different SLC carriers were detected. The most abundant was SLC 16A1 [MS – 283], a transporter known to transport lactate, pyruvate and other monocarboxylates in the plasma membrane of many cell types (315-316). Other members of the SLC family are transporters for neutral amino acids (SLC38A3, [MS – 176]), alanine/serine/cysteine/threonine (SLC1A4, [MS – 90]), organic cations, *e.g.* carnitine (SLC22A16, [MS – 177], glycine (SLC6A9, [MS – 137]), Na^+-dependent citrate (SLC13A5, [MS – 96]), Na^+-independent cationic amino acids (SLC7A3, [MS –74]), and equilibration of nucleosides (SLC29A1, [MS – 71]). Each of these carriers are of undoubted importance during the proliferation of the growth plate chondrocytes, but probably have only minor effects on the activity of released MVs. They appear to be carryovers from the plasma membrane of the chondrocytes. However, within the SLC families of carriers, of special interest to MV function are two Zn^{2+} transporters – SLC39A14, [MS – 80] and SLC39A8, [MS – 79]. Zn^{2+} is remarkably abundant in MVs (317) and it is possible that these carriers are involved in its uptake, most likely into the chondrocytes before MV formation.

9.4. Ca^{2+} channel proteins

Several types of Ca^{2+} channels are differentially expressed in growth plate chondrocytes. In early stages of growth plate development, Ca^{2+} channels of the L-type are evident; however as the calcification front is approached, the putative AnxA5 type of channel becomes dominant. While there is no evidence for L-type Ca^{2+} channels in MVs, as noted earlier, AnxA5, AnxA2 and AnxA6 – some of the most dominant proteins in cartilage MVs – may serve that function, although recent data render this unlikely. This is because AnxA5 failed to support Ca^{2+} uptake in liposomes modeled after MVs, and which readily acquired Ca^{2+} when treated with several Ca^{2+} ionophores (318).

9.4.1. L-Type Ca^{2+} channels in growth plate chondrocytes

Studies in the early 1990s indicated that L-type voltage-dependent Ca^{2+} channels are operative in growth plate chondrocytes (319-320); this was initially based on their response to various benzothiazepines that selectively block L-type Ca^{2+} channels. Their presence was later confirmed using immunostaining with antibodies to the alpha subunit, revealing that they are expressed at all stages of the growth plate (321). These channels appear to participate in chondrocyte proliferation and early differentiation. The alpha-1 subunit of L-type Ca^{2+} channels mediates influx of Ca^{2+} into cells upon membrane polarization (322-323). This subunit contains 24 transmembrane segments that form a highly selective pore through which Ca^{2+} passes into the cell (324-325). The structure of L-type Ca^{2+} channels is highly complex and consists of alpha-1, alpha-2/delta, beta, and gamma subunits in a 1:1:1:1 ratio (326). In resting zone chondrocytes, combined activities of L-type Ca^{2+} channels (327) and Ca^{2+}-ATPase (328) appear to maintain *mean* intracellular Ca^{2+} activity at around 50 nM; however, as the cells proliferate and approach the zone of hypertrophy, *average* basal Ca^{2+} levels rise to >100 nM (329). Confocal *in situ* imaging of proliferating chondrocytes in slices of PBS-bathed tibial growth plate tissue reveal dynamic fluctuations in Ca^{2+} activities in different regions of the cell (306). However, L-type Ca^{2+} channels would not be operative in MVs; they lack the voltage differential needed to drive Ca^{2+} uptake.

.

9.4.2. Annexins as Ca^{2+} channels

As alluded to earlier, SDS-PAGE analyses and initial characterizatoin by Genge *et al.* revealed that the dominant proteins in MVs isolated from growth plate cartilage were AnxA5, AnxA2 and AnxA6 (60, 61). AnxA5 was shown to be progressively and powerfully expressed in growth plate cartilage (Figure 6) (94); cells in the proliferative zone scarcely expressed the protein. Maximal expression was seen in the hypertrophic zone where MV formation is most active. Studies by Arispe *et al.* were the first to provide apparent evidence that AnxA5 exhibits Ca^{2+} channel activity when inserted into acidic phospholipid bilayers (125) – behavior predicted by Huber, based on the hydrophilic pore in its crystal structure (123) – but the experimental conditions required were not physiological. Eight years later, studies by Kirsch *et al.* confirmed elevated expression of AnxA5 in hypertrophic chondrocytes (330); they subsequently suggested that AnxA5-mediated Ca^{2+} influx may regulate growth plate hypertrophy and apoptosis (331). However, in studies using large unilamellar liposomal models of MVs designed to demonstrate under physiological conditions that AnxA5 exhibits Ca^{2+} channel activity, AnxA5 failed to support significant Ca^{2+} uptake (318). So far, only under artificial *in vitro* conditions does AnxA5 appear to exhibit Ca^{2+} channel activity. Its primary function appears to be in the nucleational core that enables MVs to induce mineral formation (288); incorporation of AnxA5 markedly accelerates the onset of mineral formation (131, 136, 332).

Figure 6. Immunolocalization of Annexin A5 in Chicken Growth Plate Tissue. Growth plate cartilage was fixed in Bouin's fixative (25 ml formalin, 5.0 ml glacial acetic acid, and 75 ml saturated picric acid) for 24 h at 4 ºC, washed three times with 50% ethanol, and then embedded in paraffin and 4 microM sections cut. Deparaffinized sections were incubated with rabbit anti-chicken 33 kDa annexin antibody diluted 1:100 in phosphate-buffered saline solution containing 3% bovine serum albumin for 2 h, washed three times over 30 min in phosphate-buffered saline, and then incubated with Fluorescein (FTIC) conjugated goat anti-rabbit IgG (ICN Biochemicals, Costa Mesa, CA) for 1 h and washed as before. Control sections were incubated with diluted rabbit preimmune serum and processed as before. Sections were viewed and photographed using a Zeiss model Photo-Microscope III epifluorescence microscope. Note that AnxA5 is almost undetectable in the proliferative zone of the growth plate (top), but progressively increases from the zone of maturation to the zone of hypertrophy and calcification, and reaches a maximum at the calcification front marked by vascular penetration. (Reproduced from (89) with permission of John Wiley and Sons, publishers.)

9.5. Inorganic phosphate (Pi) transporters

Uptake of Pi by all living cells is essential for survival and growth, inasmuch as phosphate is essential for synthesis of DNA, RNA, as well as all nucleotides involved in cellular metabolism and replication. In the "housekeeping" functions of vertebrate cells, Pi transporters use an inwardly directed electrochemical Na^+ current to support Pi influx. This Na^+ gradient, produced by the action of a Na^+/K^+ ATPase in the plasma membrane, carries Pi into living cells. However in MVs, Na^+ levels are as high as that of the extravesicular fluid (63); thus there is no Na^+ gradient to drive Pi uptake.

9.5.1. Na^+-dependent Pi transporters

In vertebrates, two unrelated families of Na^+-dependent transporters carry out general Pi transport. Remarkably, they transport different Pi species: divalent HPO_4^{2-} is carried by type II Na^+/Pi cotransporters; monovalent $H_2PO_4^-$ is carried by type III (PiT-1) Na^+/Pi cotransporters (333). Montessuit *et al.* were the first to study Pi transport in MVs (334). In MVs isolated from cartilage of mildly rachitic chickens, Pi uptake appeared to be a saturable process that could be driven by establishing an artificial Na^+ gradient (334). It appeared that Pi uptake in both MVs and chondrocytes was Na^+-dependent (334, 335). Subsequent studies by Guo *et al.* have confirmed the presence of a type III Na^+/Pi transporter using PCR analysis of RNA isolated from normal chicken tibial growth plate cartilage (336). This Pi transporter is a close homolog of human PiT-1 (Glvr-1, type III Na^+/Pi porter) showing 77% sequence identity. It appears to be a 73.5 kDa MW integral membrane protein with 12-transmembrane domains. However, *in situ* hybridization revealed that this Na^+-dependent PiT-1 Pi porter was only expressed strongly in the resting and proliferating zones; it was barely present in the hypertrophic zone (Figure 7B) (336). Subsequent studies on MVs isolated from normal chick growth plate cartilage showed that Pi transport was not strictly Na^+-dependent. Substitution of Li^+ or K^+ for Na^+ had minimal effect on Pi uptake; N-methyl D-glucamine (NMG^+) was totally inhibitory, whereas choline$^+$ was clearly stimulatory (208). Several known inhibitors of Pi transport were also used in this study. As controls, several putative intermediates in the MV mineralization pathway – ACP, PS-Ca^{2+}-Pi complex (PS-CPLX) and HAP – were studied. When incubated in synthetic cartilage lymph (SCL) matched in electrolyte composition and pH to that of the native fluid, PS-CPLX and HAP caused almost immediate uptake of Pi; pure ACP required ~1 h; but MVs displayed rapid Pi uptake only after ~3 h incubation. Phosphonoformate (PFA) delayed the onset and rate of Pi uptake by the MVs with an IC_{50} of 3–6 microM; however, it also inhibited Pi uptake by the mineralization intermediates with only slightly higher IC_{50}'s of 8.5–14 microM. Thus, PFA proved not to be a specific Pi transport inhibitor. While Na^+ substitutions had minimal effect on HAP or CPLX-seeded mineral formation, with ACP, NMG^+ totally blocked and choline$^+$ stimulated mineralization, just as with MVs. Thus, ACP appeared to mimic MV Pi uptake.

9.5.2. Na^+-independent Pi transporters

Studies on confluent, primary cultures of normal growth plate chondrocytes also detected a second type of

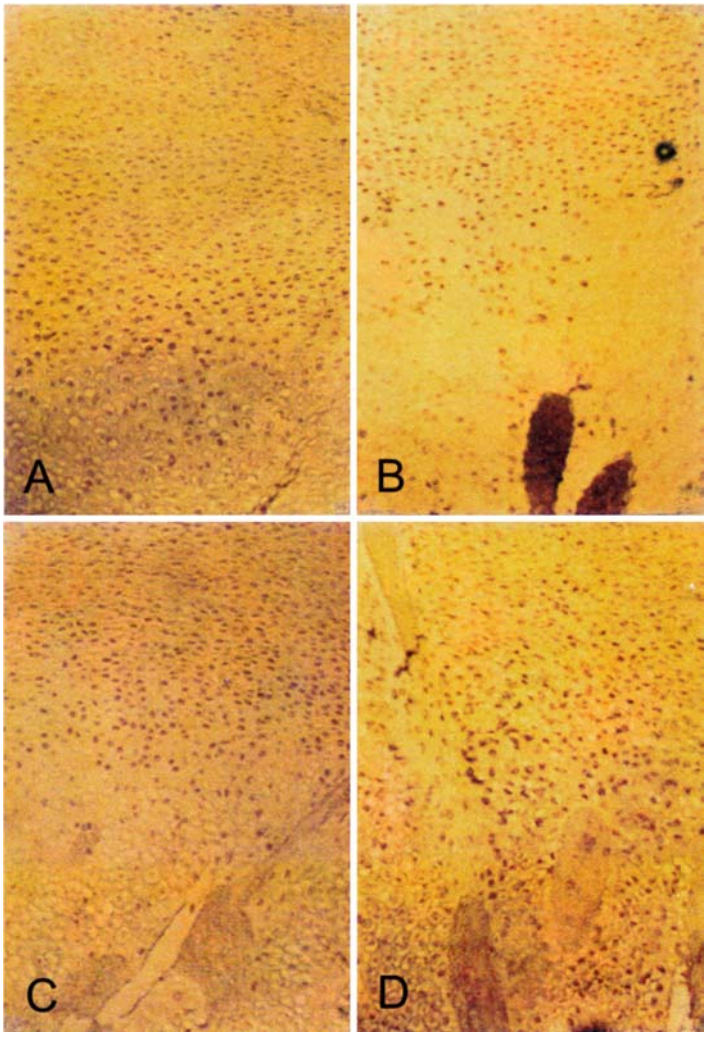

Figure 7. *In situ* Hybridization Evaluation of the Expression of Chondrocyte Pi Transporters in Different Zones of the Avian Growth Plate. The procedures used were as described by Guo (337). In brief, longitudinal samples from the proximal tibial epiphyseal cartilage from six-week-old chickens were obtained, fixed, decalcified, embedded in paraffin, and sectioned (6 microns) and mounted on glass slides. After rehydration, tissue sections were treated with proteinase K and washed with 3% H_2O_2 to inactivate endogenous peroxidase activity. For hybridization, the mounted tissue sections were treated with prehybridization buffer and then incubated with biotin-labeled primers synthesized by Invitrogen, with the following sequences: Collagen II: 5'-Biotin-CGGGGCCCTTCTCCGTCTGACCCAGT-3'; Collagen X: 5'-Biotin-GTGTGGTGGCCCCTTGATGCT-GGA-3'; PIC18: 5'-Biotin-CCTAAGATGGCGGCGGGGCGCACGC-3'; PiT type III (Glvr13): 5'-Biotin-GGTGCCACG-5TCGCCCGTGCGATAGACC-3'; Poly d(T): 5'-Biotin-$(T)_{20}$-3'. The biotin-labeled probes were denatured at 95 ºC, diluted in prehybridization buffer, and applied to the tissue sections and allowed to hybridize at 37 ºC overnight, care being taken to prevent evaporation. As negative controls, slides were incubated in the hybridization solution without probes; for positive controls a poly d(T) biotin labeled probe was used. For visualization, slides were incubated with biotinylated horseradish peroxidase in PBS and incubated for 30 min at 37 ºC. Following washing, 3'3'-diaminobenzidine tetrahydrochloride (DAB) was used for color development. The slides were rinsed with distilled water, mounted in glycerol gelatin (Sigma), viewed, and photographed using a Zeiss photomicroscope. 7A – Mitochondrial PiC phosphate transporter; 7B – Plasma membrane type III (Glvr) phosphate transporter; 7C – Collagen type II, and 7D – Collagen type X. Note in 7A that the highest level of mitochondrial PiC expression is in the hypertrophic zone, although low levels of expression were evident in the upper zones. Also notice that at the base of the hypertrophic zone where the cells have become apoptotic, that the mitochondrial PiC transporter is no longer expressed. In 7B, note that the highest levels of expression of the Na^+-dependent plasma membrane type III Pi transporter were in the upper (resting and proliferating) zones, with almost no expression in the lower (hypertrophic and calcified) zones. As positive controls, in 7C, note that collagen type II expression was high in the resting and proliferating zones – as expected, but was almost totally absent in the hypertrophic and calcified zones. In contrast, in 7D, note that the expression of collagen type X was weak in the proliferating zone, but intense in the hypertrophic and calcified zones – as expected. (Reproduced from (336) with permission from Yande Guo.)

Pi transport activity, expressed shortly before the onset of mineralization (303, 336). While the Na^+-dependency of Pi uptake early in cultures of the chondrocytes was confirmed, a different Na^+-*independent* Pi transporter was expressed as the cells approached hypertrophy. In contrast to Na^+-dependent Pi transporters whose activity is upregulated by Pi insufficiency (337, 338), this porter was upregulated by elevated Pi levels typical of the extracellular fluid of growth plate cartilage. The activity of this Na^+-*independent* Pi transporter was Cl^-dependent; but Cl^- was not co-transported (336). It had a slightly alkaline pH optimum (7.6–8.0) appropriate for the pH of growth plate extracellular fluid (63, 339). $Choline^+$ was nearly as effective as Na^+ as a co-substrate (336). The apparent K_m for Pi was 0.59±0.01 mM; its V_{max} was 0.99±0.01 nanomoles/mg protein/min. (For comparison with non-calcifiable cells, Pi uptake by Chinese hamster ovary cells tested under identical conditions had an apparent K_m for Pi of 0.046 mM and a V_{max} of 0.34 nano-moles/mg protein/min.) The activity of this Pi porter appears to represent the Na^+-independent action of the mitochondrial PiC transporter that is active when mature growth plate chondrocytes load large amounts of Ca^{2+} and Pi prior to the onset of growth plate mineralization. Support for this concept comes from the finding that the mitochondrial PiC Pi transporter is strongly up-regulated in hypertrophic chondrocytes, the opposite of the Na^+-dependent PiT-1 plasma membrane Pi transporter (Figure 7A) (336). This will be discussed further when MV formation is considered.

10. MATRIX VESICLE REGULATORY PROTEINS

About a dozen proteins involved in regulation of chondrocytes were found by proteomic analysis to be present in significant levels in MVs (78). While it can be assumed that these proteins are carry-overs from the cells that formed the MVs, they do not appear to exert a major effect on mineral formation. However, some appear to be involved in the formation of MVs.

10.1. Syntenin

The most abundant regulatory protein identified in MVs was syntenin [MS – 1158], a protein that links syndecan to the cytoskeletal protein, actin (340-341). Studies have shown that syntenin, syndecan, and actin co-localize to filamentous cell process in endothelial cells (342-343); these short cellular "villi" are closely analogous to those seen in freeze-fracture images of growth plate chondrocytes (50). However, there have been no studies to date on the role of syntenin in growth plate development. Early studies showed that drugs that disrupt actin filament formation clearly enhance release of MV in growth plate chondrocyte cultures (69, 73). On the other hand, syndecan-3, a cell-surface heparan sulfate proteoglycan that binds to syntenin, appears to play an important role in chondrocyte proliferation (344-345). Syntenin is a 32 kDa cellular PDZ-containing adaptor protein (346) that binds to the cytoplasmic domains of the vertebrate syndecans; its binding to syndecan requires the cooperation of both PDZ domains of syntenin (346). Syndecans act as co-receptors involved in docking of heparin-binding growth factors and adhesion molecules (348). Of special interest to MV formation, the development of cell membrane protrusions requires dephosphorylation of tyrosine residues in syndecan-1 (349). Apparently, at the tip of these processes, syntenin binds to syndecan, which in turn binds to type VI collagen in the extracellular matrix (348), leaving MVs attached at the points of contact. It is likely that additional matrix proteins (*e.g.* fibrillin, versican or proteoglycan link proteins), as well as the integrins, are also involved in MV formation.

10.2. G_i Protein, alpha-2

The alpha-2 subunit of G_i protein is a heterotrimeric subunit that inhibits the production of cAMP from ATP. Gi-alpha-2, with a proteomic score [MS – 660] appears to occur in significant abundance in MVs (78). In the cellular environment of growth plate cells, the function of G_i-alpha-2 is mainly to suppress cAMP dependent pathways by inhibiting adenylate cyclase activity, decreasing the production of cAMP from ATP. In turn, this would result in decreased activity of cAMP-dependent protein kinases (350). Thus, the ultimate effect of G_i is the opposite of cAMP-dependent protein kinases. In the cell, G_i protein also appears to play a role in activation of the phospholipase C pathway (351, 352). Considering its relative abundance in MVs, Gi-alpha-2 may well be important in activating the phospholipase C activity responsible for the breakdown of the MV phospholipids (PC and PE) that occurs during MV mineralization (207). (See discussion of MV phospholipases, Section 7).

10.3. Tyr/Trp mono-oxygenase activation proteins, etc.

The theta and beta subunits of the mono-oxygenase activating protein are relatively abundant in MVs, [MS – 725] and [MS –307], respectively. They are protein kinases that enhance the activity of Tyr/Trp hydrolases that would lead to the formation of serotonin and Dopa in GP chondrocytes. These gene products belong to the 14-3-3 [MS – 539] family of proteins that mediate signal transduction by binding to phosphoserine-containing proteins. This highly conserved protein family is found in plants and mammals. These enzymes appear to be carryovers from the plasma membranes of the chondrocytes that form MVs.

11. CYTOSKELETAL PROTEINS

Cytoskeletal proteins have been repeatedly implicated in the formation of membrane-derived vesicle-like structures in a variety of systems, including red blood cells, intestinal brush border cells, liver cells, and a number of other cell types (353-355). Actin was first identified as a constituent of MVs in 1982 by Muhlrad (92). Actin was subsequently implicated in MV formation by studies on primary cultures of growth plate chondrocytes showing that agents affecting the stability of actin microfilaments significantly altered MV formation (69). Cytochalasin D, a fungal metabolite that causes depolymerization of actin microfilaments greatly enhanced MV formation. In contrast, phalloidin, an agent that stabilizes actin

microfilaments, significantly decreased MV formation. Another drug, colchicine, which destabilizes microtubules, also stimulated the release of MVs. In an earlier study, Hale showed that the localization of cytoskeletal proteins in cultured growth plate chondrocytes indicated that both microtubules and microfilaments were involved in the formation of cell processes from which MV were shown to derive (68). Subsequent studies, in which the enzyme, protein, and lipid composition of chondrocyte microvilli and MVs were compared, indicated that vesicles must derive from these structures. Twenty five years later, proteomic analysis of MVs confirmed that numerous cytoskeletal proteins are present in collagenase-released MVs from embryonic chick femoral cartilage (78). Of these, by far the most abundant was beta-actin [MS = 1139]. Among other cytoskeletal proteins detected were: filamin B, beta [MS – 398], actinins alpha-1 and -4 [MS – 698], tubulins beta-6 and alpha-8 [MS – 840], radixin [MS – 439], gelsolin/vilin related proteins [MS – 433], as well as other minor proteins. The author acknowledges the online use of Wikipedia as a valuable resource for information on several of these cytoskeletal proteins.

11.1. Actin

Actin is a globular, ~42-kDa protein found in nearly all eukaryotic cells; it is typically present in high concentrations (over 100 microM). Actins are one of the most highly-conserved proteins, differing by no more than 20% in species as diverse as algae and humans. Actin represents the monomeric subunit of two types of filaments in cells: microfilaments, and thin filaments; it is a critical part of the contractile apparatus in muscle cells. Actins participate in important cellular processes including muscle contraction, cell motility, cell division and cytokinesis, vesicle and organelle movement, cell signaling, and the establishment and maintenance of cell junctions and cell shape. Many of these actions are mediated by extensive and intimate interactions between actin and cellular membranes. In vertebrates, three main groups of actin isoforms, alpha, beta, and gamma have been identified. The alpha-actins are found in muscle tissues and are a major constituent of its contractile apparatus. The beta- and gamma-actins co-exist in most cell types as components of the cytoskeleton and are mediators of internal cell motility. Beta-actin is one of six different actin isoforms that have been identified in humans and is one of the nonmuscle cytoskeletal actins. As noted above, beta-actin is a dominant MV cytoskeletal protein; and as noted earlier in cultured growth plate chondrocytes, drugs that block formation of actin microfilaments significantly stimulate the release of MVs (68, 69, 73).

11.2. Filamin B, beta

This protein, also known as FLNB, is a cytoplasmic protein that binds to actin. It regulates intracellular communication and signaling by cross-linking with actin to allow direct communication between the cell membrane and cytoskeletal network. Filamin B is thought to be important for proper skeletal development (356). Mutations in the FLNB gene are involved in several lethal bone dysplasias, including boomerang dysplasia and atelosteogenesis type I (357). The finding of filamin B in MVs [MS – 398] appears to be linked to the abundant presence of beta-actin.

11.3. Actinin

Actinin belongs to the spectrin gene superfamily that represents a diverse group of cytoskeletal proteins, including the alpha- and beta-spectrins and dystrophins. Actinins, alpha-1 and -4 are actin-binding proteins with various roles in different cell types. In nonmuscle cells, these cytoskeletal isoforms are found in microfilament bundles and adherens-type junctions, where they are involved in binding actin to the membrane. In contrast, the skeletal-, cardiac-, and smooth-muscle isoforms of actinin are localized to the Z-disc and analogous dense bodies, where they help anchor the myofibrillar actin filaments. The presence of both actinin alpha-1 [MS – 440] and alpha-4 [MS – 258] in MVs again appears to relate to their high affinity for actin.

11.4. Tubulin

Tubulin is one of several members of a small family of globular proteins. The most common members of the tubulin family are alpha- and beta-tubulin, proteins that make up microtubules. Each has a molecular weight of approximately 55 kDa. Microtubules are assembled from dimers of alpha- and beta-tubulin. These subunits are slightly acidic with an isoelectric point between 5.2 and 5.8 (358). To form microtubules, the dimers of alpha- and beta-tubulin bind to GTP (359) and assemble onto the (+) ends of microtubules while in the GTP-bound state (360). After the dimer is incorporated into the microtubule, the molecule of GTP bound to the beta-tubulin subunit can hydrolyze into GDP through inter-dimer contacts along the microtubule protofilament (361). Whether the beta-tubulin member of the tubulin dimer is bound to GTP or GDP influences the stability of the dimer in the microtubule. Dimers bound to GTP tend to assemble into microtubules, while dimers bound to GDP tend to fall apart; thus, the GTP cycle is essential for the dynamic instability of the microtubule network. Work by Hale *et al.* (69) reveals that tubulin depolymerization stimulates MV formation. Since GP chondrocytes that form MVs are typically in an energy-depleted state, the guanine nucleotides would tend to be in the GDP form and would thus favor disassembly of microtubules, and hence stimulate MV formation. In the MV proteome, three tubulin forms were detected: general tubulin [MS – 296], beta-6 [MS – 456], and alpha-8 [MS – 89]. Since tubulin is essential for cell division, it would clearly be essential during chondrocyte proliferation. The presence of tubulin in MVs may result from being in disassembled form in the cytosol that was encapsulated during MV formation.

11.5. Radixin

Radixin is a cytoskeletal protein that acts as an adapter and signaling protein (362). It functions as a plasma membrane-cytoskeletal cross-linker in actin-rich cell surface structures. It appears to be required for cytoskeletal functions such as transmembrane signaling, growth regulation, differentiation, cell motility, adhesion and proliferation. Radixin is a member of the ERM (ezrin-radixin-moesin) protein family that share highly similar

amino acid sequences. Radixin is a 583 amino acid (~80 kDa) protein with an extremely long alpha-helical domain (residues 310–477, ~240 Angstroms in length). The N-terminal FERM domain (residues 1-309) is 85-90% identical to those of ezrin and moesin and acts as a conditional membrane-binding site. The shorter C-terminal domain (residue 478–583) binds to f-actin; thus radixin forms a bridge between phosphatidylinositol 4,5-bisphosphate (PIP_2) in the plasma membrane and actin. Thus, it is not surprising to find that radixin has a significant proteome score [MS – 439]; it is apparent that it plays a role in the binding of actin to the plasma membrane.

11.6. Gelsolin and proteins with gelsolin/villin domains

There were significant levels of proteins with gelsolin/villin domains in the MV proteome [MS – 356], with lesser levels of gelsolin itself [MS – 77]. Gelsolin is an actin-binding protein that regulates actin filament assembly and disassembly. Gelsolin is one of the most potent members of the actin-severing gelsolin/villin superfamily; it severs f-actin with nearly 100% efficiency (363). It is an 82-kD protein with six homologous subdomains, referred to as S1–S6; each subdomain is composed of a five-stranded beta-sheet, flanked by two alpha-helices, one positioned perpendicular with respect to the strands and one positioned parallel. The N-terminus (S1-S3) forms an extended beta-sheet, as does the C-terminal (S4-S6) (364). As an important actin regulator, gelsolin plays a role in podosome formation (365-366). Podosomes are protrusions from the cell membrane that extend into the extracellular matrix (363). Apparently growth plate chondrocytes in the process of MV formation first produce actin-rich structures akin to these structures. Gelsolin inhibits apoptosis by blocking mitochondrial membrane potential loss and cytochrome C release (367). Prior to cell death (such as occurs upon chondrocyte hypertrophy), mitochondria lose membrane potential and become more permeable. Gelsolin can impede the release of cytochrome C, obstructing the signal amplification that would lead to apoptosis. Actin can be cross-linked into a gel by actin-cross-linking proteins. Gelsolin can turn this gel into a sol, hence the name gelsolin. Thus, although present in modest levels, gelsolin likely plays an active role in regulating MV formation.

11.7. Plastins

Plastins comprise a family of actin-binding proteins that are conserved throughout eukaryote evolution and are expressed in most tissues of higher eukaryotes. In humans, two ubiquitous plastin isoforms (L and T) have been identified. The L isoform of plastin is expressed only in hemopoietic cell lineages, while the T isoform has been found in all other normal cells of solid tissues that have replicative potential (fibroblasts, growth plate chondrocytes, endothelial cells, etc.). The C-terminal 570 amino acids of the T-plastin and L-plastin proteins are 83% identical and contain a potential Ca^{2+}-binding site near the N terminus (368). Of special interest to MV formation, T-plastin 3 appears to contribute to the assembly and maintenance of the actin cytoskeleton of plasma membrane protrusions that are characteristic of growth plate chondrocytes *in vivo* and from which MVs appear to bleb. The proteomic score of plastin 3 is not high [MS – 151], but the protein would appear to be involved with MV formation.

12. MATRIX VESICLE LIPIDS

The early discovery of extracellular lipids at sites of mineralization by Irving & Wuthier (16-19) found its explanation in the discovery of membrane invested MVs (1-4). The development of facile methods for quantitation of the complex mixture of lipids present in MVs was critical to the success in this endeavor (222, 369-370). Early investigations of the lipid composition of MVs (29-31) established several unusual features. MVs were enriched in nonpolar lipids and depleted in phospholipids compared to the plasma membrane, or the total cell. The ratio of free cholesterol to phospholipids in MVs was double that of the plasma membrane, and nearly 5-fold higher than in the cells. Thus some MV lipids must not reside in the vesicle membrane, but rather in some other form (proteolipids?) within the vesicle lumen (74, 93). This may explain: 1) the marked osmiophilicity of the luminal contents of many MV (3), 2) the presence of a "low-density nucleation factor" in MVEM (66), and 3) the abundant presence of milk-fat globule protein in the proteome of MVs (78).

12.1. Phospholipids

MV phospholipid composition was significantly different from that of the cell, or 'membrane' fractions (29-31). Among the notable differences were an enrichment in phosphatidylserine (PS) (3.2–4.5 fold), sphingomyelin (SM) (2.2–2.5 fold), and total lysophospholipids (LPL) (1.8–2.2 fold), as well as depletion in phosphatidylcholine (PC) (0.6-0.7 fold) – when compared to the cells (Table 1). A similar enrichment in SM and LPL was evident in hypertrophic *vs.* proliferating cells of the growth plate, suggesting that phospholipases are active in the process of hypertrophy, a phenomenon that precedes MV formation. This finding agrees with earlier studies showing elevated phospholipase activity in the hypertrophic zone of growth plate cartilage (223).

12.1.1 Fatty acid composition of MV phospholipids

Fatty acid analyses of the LPL of MVs showed enrichment of saturated fatty acids (stearic) and reduction in unsaturated fatty acids (oleic and palmitoleic) compared to the diacyl forms (227). This indicates that the LPL must arise from action of phospholipase A_2 type activity. The abundant presence of zwitterionic type LPLs, and the depletion of PC in MVs, indicates that phospholipase A_2 must be active during MV formation. More will be made of this in the discussion of the mechanism of MV formation.

12.1.2. Physical form of MV phospholipids

Studies also have been directed toward elucidation of the physical form of phospholipids in MV (64). This was done to ascertain whether the acidic phospholipids present in MV were complexed with the newly forming calcium phosphate mineral. Earlier studies on the phospholipids of growth plate cartilage had shown

Table 1. Total phospholipid composition of growth plate tissues: chondrocytes, membranes, and matrix vesicles

% of Total Lipid P					
		Chondrocytes			
Phospholipid	**Whole Cartilage**	**Proliferating**	**Hypertrophic**	**Cell Membranes**	**Matrix Vesicles**
Sphingomyelin	8.6 ± 0.7	5.8 ± 0.4	8.0 ± 0.8	8.1 ± 0.8	13.4 ± 1.8
Phosphatidylcholine	45.2 ± 1.9	47.6 ± 1.5	38.0 ± 1.5	53.2 ± 2.2	41.8 ± 2.5
Lysophosphatidylcholine	2.0 ± 0.6	1.9 ± 0.4	1.8 ± 0.4	3.5 ± 0.8	3.4 ± 0.8
Phosphatidylethanolamine	17.6 ± 1.0	16.9 ± 0.7	14.7 ± 0.8	14.6 ± 1.8	14.9 ± 1.8
Lysophosphatidylethanolamine	2.0 ± 0.4	3.3 ± 0.7	2.4 ± 0.4	4.9 ± 1.2	6.5 ± 1.2
Phosphatidylserine	5.1 ± 0.8	3.3 ± 0.3	5.0 ± 1.0	5.4 ± 0.7	9.3 ± 1.1
Lysophosphatidylserine	0.5 ± 0.2	0.2 ± 0.1	0.3 ± 0.2	2.2 ± 0.7	2.4 ± 0.8
Phosphatidylinositol	7.2 ± 0.8	6.2 ± 0.8	6.4 ± 0.8	6.1 ± 0.8	6.6 ± 0.6
Lysophosphatidylinositol	1.1 ± 0.7	1.0 ± 0.6	0.5 ± 0.4	0.3 ± 0.2	1.1 ± 0.3
Phosphatidic Acid	2.0 ± 0.5	0.8 ± 0.3	1.6 ± 0.5	1.1 ± 0.2	0.9 ± 0.3
Phosphatidylglycerol	1.2 ± 0.6	0.7 ± 0.3	1.2 ± 0.6	0.9 ± 0.2	1.3 ± 0.3
Diphosphatidylglycerol	3.0 ± 0.6	2.5 ± 0.4	2.9 ± 0.6	1.7 ± 0.3	1.5 ± 0.4
Number of Analyses	(18–45)	(15–29)	(9–21)	(15–36)	(37–72)

Values presented represent the combination of lipids extractable before demineralization, and those extractable after treatment of the tissue with EDTA. The means ± S.E.M. of these composite analyses are derived from 11 reported publications (28, 30, 31, 64, 73, 207, 222-223, 267-268, 398) spanning over 30 years. The majority of the analyses were performed using 2-dimensional chromatography on Whatman silica gel-loaded papers as described by Wuthier (370). The two latest analyses were based on the HPLC method of Genge *et al.* (222) using evaporative light scattering for quantitative analysis. The "Cell Membranes" fraction represents more dense membranous material that sediments more rapidly than MVs; it probably contains some MVs that are partially calcified. It does not specifically represent the plasma membrane. In comparing the lipid composition of MVs with proliferating chondrocytes, note the 10-fold enrichment in LPS, the almost 3-fold enrichment in PS, the over 2-fold enrichment in SM, and nearly 2-fold enrichment of LPC and LPE. Levels of PC and PE are commensurately reduced.

that a large portion of the acidic phospholipids were complexed with the mineral and were extractable only after demineralization of the tissue (20, 371). These mineral-complexed phospholipids had a turnover pattern different from that of the non-complexed lipids (28). In fact, nearly half of the PS and PI present in MVs were complexed with the newly forming mineral phase (64). About 10% of the total Ca^{2+} and Pi in the vesicles was extractable into organic solvents as acidic phospholipid-Ca^{2+}-Pi complexes (CPLX). This phenomenon is based on the fact that Pi markedly enhances the affinity of Ca^{2+} for acidic phospholipids like PS, giving rise to PS-CPLXs that are soluble in organic solvents (266). CPLXs have been shown to have potent mineral nucleating properties (131, 136, 221, 288, 372). In forming these complexes, it is critical that Pi be present prior to exposure of PS to Ca^{2+} (373). If Pi is not present first, PS forms a ternary $(PS)_2$-Ca^{2+} complex that excludes Pi binding and has no nucleational activity. This is an important clue to the sequence of events that leads to formation of PS-CPLX and formation of MVs.

12.1.3. Topological distribution of MV phospholipids

Studies by Majeska *et al.* also have shown that the bulk of MV PS resides in the inner membrane leaflet; surprisingly, PE a lipid typically found in the inner leaflet of the plasma membrane is equally abundant on the external membrane (259). However, this redistribution appears to result from the activity of scramblases recently shown to be present in MVs (287). The internal localization of PS is consistent with findings in many other tissues (374-376) and has important physiological ramifications. The formation of the PS-CPLXs in MVs would occur inside the vesicle lumen and would not be accessible to the extracellular fluid until the membrane was breached. While phospholipase and scramblase activities appear to be involved in MV formation, since much of the PS is complexed with Ca^{2+} and Pi, it is resistant to the action of these enzymes, as has been shown by Boskey *et al.* (377).

12.1.4. Ca^{2+}-binding properties of MV phospholipids

While it was known that PS binds with moderate affinity to Ca^{2+} (24-27), Holwerda *et al.* (373) determined that the K_f of Ca^{2+} for PS was 3×10^4 using biphasic solvent partition assays. Through use of ^{13}C and ^{31}P nuclear magnetic resonance (NMR) studies of Ca^{2+}-binding to PS and PE, it was established that both the carboxylate and phosphate groups were essential for Ca^{2+} binding; and that the amino group of PS exerts a significant repulsive effect (373). Later, it was discovered that the annexins bind to Ca^{2+} in an acidic phospholipid-dependent manner (378-379). The affinity of binding between the annexins and the acidic lipids is such that physiological changes in cytosolic Ca^{2+} ion activity can markedly alter the association between these proteins and PS on the inner surface of the plasma membrane. Acidic phospholipid-dependent Ca^{2+}-binding annexins have been found to constitute a major fraction of the MV proteins (60, 61) and have PS-dependent Ca^{2+}-binding constants in the 250–500 nM range (Figure 5). One of the earliest biochemical clues implicating acidic phospholipids in the mechanism of growth plate calcification was the discovery that substantial amounts of acidic phospholipids, and PS in particular, are complexed with Ca^{2+} in the mineralizing tissue (19, 20). Growth plate cartilage was dissected from successively more calcified zones: resting, proliferating, hypertrophic, and calcified cartilage, and compared with cancellous and compact bone. With increasing mineralization, progressively more and more of the acidic phospholipids could not be extracted until the tissues were demineralized with EDTA (371). Most of the Ca^{2+}-bound phospholipids are present in the form of PS-CPLXs.

Table 2. Electrolytes of growth plate tissues: chondrocytes, matrix vesicles, extracellular fluid and blood plasma

	Chondrocytes		Matrix Vesicles	Extracellular Fluid		Blood Plasma
	Proliferating	Hypertrophic	(Nascent)	Proliferating	Hypertrophic	(Arterial)
Electrolyte	**Total Millimoles/liter water**					
Na^+	42 ± 4	59 ± 1	164 ± 8	117.1 ± 1.2	115.5 ± 2.2	156 ± 7
K^+	122 ± 5	103 ± 11	19 ± 2	9.5 ± 1.2	14.7 ± 3.3	11 ± 1
Ca^{2+}	2.1 ± 0.3	1.4 ± 0.2	65 ± 8	3.30 ± 0.08	3.14 ± 0.02	3.19 ± 0.19
Mg^{2+}	9 ± 1	9 ± 1	5.4 ± 1.1	0.90 ± 0.01	0.91 ± 0.02	1.14 ± 0.07
Cl^-	31 ± 6	28 ± 2	–	111.0 ± 1.3	111.1 ± 3.1	118 ± 4
Pi	23 ± 1	22 ± 1	38 ± 4	2.35 ± 0.28	2.23 ± 0.19	2.39 ± 0.05
HCO_3^-	–	–	–	22.3 ± 0.7	26.2 ± 1.5	22.3 ± 3.0
Electrolyte	**Ultrafilterable Millimoles/liter water**					
Na^+	42 ± 4	59 ± 1	164 ± 8	103.7 ± 1.1	104.5 ± 2.1	149 ± 6
K^+	122 ± 5	103 ± 11	19 ± 2	9.4 ± 1.0	12.7 ± 1.9	8 ± 1
Ca^{2+}	0.16 ± 0.04	0.11 ± 0.03	1.5 ± 0.1	1.17 ± 0.20	1.27 ± 0.16	1.97 ± 0.16
Mg^{2+}	1.54 ± 0.02	1.50 ± 0.03	2.7 ± 0.5	0.72 ± 0.11	0.83 ± 0.15	0.77 ± 0.01
Cl^-	31 ± 6	28 ± 2	–	107.3 ± 1.3	100.6 ± 2.7	118 ± 4
Pi	23 ± 1	22 ± 1	20 ± 2	2.32 ± 0.26	2.21 ± 0.28	2.01 ± 0.08
Electrolyte	**Ion Activities**					
Ca^{2+}	0.40 ± 0.04 μM	0.49 ± 0.06 μM	7.44 ± 0.34 μM	0.95 ± 0.15 mM	1.15 ± 0.15 mM	1.52 ± 0.12 mM
Pi	21 ± 1 mM	20 ± 2 mM	15 ± 3 mM	2.30 ± 0.23 mM	2.15 ± 0.22 mM	2.00 ± 0.10 mM
H^+ (pH)	7.1 ± 0.1	7.2 ± 0.1	6.85 ± 0.15	7.39 ± 0.01	7.45 ± 0.02	7.39 ± 0.04

Values presented for total and ultrafilterable electrolytes in ECF and blood plasma are mean values derived from rats and chickens (63, 64, 317, 339). Ion activities of Ca^{2+} and H^+ in chondrocytes and MVs are means derived from values based on live avian tissue using fluorescent probes and confocal imaging (306). Activities in the extracellular fluid are based on Howell *et al.* (339). HCO_3^- levels are based on an assumed pCO_2 of 38 mm Hg.

12.2. Nonpolar lipids

Compositional analysis of the nonpolar lipid fraction from MV (30) revealed significant differences from that of the plasma membrane or the total cell. Triacylglycerols (TG) were the major nonpolar lipid in cells, accounting for 44.0±0.7% of the total; this was followed by free cholesterol (19.3±1.9%), free fatty acids (10.2±2.0%), cholesterol esters (8.4±0.8%) and 1,2-diacylglycerols (6.4±0.4%). Only trace amounts of 1,3-diacylglycerol (0.3±0.2%) were present, although there was ~10% of partially characterized hydroxysterols (223). In contrast, in MV, free cholesterol was dominant, accounting for 31.7±4.8% of the nonpolar lipid. Levels of TG in MV were only half that seen in the cells (22.4±3.6%); levels of free fatty acids, cholesterol esters and 1,2-diacylglycerols were not significantly changed, whereas the level of 1,3-diacylglycerols increased significantly to 2.5±0.7% of the total nonpolar lipid. Thus, MVs were significantly richer in free cholesterol and depleted in triacylglycerols compared to the plasma membrane and total cells. The finding of marked enrichment in free cholesterol, the high levels of SM and polyhexosyl ceramides (see next), as well GPI-anchored TNAP in MV (207) suggests that formation of lipid platforms is involved in MV formation (287) and may contribute to the nucleation of mineral formation by MVs.

12.3. Glycolipids

The non-phosphorus-containing polar lipid composition of MVs, plasma membranes and total cells of avian growth plate cartilage has been only minimally explored (30). While these polar lipids account for a significant amount of the total lipid, they have not been well characterized. (There is no evidence that these glycolipids are complexed with the mineral phase of MVs.) MVs and the plasma membrane fraction of growth plate chondrocytes were found to be enriched in the polyhexosyl ceramides (24.6% in MVs *vs.* 7.0% in cells) and acidic glycosyl ceramides (24.1% in MVs *vs*. 8.4% in cells). Consistent with this early finding of acidic glycosyl ceramides in MVs, over 30 years later studies on detergent-resistant membrane fractions of growth plate chondrocytes report the presence of ganglioside-1 (GM1) as the principal neuraminic acid-containing glycosyl ceramide (287). These membrane fractions also contain GPI-anchored TNAP that becomes incorporated into MVs. These chemical features, as well as morphological studies, all indicate that MVs derive from the plasma membrane.

13. MATRIX VESICLE ELECTROLYTES

Endochondral calcification is a complex process in which Ca^{2+} and Pi (HPO_4^{2-} and $H_2PO_4^-$) in solution are processed and brought together to induce precipitation of a mineral phase that ultimately forms hydroxyapatite ($Ca^{2+}{}_{10}{\cdot}PO_4^{3-}{}_6{\cdot}OH^-{}_2$, HAP), the principal mineral of bone. To properly understand the role of MVs in the induction of growth plate mineralization, the levels of MV electrolytes 1) need to be compared with: 2) those present in the intracellular fluid of chondrocytes from which the MVs form, 3) the extracellular fluid (ECF) where mineralization occurs, and 4) the blood plasma – the central source of electrolytes that is controlled by various endocrine systems to maintain relatively constant levels. Presented in Table 2 are chemical analyses of levels of major ion species in these four compartments. Because the precipitation process involves interactions between the ionic *activity* of Ca^{2+} and HPO_4^{2-}, and also other ionic species, the levels of these and other electrolytes are expressed as: a) total, b) ultrafilterable and c) ion activities. Mean values for Na^+, K^+, Mg^{2+}, Ca^{2+}, Pi, Cl^- and HCO_3^- from growth plates of rat (339) and chicken cartilage (63) are presented. Supporting data obtained

from ultrastructural electron probe analyses (380) are also considered. The physical properties of the mineral present in MVs are also discussed in detail.

13.1. Chemical analyses of intracellular electrolytes in growth plate chondrocytes

Electrolyte levels in living cells constitute an analytical challenge because of their dynamic character. This is particularly true of cells entrapped in a dense proteoglycan- and type II collagen-rich matrix such as occurs in growth plate cartilage. Different approaches have been taken to solve this problem. First, by careful release using controlled enzymatic digestion of the matrix proteins, chondrocytes can be obtained in essentially intact form, particularly if they are quickly restored to an ionic environment (*e.g.* synthetic cartilage lymph, SCL) that matches the electrolyte composition and osmolarity of the native extracellular fluid. However, when feasible, ion activities are even better assessed *in situ* using fluorescent probes specific for the ion in question. Using the first approach, we performed zonal dissection of the tibial growth plates of young (6–8 week old) rapidly growing chickens to obtain tissue from the proliferative and hypertrophic zones. The cells were released and equilibrated in SCL containing glucose to restore native electrolyte values (63). ^{3}H-labeled H_2O and ^{14}C-labeled inulin (a high molecular weight inert polysaccharide that does not penetrate into living cells) were then used to enable determination of the intracellular volume for accurate electrolyte concentrations in these living cells (63).

Table 2 presents data from that study. Shown in the first two columns are the cellular concentrations of the major electrolytes. Immediately obvious is the fact that the proliferating cells, like all normal vertebrate cells, were rich in K^+ (~120 mM) and relative low in Na^+ (~40 mM). K^+ levels in the hypertrophic cells were slightly lower (~100 mM) and Na^+ levels higher, evidently because ATP levels were reduced as these cells approach their apoptotic demise. The levels of *total* Mg^{2+} were relatively high (~9 mM) typical of living cells; *total* Ca^{2+} levels was much lower (1.5–2.0 mM). However, both of these divalent cations are largely protein bound – as is evident in the marked reduction in the ultrafiltrates (Mg^{2+} = ~1.5 mM, Ca^{2+} = 0.10–0.15 mM). Concerning the anions, note that intracellular Cl^- (~30 mM) is markedly lower than is seen in the extracellular fluid (~110 mM) – as is typical of all living vertebrate cells. The only remarkable difference from typical soft tissue cells is the presence of high levels of Pi (22–23 mM), a value consistently observed in growth plate chondrocytes. This appears to be a modification designed to facilitate subsequent mineral formation. Note further that overall *average* cellular Ca^{2+} ion *activities* (0.4–0.5 *micromolar*), determined *in situ* using a Ca^{2+}-specific fluorescent probe in thin slices of live growth plate tissues incubated in phosphate-buffered saline (306), are only 1/250 – 1/300 of the ultrafilterable levels. However, *average* Ca^{2+} activity levels are poor indicators of the dynamics of chondrocyte Ca^{2+} metabolism. Major differences in local intracellular Ca^{2+} levels in different zones of the growth plate have important bearing on MV formation.

13.2. Chemical analyses of electrolytes in isolated matrix vesicles

In comparing electrolyte levels in MVs with those in the cells from which the vesicles arise, note that the Ca^{2+} and Pi levels represent those present in *nascent* vesicles. Much additional acquisition of Ca^{2+} and Pi occurs rapidly upon exposure of the MVs to the extracellular fluid. Note first that the levels of total Pi (35–40 mM) in the MVs are not all that much higher than those present in the cells (20–25 mM). In contrast, note the markedly higher levels of *total* Ca^{2+} (60–70 mM) in MVs compared to the average levels of *total* Ca^{2+} (1–2 mM) in the cells. (How this remarkable enrichment occurs will be delineated in a subsequent section). The levels of *total* Ca^{2+} and Pi in MVs are also much higher than those in the ECF. This seems paradoxical from a thermodynamic perspective – until one examines MV Ca^{2+} ion *activity*, which is only 1.2–1.5% of that in the extracellular fluid. (MV Ca^{2+} ion activity levels were analyzed *in situ* as just described for the chondrocytes.) Another remarkable finding is that levels of Na^+ (~165 mM) and K^+ (~20 mM) in the MVs are just the reverse of what is seen in the chondrocytes from which they arise. MV Na^+ and K^+ levels are very similar to those in the ECF and blood plasma. These levels of MV Na^+ and K^+ show that despite the presence of Na^+/K^+-ATPase protein in MVs noted previously (78), the pump is obviously not operational. This is due to lack of ATP needed to drive the ion pump. Other MV electrolyte features justify comment. The pH of the *nascent* MVs is only about 6.8, similar to that in the perimeter of the hypertrophic cells from which the vesicles arise (307). However, after exposure to the ECF, the intravesicular pH rises significantly to ~7.6 (77). This appears to be in response to carbonic anhydrase activity that is part of a two-component system for regulating intravesicular pH (160). In addition to carbonic anhydrase that enables CO_2 to combine with H_2O to form carbonic acid (H_2CO_3), there is a HCO_3^-/Cl^- exchange channel (311) that enables entrance of HCO_3^- to buffer H^+ released when Ca^{2+} reacts with HPO_4^{2-}, to form ACP ($Ca^{2+}_3 \cdot PO_4^{3-}_2$) ion clusters in route to OCP and HAP formation. This specific intravesicular buffer system is vital to mineral induction.

13.3. Chemical analyses of electrolytes in the extracellular fluid and blood plasma

As is true of all vertebrate species, Na^+ and Cl^- comprise the major ion-pair in blood plasma (Table 2), with levels of ~150 mM and ~120 mM, respectively. In cartilage ECF Na^+ levels are significantly lower (115–117 mM) because of extensive binding to proteoglycans that are present in high levels (25–35 mg/mL). The levels of Na^+ in *ultrafiltrates* of blood plasma are significantly reduced – compared to the total – because of binding to plasma proteins (*e.g.* albumin and globulins). Cl^- levels in ultrafiltrates are much less affected, presumably because proteins generally do not tightly bind Cl^-. Levels of *ultrafilterable* K^+ in cartilage ECF are higher than those in blood plasma; they appear to be caused by Ca^{2+}-activation of a K^+ channel in growth plate chondrocytes (381). The

levels of *total* Ca^{2+} in blood plasma (3.2 mM) and cartilage ECF (3.1–3.3 mM) are very similar; however, major reduction is seen in *ultrafilterable* Ca^{2+} in cartilage ECF (1.2–1.3 mM) compared to plasma (2.0 mM). In cartilage ECF only about 35-45% of the Ca^{2+} is not protein bound (*i.e.* ultrafilterable), whereas in blood plasma about 67% is ultrafilterable. In cartilage fluid this reduces the activity of Ca^{2+}, but the proteoglycan-bound Ca^{2+} can act as a reservoir – available for subsequent mineral growth. On the other hand, the levels of Pi in the ECF ultrafiltrate are 10–15% higher than the levels in plasma, presumably from intracellular leakage. This would provide a significant boost in the ability of the ECF to support apatitic mineral growth. Note that substantial levels of HCO_3^- appear in both blood plasma and cartilage ECF; this anion provides part of the important buffer systems in both tissue fluids. Some data presented in Table 2 are derived from chemical analyses of electrolytes in extracellular fluid of growth plates made by Howell and Pita using their elegant micropuncture techniques (340). The bulk of the data are from expressed extracellular fluid from premineralizing and mineralizing zones of rapidly growing broiler-strain chickens (63, 64). Direct chemical analyses of electrolytes were also made on isolated cells and MVs (63, 64, 318) as well as MV-enriched microsomes isolated by non-enzymatic methods (55, 56).

13.4. Ultrastructural analyses of Ca^{2+} and P in chondrocytes and MVs

Electron probe analyses of *in situ* Ca and P in the cells and matrix of chicken growth plate cartilage have been reported (381). It is important to note that use of this method to determine concentrations of Ca^{2+} and P is problematic because of the difficulty in measuring the volume of tissue analyzed. Nevertheless, the general patterns obtained by chemical and microprobe analyses agree quite well, *qualitatively*. Chemical analyses of MVs isolated from the proliferative and hypertrophic zones yielded levels of *total* Ca^{2+} (43 ± 3, and 98 ± 14 mM, respectively) (63); electron probe *in situ* estimates of MV levels from similar zones reported values of Ca^{2+} 277 ± 46, and 882 ± 101 mM, respectively – values 5–9-fold higher. Similarly, chemical analyses of total inorganic P (Pi) in MV isolated from the two zones were 30 ± 4, and 50 ± 10 mM, respectively; electron probe estimates of total P (organic and inorganic) yielded values of 173 ± 32, and 603 ± 69 mM, respectively – values 6–12-fold higher. Thus, while the *quantitative* values obtained do not agree, *qualitatively* they show the same pattern. In either case, it is obvious that the levels of Ca^{2+} and Pi present far exceed what could occur free in solution. Using a special potassium pyroantimonate Ca^{2+} stain, Brighton and Hunt carefully studied the levels of Ca^{2+} in chondrocytes at different zones of epiphyseal cartilage of rat costal cartilage (Figure 8A–C) (382-384). Their findings showed that growth plate chondrocytes accumulated Ca^{2+} in their mitochondria reaching maximal levels in the hypertrophic cells just prior to the onset of mineral formation. Their studies indicated that this stored Ca^{2+} was transferred via cytoplasmic processes to the extracellular matrix in the form of Ca^{2+}-loaded MVs. Although controversial at the time of first discovery subsequent biochemical and confocal studies using ion probes for Ca^{2+} have essentially confirmed these early observations.

13.5. Chemical analyses of microelements in MVs

Sauer, in particular, focused attention on levels of various microelements in MVs (317). These studies were prompted by the discovery that chelators of transition metal ions (*e.g. o*-phenanthroline) markedly stimulated the rate of Ca^{2+} loading by mineralizing MVs (76). These analytical studies revealed remarkable levels of *total* Zn^{2+} (1.0-1.5 mM) in MVs. Levels of other trace elements were at background values, although low levels of total Cu^{2+} (50-100 microM*)* were detected. Further studies revealed that addition of 5 microM Zn^{2+} to the mineralizing medium markedly inhibited MV Ca^{2+} loading (385). This will be detailed later when the regulatory role of Zn^{2+} in the induction of mineralization by MV is considered.

13.6. Physico-chemical properties of MV mineral forms

Knowledge of the chemical form of the mineral ions at different stages of MV development is essential for proper understanding of the mechanism of MV mineral formation. For example, crystalline HAP is not the first mineral formed by MV; to the contrary, there is strong evidence that ACP and complexes of it with certain proteins and lipids are the first solid- phase mineral form present in MVs. This is evident from the following data.

13.6.1. X-ray Diffraction Analyses

A variety of physico-chemical methods have been applied to ascertain the physical form of Ca^{2+} and Pi present in MV. Early X-ray powder diffraction studies on freeze-dried collagenase-released MV isolated from avian growth plate cartilage revealed that no crystalline HAP mineral is present initially (63) (Figure 9). Nevertheless, chemical analyses reveal that nascent vesicles contained large amounts of Ca^{2+} and Pi – much more than could exist in solution phase. It is now apparent that this is largely amorphous (ACP), but because of its diffuse X-ray diffraction pattern (386), it is obscured in the diffuse diffraction halo of the MV proteins and lipids. X-ray diffraction studies on MV-enriched microsomal fractions purified by isosmotic Percoll density gradient fractionation, also revealed the absence of crystalline mineral (57). However, upon incubation in SCL for 16 h these MVs accumulated large amounts of Ca^{2+} and Pi, which X-ray diffraction analysis then clearly showed was HAP-like crystalline mineral.

13.6.2. FT-IR and FT-raman analyses

Using solid-state spectroscopic (FT-IR and FT-Raman) methods, Sauer *et al.* also examined the initial mineral phases present in nascent MVs, as well as that subsequently formed after incubation in SCL (387-388). MVs prepared by mild collagenase digestion accumulate large amounts of Ca^{2+} and Pi from SCL – without the addition of organic phosphate substrates (76). These vesicles were incubated in SCL and harvested at different stages of ion accumulation, lyophilized, incorporated into

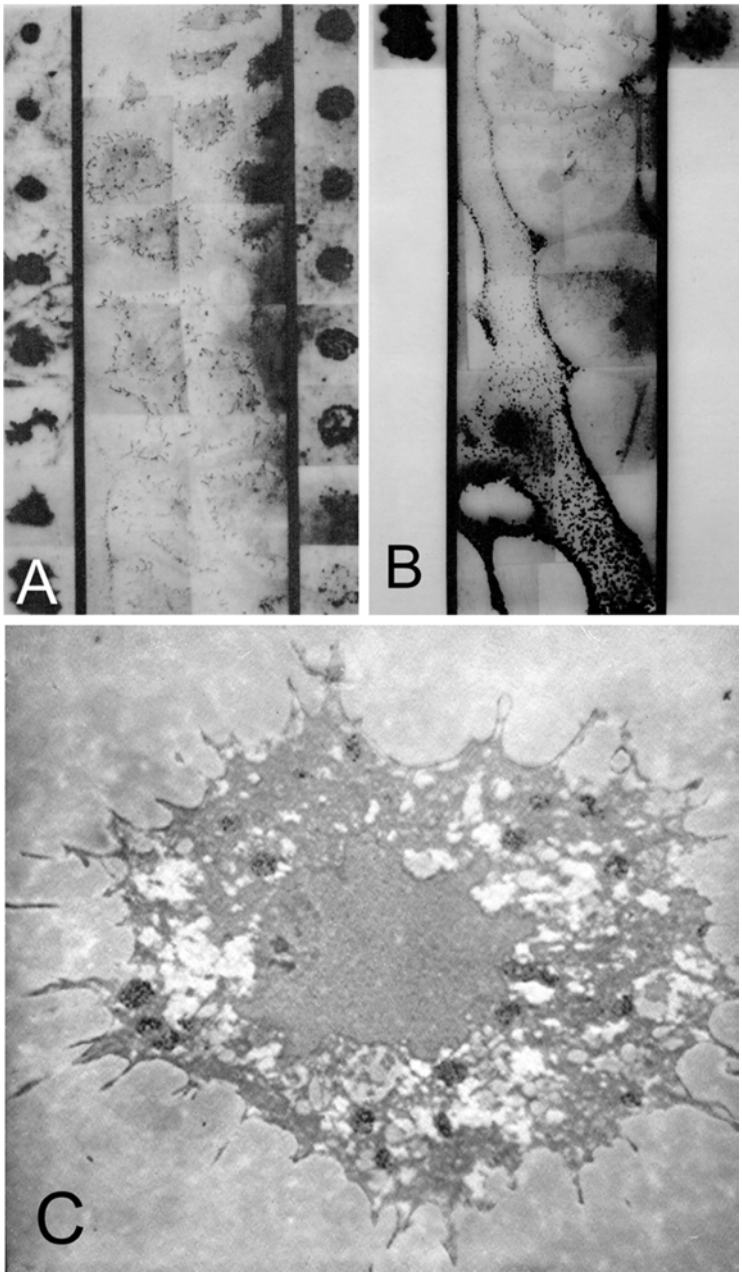

Figure 8. Ultrastructural Montage of Potassium Pyroantimonate Staining of Ca^{2+} in Rat Epiphyseal Cartilage. Costochondral junctions of 21-day-old Sprague-Dawley rats were processed as described (383). In brief, the tissues were bisected longitudinally and fixed in a solution of 2% potassium pyroantimonate (PPA) and 2% osmium tetroxide, brought to pH 7.5 by addition of acetic acid. The tissues were cut longitudinally into thin slices, dehydrated, embedded in SPURR, and sectioned using a diamond knife. Sections were observed and photographed using a Carl Zeiss EM9S-2 electron microscope. (PPA, which is several orders of magnitude more sensitive for Ca^{2+} than for Na^{+} and does not precipitate K^{+} at all, forms electron-dense precipitates with cellular Ca^{2+} readily visualized at the ultrastructural level. Note that the PPA-Ca^{2+} stain is localized predominantly in mitochondria and cell membranes. 8A – Three-panel montage of maturation to late hypertrophic zones of the growth plate revealing transfer of Ca^{2+} from mitochondria to MVs. After reaching peak Ca^{2+} levels in the zone of maturation (top 4-5 cells in center panel), there is subsequent loss of mitochondrial Ca^{2+} (right panel) and a concomitant accumulation of the PPA-Ca^{2+} complex by MVs (left panel). 8B – Montage of late hypertrophic and calcifying cartilage zones showing onset of mineralization at MV loci (upper perilacunar region), with subsequent spreading throughout the matrix (lower region). 8C – Higher magnification of a PPA-stained hypertrophic cell. The chondrocyte shows intense Ca^{2+}-PPA stain in numerous mitochondria. (Adapted from (382) with permission from C.T. Brighton, M.D.).

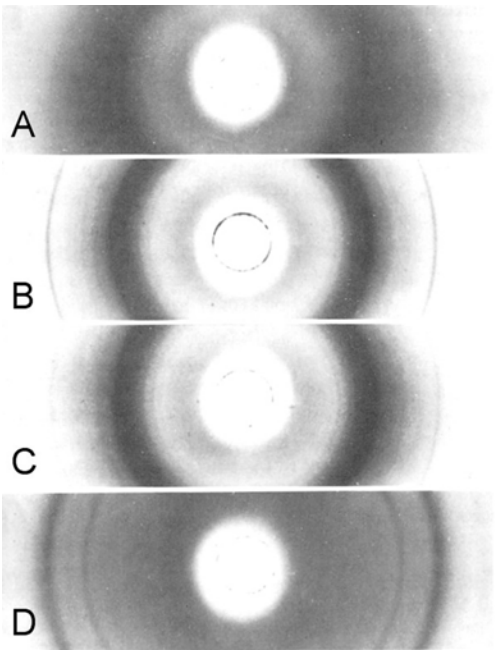

Figure 9. X-Ray Diffraction of Freeze-Dried Epiphyseal Cartilage Fractions. X-ray powder diffraction patterns of freeze-dried epiphyseal cartilage fractions. After sequential hyaluronidase-collagenase digestion of 3–5 g of fresh cartilage as described by Majeska and Wuthier (54), the digestate was differentially centrifuged: Fraction 1 (cell pellet) was sedimented for 10 min at 150 ×g; Fraction 2 (membrane fraction) for 15 min at 13,000 ×g; Fraction 3 (MV fraction) for 60 min at ~100,000 ×g. The cell pellet was treated for 15 min at 38ºC with 20 ml of 0.1 M sodium citrate, pH 6.0, to dissolve any mineral debris, rinsed with 20 ml of synthetic cartilage lymph (SCL) and incubated for 2–3 h in 5 mM glucose- and 0.1% bovine serum albumin containing SCL to permit restoration of normal electrolyte balance as previously described (391). The chondrocytes (9A) were then sedimented as above and freeze-dried. The membrane fraction (9B) and the nascent MV fraction (9C) were freeze-dried immediately after ultracentrifugation (30). The non-digestable residue (early mineral deposits, 9D) was freeze-dried immediately after washing with SCL. Specimens were examined using a 57.3 mm DeBye Scherrer powder camera using Cu K-alpha radiation. Note the absence of hydroxyapatite (HAP) diffraction bands in the membrane (9B) and MV (9C) fractions, despite the fact that they contained over 50 and 100 mM (wet wt) Ca^{2+}, respectively. (In 9B and 9C, the sharp weak outer diffraction band is that of NaCl present in the SCL used to isolate these fractions.) The presence of poorly crystalline HAP diffraction bands is clearly evident in the non-digestible mineral residue (9D). (Reproduced from (63) with permission from Springer).

KBr pellets, and examined by FT-IR. The baseline spectrum of the nascent MV was computer-subtracted from that of MV at progressive stages of mineralization, revealing the formation of mineral by the vesicles. The first detectable *crystalline* phase was found to be an HPO_4^{2-}-containing octacalcium phosphate (OCP)-like mineral (Figure 10); this finding was later confirmed using FT-Raman spectroscopy (388). In these intact MVs, no obvious spectra of ACP were evident, presumably again because the patterns of lipids and proteins obscured it. However, when the nucleational core of MVs was isolated and characterized (See Section 16), FT-IR analyses provided clear evidence for the presence of ACP. However, the mechanism of mineral formation by MVs is not a straight-forward process; it involves a number of staged events that progressively lead to the formation of biological apatite.

13.7. Solubility properties of nascent MV mineral

A variety of studies have explored the solubility properties of the initial MV mineral. *First,* analyses of CRMVs using biphasic solvent partition of electrolytes revealed that the great majority of the Ca^{2+} (>90%) was in an insoluble form, including about 8–10% of the Ca^{2+} being present as acidic phospholipid-Ca^{2+}-Pi complexes (64). Less than 5% of the MV Ca^{2+} appeared to be free in solution. In contrast, much of the MV Pi and Mg^{2+} (about 50%, each) and Na^+ and K^+ (70-80%, each) were free in solution. These findings suggested that at least half of the Pi and Ca^{2+} present in nascent MVs are not initially combined together; about 40% of the total Ca^{2+} appeared to be bound to proteins and lipids. Subsequent studies by McLean *et al.* (67) supported these observations. Sucrose gradient analysis of MV-enriched microsomes revealed that in the low-density fractions, much of the Ca^{2+} and Pi were not combined; Ca^{2+} appeared to be largely bound to proteins, whereas most Pi appeared to be unbound in the vesicle fluid. *Second*, in the McLean study, brief exposure (10 min) of the MVs to isosmotic citrate (pH 6.0) buffer removed 85-90% of the Pi and 70-80% of the Ca^{2+} (67). This destroyed their ability to subsequently accumulate mineral ions. Such brief, mild treatments should not dissolve crystalline HAP protected within the MV lumen, but would readily dissolve ACP, which is very acid labile. Subsequent studies on the properties of nascent MV mineral have led to the discovery of a nucleational core

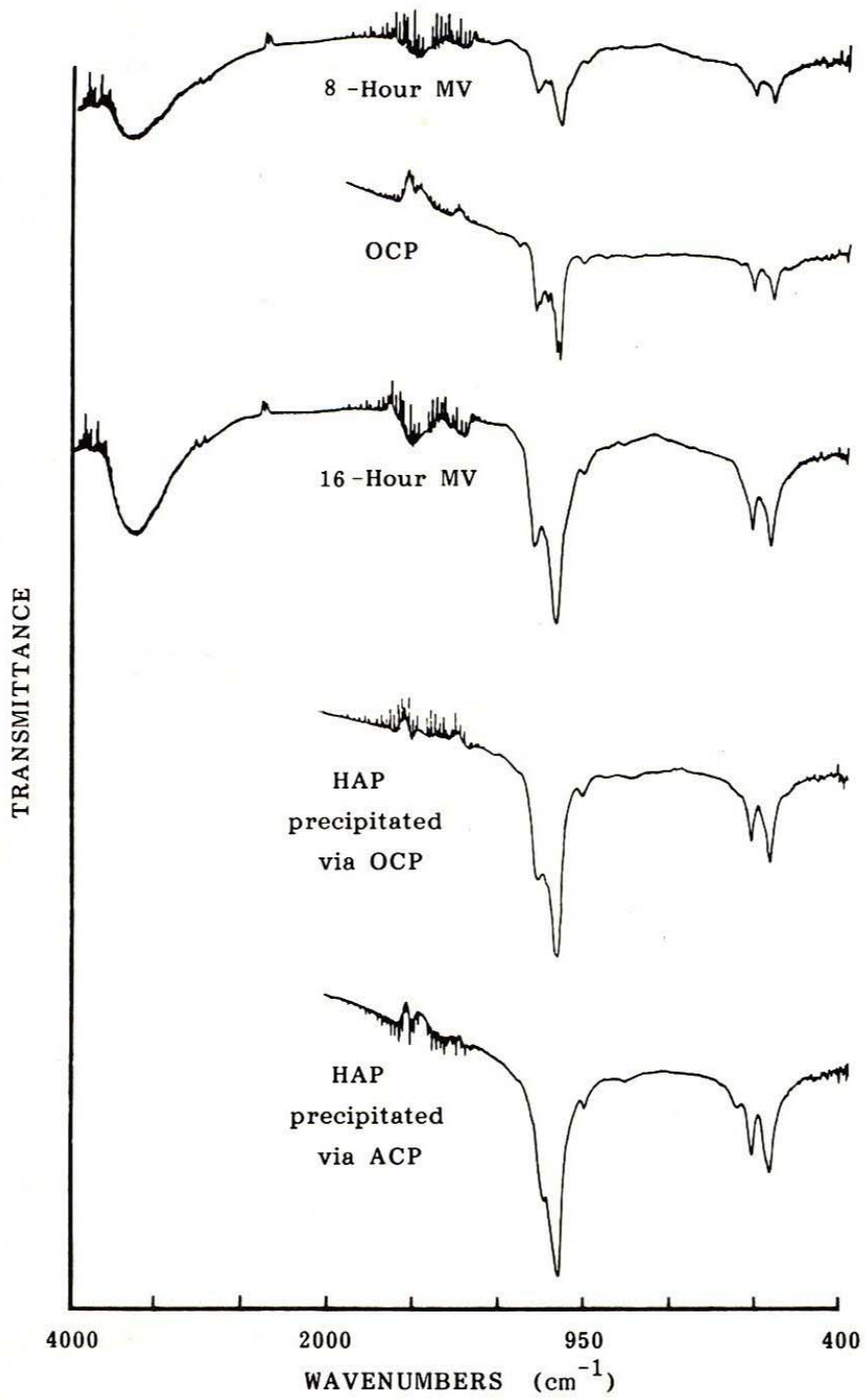

Figure 10. Fourier-Transform Infrared (FTIR) Difference Spectra of MVs during Mineral Formation – FTIR *difference* spectra of MVs at two key times during incubation in SCL to induce mineral formation. *Difference* spectra were obtained by subtracting the spectrum of unmineralized MVs from that of MVs incubated in SCL for the indicated time periods, 8 and 16 h. These were compared with similar levels of three mineral standards: octacalcium phosphate (OCP), hydroxyapatite (HAP) precipitated *via* an OCP intermediate, and HAP precipitated *via* an amorphous calcium phosphate (ACP) intermediate. Note that the first clearly discernible crystalline mineral phase is OCP-like – evident from the doublet at 600–560 cm^{-1} and the triplet at 1130–1030 cm^{-1} – was dominant at 8 h near the end of the rapid uptake period (2–6 h, see Fig. 16A, later). The spectrum of the initial mineral (8 h) most closely matched the spectrum of OCP; later (16 h) the mineral appeared like HAP precipitated *via* OCP, not *via* ACP. (Adapted from (455) with permission from the Institute for Scientific Information).

that is directly responsible for induction of crystalline mineral. How it was discovered and how it functions will be described later. However next, attention will focus on how MVs are formed by growth plate chondrocytes.

14. FORMATION OF MATRIX VESICLES

Formation of MVs is a complex physiological process that involves a series of progressive changes in growth plate chondrocytes that ultimately lead to a modified form of apoptosis. The cells shed calcifiable MVs into the extracellular matrix – capable of inducing mineral formation. MV formation stems from the fact that in the proliferative zone of the growth plate, chondrocytes become embedded in a highly impervious matrix of their own making. This proteoglycan-rich gel impedes diffusion of O_2, albumin-bound fatty acids (389), and other nutrients and electrolytes to the proliferating cells. Thus, during their rapid growth, the epiphyseal chondrocytes become separated from their vascular supply and become hypoxic (390-391). They express high levels of glycolytic enzymes (392-394) and become dependent on anaerobic glycolysis for energy (216). The cells adapt to their cloistered, hypoxic environment; they maintain a normal energy charge (216). However, upon penetration of blood vessels to near the maturing chondrocytes, delivery of nutrients, Ca^{2+}, and Pi – and especially of O_2 – leads to a sudden increase in oxidative metabolism. Delivery of O_2 to these hypoxic cells causes oxidative stress; their mitochondria begin to store Ca^{2+}; becoming loaded with Ca^{2+}, they can no longer efficiently produce ATP. The cells undergo a physiological "ischemia-reperfusion" crisis. The cells become depleted of ATP; they swell and become hypertrophic. They generate reactive oxygen species that along with elevated Pi from ATP hydrolysis trigger the opening of the mitochondrial permeation transition pore (395). This leads to rapid unloading of the stored Ca^{2+} and Pi, and this in turn leads to a type of cellular apoptosis (396-397). During this event Ca^{2+}-loaded vesicles are released from the cells into the matrix, forming MVs. This introduction is a snap-shot from a physiological perspective. Presented next, is a morphological view of MV formation. Following that, are various biochemical studies that describe how the cells form the MVs and enable them to induce rapid mineral formation – once they are released into the extracellular matrix.

14.1. Electron microscopic studies

The first studies that directly addressed the question of how MVs are formed were those of Bonucci in 1970 (4). Using serial TEM sections of growth plate cartilage, data were obtained that indicated MVs form from cellular projections, either by fragmentation, or by budding from the tips. Studies by Thyberg and Friberg (37, 38) a short time later presented evidence that there may be different types of MV. These early TEM studies indicated that MVs largely derive by exfoliation of vesicles from the outer membrane of growth plate chondrocytes. As noted previously, freeze-fracture analyses of growth plate cartilage contributed definitive evidence that the distribution of membrane-associated particles on cellular processes was identical to that on MVs (Figure 3) (47, 48, 50, 55). This revealed that MVs arise from the cell by mechanisms that do not alter the inside/outside orientation of the membrane. Subsequent TEM studies of MV formation by Akisaka *et al.* (46) presented evidence that some MVs form by extrusion of preformed osmiophilic cytoplasmic material. Images presented by Arsenault (40, 42, 43) using slam-freezing techniques revealed the presence of high levels of Ca^{2+} and Pi in MVs prior to crystal formation (Figure 2). Ca^{2+} and Pi were not always co-localized, suggesting that they were not present only as calcium phosphate mineral *per se* – a finding in accord with solubility studies noted previously (64, 67). Studies in which tissue sections were collected by flotation on nonaqueous media and left unstained also suggested that Ca^{2+} and Pi in MV were not in a crystalline form (46).

14.2. Biochemical studies

Much of the evidence providing data on the chemical processes by which MV formation occurs has come from metabolic studies. These have been both *in vivo* and *in vitro* experiments demonstrating that incorporation of precursors into MV lipids, electrolytes and proteins is a very active, rapid process.

14.2.1. Phospholipid metabolic studies

The phospholipid composition of MV shows many similarities to that of the plasma membrane, with some notable exceptions (73). While supporting morphological studies that MVs derive from the plasma membrane, metabolic studies have provided more explicit information. *In vivo* studies on the incorporation of ^{32}Pi into phospholipids of chondrocytes and MV have revealed that MV formation is a dynamic process in which labeling of MV PC and PE – which tend to be depleted – was nearly as rapid as that of the cellular lipids. In contrast, labeling of PS and SM – which are enriched in MV – was significantly slower (398). This paradox suggests that MV formation involves processes in which the plasma membrane becomes modified by action of phospholipases that selectively degrade PC and PE, while retaining PS and SM. The very limited ability of isolated MVs to incorporate radiolabeled fatty acid lipid precursors demonstrated that the rapid labeling of MVs seen *in vivo* resulted from prelabeling of the MV membrane lipids while they were part of the cell (268). However, isolated MVs can incorporate ^{14}C-serine into both PS and its lyso-form, LPS, *via* Ca^{2+}-dependent non-ATP-dependent base-exchange (PS synthase). This reveals that MVs retain the ability to synthesize PS, a key Ca^{2+}-binding lipid, enabling its further enrichment in the MV membrane.

14.2.2. Cell culture studies

Further insight into the mechanism of MV formation has come from studies on primary cultures of growth plate chondrocytes. However, it is important to distinguish between vesicles released into the culture media (media vesicles, MeVs) from those that become entrapped in the extracellular matrix (matrix vesicles,

MVs). MeVs do not appear capable of inducing mineral formation, whereas MVs clearly do (74, 399). It is noteworthy that both MeVs (68, 91), and MVs are rich in TNAP. The kinetics of MeV formation can be modulated by a variety of drugs that affect the cytoskeletal system and the acidic phospholipid-dependent Ca^{2+}-binding proteins (annexins). Cytochalasin D, a drug that blocks actin microfilament formation, markedly enhanced the rate of MeV formation, whereas phalloidin, a drug that prevents actin filament disassembly, clearly inhibited it (69). Coupled with the observation that isolated chondrocyte microvilli have a phospholipid composition almost identical to that of collagenase-released MVs (73), this provides biochemical confirmation of freeze-fracture studies that show MVs being formed from cellular microvilli (47, 50). While MVs contain some actin (78), chondrocyte microvilli contain abundant filamentous actin (69). This reveals that MVs form by mechanisms that involve depolymerization of actin filaments. On the other hand, studies using tricyclic amine drugs that selectively bind to the annexins also stimulate release of MeVs from cultured chondrocytes (70). Taken together, these findings indicate that processes that uncouple the annexins from the cytoskeletal network must be involved in MV formation. Further, the discovery that ascorbate, a vitamin required for normal collagen synthesis and fibril formation, strongly stimulates MV formation and matrix mineralization by cultured chondrocytes (75), suggests that MV formation is linked with synthesis of extracellular matrix collagens (400-401). The demonstration that both TNAP and at least two of the MV annexins (AnxA5 and AnxA6) bind tightly to both type II and X collagen (95, 102), suggests that MV formation involves the attachment of proteins present in microvilli-like extensions of the chondrocyte plasma membrane to matrix collagens (95, 402-403). Further, the finding of various integrins by proteomic analyses of MVs (78) indicates that they also contribute MV formation. Thus, binding of extracellular proteins to receptors on the outer membrane of the chondrocytes facilitates MV formation.

14.3. Role of cellular Ca^{2+} and Pi metabolism in MV formation

There is clear evidence that cellular metabolism of both Pi and Ca^{2+} is involved in MV formation and subsequent mineralization (404). Here is a brief preview of what will be discussed on this topic. When mitochondrial Ca^{2+} is released via the mitochondrial transition pore into the Pi rich cytosol, the released Ca^{2+} interacts simultaneously with both Pi and PS forming PS-Ca^{2+}-Pi complexes, as well as with PS and AnxA5 to form PS-Ca^{2+}-AnxA5 complexes. Both types of complexes are attached to the PS-rich inner leaflet of the plasma membrane of the chondrocytes becoming incorporated into and facilitating MV formation. Much of the mitochondrial Ca^{2+} released into the cytosol appears to become tied up in these complexes. Confocal imaging of Ca^{2+} ion activity in the hypertrophic cells show that central cytosolic Ca^{2+} levels drop to $<10^{-7}$ M, but peripheral Ca^{2+} levels rise markedly to $\sim 7.5 \times 10^{-6}$ M (307). Because of this Ca^{2+} depletion, cytoskeletal structural proteins like f-actin depolymerize and allow blebbing of MVs from the plasma membrane (69, 73). Upon binding of TNAP to types II and X collagens (95) and proteoglycan core and link protein (95), the tips of the membrane-enveloped cellular microvilli detach and form MVs. These vesicles envelop various cytoplasmic proteins, the PS-Ca^{2+}-Pi complexes, as well as Pi, Mg^{2+}, and other electrolytes, and attach tightly to the extracellular matrix proteins. Subsequently, phospholipase activity in the MV membrane (207) apparently enable externalization of PS-Ca^{2+}-annexin complexes that is facilitated by binding to extracellular proteins like types II and X collagen (405). Based on recent proteomic data (78) it is evident that type VI collagen is also involved in MV attachment.

14.3.1. Histology of cellular Ca^{2+} metabolism during MV formation

The early discovery by Martin and Matthews (271-272) that growth plate chondrocytes accumulate significant amounts of Ca^{2+} in the form of mitochondrial granules prior to the onset of extracellular mineralization in the growth plate provided the first indication of how cells load Ca^{2+} into MVs. The fact that all mitochondria possess the ability to accumulate massive amounts of Ca^{2+} had been known for some time (406-407). Further, studies on Ca^{2+} accumulation by isolated growth plate mitochondria by Shapiro and Lee (408-409) showed that even under hypoxic conditions these mitochondria could accumulate Ca^{2+} – significantly more than those from noncalcifying cells. And as was noted earlier, ultrastructural studies by Brighton and Hunt (382-384) using pyroantimonate staining (Figure 8A–C), as well as the electron probe studies by Hargest *et al.* (380), revealed that the accumulated mitochondrial Ca^{2+} becomes subsequently transferred to MV during growth plate development. These ultrastructural findings were confirmed by Whitson *et al.* (410) using a completely different Ca^{2+} stain which showed that Ca^{2+} accumulated on the inner aspect of the plasma membrane; it became concentrated at the termini of cellular processes from which MV appeared to form. Nearly a dozen different investigations using a variety of chemical and histological methodologies document that mitochondria play a key role in growth plate calcification. These were critically reviewed by Matthews nearly a quarter of a century ago at the Fourth International Conference on Matrix Vesicles (411). And the evidence continues to mount.

14.3.2. Confocal imaging of Ca^{2+} in living growth plate chondrocytes

Imaging studies published first in 1993 (404), and reconfirmed in 1997 (306), document that growth plate chondrocytes exhibit highly active metabolism of Ca^{2+}. Laser confocal imaging of sections of living avian growth plate cartilage using a sensitive Ca^{2+} probe (Indo 1) at low magnification revealed marked differences in Ca^{2+} ion activities within individual chondrocytes in different regions of the growth plate (Figure 11A–B). More detailed study revealed that in the **proliferative zone**, while there were generally lower overall levels of Ca^{2+} (Figure 12A), there were also marked differences in Ca^{2+} levels within sharply defined regions, presumably

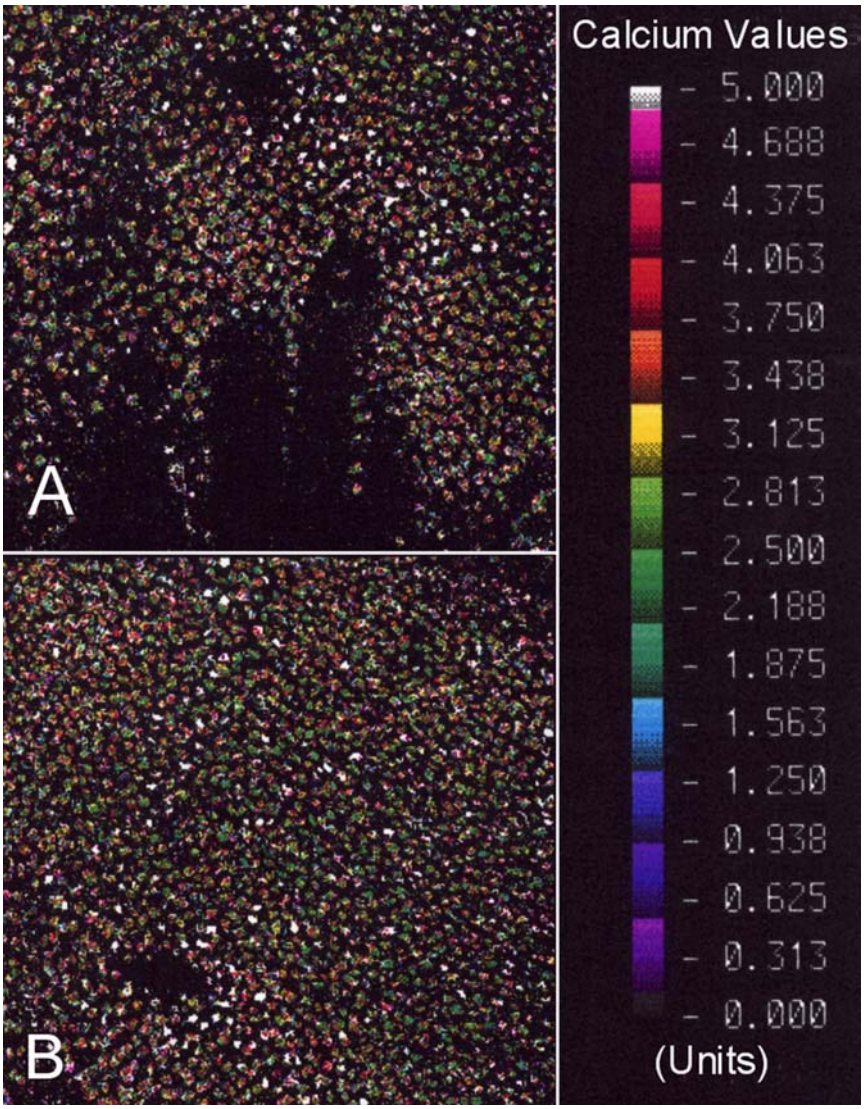

Figure 11. Low Magnification Confocal Imaging of *In situ* Ca^{2+}-Ion Activities in Living Chick Growth Plate Chondrocytes. Sections 50-micron thick of growth plate cartilage from the proximal end of the tibia of 6- to 8-week-old broiler strain chickens were collected in synthetic cartilage lymph (SCL) (54) and incubated in a fluorescent Ca^{2+} indicator, Indo 1-AM (0.5–2.5 microM) (580) at 25 ºC in the dark for 30 to 60 min. The tissue slices were rinsed with phosphate buffered saline (PBS), (10 mM Na phosphate, 150 mM NaCl, pH 7.5) and mounted on glass slides with a drop of PBS under a thin cover slip, then examined at room temperature using an ACAS 570 laser Confocal imaging system (Meridian Instruments, Inc., Okemos, MI). The excitation wavelength was set at 355 nm and the emission wavelengths at 405 and 485 nm. The ratio of Ca^{2+}-chelated Indo 1 to free Indo 1 (405/485) in the cells was used to estimate intracellular Ca^{2+} levels. Generally, the following settings were used: photomultiplier tube-1, 485 nm (40%); photomultiplier tube-2, 405 nm (60%); step size, 0.5 micron; x,y points, 180; scan delay, 40 sec; step speed, 0.5 mm/sec; argon laser power, 100 mw; scan strength, 10%; sample points, 128; Confocal mode; pinhole size, 125. For low magnification maps, a step size of 5 microns was used. 11A – Longitudinal imaging. The invasion of capillaries (black areas) is from the bottom of the tissue section. Note the much higher Ca^{2+} ion activity (white and red colored) in numerous cells just ahead of the invading capillary tips. 11B – Cross-sectional imaging. The invading capillaries (black areas, bottom left) are associated with numerous white colored (high Ca^{2+}) cells; further away the cells tend to stain green (lower Ca^{2+}). These low magnification sections provide a broad sense of the relationship between capillary invasion and levels of cellular Ca^{2+}-ion activity. The range in size of the cells is ~20 microns near the invading blood vessels to ~6–8 microns in the deeper areas. The bar (right) shows relative Ca^{2+} values: black–purple–blue (0.0–1.25 Ca^{2+} values) ~0.02–0.05 microM; green shades (1.6–2.7 Ca^{2+} values) ~0.1–0.3 microM; yellow–orange shades (2.7–3.5 Ca^{2+} values) ~0.3–0.5 microM); red shades (3.6–4.7 Ca^{2+} values) ~0.5–1.5 microM), white (5.0 Ca^{2+} value, >10 microM). In subsequent figures, where indicated, Ca^{2+} ion activities were calculated from standard curves using separate scans. (Unpublished data, with permission from Licia N.Y. Wu)

.

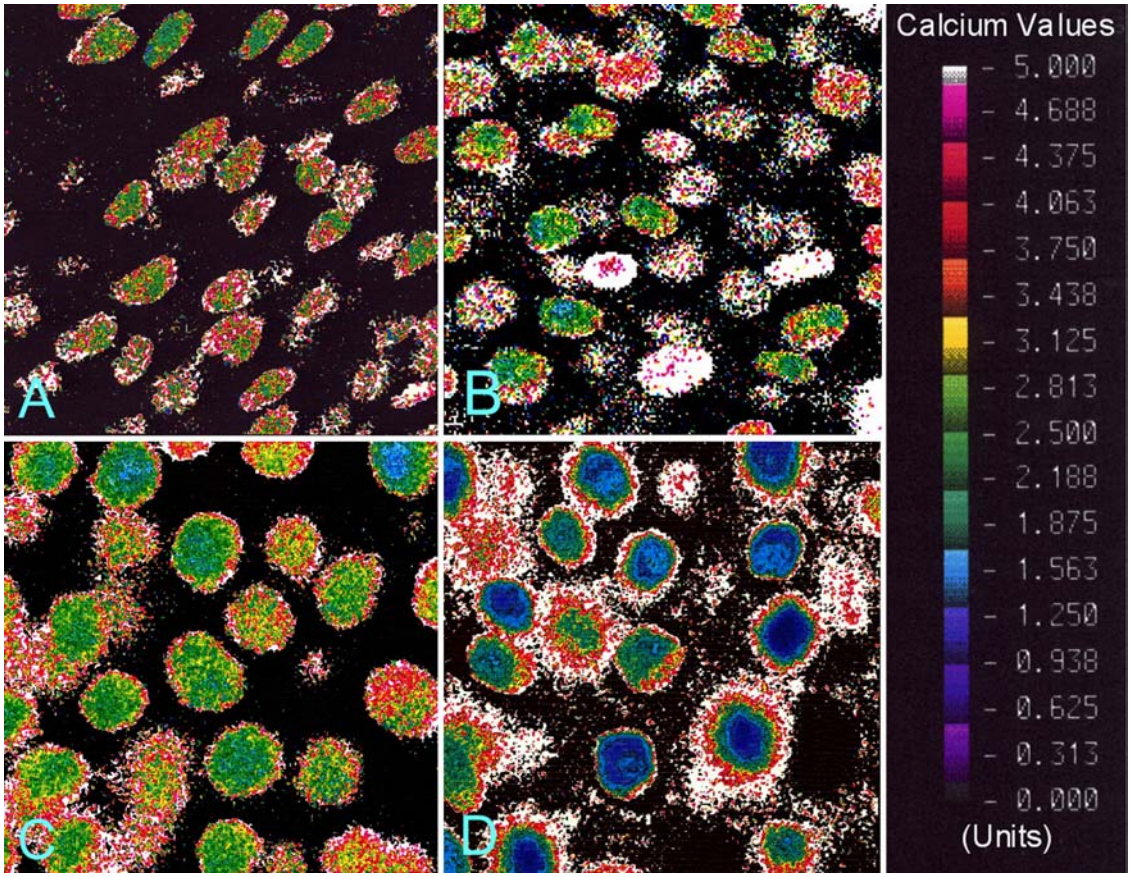

Figure 12. Confocal Images of *In situ* Ca^{2+} Ion Activities in Living Chondrocytes in Different Zones of the Growth Plate. For this medium magnification imaging, the scanning parameters used were as described in Figure 11; but here a step size of 0.5 microns was used. 12A –Proliferating zone. These proliferating cells were much smaller and flatter than in the successive zones (6–8 micron diameters) and that the cells generally had inter-mixed many different levels of Ca^{2+} in the subcellular organelles. The cell nuclei were typically lower in Ca^{2+} (green, <0.1 microM) than the surrounding cytoplasmic compartments. Generally, the overall average level of Ca^{2+} was low. 12B – Maturation zone. The cells were considerably larger (8–10 micron diameters) than in the preceding zone. Numerous cells contained high levels (red – white, 1.5–>10 microM) levels of Ca^{2+}, although these levels of Ca^{2+} were continually rising and falling (See Figure 13). The Ca^{2+}-rich maturation cells were closely associated with the invading capillaries. 12C – Hypertrophic zone. The hypertrophic cells are much larger (17–25 micron diameters) and rounder than those in the preceding zones and show marked difference in Ca^{2+} levels from cell to cell – some with relatively high levels of Ca^{2+} (much of the intracellular area red, *ca.* 4 microM); others with much lower (0.1 microM) Ca^{2+} activity (green). In these hypertrophic cells, Ca^{2+} activity was significantly higher near their cell periphery. Some of the Ca^{2+}-loaded cells appear to be shedding off Ca^{2+}-rich vesicles from their perimeters. 12D – Calcifying zone. The cell size was somewhat reduced (~15–17 micron diameters). There were marked differences in Ca^{2+} ion activity in these cells; some had extremely low activity (<0.05 microM, blue) and others had very high Ca^{2+} activity, especially near their perimeters where a large number of Ca^{2+} rich (white, >10 microM) particles (vesicles) were being exfoliated from the peripheral surfaces. (These particles are membrane-enclosed vesicles; otherwise the Indo 1 dye would have dissipated into the surrounding medium.) (Adapted from (306) in color.)

corresponding to endoplasmic reticulum, mitochondria and nuclei. Although marked variations were seen between different regions within the cells and between individual cells, few cells had overall high levels and the nuclei obviously had very low Ca^{2+} levels. In the **maturation zone** there was a marked increase in the differences in Ca^{2+} levels of individual chondrocytes (Figure 12B); some had very high overall levels; others had quite low levels; some had intermediate levels similar to those in the proliferative zone. Ca^{2+} levels near the plasma membrane were clearly the highest. In individual cells, overall Ca^{2+} levels rose and fell within a matter of minutes; cells with high levels of Ca^{2+} tended to loose it, while those with low levels tended to gain it (Figure 13A). In the greatly enlarged cells of the **hypertrophic zone**, the previous Ca^{2+} oscillations appeared to have transferred much of the Ca^{2+} to the cell perimeter (plasma membrane), where it was then shed as highly-Ca^{2+}-enriched microstructures (MVs) into the extracellular matrix (Figure 12C). The volume of the cells in this region of the growth plate was almost ten-fold larger than those of the proliferative zone (306). In the **calcifying zone**, as the cells shed Ca^{2+}-loaded MVs, the central cytosol became

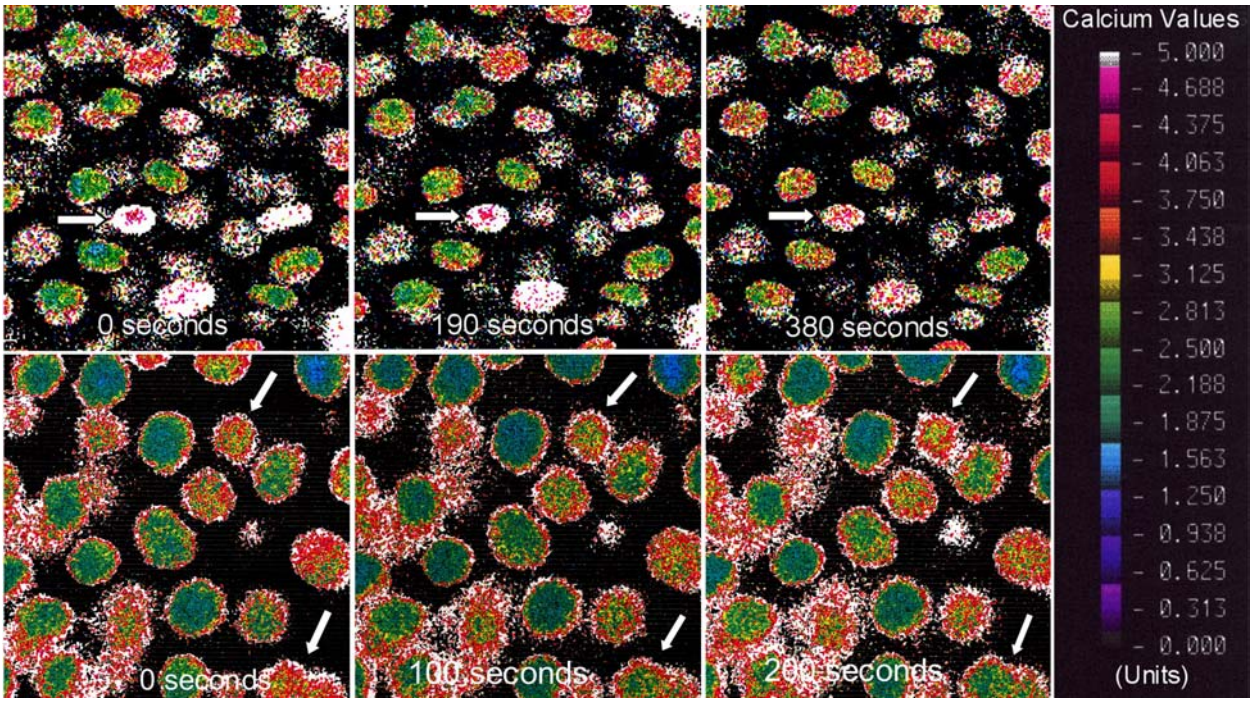

Figure 13. Dynamic Variations in Intracellular Ca^{2+} Ion Activities in Chondrocytes from the Maturation and Hypertrophic Zones of Chick Growth Plate Cartilage Multiple scans of the same area in different zones of the growth plate were performed using the scanning parameters described above, except that the scan delay was typically set at 95 seconds and 5 successive scans were obtained with an interval of 0 to 5 seconds between scans. 13A – Maturation zone. The first scan (0 seconds, left panel) reveals marked differences between individual cells. In the lower left center (white arrow) a high-Ca^{2+} cell (red center, 2–4 microM; white periphery, >10 microM) is surrounded by three low-Ca^{2+} cells (green centers – 0.2 microM, orange periphery – 0.8 microM). 190 seconds later (center panel) the Ca^{2+} level of the central cell has decreased significantly, whereas in the surrounding cells, Ca^{2+} levels have increased. At 360 seconds (right panel), the level of Ca^{2+} in the center cell of the cluster has further declined, whereas that of the surrounding three cells has increased. 13B – Hypertrophic zone. At time zero (left panel) there were marked differences in the levels of different cells, many cells appearing to be shedding Ca^{2+}-rich vesicles. In the successive 100-second time periods, note the numerous changes in intracellular Ca^{2+} actitivy. Some Ca^{2+}-rich cells (*e.g.* upper arrow and another one cell removed to its left) were increasing in ion activity from one with a green and red center to one with a red and white periphery beginning to shed Ca^{2+}-rich vesicles. In contrast, other high Ca^{2+} cells (two pointed at by lower arrow, one above the cell pointed to by the upper arrow) were obviously decreasing in Ca^{2+} activity. (Adapted from (306) in color.)

markedly lower in Ca^{2+} than in the preceding zone (Figure 12D). The overall impression was that after a crescendo of rising and falling Ca^{2+} levels, the cells exfoliated the accumulated Ca^{2+} *via* a burst of Ca^{2+}-loaded vesicles that were shed from their perimeter (Figure 13B).

14.3.3. Biochemistry of mitochondrial Ca^{2+} metabolism

TEM studies of the growth plate showed clear evidence of Ca^{2+} loading in mitochondria, with subsequent transfer to MVs (383, 384). On the other hand early biochemical studies by Lee and Shapiro indicate that functional mitochondria can be isolated from epiphyseal chondrocytes that are able to carry out oxidative phosphorylation (412-413). These isolated chondrocyte mitochondria accumulated maximal Ca^{2+} when ATP and a respiratory substrate (*e.g.* citrate or alpha-ketoglutarate) were available (409). Uncouplers of oxidative phosphorylation, or inhibitors of respiration, impeded Ca^{2+} uptake – as is seen in mitochondria isolated from non-calcifying cells. Further, there was heterogeneity in the extent of Ca^{2+} loading (*i.e.* density) of the growth plate mitochondria. Ca^{2+} accumulation increased from the proliferative zone to the early hypertrophic zone of the growth plate (414). Then in the hypertrophic zone where MVs most rapidly form, mitochondrial levels abruptly fell – a finding later confirmed by Hargest (380). Accumulation of excessive Ca^{2+} is known to inhibit mitochondrial respiration – as is true in all mitochondria (415). However, growth plate mitochondria appear to be more tolerant of Ca^{2+} accumulation than most (409). The general mechanisms by which mitochondria transport Ca^{2+} have been thoroughly reviewed by Gunter and Pfeiffer (416-417). Mitochondria primarily utilize a uniporter system for transporting Ca^{2+} into the inner matrix, driven by the electro-chemical gradient produced by mitochondrial respiration. It can be best described as a "very fast gated pore" (416). This property was studied in growth plate mitochondria by Lee and Shapiro (418) who found that Ca^{2+} uptake was similar to that from noncalcifying cells. They observed that inhibitors of mitochondrial respiration caused rapid loss of greater than 80% of the Ca^{2+}. However, in mitochondria isolated from

the "most calcified" zone there was increased "nonspecific Ca^{2+} binding"; and, a high percentage of the accumulated Ca^{2+} was "non-extrudable", apparently in the form of mitochondrial granules – in agreement with the ultrastructural observations noted previously. There are two primary mechanisms by which mitochondria are able to release stored Ca^{2+}; these are Na^{+}-dependent and Na^{+}-independent pathways – evident in all cells studied (416). For most cells, including growth plate chondrocytes up to the zone of maturation, mitochondria primarily regulate cytosolic Ca^{2+} ion activities by these two Ca^{2+} carriers. However, another more substantial pathway of mitochondrial Ca^{2+} release is of special importance to growth plate mineralization. This is the so called "mitochondrial permeability transition" (MPT), a mechanism involving a marked change in the permeability of the inner mitochondrial membrane. It involves a dramatic loss of membrane potential, as well as rapid leakage of K^{+}, Mg^{2+}, Ca^{2+}, Pi and other small ions and molecules from the mitochondrial matrix (419-420). This massive release of mitochondrial electrolytes is closely associated with the onset of apoptosis in many cell types (421-424); however, it is of key importance in the formation of MVs by growth plate chondrocytes. The MPT is brought about by first preloading of mitochondria with Ca^{2+}; and then by inducing Ca^{2+} release *via* an agent that activates the MPT pore. Among the various cofactors known to function as Ca^{2+}-releasing agents in the MPT, the most potent and best studied is inorganic phosphate (Pi) (416).

14.4. Growth plate cellular Pi metabolism

Thus, cellular Pi metabolism is deeply entwined with Ca^{2+} metabolism. Cells require Pi for a plethora of basic cellular functions ranging from synthesis of DNA and RNA to metabolic intermediates directly involved in energy metabolism. Over and beyond this in the growth plate, Pi is needed for formation of the calcium phosphates that initiate solid phase formation during bone growth. Growth plate cartilage has been shown to possess unusually high levels of both cytosolic (20-25 mM) and extracellular (2.2-2.5 mM) Pi (63). In fact, studies by Mansfield *et al.* (425-426) have documented that exposure of terminally differentiated, cultured tibial growth plate chondrocytes to even modestly elevated levels (3 mM) of extracellular Pi induces 'apoptotic' cell death within 48 h. Apoptosis of these cells is mediated *via* the MPT mechanism (314). It is noteworthy that the release of mitochondrial Ca^{2+} via the PMT also activates uptake of Ca^{2+} by the endoplasmic reticulum, which in turn releases Ca^{2+} into the cytosol (427). These findings explain how Ca^{2+}, first stored in mitochondria of growth plate chondrocytes, becomes released. It causes elevation in cytosolic Ca^{2+} levels – ultimately at the cell periphery, as confocal imaging of Ca^{2+} metabolism has indicated (306). Of direct interest to growth plate mineralization, Type VI collagen receptors on the cell surface (109, 110) act as transducers to mitochondria, affecting opening of the MPT pore for Ca^{2+} (111). This appears to trigger mitochondrial Ca^{2+} unloading (112).

14.4.1. Chondrocyte mitochondrial PiC Pi-transporter

To better understand the processes by which mitochondria take up Pi, the PiC transporter will now be discussed. Mitochondrial acquisition of Pi is essential for oxidative phosphorylation – an energy-capture process vital to all aerobic eukaryotic cells. Mitochondrial uptake of Pi is largely accomplished by PiC, an H^{+}/Pi symporter (or Pi/OH^{-} antiporter) (428-429). PiC is an integral membrane protein, a homodimer that resides in the inner mitochondrial membrane that translocates or exchanges Pi from the cytosol into the mitochondrial matrix (430). PiC is Na^{+}-*independent* and is responsible for the rapid import of Pi used for ATP synthesis. The mitochondrial PiC transporter has been cloned and sequenced from chicken growth plate cartilage (336). The molecular mass of the mature protein is 34,985. Hydropathy plots indicate that PiC is a highly compact protein with 6 transmembrane domains; both the N-terminal and C-terminal ends reside in the mitochondrial matrix lumen. *In situ* hybridization analysis reveals that mitochondria PiC is most strongly expressed in the maturation/prehypertrophic zone, although it is expressed at low levels throughout the growth plate (Figure 7A) (336). However, note that at the terminus where the cells become apoptotic and vascular penetration occurs, many cells are devoid of PiC message. Of pertinence here, analysis of PiC gene expression in primary mineralizing cultures of chicken growth plate chondrocytes reveal that the gene is only weakly expressed *early* in culture; it becomes progressively more highly expressed as the cultures mature and calcify. These features match the Na^{+}-*independent* Pi porter described by Wu *et al.* Thus it is apparent that this high-capacity mitochondrial PiC porter is the one whose expression is enhanced by elevated Pi levels in the culture medium (303).

14.4.2. Chondrocyte plasma membrane Pi-transporters

At this point, we need to return to Pi uptake and transport in the plasma membrane of growth plate chondrocytes. Recall that two Na^{+}-dependent (type III Glvr-1 and type II) plasma membrane Pi transporters (334-335, 426, 431) are present in growth plate chondrocytes and MVs. Subsequent studies have confirmed the presence of the PiT type III (Glvr-1) Pi porter in growth plate chondrocytes, but *in situ* hybridization studies reveal that it is expressed strongly only in the resting and proliferative zones; there is almost no expression in the maturation/hypertrophic zone (Figure 7B) (336). Again, note that it is also expressed in the early growth plate chondrocyte cultures, but declines as the cells mature and begin to induce calcification (303). As indicated above, these studies also uncovered evidence for a Na^{+}-*independent* Pi transporter whose expression was upregulated as the cells approached hypertrophy. In contrast to the Na^{+}-dependent Pi transporters that are upregulated by falling Pi levels, expression of this porter is induced by culturing the chondrocytes in media containing slightly elevated levels of Pi (2–3 mM) – levels typical of the extracellular fluid of growth plate cartilage. This Na^{+}-*independent* Pi transporter had a pH optimum of 7.6–8.0, appropriate for the pH of growth plate extracellular fluid (63, 338).

14.4.3. Growth Plate Chondrocyte Mitochondrial Permeability Transition (MPT) Pore

The key Pi-sensitive MPT pore appears to be

directly involved in the apoptotic demise of hypertrophic chondrocytes (314). Under conditions of mitochondrial Ca^{2+} overload, especially when accompanied by oxidative stress, elevated Pi levels and ATP deletion, this non-specific MPT pore opens in the inner mitochondrial membrane (432-436). This allows rapid release of mitochondrial electrolytes, including both Pi and Ca^{2+}. Immediately, ATP synthesis effectively stops; and as noted before, there is clear evidence that hypertrophic growth plate chondrocytes rapidly become energy depleted. Several independent studies reveal that the levels of ATP in hypertrophic cells are greatly reduced compared to resting or proliferating cells (302, 437-439). Hydrolysis of ATP, which is typically present in 5–10 mM levels in healthy, active cells, would release large amounts of Pi. And direct analyses of the Pi levels of isolated growth plate chondrocytes reveal the presence of high cytosolic levels in the range of 20–25 mM (63). This has been confirmed by ^{31}P-NMR analysis of growth plate chondrocytes (404, 438). However later in this process, breakdown of cellular phospholipids through the action of phospholipases (223) and the action of PHOSPHO-1 (202-203), may also contribute to the elevated Pi levels in the cytosol of growth plate chondrocytes. Taken together, these findings reveal an intricate scenario in which Ca^{2+}-loaded mitochondria, subjected to oxidative stress, and exposed to elevated levels of cytosolic Pi, release their electrolytes via the MPT into the cytosol. In this process, they induce a specialized form of apoptosis in which the released Ca^{2+} and Pi combine with PS and AnxA5 to form complexes that contribute to MV formation, and ultimately to mineral formation. Upon Ca^{2+} release, microvilli-like cellular membrane extensions are formed, a process that depends on the activity of phospholipases and scramblases that modify the membrane lipid composition, as well as the inside/outside orientation of the lipids in the membrane. During this complex event, membrane-associated proteins like TNAP become externalized allowing them to interact with matrix proteins. Upon binding to the extracellular collagens (Types II, VI, X) these cellular extensions bleb off to form of vesicles – MVs – primed with sufficient levels of both Ca^{2+} and Pi in the form of a nucleational core of ACP-PS-AnxA5 complexes that serve as the nidus for triggering extracellular mineral formation.

14.5. Growth plate cellular H^+ (pH) metabolism

The pH of both the extracellular and intracellular fluids also has a profound effect on the process of MV formation. Because growth plate chondrocytes are embedded in a highly viscous tissue comprised of large amounts of high molecular weight proteoglycans, their pH is largely governed by their anaerobic metabolic activity. However, in weight-bearing joints, the on-off pressure exerted by body movements enables exchange of fluid despite the limited vasculature of the tissue. This exchange of fluid ameliorates the tendency toward acidification. There are also zonal differences in cellular metabolism ranging from the quiescent "resting" zone through the zone of rapid cellular proliferation to the zone of hypertrophy where the cells undergo apoptotic formation of MVs. These changes in metabolic activity influence the cellular pH, which has been documented by confocal imaging using the fluorescent probe, BCECF.

14.5.1. Confocal imaging of H^+ (pH) in living growth plate chondrocytes

The pH of growth plate chondrocytes *in situ* has been measured using confocal imaging with BCECF as a fluorescent probe (306). Low magnification confocal imaging shows that in different regions of the growth plate there are sharp differences in pH between individual cells (Figure 14A–B). At higher magnification, it became evident that this occurred in various intracellular compartments where pH levels ranged from pH 6.2–8.0. In the proliferating zone, *average* cytosolic pH (pH 6.95±0.05) was generally lower than in the other zones, although there were many focal regions of lower and higher pH (Figure 15A). For example, the pH of the nuclei of the cells tended to be low (pH 6.5-6.7), a finding not as apparent in the maturing and hypertrophic zones. In the zone of maturation, the *average* pH (7.39±0.04) was significantly higher and was characterized by the presence of many focal regions of distinct alkalinity (pH 7.8–8.0) (Figure 15B). In the hypertrophic zone, the overall pH (7.19±0.04) was slightly lower than in the maturation zone. While there were many regions of alkalinity, notice that in the periphery of the cells, the pH was significantly more acidic (Figure 15C). In the zone where extracellular calcification was already occurring, the intracellular pH was lowered even further (6.76±0.03); there were few focal areas of alkalinity (Figure 15D). These findings are interpreted as follows:

In the **proliferating zone**, the key cellular activity is replication, whose rate is governed by both genes and growth factors (440). Cell replication requires a constant source of raw materials for DNA and RNA synthesis, as well as metabolic energy. Because of their cloistered avascular environment, there is low O_2 tension in these cells (216, 390, 441). Most of their energy is derived from glycolytic production of ATP (216). The generally lower cellular pH in the proliferative zone appears to result from glycolytic production of lactic acid. In the **zone of maturation**, different forces are operative. Cell division has largely ceased; and the cells, because of their closer proximity to the invading blood supply, are affected by the increasingly available supply of O_2, nutrients, Ca^{2+} and Pi (395). There is an awakening of mitochondrial oxidative metabolism, as well as the active acquisition and storage of Ca^{2+} within the mitochondria (382, 409). With the increased metabolic activity, there is synthesis of a variety of new proteins that become involved in the mineral-forming process. At this stage, the cells begin to undergo a measurable increase in volume (306). Apparently due to the sharply increased oxidative phosphorylation, these maturing cells show marked alkalinization in areas that appear to be organelles like the mitochondria and the endoplasmic reticulum (306). At this stage there is maximal Ca^{2+} storage by the mitochondria (409), which adversely affects their ability to produce ATP (408). When the demand for ATP exceeds the ability of the impaired Ca^{2+}-loaded

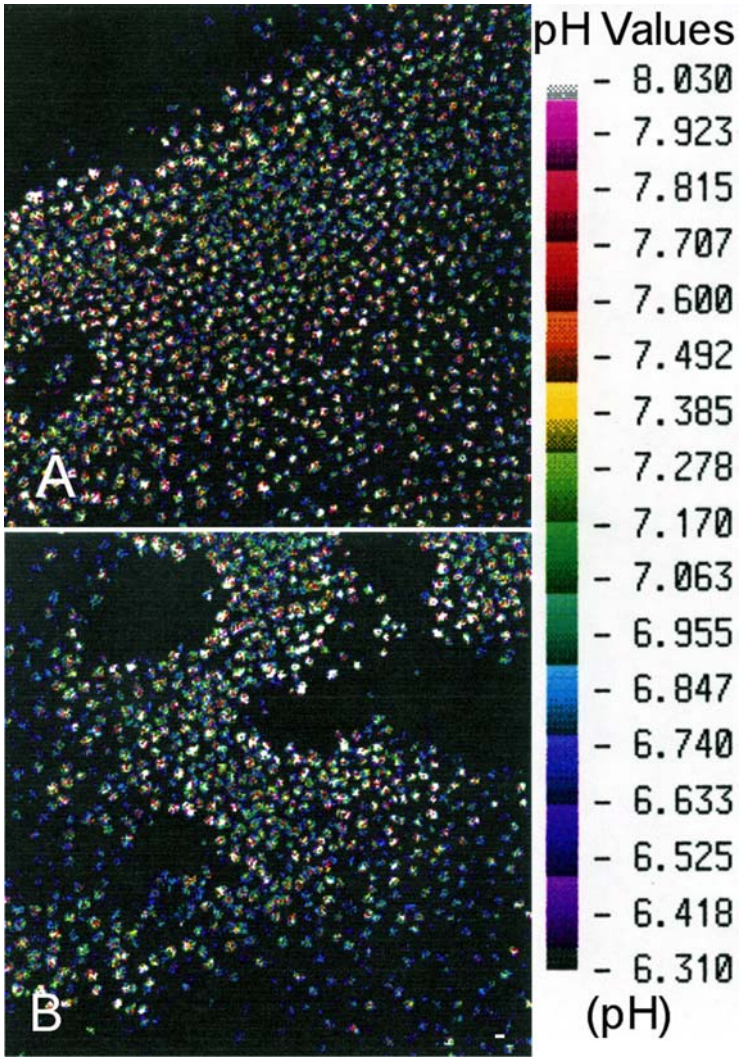

Figure 14. Low-Magnification Confocal Imaging of *In situ* H^+ Ion Activity (pH) in Living Chick Growth Plate Chondrocytes. Growth plate tissue slices were prepared as described for Ca^{2+}. For loading BCEF acetoxymethyl ester (BCEF-AM), the fluorescent probe for pH, a dimethylsulfoxide stock solution was added to slices of cartilage in SCL to give a final concentration of 0.5 microM. After incubation for 30 to 60 min at RT, tissue slices with BCECF-loaded cells were rinsed with PBS before making intracellular pH studies. The excitation wavelength was 488 nm and emission wavelengths of 530 (photomultiplier tube-1) and 650 nm (photomultiplier tube-2, free form) were used. The following settings were used: laser power, 100 mW; scan strength, 15%, 10% neutral density filter; photomultiplier tube-1 (40%)/photomultiplier tube-2 (70%); step speed, 0.5 mm/sec; sample points 128; X, Y points, 180; Confocal mode; pinhole, 124. The ACAS ratio quantitation program of photomultiplier tube-1/photomultiplier tube-2 was used. 14A – Cross-section showing showing proliferative and maturation cells. The lowest pH values (7.2–6.8, green–blue-green) were generally seen in the cells away from the penetrating capillary and edge of tissue. 14B – Cross-section showing mainly hypertrophic and calcifying cells. Black areas are penetrating capillaries. The highest pH values (7.8–8.0, red–white) were generally seen in cells nearest to the capillaries. Cells deeper in the calcified cartilage had significantly lower pH (6.7–6.9, blue–blue-green). pH *vs*. color scale at right. (Unpublished data, with permission from Licia N.Y. Wu.)

mitochondria to supply, levels of Pi build up in the cytosol (63, 438, 442) setting up eventual apoptosis. In the cell's struggle to control cytosolic Ca^{2+}, there is a cyclical rise and fall of Ca^{2+} levels (306) (Figure 13A–B).

Approaching the **zone of hypertrophy** a crisis point is reached that triggers the opening of the mitochondrial transition pore described earlier (314). ATP synthesis ceases. A flood of stored Ca^{2+}, electrolytes, nucleotides, and small proteins leaves the damaged mitochondria. The rising levels of cytosolic Ca^{2+} activate intracellular proteases and phospholipases that in turn begin to release large amounts of free amino acids – as well as damage the intracellular membranes.

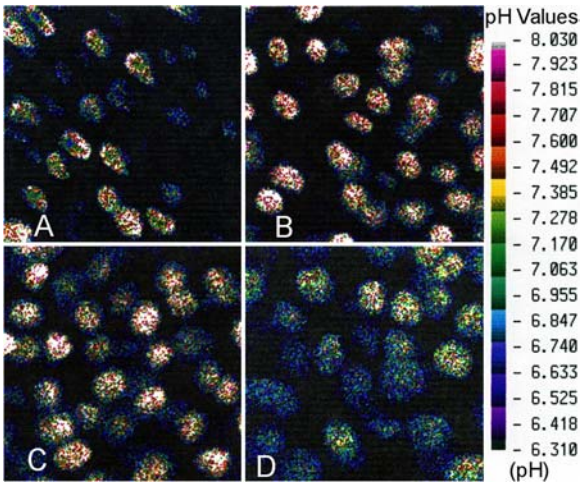

Figure 15. Confocal Imaging of *In situ* H^+ Ion Activity (pH) in Chondrocytes in Different Zones of the Living Chick Growth Plate. 15A – Proliferating zone. Note the marked variety in pH level within individual cells and within intracellular areas. The nuclei of several cells have a significantly lower pH (~6.8) than the surrounding organelles and cytoplasm which have a range of pH (6.8–7.9). Some cells deeper in the section are more acidic (bluish green, pH ~6.7). 15B – Maturation zone. More of the cells have areas of intense alkalinity (red and white, pH 7.8–8.0); relatively few cells have low pH (6.8). 15C – Hypertrophic zone. There is more variability in pH than in the maturation zone; fewer cells have areas of intense alkalinity. The pH at the periphery of all the cells is distinctly more acidic (pH 6.6–6.8) than in the central cytosol. 15D – Calcifying zone. Most of the cells have large areas of more acidic pH (6.6–6.8); all cells tend to be acidic in the periphery. (Adapted from (306) in color.)

The level of ATP plummets as metabolic demand exceeds the available supplies (395, 442). Intracellular levels of Pi increase dramatically (63, 438). With the rise in amount of low molecular weight solutes, there is influx of water that causes marked osmotic swelling; the cells become hypertrophic. At this time, there is movement of both Ca^{2+} and H^+ to the cell periphery where pH levels fall (306). Facilitated by the presence of the annexins, Ca^{2+} and Pi bind to PS on the inner leaflet of the plasma membrane to form PS-Ca^{2+}-Pi complexes (PS-CPLXs) (60, 61). Dissociation of cytoskeletal actin fibrils facilitates the blebbing of MVs from cell processes (69, 73). The newly forming vesicles carry with them the annexins (60, 61), the PS-CPLXs (64), the encompassed electrolytes (Pi, Mg^{2+}, Ca^{2+}, K^+, Na^+) (63), as well as various cytosolic enzymes (*e.g.* the family of glycolytic enzymes) and proteins (78). Because the pH near the plasma membrane of these cells is slightly acidic (pH 6.5-6.9), even though the levels of Ca^{2+} and Pi are sufficiently high, ACP cannot form (77). However at this pH, Mg^{2+}-containing PS-CPLXs can form readily (266) and become a key component of the nucleational core of MVs (288, 443). Upon release of the MVs into the extracellular space where the pH is more alkaline (pH 7.5–7.6) (63, 339), the high levels of enclosed Ca^{2+} and Pi readily combine to form ACP. But because of abundant Mg^{2+}, ACP is stabilized and does not immediately dismutate to OCP or HAP (444). In the **zone of calcification** when the hypertrophic chondrocytes are "spent" and the extracellular matrix around them begins to calcify around the MVs, the levels of intracellular Ca^{2+} markedly decline (Figure 12D, Figure 13B) and the aveage pH of the cytosol falls to 6.76±0.03 (Figure 15D). There are few focal areas of high pH such as was seen in the maturing and hypertrophic cells. These cells generally are eliminated by macrophages during the invasion of the capillaries from the marrow cavity. In avian species, however, there is evidence that some growth plate cells survive, become reprogrammed (445-446), and express osteoblast-like character (447), producing type I instead of type II collagen, etc. Attention must now be directed toward the mechanism by which newly formed MVs induce *de novo* crystalline mineral – once they are released into the extracellular matrix.

15. THE KINETICS OF MINERAL FORMATION BY MATRIX VESICLES

15.1. Differing views of MV mineral formation

Many types of *in vitro* studies have been conducted to explore the ability of isolated MV to accumulate Ca^{2+} and Pi and form crystalline mineral deposits. It should come as no surprise that numerous differences have been reported with regard to: 1) the requirement for ATP (82, 187, 448) or other organic phosphates (66, 449), 2) the regulatory effects of Zn^{2+} (317, 385, 450), 3) the kinetics of mineral ion accumulation (332, 451-453), and 4) the nature of the first mineral phase produced (57, 65, 77, 387-388, 454). Most of these differences can be traced to the differing methods of MV preparation, the species from which they were obtained, the extent of damage imposed on the structures during isolation from the tissue, and the method used for assessing the timing, rate, and amount of mineral formation. Rather than dwell on these differences, attention will be focused on MVs that have been released from normal avian cartilage using carefully controlled levels and timing of protease exposure. These MVs can be obtained in a good yield, in a high state of purity, and induce mineral formation within a few hours when incubated in a synthetic cartilage lymph (SCL) matched to that of the extracellular fluid in growth plate, with no added organic P substrates required (60-62, 76). Their activity will be compared with MV-enriched microsomes that have not been exposed to exogenous proteases.

15.2. Radio-isotope analyses of the kinetics of Ca^{2+} and Pi accumulation

MVs isolated by modified collagenase digestion of growth plate cartilage from broiler-strain chickens, or MVEM isolated by the previously-described nonenzymatic tissue homogenization methods, acquire mineral ions from synthetic lymph and rapidly induce the formation of crystalline solid phase mineral in a sequence of predictable stages (Figure 16A) (62, 65-67, 317, 332) Studies measuring simultaneous uptake of $^{45}Ca^{2+}$ and ^{32}Pi during MV mineralization indicated that an OCP-like, low

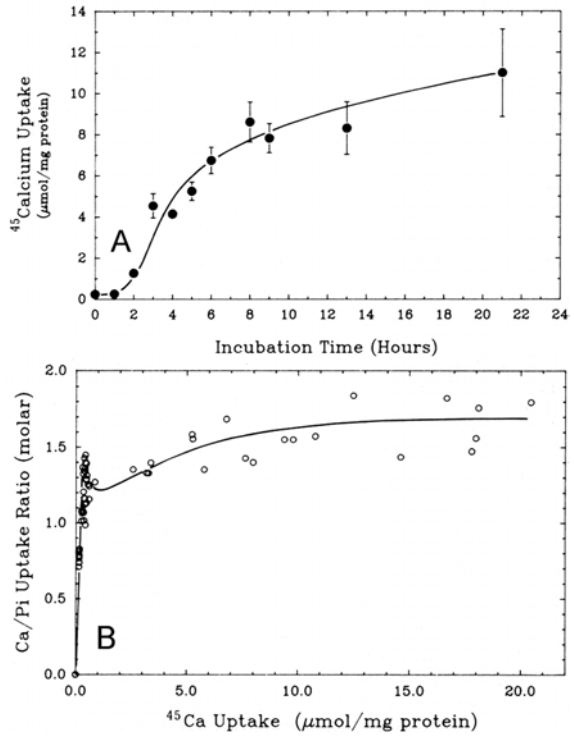

Figure 16. Time-Course of $^{45}Ca^{2+}$ Accumulation and Change in $^{45}Ca^{2+}/^{32}Pi$ Molar Ion Uptake Ratio during MV Ion Loading from SCL *in vitro*. 16A – $^{45}Ca^{2+}$ accumulation. MV were incubated in SCL at 37ºC for the indicated times, collected by micro-filtration, and assayed for $^{45}Ca^{2+}$ uptake (449). Values are the mean ± standard error of 4 separate incubations. 16B – Change in Ca^{2+}/Pi molar ion uptake ratio. MVs were incubated in $^{45}Ca^{2+}$ and ^{32}Pi double-labeled SCL at 37 ºC as indicated in A. Note the rapidly increasing Ca^{2+}/Pi uptake ratio during the early limited ion accumulation. This is followed by a brief decline in Ca^{2+}/Pi ratio to about 1.3 during the rapid formation period, followed by a gradual increase in Ca^{2+}/Pi ratio to 1.60 during the slow formation period. (Reproduction from (455) with permission from the Institute for Scientific Information.)

(1.33) Ca/P-ratio mineral forms during the early phase of rapid mineral ion accumulation (Figure 16B) (65, 455). Later during the slow uptake period, the Ca/P ratio rose to ~1.60, indicating progressive transformation into HAP-like mineral (Figure 16B). These findings are in close accord to studies using FT-IR, which reached the same conclusion (Figure 10) (387). Both approaches reveal that mineral formation by MVs is not a simple process; it involves several solid phases prior to the formation of the thermodynamically stable HAP, the major mineral of mature bone. Based on extensive studies, the kinetics of MV calcification generally involve the following sequence of events: 1) exchange of ions at the vesicle membrane surface, 2) selective acquisition of Ca^{2+} in preference to Pi during a lag period in which very limited ion uptake occurs, 3) a transient induction period in which the Ca^{2+}/Pi uptake ratio rapidly declines, indicative of selective Pi uptake, followed by 4) a rapid accumulation of both Ca^{2+} and Pi at a Ca^{2+}/Pi stoichiometry of close to 1.33, and 5) finally, an extended period of slower acquisition of both mineral ions at a gradually rising Ca^{2+}/Pi ratio approaching that of Ca^{2+}-deficient apatite (~1.60) by the end of 24 h. Interpretation of these five stages of MV mineral formation now follows.

15.2.1. Stage 1 – initial exchange period

When isolated MVEM are exposed to $^{45}Ca^{2+}$- or ^{32}Pi-labeled SCL, there was initially a rapid, but very limited uptake of both ions that corresponds to an exchange with ions bound to proteins and/or acidic phospholipids at the vesicle surface (Figure 16A) (65, 449, 456). During this brief period, $^{45}Ca^{2+}/^{32}Pi$ uptake ratios rapidly increased from very low values (<0.7) to values typically above 1.5, indicating a preferential binding of Ca^{2+} (Figure 16B) (57, 455).

15.2.2. Stage 2 – the lag period

Stage 1 is followed by a lag period of variable duration during which little further accumulation of Ca^{2+} and Pi occurs. The lag period can be extended in several ways that do not preclude eventual induction of mineral formation. For example, by adding low (*i.e.* 5 micromolar) levels of Zn^{2+} to the SCL in which the MVs are incubated, Ca^{2+} accumulation is essentially blocked (Figure 17A). The inhibitory effect of Zn^{2+} can be rapidly eliminated by treatment of MVs with *o*-phenanthroline, a group 2B metal ion chelator that binds tightly to Zn^{2+} (Figure 17B) (76, 317, 385). Thus, one explanation of the lag period is that it represents the time needed for displacement of Zn^{2+} by Ca^{2+} at key sites that enables rapid ion acquisition. Zn^{2+} binds tightly to AnxA5 in the presence of PS (Figure 4C) (60). While Zn^{2+} has been shown to block the apparent Ca^{2+}-channel activity of AnxA5 in planar PS bilayers (125), the high levels of Ca^{2+} used and the excessive amount of Zn^{2+} required, cast doubt that this is the physiological action of AnxA5. The lag period also can be greatly extended by exposing active MV to proteases such as trypsin or chymotrypsin (76). In this case, when ion uptake finally begins, it does so at a much lower rate than in the untreated control. However, as noted previously, if these protease-inactivated MVs are treated with detergents that permeabilize the vesicle membrane, mineral formation then rapidly ensues (288, 457). This indicates that the lag period is a rate-limiting step that represents the inability of mineral ions to pass through the vesicle membrane and reach the nucleational core. In modeling MV mineralization using liposomes encapsulating Pi-buffered intracellular electrolytes (See Section 18), Blandford *et al.* explored several methods for enabling Ca^{2+} to enter the liposomes (318). The most rapid means was found to be by addition of phospholipase A_2 to the incubation mixture; it triggered almost immediate rapid uptake of $^{45}Ca^{2+}$. Since latent phospholipases are evident in MVs, activation of these enzymes would be natural way to breach the membrane block. In fact, in studies of changes that occur in MVs during mineral formation, Wu *et al.* found that phospholipids levels began to decline upon introduction of the MVs into the SCL, accompanied by increased levels of FFA and 1,2-DAG (207). This is evidence of

phospholipase activity, which would increase membrane leakiness and allow entrance of Ca^{2+} and Pi. Thus, the event that signals the end of the lag period appears to be partial degradation of the MV membrane brought about by activation of endogenous phospholipases. This allows access of Ca^{2+} and Pi to the nucleation site, which then can initiate rapid onset of mineralization.

15.2.3. Stage 3 – the induction phase

However, approaching the end of the lag period there is a transient sharp decline in the Ca^{2+}/Pi uptake ratio from ~1.5 to 1.25 (Figure 16B) (57, 455). This is indicative of conversion of ACP to crystalline OCP. In fact, for the induction of rapid mineral formation, two conditions need to be met. First, there must be a means by which the extravesicular Ca^{2+} and Pi can gain access to the nucleation core. Second, there needs to be present within the MV lumen crystalline nuclei that can engender crystal growth. FT-IR analyses reveal subtle conformational changes in MV structure during this period – apparently caused by induction of the first crystalline nuclei (387). Two factors can prevent the conversion of the ACP-containing nucleational core to OCP crystalline nuclei: 1) elevating the pH of SCL to 8.0 (77), which delays induction indefinitely; or 2) incorporation of Mg^{2+} (131, 137), which delays onset of rapid mineral formation for at least 10–12 h. In typical MV mineralization induction of rapid mineral formation occurs within 1–3 h after exposure of the vesicles to the extracellular fluid.

15.2.4. Stage 4 –the rapid acquisition phase

After induction has occurred, rapid acquisition of both Ca^{2+} and Pi ensue. This phase corresponds to the proliferation of the first crystalline mineral phase – an OCP-like, HPO_4^{2-}-containing calcium phosphate mineral (387). The Ca^{2+}/Pi stoichiometry of ion acquisition during this rapid mineral formation period is close to 1.33, characteristic of OCP (450, 457). Both FTIR and FT-Raman spectroscopic analyses of this early mineral phase are consistent with the formation of a poorly-crystalline OCP-like mineral (Figure 10) (387-388). This stage generally lasts for 2-3 h (Figure 16A) and coincides with rapid OCP formation. The acquired $^{45}Ca^{2+}$ by the MVs is not exchangeable with ion-exchange resins until the beginning of the plateau phase (67), indicating that it must occur within the vesicle lumen. This is supported by the fact that the ionic environment within the vesicle lumen would favor growth of OCP in preference to HAP. The fluid is rich in Mg^{2+} and Pi (63, 64), and contains low levels of Zn^{2+} (317) – a combination of factors known to suppress HAP and favor OCP-crystal formation (385). It is also evident that the acidic phospholipid-rich inner membrane, in combination with the MV annexins, facilitates growth of OCP-like crystals along the membrane fluid interface. Crystal growth within MVs is typically seen in close association with the vesicle membrane (2). Such crystal growth, in conjunction with Ca^{2+}-activated phospholipases, would lead to further destabilization and rupture of the vesicle membrane. Crystal growth is also closely associated with TNAP, whose catalytic activity declines progressively as mineralization ensues (76).

15.2.5. Stage 5 – the plateau phase

At the end of the rapid uptake phase there is an extended period of slow accumulation of both Ca^{2+} and Pi, with gradually rising Ca^{2+}/Pi uptake stoichiometry (Figure 16A) (57, 65, 449, 455). The plateau phase appears to coincide with the complete breaching of the vesicle membrane and direct exposure of the nascent crystals to the extravesicular environment. This interpretation is based on the finding that only after this point does the acquired Ca^{2+} become readily exchangeable with ion-exchange resins (67). The nature of the mineral phase formed during the plateau phase is a poorly crystalline HAP; FTIR patterns confirm that it is HAP formed from an OCP precursor, rather than from ACP (Figure 10). The obvious decrease in the *rate* of mineral ion uptake relates to several factors: 1) the progressive depletion of mineral ions available from the SCL, 2) the apparently slow, gradual dismutation of the OCP to HAP, and 3) the adsorption of MV regulatory proteins to the growing HAP crystals. Typically, during 24 h incubation, at most 30-40% of the original Ca^{2+} and Pi in the SCL become incorporated into the newly forming mineral (57, 65, 385, 449, 456). In contrast, if pure HAP crystals are seeded into protein-free SCL, acquisition of about 70% of the mineral ions occurs during a similar incubation period. This marked difference suggests that various factor(s) associated with MVs limit the extent of crystal growth.

16. THE NUCLEATIONAL CORE: THE DRIVING FORCE IN MV Ca^{2+} AND Pi ACCUMULATION

A key question with regard to MV mineralization is what drives the accumulation of Ca^{2+} and Pi by MV? At the outset, let it be stated that it is highly doubtful that ATP-driven active transport processes are involved. This conclusion is based on several facts. *First***,** as has been already argued, the orientation of the Ca^{2+}/Mg^{2+} ATPase pump in the vesicle membrane would be facing outward – favoring loss, not gain, of Ca^{2+}. (There is no evidence that the plasma membrane becomes everted during MV formation.) *Second***,** while there is strong evidence for the abundant presence of Na^+/K^+-ATPase pump proteins in MVs – based on proteomic studies (78), it is obvious that they are not operative. *Third*, there is insufficient ATP in the extravesicular fluid to power such an ion pump (302). Supporting this contention is the finding that MVs have high levels of Na^+ and low levels of K^+ (63), the opposite of what would occur if the Na^+/K^+ pump were operative. Thus, the most logical force for driving Ca^{2+} uptake by MVs is the nucleational core, which provides "sink conditions" – *i.e.* by reducing the ion *activity* of Ca^{2+} within the vesicle lumen to levels significantly lower than those in the extravesicular fluid. MVs create sink conditions by forming an insoluble, metastable Ca^{2+}-Pi phase within the vesicle lumen. Strange as it may seem, while *total* Ca^{2+} (65 ± 8 mM) levels in newly formed MV are much higher than those in the extravesicular fluid (3.2±0.5 mM) (63), the *ionic activity* of Ca^{2+} in the MV lumen is much lower. Based on *in situ* confocal imaging of MVs, the Ca^{2+} *activities* are 7.4 ± 0.3 micromolar (306). These levels are far lower than the 1,000 ± 200 micromolar (*i.e.* 1.0 ± 0.2

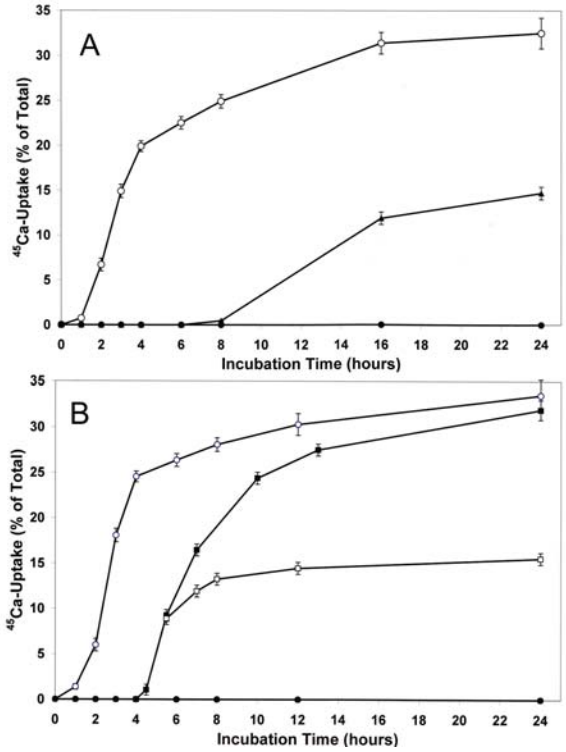

Figure 17. Effect of Zn^{2+} Levels in SCL, and Counter-Effects of *o*-Phenanthroline (OP), on Matrix Vesicle Ion-Loading *in vitro.* $^{45}Ca^{2+}$ accumulation was used as an indication of MV mineralization. Ca^{2+} uptake was assayed by incubating collagenase-released MV samples (80 micrograms protein) in capped polypropylene test tubes with 2 ml of $^{45}Ca^{2+}$-labelled SCL (1 x 10^6 dpm/ml) using a constant temperature (37 ºC) shaker bath. At timed intervals, 0.1-ml aliquots of the SCL incubations were sampled by rapid vacuum microfiltration (57) and assayed for radioactivity by liquid scintillation counting. 17A – Inhibitory effect of graded levels of Zn^{2+}. $ZnCl_2$ was added from a stock solution to achieve the final concentrations (2–20 microM). Shown are data for 0 microM (*open circles*), 2 microM (*closed triangles*) and 5 microM (*closed circles*) Zn^{2+}, the lowest concentration required for complete inhibition. The inhibitory effect of Zn^{2+} was to extend the lag period (*i.e.* delay the onset) and reduce the rate of mineral formation. 17B – Rapid counter-effects of OP on Zn^{2+} inhibition. The control MVs with no Zn^{2+} or OP additions show typical rapid $^{45}Ca^{2+}$ uptake (*open circles*). MVs fully inhibited by 20 microM Zn^{2+} (*closed circles*) were treated at 4 h with 100 microM OP, a potent Zn^{2+} chelator (*closed squares*) initiating almost immediate restoration of mineral formation. At 6 h, addition of 100 microM Zn^{2+} (*open squares*) obviously blocked recovery of $^{45}Ca^{2+}$ accumulation. Each point is the mean ± SE (n = 4). (Adapted from (317) with permission from Elsevier.)

mM) Ca^{2+} *activity* present in the extracellular fluid (339). Thus, the vast majority (~99%) of Ca^{2+} in MVs must be tied up in insoluble forms (64); these are embodied in the nucleational core.

16.1. Discovery of the nucleational core

A long series of observations ultimately led to the discovery that it was the presence of a nucleational core that drives MV Ca^{2+} and Pi accumulation. The roots of the discovery of the nucleational core go back to 1977 when it was first documented that MVs contain sizeable amounts of Ca^{2+}, Pi, and other mineral ions (63); this mineral was amorphous to x-ray diffraction (Figure 9), and occurred in various solubility states (64). A significant breakthrough occurred in 1986 when the marked acid lability of the mineral in MVs was first documented (66). The mineral was shown to be inside the vesicle lumen, and when lost, the MVs would not mineralize (67). Ca^{2+} uptake by MV was shown to be highly sensitive to pH, being limited to a range very similar to that observed with ACP (77). The next step was a major improvement in MV isolation, yielding purer, highly active, mineralization-competent vesicles (76). Importantly, the ability of these MVs to induce mineral formation could be readily ablated by chymotrypsin. Amazingly, if these damaged vesicles were then treated with detergents, their nucleational competence was restored (288). This series of observations led to the conclusion that a "nucleational core" was responsible for accumulation of Ca^{2+} and Pi by MVs.

The discovery process evolved in this way. *First*, one of the most effective ways to prevent Ca^{2+} ion uptake by isolated MVs was to briefly (*ca.* 10 min) expose them to isosmotic, pH 6 citrate buffer (66). After this simple treatment, their ability to accumulate Ca^{2+} (and Pi) was almost totally abrogated. Such treatment was shown to remove 80-85% of the total Ca^{2+} and Pi from the vesicles (67). These findings revealed that the main contributor to the driving force for Ca^{2+} uptake must be an insoluble, but highly acid-labile Ca^{2+}-Pi-rich phase. *Second*, it was found that accumulation of mineral ions by MVs from SCL only occurred within a very narrow pH range – between 7.4–7.8 (77) (Figure 18A). Either below or above this range, the rate of Ca^{2+} uptake was dramatically reduced; for example, at pH 8.0 there was simply no uptake of $^{45}Ca^{2+}$ by MVs. (In contrast, upon seeding of HAP at pH 8.0, there is a slow, steady accumulation of $^{45}Ca^{2+}$ for at least 24 h (77)). On the other hand, it became evident that below pH 7.4, the *solubility* of the mineral phase in MVs was too high to reduce Ca^{2+} activity in the *intravesicular* fluid to levels that enabled Ca^{2+} acquisition. Above pH 7.8, it was evident that the *stability* of this phase was so great that it could not convert to a crystalline state that could acquire additional Ca^{2+}. Between pH 7.6 and 7.8 this phase exhibited optimal *low solubility* and sufficient *metastability* to support rapid Ca^{2+} and Pi acquisition from the extravesicular fluid. It is physiologically significant that the pH of the extracellular fluid in the hypertrophic region of the growth plate is poised at 7.6 (63, 339); this is the center of the active pH range for MV mineralization. *Third,* the only known calcium phosphate phase with the properties described above is ACP (amorphous calcium phosphate) (444). However, in intact MVs, ACP is in a hidden form not readily discernible with FT-IR or FT-Raman (387-388) or X-ray diffraction (63). It was only

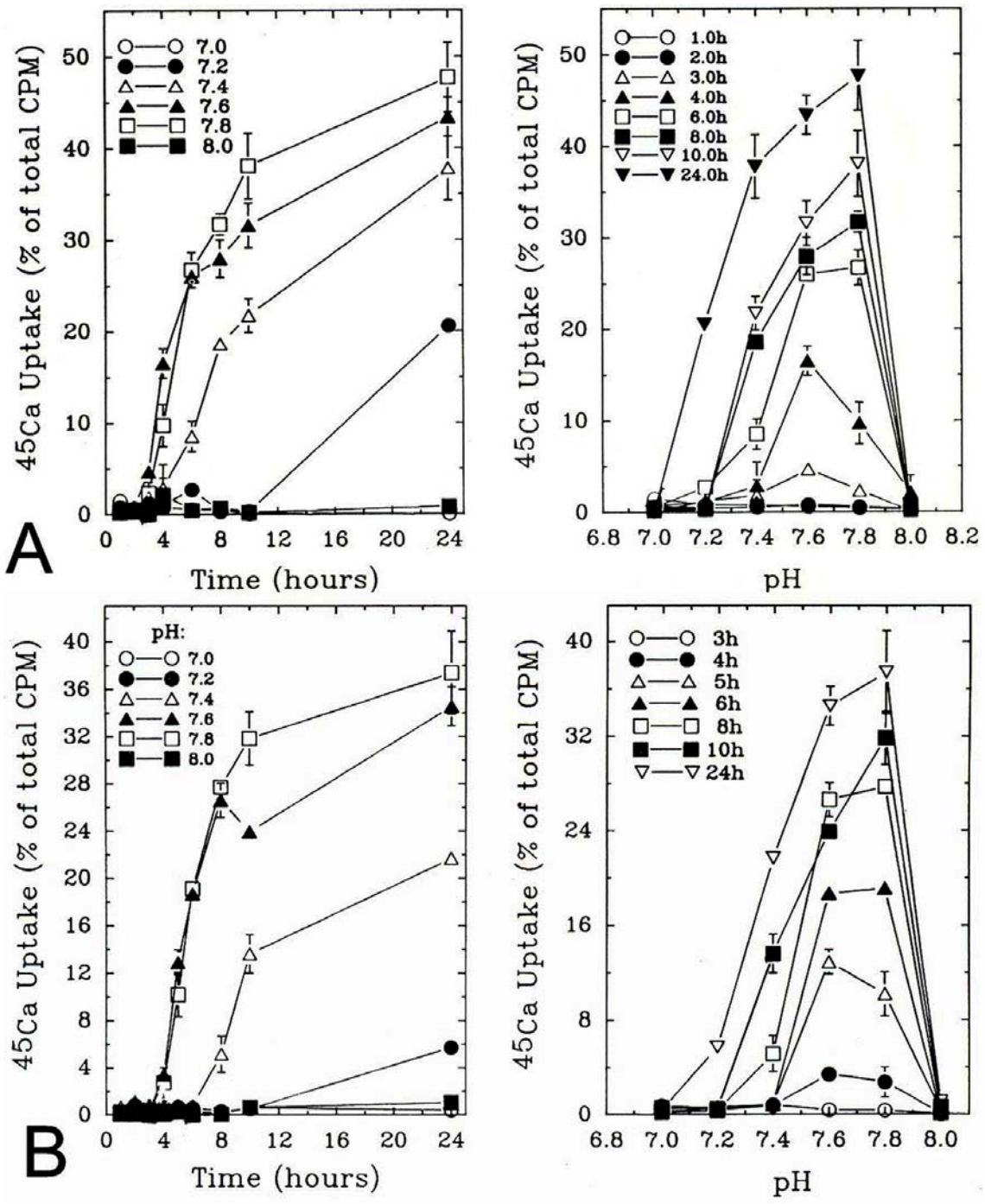

Figure 18. Effect of pH on Rate and Amount of Mineralization by MVs and the MV Nucleational Core. 18A – MV mineralization. CRMV were incubated in $^{45}Ca^{2+}$-labelled SCL at a Ca^{2+}/Pi molar ratio of 1.30 and a Ca^{2+} x Pi ion product of 2.63 mM^2. The pH of the incubation medium was varied from 7.0 to 8.0 in increments of 0.2 pH units. *Left Panel* – Time course of $^{45}Ca^{2+}$ accumulation. During the early stages of rapid uptake (<5 h) pH 7.6 exhibited the fastest rate of uptake; pH 7.8 was most rapid after 5 h. *Right Panel* – pH profile of $^{45}Ca^{2+}$ accumulation. Note the extremely narrow range in which MVs are able to accumulate $^{45}Ca^{2+}$, and that at pH 8.0 uptake essentially ceased. 18B – Mineral formation by the MV nucleational core. CRMV were extracted with 0.5% Triton X-100 at RT for 10 min. The mixture was centrifuged to sediment the insoluble residue (the nucleational core). $^{45}Ca^{2+}$ deposition was studied under the same conditions as in 18A. (Note that the pH effects on the nucleational core are almost identical to those of native CRMV.) (Adapted from (77) with permission from Elsevier.)

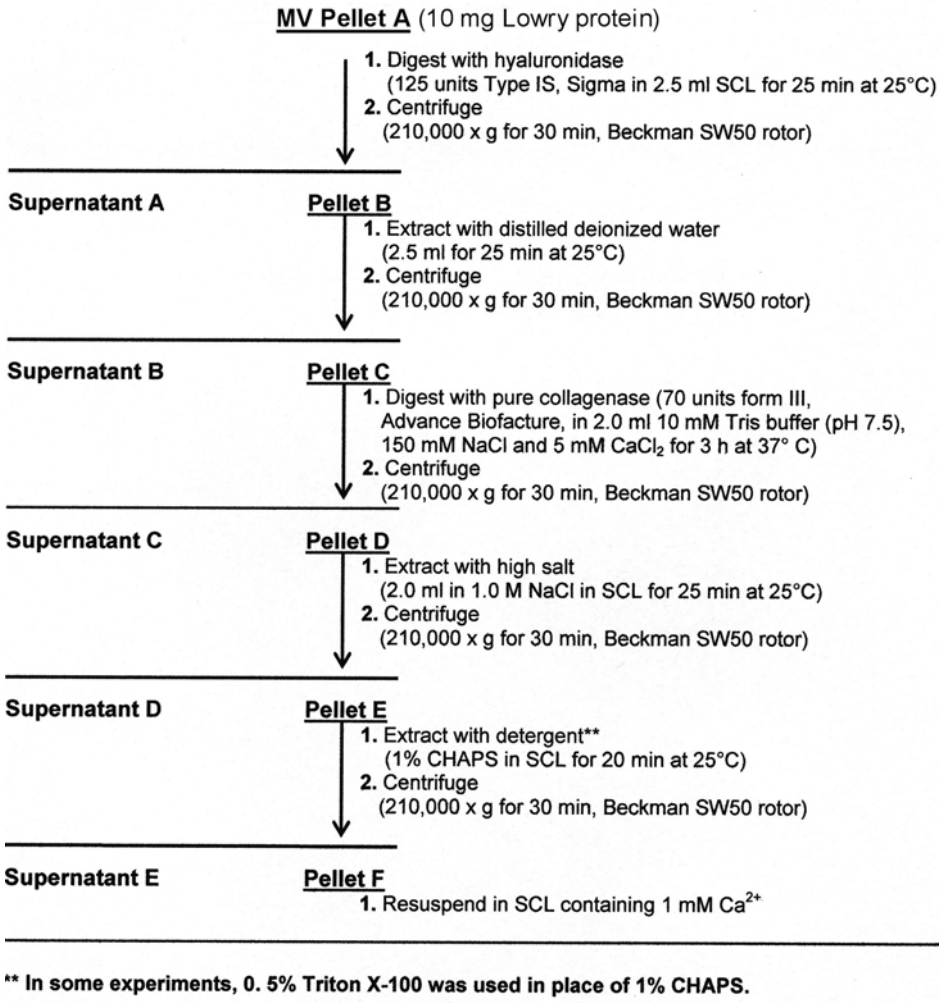

Figure 19. Sequential Extraction Scheme for Isolating the Nucleational Core of MVs. Collagenase-released MVs (CRMVs) (61) were used for the isolation of the nucleational core. This fractionation scheme was used to remove nonessential materials from the vesicles and reveal the functionally active nucleational core. (Originally published in (457) by the American Society for Biochemistry and Molecular Biology.)

by careful biochemical dissection of the nucleational core from isolated MVs that the true nature of the nucleational complex was revealed.

16.2. Isolation of the nucleational core

The following chemical dissection procedure describes how the nucleational core was isolated (Figure 19) (288, 443, 457). It entailed *sequential* extraction of *active* MVs: 1) with hyaluronidase to remove hyaluronate, 2) with water to dissociate proteoglycan link and core proteins, 3) with pure collagenase to remove attached collagens, and 4) with 1 M NaCl to dissociate other vesicle proteins. (Critically, the 1 M NaCl had to be made in Ca^{2+}-containing SCL to prevent dissolution of the ephemeral mineral.) Finally, 5) a detergent, *e.g.* CHAPS, was used to remove MV membrane phospholipids. The properties of the nucleational core isolated by this procedure – taken with data from the preceding studies – revealed that this was the material responsible for induction of mineral formation by MV.

16.3. Chemical characterization of the nucleational core

What are the morphological, chemical and physical properties of the nucleational core? While the just cited studies revealed much of what is currently known about this ephemeral material, much more is now understood.

16.3.1. Electrophoretic Analysis of Proteins of the nucleational core

Proteins remaining in the nucleational core appear to contribute significantly to its ability to lower the intravesicular Ca^{2+} ion activity. The most obvious of these are the MV annexins. And indeed, SDS-PAGE electrophoretic analysis of the nucleational core reveals that AnxA5 is the main protein component (Figure 20). AnxA5 has been shown to bind to Ca^{2+} in the presence of acidic phospholipids with a dissociation constant in the range of 5 x 10^{-7} M (Figure 5) (60). Taken with its abundance in MVs (78), it is evident that it could trap significant

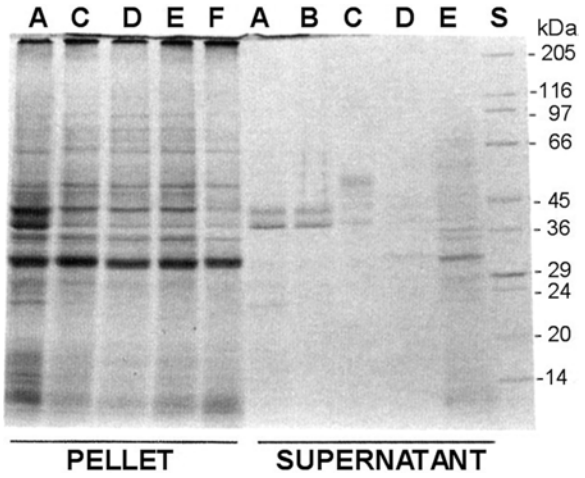

Figure 20. SDS-PAGE Analysis of the Proteins Present in CRMV and in the Various Sequential Subfractions. CHAPS (1% in SCL) was used as the detergent. The *capital letters* above the gel correspond to those shown in Fig. 19. *Pellet A*, original CRMV; *Pellet B*, after digestion with hyaluronidase (not shown); *Pellet C*, after extraction with deionized distilled water; *Pellet D*, after digestion with collagenase; *Pellet E*, after extraction with 1 M NaCl in SCL; *Pellet F*, after extraction with CHAPS. *Supernatant A*, after digestion with hyaluronidase; *Supernatant B*, after extraction with deionized distilled water; *Supernatant C,* after digestion with collagenase; *Supernatant D,* after extraction with 1 M NaCL in SCL; *Supernatant E*, after extraction with CHAPS. Note the selective removal of proteins (seen in the supernatants) by the sequential extraction steps. Note in *Pellet F* the much cleaner and simpler protein pattern of the NC (*Pellet F*) compared with that of the CRMV (*Pellet A*). Note that the dominant protein in the NC (*Pellet F*) is the 33-kDa AnxA5. (Originally published (457) by the American Society for Biochemistry and Molecular Biology.)

amounts of Ca^{2+}. Importantly, Pi was shown not to interfere with the formation of these ternary PS-Ca^{2+}-annexin complexes (Figure 4C) (61). Before development of the procedure for isolating the nucleational core an earlier type of biochemical dissection of MVs revealed that the MV annexins can only be removed by using powerful Ca^{2+}-chelating agents such as EGTA (Figure 4A) (60, 61). Further, this family of proteins is uniquely able to be partitioned into organic phases under highly acidic conditions, revealing their amphipathic nature (93). In fact, the annexins cannot be removed from MVs without destroying the ability of the MVs to mineralize. Thus, it is not surprising that AnxA5 was the major protein in the nucleational core.

16.3.2. Chromatographic analysis of lipids in the nucleational core

On the other hand, the detergent, CHAPS used to expose the nucleational core, extracted nearly all of the resident phospholipids. The only lipids that remained were free cholesterol and an unidentified lipid. After 1M-NaCl treatment, CHAPS displaced most of the phospholipid. (Another detergent, Digitonin, while removing most of the cholesterol, left the nucleational core phospholipids intact.) However, the fact that the nucleational core was still functional after CHAPS treatment indicates that CHAPS must have substituted for the phospholipids in the core structure, somehow preserving its activity. However, in the native nucleational core, significant amounts of PS-CPLX are present. About 10% of the total Ca^{2+} and Pi in MV is in the form of organic solvent-soluble PS-ACP complexes (64); the great majority of the Ca^{2+} (85-90%) and about half of the Pi and Mg^{2+} in MV are insoluble in organic solvents – *i.e.* present as non-lipid-soluble complexes. It is now evident that the PS-ACP complex (PS-CPLX) is a key component of the nucleational core of native MVs.

16.4. Physical characterization of the nucleational core

Several types of physical measurements were made on the CHAPS-isolated nucleational core. TEM and FTIR, as well as ^{31}P-NMR and its solubility properties were used to analyze the structure of the nucleational core (443, 457).

16.4.1. Transmission electron microscopy (TEM)

TEM reveal that the nucleational core is composed of aggregates of particles ~110 nm in diameter, with ~1.0 nm diameter subunits apparently composed of clusters of Ca^{2+} and Pi ions (457). The ~1.0 nm diameter of the subunit is similar in size to the core structure of ACP measured by radial distribution function analysis (458). This finding supports the conclusion that ACP is a major component of the nucleational core. There was no evidence for the presence of crystalline mineral in the nucleational core.

16.4.2. FT-IR analysis

FT-IR spectral analysis of the nucleational core revealed the presence of a number of characteristic features: strong, sharp C–H stretch bands (2922 and 2851 cm^{-1}) characteristic of acyl chains (lipids), strong amide bands (~1654 and ~1545 cm^{-1}) characteristic of proteins, a strong P-O stretch band (1054 cm^{-1}) characteristic of all calcium phosphate minerals, and a broad, unsplit P-O absorption band (~558 cm^{-1}) characteristic of ACP (Figure 21). These data reveal chemical features that distinguish it from those of the MVs from which it was isolated. The most obvious difference is the marked increase in the intensity of the *unsplit* P-O absorption band at ~558 cm^{-1} and the strong P–O stretch band at ~1054 cm^{-1}; these absorbencies finally reveal the obvious presence of ACP in the nucleational core – in contrast to its being masked in intact MVs. Further, the strong absorbencies at ~1654 cm^{-1} and ~1545 cm^{-1} represent the amide-I C=O stretch bands and the amide-II N–H stretch bands, respectively, clearly show that significant amounts of protein are also present in the nucleational core. The C–H stretch bands at 2922 and 2851 cm^{-1} are not as intense as those in native MVs, in agreement with the reduction in lipids evident in TLC chromatograms of the nucleational core. Further, the sharp strong bands at 3507 and 3441 cm^{-1} evident in the nucleational core, but not native MVs, appear to be due to the presence of the three hydroxyl moieties in the sterol nucleus of the CHAPS detergent. This supports the

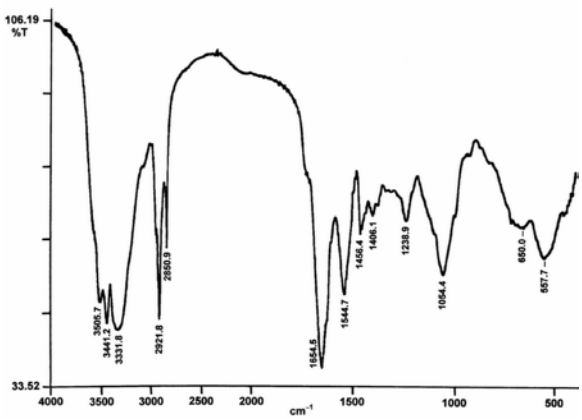

Figure 21. FT-IR Analysis of the Nucleational Core Obtained by CHAPS Treatment. CRMV were sequentially extracted to yield the CHAPS-NC as described in Fig. 19 and lyophilized. Approximately 1 mg was incorporated into ~300 mg KBr, compressed into a transparent pellet and examined by FT-IR. (In addition to the various lipid and protein structures identified in the text, in particular, note the *unsplit strong absorption band at ~558 cm^{-1}, typical of ACP*.) (Reproduced from (443) with permission from Informa Medical and Pharmaceutical Science.)

contention that the detergent displaced phospholipids in the nucleational core. The intense broad band at 3332 cm^{-1} represents the presence of tenacious water, despite vacuum drying.

16.4.3. ^{31}P-NMR analysis

The mineral initially present in MVs was also studied by solid-state, magic-angle ^{31}P-NMR using proton cross-polarization (Figure 22) (457). A distinct central peak at 3.2 ppm characteristic of all calcium phosphates, including ACP, OCP or HAP, was evident, but x-ray diffraction studies of either isolated MVs (Figure 9C) (63) or the nucleational core (457) showed no evidence of crystallinity. The cross-polarization spinning sideband *pattern* was highly distinctive and matched that of the PS-CPLX; it did not resemble that of any of the known crystalline calcium phosphates (459-460). By measurement of the relative size of the central peak and the spinning sidebands and comparing them with known mixtures of ACP and PS-CPLX, it was estimated that only about 8-10% of the total MV-P was as the PS-CPLX; the bulk, about 90%, was present as ACP. The proportion of MV-P present as CPLX closely agrees with the ~5-10% value obtained by solvent partition of MV by Wuthier and Gore (64) noted earlier.

16.4.4. pH Sensitivity of the nucleational core

One of the most effective ways to destroy the nucleational core is to expose it to isosmotic, pH 6 citrate buffer (288). After this simple treatment, its ability to induce mineral formation was totally destroyed. This reveals that it is highly sensitive to even mildly acidic conditions. On the other hand, at pH 8, the nucleational core is highly stable and insoluble. As was discussed earlier, the nucleational activity of the MVs and the nucleational core is operative only within a very narrow pH range – between 7.4–7.8 (77) (Figure 18B). Either below or above this range, its ability to nucleate mineral formation is dramatically reduced. Below pH 7.4, the *solubility* of the nucleational core is too high to accrete Ca^{2+} and Pi from the intravesicular fluid to enable crystal growth. Above pH 7.8, the *stability* of the nucleational core is so great that it can not convert to a crystalline form that could acquire additional Ca^{2+}. Only between pH 7.6 and 7.8 does the nucleational core exhibit sufficiently *low solubility* and adequate *metastability* to induce rapid mineral formation. As noted previously, the extracellular fluid at the site of calcification in the growth plate in fact has a pH of 7.6 (63, 339); this enables a maximal rate of mineral formation. Thus, in accord with all the data just presented, the solubility properties of the nucleational core also match those of ACP (444); but the story gets more complicated.

16.5. Summary of nucleational core structure and composition

To summarize, SDS-PAGE electrophoresis, X-ray diffraction, TEM, FTIR and ^{31}P-NMR findings – as well as the solubility properties of the nucleational core – all clearly indicate that ACP is a major component of the nucleational core. Localized within the vesicle lumen, this quasi-stable highly hydrated solid phase of amorphous mineral forms the bulk of the nucleational core. However, ^{31}P-NMR and the early solvent partition assays indicate that only about 10% of the Pi is present in the form of PS-CPLX. Off hand, this small percentage suggests that PS-CPLX would have little to do with nucleation of mineral formation. However as we shall soon discover, this small critical amount of PS-complex is the trigger for mineral nucleation. The *insolubility* of the nucleational core is the initial driving force for Ca^{2+} and Pi accumulation. Its *metastability* is what enables the nucleational core to convert to crystalline OCP and drive rapid mineral formation.

17. RECONSTITUTION OF THE NUCLEATIONAL CORE: ROLE OF PS-Ca^{2+}-Pi COMPLEX (PS-CPLX) IN MV CRYSTAL NUCLEATION

To fully understand how the native MVs work, it has been necessary to take them apart and put them back together again. Being able to chemically dissect and then reconstitute MVs and their key components provides assurance that a proper understanding of the *modus operandi* of these intriguing biological nanostructures has been achieved. After it was possible to consistently isolate functionally operational MVs that induced mineral formation in a predictable manner in an ionic environment closely matched to that occurring in the native tissue, it became possible to disassemble the native vesicles by biochemical dissection. As noted previously, this led to the important discovery that a nucleational core exists in MVs that enables them to induce mineral formation – even in the absence of the protective environment of the vesicle lumen. The next challenge was to reconstruct from pure components a functional nucleational core that was capable

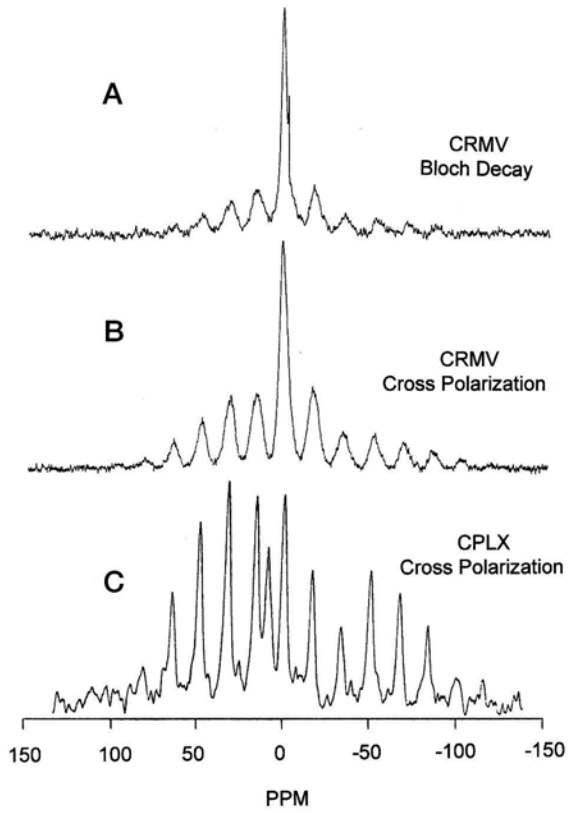

Figure 22. Solid-State ^{31}P NMR Analysis of Native CRMV. Lyophilized CRMV (10–20 mg) were packed into 7-mm Doty Scientific SiN_3 rotors, spun at 2 kHz, stabilized to a precision of ± 1 Hz, and recorded at RT. Solid-state ^{31}P NMR spectra of the CRMV and synthetic PS-Ca^{2+}-Pi complex were obtained using a Varian Unity+ spectrometer operating at 121.42 mHz for ^{31}P. Pulse widths were 4.4 μs, and a contact time of 2.5 ms was used. Chemical shifts were referenced to external H_3PO_4 at 0 ppm (581). Bloch decay and cross-polarization pulse sequences were employed with high proton decoupling: 10-s recycle time was used for Bloch decay; 3-s times were used for cross-polarization experiments. 22A – CRMV, Bloch decay; 22B – CRMV, proton cross-polarization; 22C – PS-CPLX, proton cross-polarization. Note the marked increase in intensity of the spinning sidebands in B compared to A, when subjected to proton cross-polarization. Note the close similarity in the *position* and relative intensity of the spinning sidebands of the CPLX and CRMV upon proton cross-polarization. The large central band in *A* and *B* is due to the presence of ACP. Based on the relative intensity of the central peak and the sidebands, compared to known mixtures, ~8% of the P in the CRMV is composed of the CPLX. (Originally published in (457) by the American Society for Biochemistry and Molecular Biology.)

of inducing mineral formation of a type and character that matched that of the native vesicles. The final challenge to demonstrating that the mechanism of MVs was truly understood was to reconstitute functional synthetic vesicles (liposomes) from pure precursors that were capable of inducing the same mineral type produced by native MVs. This has been largely accomplished, although there will always be room for continued refinements to make the constructs match ever more closely the native structure.

17.1. Reconstitution of the nucleational core

The discovery of the nucleational core (NC) prompted attempts to reconstitute it from known pure materials. This required extensive characterization of its components (288, 457). As already noted, these studies revealed that key components of the NC were: ACP, AnxA5, and PS-CPLX. Also evident were regulatory factors that alter the rate at which the NC could induce mineral formation. A key regulatory component was found to be Mg^{2+}, the principal intracellular divalent cation. Another important factor was the lipid composition of the NC; for example, PS was the most efficacious lipid. Dilution of PS with other phospholipids normally present in MVs, or nonpolar lipids such as free cholesterol, had a progressively inhibitory effect on the activity of the synthetic NC. The first effort to reconstitute the NC was made in 1996 by Wu *et al.* (443), who centered on the PS-Ca^{2+}-Pi complex. Various pure lipids, electrolytes and proteins were combined to form a synthetic nucleationally active complex, analyzing its rate and extent of mineral formation. While inclusions of PE or SM with PS were strongly inhibitory, co-incorporation of AnxA5 increased nucleation activity, but much more was needed to refine the reconstruction of the physiological complex.

17.2. Mathematical analysis of the kinetics of mineral formation

It was not until a decade later that a systematic attempt was made to reconstitute the NC using a biomimetic approach. To accurately ascertain the effects of each permutation, a more precise method for measuring the onset time, the kinetic rate and the amount of mineral formed needed to be devised. This led to the development of a high throughput method for studying the kinetics of mineral formation using *in vitro* modeling of MV mineralization (332). The method was based on light scattering by nascent crystallites at 340 nm (461) that enabled monitoring of mineral formation at regular intervals without disturbing the system using an automated plate reader. It yielded precise replicate values that typically agreed within <5%. Using a Mg^{2+}-containing biomimetic PS-CPLX as the nucleating material, it was found that mineral formation followed a sigmoidal pattern – as it does with authentic MVs. There was a quiescent induction period; then rapid formation ensued for a limited time; this was followed by a distinct decline in rate that continued to slow, ultimately reaching a maximal asymptotic value. Key to quantization of mineral formation was the use of first-derivative analysis that defined the induction time, the rate, the length, and the amount of initial mineral formation (Figure 23). Through use of a five-parameter logistic curve-fitting algorithm, the maximal amount of mineral formation could be predicted accurately.

17.3. The Physical and nucleational properties of pure PS-CPLX

Studies aimed at reconstituting the nucleational

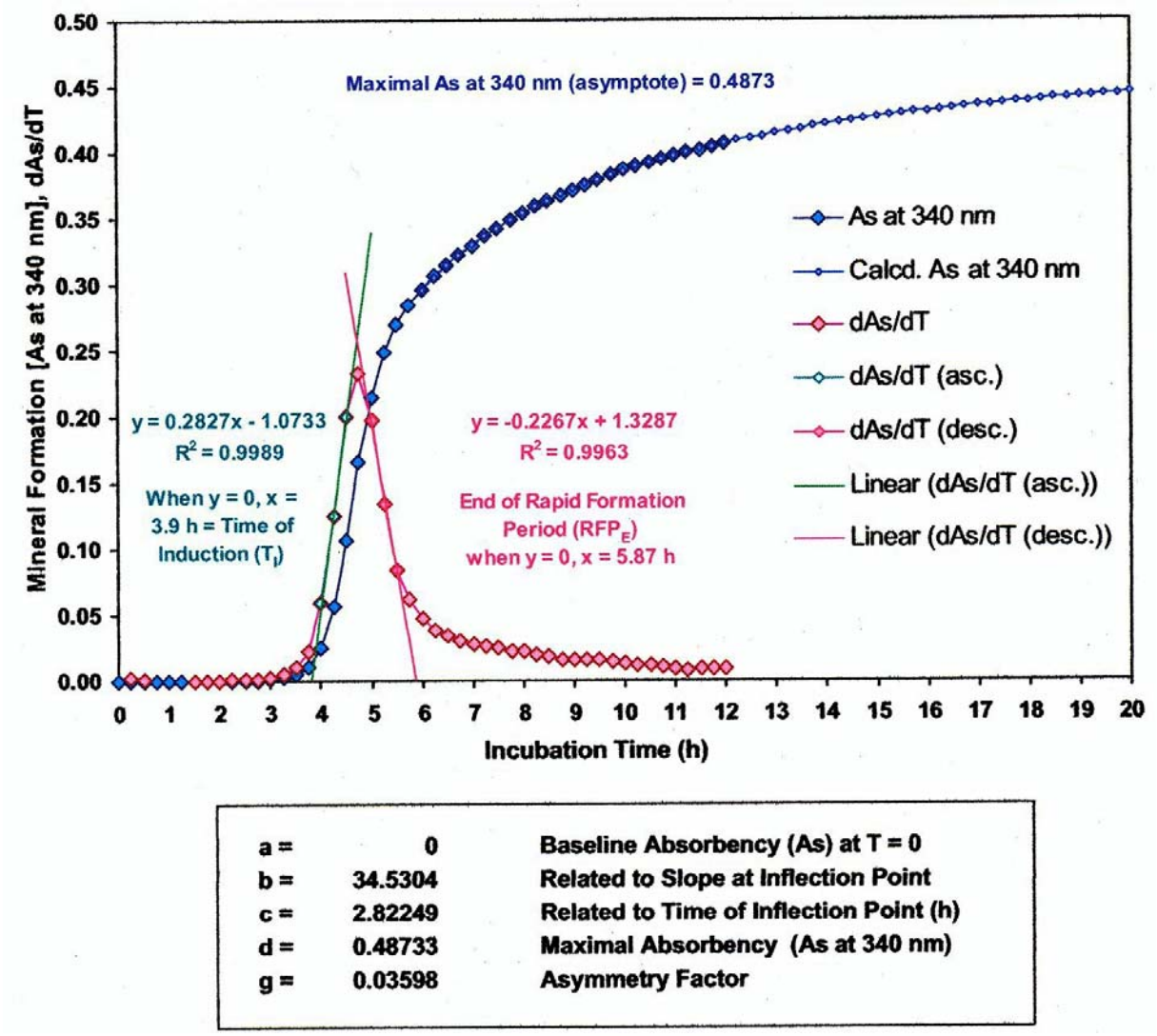

Figure 23. Mathematical Analysis of a Typical Mineral Formation Curve. The sigmoidal curve shows mineral formation from 0 to 12 h incubation (large blue diamonds). The five-parameter logistic curve-fitting equation for sigmoidal curves is as follows:

$$y = d + \frac{(a-d)}{\left(1 + \left(\frac{x}{c}\right)^{b}\right)^{g}}.$$

The box below the figure shows values of the five parameters for the equation that closely fit the mineral formation curve (*SSE* = 3.0 x 10^{-6} As at 340 nm). From this equation, data points have been calculated (Calc.) from 5.5 to 20.0 h (*small blue diamonds*). The figure also shows the first derivative (dAs/dh) curve (*large pink diamonds*), with superimposed lines, *green with small diamonds* for the ascending (asc.) portion and *red with small red diamonds* for the descending (desc.) portion. The ascending region extrapolates to the time of induction (T_I = 3.79 h) at y = 0; the descending region extrapolates to the end of the rapid formation period (RFP_E = 5.87 h) at y = 0. The rate of rapid mineral formation (RMF_R), the average slope of the mineral formation curve between T_I and RFP_E (0.1397 *d*As/*d*h), is calculated by dividing the As at RPE_E (0.2903) by the length of the rapid formation period (5.87 – 3.79 = 2.08 h). The nucleation potential, the ratio (RMF_R/T_I) x 100, is a sensitive measure of the potency of each nucleator. AMF_{Mas} (0.4873) (parameter *d* in the five-parameter equation) is the asymptotic As value, indicating maximal mineral formation. (Reproduced from (332), with permission from Elsevier.)

core revealed that the entity most responsible for nucleation of crystalline mineral was PS-CPLX. TEM analysis of the pure synthetic PS-CPLX revealed extended membrane-like structures composed of PS-CPLX units 7.6–8.0 Angstroms in diameter that form quasi-crystalline arrays; these appear to be nucleating mineral (arrows, Figure 24). Evidence of this short-range two-dimensional order comes from FT-IR analyses which consistently

Figure 24. TEM of PS-CPLX Showing Extended Two-Dimensional Membrane-Like Structures with Quasi-Crystalline Arrays of Particles. PS-CPLX was prepared and processed for TEM examination as previously described (131). The fresh complex was harvested by centrifugation and incubated with SCL for ~2 h. Careful inspection reveals that the membrane-like structures are in fact composed of an assembly of semi-ordered particles of PS-CPLX, ~8.5 angstroms in diameter. At various sites on the "membrane" there are more ordered assemblies of the particles (*arrows*) that appear to be sites of mineral nucleation.. (Unpublished data from 1997.)

reveal splitting of the 560 – 600 cm^{-1} P–O bond resonance. Pure *Mg^{2+}-free* PS-CPLX can nucleate calcium phosphate microcrystalline mineral almost immediately upon exposure to SCL, very much like that induced by HAP (Figure 25) (444). Thus, while the PS-CPLX comprises only a quantitatively minor component of the NC (289, 458), it is vital to its nucleation properties.

17.4. Requirements for PS-CPLX formation

During MV formation, PS-CPLXs can readily form at pH 6.7 (266), conditions like that present in the perimeter of growth plate chondrocytes (Figure 15C). In contrast, the ACP component of the nucleational core cannot form at this pH and can occur only after the vesicles are released into the extracellular fluid where the pH (7.6) favors ACP formation. Other requirements for PS-CPLX formation were studied recently by Wu *et al.* (131) using the just described *in vitro* model system (332). A key requirement in the formation of PS-CPLX is that excess Pi must be present with the lipid before introduction of Ca^{2+} (266, 443, 462). This feature occurs in cells during formation of MVs. There, levels of cytoplasmic Pi are high (63) and levels of Ca^{2+} are low (306) – prior to Ca^{2+} being released during the mitochondrial permeation transition that engenders MV formation (306, 314, 383). If Ca^{2+} interacts with PS in the absence of Pi, it leads to formation of 2:1 PS-Ca^{2+} complexes that have no nucleational activity (266, 373). This reveals that only under circumstances in which high cytosolic Pi is present, is it possible to form PS-CPLX *in vivo*. On the other hand, addition of high levels of Ca^{2+} to neutral solutions rich in Pi leads to formation of amorphous calcium phosphate (ACP) an ephemeral phase that spontaneously converts to HA (386, 444) unless stabilized with various agents such as Mg^{2+} (463-464), certain proteins (465-467), and acidic lipids such as PS (266). Interaction with PS during ACP formation *spontaneously* leads to production of PS-CPLX (221). However, PS-CPLXs do not form *instantly* when Ca^{2+} comes in contact with PS and Pi.

17.5. Molecular rearrangements during PS-CPLX formation

In recent studies by Wu *et al.* (131), micelles of PS in a K^+- and Pi-rich intracellular buffer were used to model *in vivo* PS-CPLX formation. Addition of 4 Ca^{2+} per PS was minimally required to form nucleationally competent complexes. During the initial 10-min "ripening" period, light-scattering data revealed significant contraction in the size of the nascent PS-CPLX particles. FT-IR analyses showed that this was accompanied – not only by major deprotonation of HPO_4^{2-} to PO_4^{3-} – but with rearrangement of the phosphate groups, producing features that mimic those seen in crystalline calcium phosphate mineral (*i.e.* splitting of the P–O band in the 560–600 cm^{-1} region (Figure 26) (131). Molecular dynamic simulations indicated that the initial interactions between Ca^{2+} and Pi, and PS (*i.e.* its carboxyl, amino, and phosphodiester groups) produced interatomic distances in the incipient PS-CPLX that agreed closely with previous RDF-EXAFS (radial distribution function x-ray-absorption fine structure) measurements on the mature complex (468) – except for an elongated Ca–N distance. During this critical period, atomic rearrangements involving deprotonation of the PS amino group, led to contraction and stabilization of the PS-ACP complex. Molecular simulations revealed the following: interaction between Ca^{2+} and the (PS-$NH_3^+\cdots HPO_4^{2-})^-$ ion-pair leads to formation of a ($Ca^{2+}\cdots$PS-$NH_3^+\cdots HPO_4^{2-})^+$ adduct. Because of its net positive charge, deprotonation of the PS-NH_3^+ (pK_a = 9.8) rather than the HPO_4^{2-} (pK_a = 12.3) group would lead to ($Ca^{2+}\cdots$PS-$NH_2\cdots HPO_4^{2-})^0$ as a product. The electrically neutral R–NH_2 group, having a pair of unshared electrons, would interact with Ca^{2+}, forming a shortened Ca–N bond. Such Ca–N bonding is an important feature of strong chelating agents like EDTA, but in PS-CPLX the affinity for Ca^{2+} is weaker and the reaction occurs more slowly. Contraction in the size of the polar head group would enable construction of planar hexagonal assemblies that closely match the lattice parameters of OCP and HAP, forming an almost perfect nucleational agent – as was evident from the rapidity in which mineral formation occurred upon addition

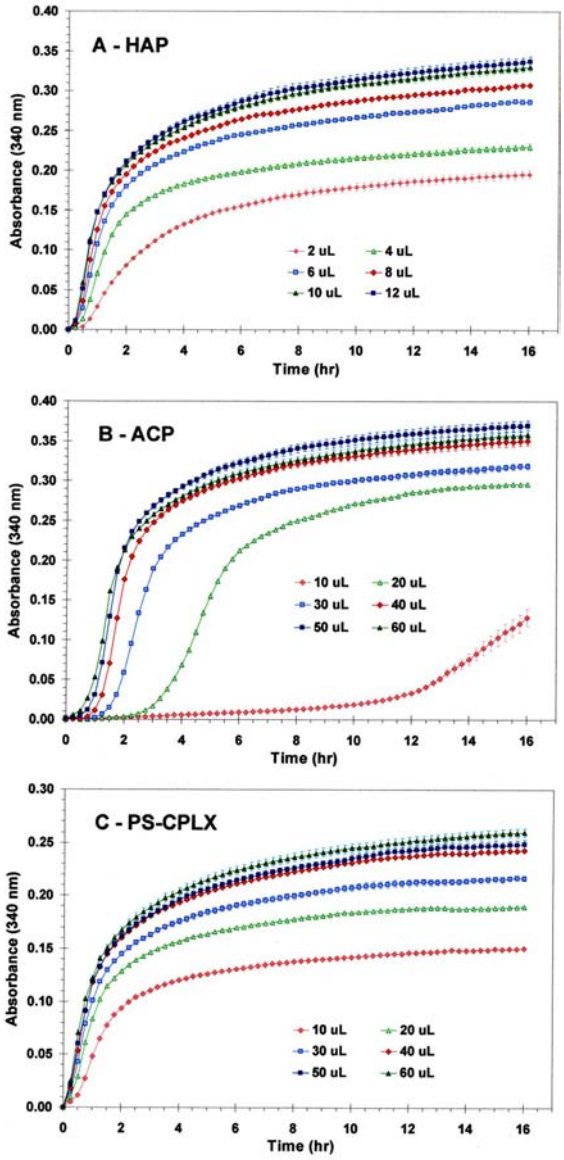

Figure 25. Comparative Nucleational Properties of PS-CPLX, Hydroxyapatite (HAP) and Amorphous Calcium Phosphate (ACP) on the Kinetics of Mineral Formation. The effect of amount of seeding on mineral formation from pure Mg^{2+}-free PS-CPLX, and for comparison, HAP and ACP were studied. Shown are the increases with incubation time in absorbance at 340 nm caused by light scattering from the formation of mineral crystallites when increasing volumes of nucleation seed suspensions were added to 1 ml of SCL and incubated at 37 ºC for the indicated times. Upon addition of PS-CPLX (C) and HAP (A) mineral formation began to occur almost immediately after addition, regardless of the volume added. In contrast, the timing of onset of mineral formation from ACP (B) was strongly dependent on seeding volume. The fact that PS-CPLX can initiate mineral formation so rapidly indicates that it is a powerful nucleational agent, nearly as potent as HAP itself. (Reproduced from (137), with permission from Elsevier).

of the PS-CPLX to SCL (Figure 25). These events obviously occur intracellularly during the critical period after release of mitochondrial Ca^{2+} that sets in motion the formation of PS-CPLX on the inner surface of the plasma membrane and becomes incorporated into the MVs when they are released from the cell. In the more alkaline (pH 7.5) extracellular environment, the excess Ca^{2+} and Pi in the nascent MVs rapidly form ACP, which becomes the quantitatively major component of the NC. However, the nucleational properties ascribed to the NC for crystal formation largely reside in the PS-CPLX.

17.6. Effect of Mg^{2+} incorporation on the nucleational activity of PS-CPLX

A complicating factor in understanding crystal nucleation is the fact that *in vivo* ACP and PS-CPLX both contain high levels of Mg^{2+} (64); this is true simply because Mg^{2+} is far more abundant than Ca^{2+} in the cytoplasm. Mg^{2+} stabilizes both ACP and the PS-CPLX in the NC, inhibiting their conversion to crystalline calcium phosphates. As noted above, Mg^{2+}-free PS-CPLXs are almost as potent as HAP in nucleating crystal formation, initiating mineral formation in a matter of seconds (Figure 25). Mg^{2+}-containing PS-Ca^{2+}-Pi complexes are much less active, requiring much more time; incorporation of a little as 0.5 mM Mg^{2+} is sufficient to extend the induction time by 3 h; increasing this to 0.75 mM or higher delay induction for many additional hours (Figure 27A) (137). How Mg^{2+} does this is readily apparent from FT-IR analysis, which reveal that it prevents the formation of the highly ordered P–O bonds evident as splitting of the 560–600 cm^{-1} resonances observed in all crystalline calcium phosphates (Figure 27C).

17.7. Role of AnxA5 in MV crystal nucleation

Here is where AnxA5 has been shown to play a critical role; its presence counteracts the inhibitory effects of Mg^{2+}. If AnxA5 is incorporated at the time of PS-CPLX formation, the induction time to mineral formation can be reduced from 16 h to only 3–4 h (Figure 28) (136). This acceleration in nucleation is of key importance in rapidly growing species like broiler-strain chickens where longitudinal growth can be up to 50–60 micrometers per hour. Since hypertrophic chondrocytes are ~20 micrometers in diameter, this means that mineralization of 2–3 cells must be completed every hour to maintain structural integrity. How can AnxA5 so greatly enhance the rate of mineral formation? There are several important clues. *First*, high resolution scanning electron micrographs of AnxA5 associated with PS-rich bilayers reveal an orderly hexagonal pattern of triskelion shaped trimers on the membrane surface (126, 128-130). *Second*, the dimensions of this hexagonal pattern closely coordinate with the dimensions of hexagonal crystal structures of OCP and HAP. *Third*, at the interfacial regions where AnxA5 interacts with Ca^{2+} and the PS polar head groups, domains are created that apparently exclude Mg^{2+}. This is because in the presence of PS, AnxA5 has no affinity for Mg^{2+} – in stark contrast to its high affinity for Ca^{2+} (60, 61). For example, if AnxA5 and PS micelles are co-incubated with low levels of Ca^{2+}, they rapidly form complexes that co-sediment with the PS liposomes. In

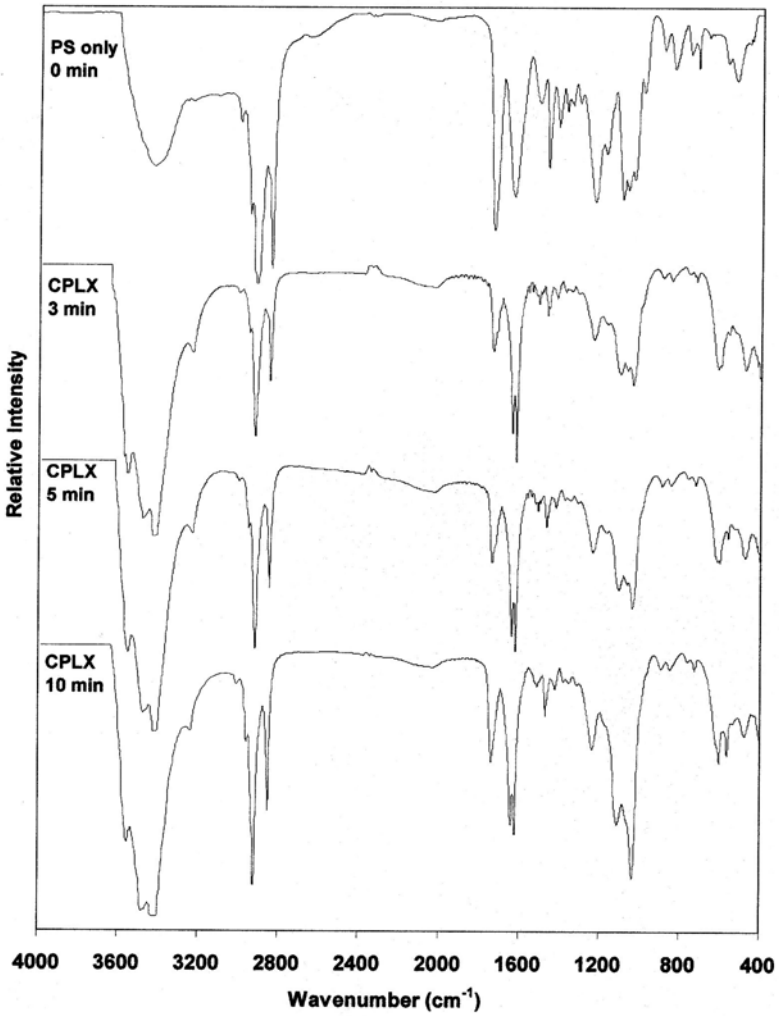

Figure 26. FTIR Analysis of the Reaction Time Needed for Formation of PS-CPLX. PS-CPLX was synthesized by drying 5 mg PS in chloroform under N_2 to form a thin film in a test tube. Then 2 ml of KCl (150 mM)-KP_i buffer (10 mM, pH 7.5) was added; and the tube then sonicated for 1–2 min in a water bath at 25°C to form small unilamellar liposomes. Of this PS stock, 50 microliters (0.16 micromol) was diluted with 150 microliters of the KCl-KP_i buffer for making 200 microliters of CPLX. Then 9.6 microliters of 100 mM $CaCl_2$ was added dropwise with constant stirring to form 6:1 Ca^{2+}/PS (molar ratio) complexes and allowed to react for up to 10 min. After the indicated incubation times (see below) CPLX samples were chilled to 0°C and harvested by centrifugation at 13,000 x g for 5 min. The supernatant fluid was decanted, and tubes were allowed to drain, wiped to remove residual fluid and then lyophilized after freezing at –80°C. For FTIR analysis, samples of the dried pellet (1 mg) were incorporated into KBr (300 mg) pellets formed under vacuum at 12,000 psi pressure, and then examined over a range from 4000 to 400 cm^{-1}. Spectrum 1 – PS only, 0 min; Spectrum 2 – CPLX, 3 min; Spectrum 3 – CPLX 5 min; Spectrum 4 – CPLX, 10 min. Note the similarities and the differences between the FTIR spectra of pure PS (top) with those of PS-CPLX (below) during the early reaction period (3 min, 5 min and 10 min). From left to right, the deep, broad O–H stretching peaks at ~3450 cm^{-1} is due to the presence of bound water. The sharp C–H stretch peaks of the lipid chains are at ~2920 and ~2850 cm^{-1}; the strong carbonyl C=O peak of fatty acid esters is at ~1740 cm^{-1}. The strong peak at 1640 cm^{-1} of the C-NH_2 group in PS became split in the CPLX samples, indicative of increased ordering. The sharp C–H scissoring peak at ~1470 cm^{-1}, and the C–O peak at ~1234 cm^{-1} are characteristic of fatty acid esters. With increasing reaction time, the P–O stretch peaks characteristic of calcium phosphates became progressively more and more intense: the 1032 cm^{-1} nu_3 band of PO_4^{3-}; the 1110 cm^{-1} nu_3 band of HPO_4^{2-}; and the 1063 cm^{-1} nu_3 band characteristic of disordered HPO_4^{2-} in poorly crystalline biological apatitic mineral (582). Notice in the 560–600 cm^{-1} region of CPLX that at 3 min only a broad peak characteristic of ACP is evident. Then, barely noticeable at 5 min, but clearly evident at 10 min are two sharp peaks at ~600 and ~560 cm^{-1}, nu_4 antisymmetric P–O bands characteristic of highly ordered (crystalline) calcium phosphates. It is this highly ordered two-dimensional structure that enables PS-CPLX to become a powerful nucleational agent. (Originally published in (131) by the American Society for Biochemistry and Molecular Biology.)

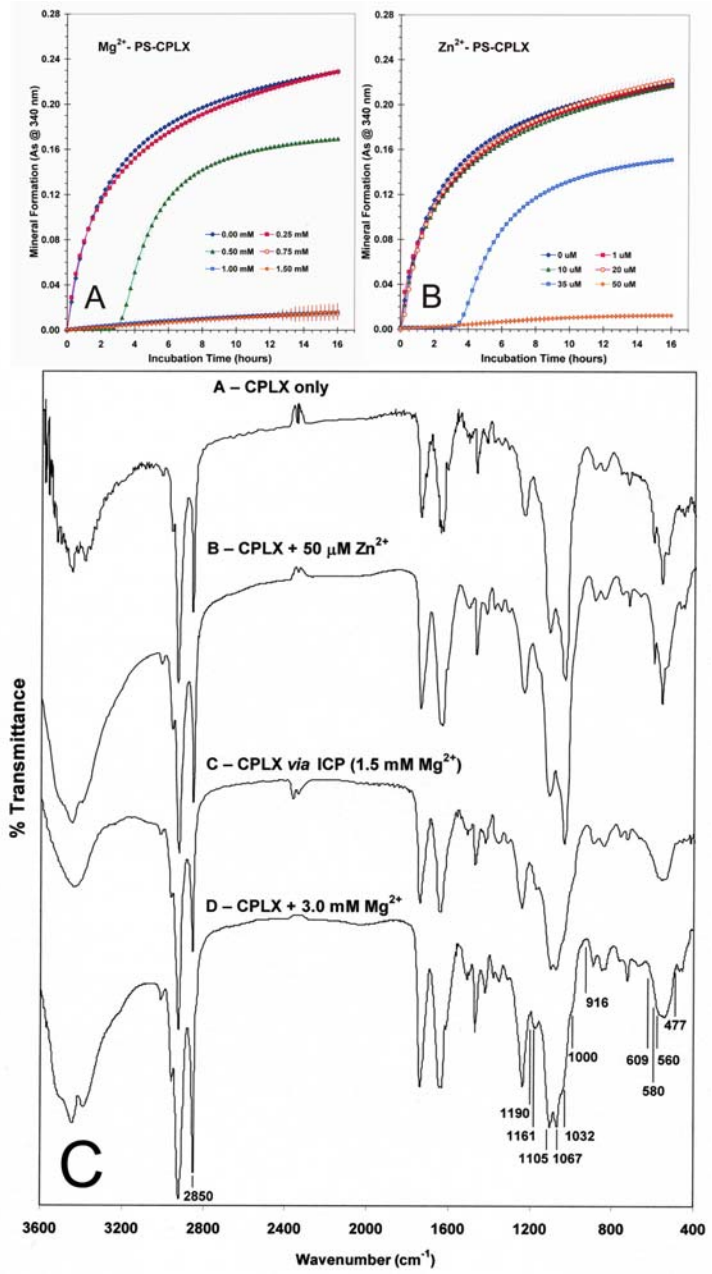

Figure 27. Effect of Incorporation of Mg^{2+} and Zn^{2+} on Properties of PS-CPLX. The effects on mineral formation were assessed by incubation in normal SCL. 27A-B – Effects on nucleational properties, the pattern of mineral formation observed when 50 microliters of PS-CPLX were seeded into SCL. **27 A** – Effects of Mg^{2+} incorporated into PS-CPLX: 0, 0.25, 0.50, 0.75, 1.00, and 1.50 mM are shown; levels below 0.25 mM caused no effect on mineral formation. At 0.5 mM, there was a 3 h delay; whereas levels at 0.75 mM and higher caused complete arrest of mineral formation within the 16 h period studied. **27B** – Effects of Zn^{2+} incorporated at 0, 1, 10, 20, 35, and 50 microM are shown; levels up to 20 microM had no significant effect on the induction time or overall mineral formation. At 35 microM Zn^{2+} delayed the induction time by ~3 h; at 50 microM Zn^{2+} completely blocked mineral formation for at least 16 h. **27C** – Effects on structural properties, as evaluated by FT-IR spectroscopy: in A – the control PS-CPLX with no additions; in B – PS-CPLX in which 50 microM Zn^{2+} was incorporated; in C – PS-CPLX formed from intracellular phosphate (ICP) buffer which contained 1.5 mM Mg^{2+}; and in D – PS-CPLX in which 3.0 mM Mg^{2+} was incorporated. While the general FTIR patterns were similar, there were significant effects of incorporated Mg^{2+} on the P–O stretch regions typically associated with phosphate-containing minerals. Note in the two Mg^{2+}-containing samples the lack of splitting in the 560–600 cm^{-1} region and that the P–O stretch complex between 1270 and 990 cm^{-1} were significantly different from that of the control. The Zn^{2+}-containing PS-CPLX did not show these features. (Reproduced from (137) with permission by Elsevier.)

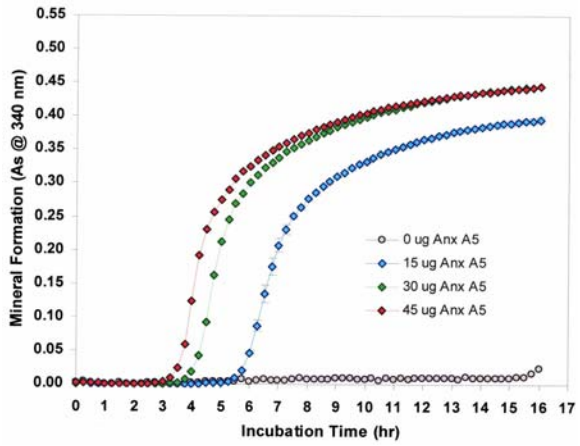

Figure 28. Effect of Annexin A5 on the Nucleation of Mineral Formation by Mg^{2+}-Containing PS-CPLX. PS stock (4x, 75 microliters) was mixed with 225 microliters of ICP buffer containing 0, 75, 150, or 225 micrograms of avian liver AnxA5; the volume was adjusted to 300 microliters, and then 6 microliters of 100 mM $CaCl_2$ was added (*ca*. 2 mM final concentration) and stirred for 10 min. After centrifugation, the CPLX pellet was resuspended by sonication in 300 microliters of SCL; 80 microliters of the suspension was diluted to 1 ml with SCL. Quadruplicate 140 microliters samples were transferred to four wells of a 96-well microplate. Mineral formation was monitored by light scattering (461) using the multiwell microplate assay system described by Wu *et al.* (457). In the control (0 micrograms Anx 5) Mg^{2+}-containing PS-CPLX prepared from ICP that contained 1.5 mM Mg^{2+} (gray circles) there was a nearly 16 h delay before the onset of mineral formation. Incorporation of 15 micrograms AnxA5 (blue diamonds) caused a dramatic shortening of the lag period from ~16 h to ~6 h; higher additions of AnxA5 (30 microgram, green diamonds; 45 micrograms, red diamonds) resulted in further shortening of the time to onset of rapid mineral formation. (Originally published in (136) by the American Society for Biochemistry and Molecular Biology.)

contrast, if Mg^{2+} is substituted for Ca^{2+} even at much higher levels, AnxA5 does not bind Mg^{2+} or co-sediment with the PS liposomes (Figures 4B–C). This is because the coordination chemistry of Mg^{2+} is very different from that of Ca^{2+} (469-471). Whereas Ca^{2+} can form flexible bond lengths and angles with as many as 7 different ligands, Mg^{2+} coordinates with only 6 ligands in a highly rigid, precise geometry (472-473). Thus, Mg^{2+}, because of its rigid coordination geometry, blocks the nucleational activity of PS-CPLX, and prevents ACP dismutation to HAP or OCP.

17.8. Mechanism of MV nucleation of OCP

A key event occurs during the induction phase that immediately precedes rapid mineral formation (332). At this time the PS-CPLXs, in conjunction with AnxA5, come together to produce a template from which OCP-like crystals rapidly proliferate. As previously noted, the Ca^{2+}/Pi stochiometry of Ca^{2+} and Pi accumulation during the rapid mineral formation period is 1.33 (Figure 10; Figure 16B), much lower than that of stoichiometric HAP (1.67) (57, 65). In fact the stoichiometry of Ca^{2+}/Pi during the rapid formation period is 1.33 – very close to the Ca^{2+}/Pi ratio of OCP (1.33) (317, 385, 449). However, it is evident that the initial mineral formed is not simple stoichiometric OCP, which when mature forms large platy crystals (474-476). Solid-state ^{31}P-NMR analyses of the initial mineral forms by Glimcher's group (477) show that the chemical shifts of the HPO_4^{2-} groups match those of both OCP (isotropic) and dicalcium phosphate dihydrate (anisotropic). The data reveal a HPO_4^{2-}-rich Ca^{2+} phosphate that is distinct from these well established crystalline phases. This is consistent with FT-IR analyses of initial MV mineral formation, which also indicates a HPO_4^{2-}-rich mineral phase (387). Thus, the initial crystalline phase is unique and transient, but over a matter of a few hours progressively converts to a non-stoichiometric, carbonate-containing HAP with a Ca^{2+}/Pi ratio of ~1.60 (160).

18. MODELING OF MATRIX VESICLES USING SYNTHETIC UNILAMELLAR LIPOSOMES

The ultimate challenge in understanding how MVs work is to reconstruct functional biomimetic models from pure components in proportions like those present in native vesicles. Our initial efforts involved incorporation of pure lipids, electrolytes and protein constituents into an emulsion made from a mild detergent, *n*-octyl beta-D-glucopyranoside (318). Using dialysis in an intracellular-like high-Pi buffer to remove the detergent, large (~300 nm diameter), stable, unilamellar vesicles (LUV) were formed; they encapsulated the Pi-rich buffer, and can include proteins like AnxA5. The LUV membrane contained PC, PS and free cholesterol (7:2:2, molar ratio); they enclosed 25–100 mM Pi, and had a ~300 nm diameter – each simulating values found in native MVs. When these LUVs were tested for their ability to induce mineral formation, incubation in SCL for periods as long a 48 h caused no $^{45}Ca^{2+}$ uptake. This documented that the LUVs were stable and not leaky.

18.1. Effects of Ca^{2+} ionophores on $^{45}Ca^{2+}$ uptake

To enable entrance of Ca^{2+}, various ionophores were initially used. Mineral formation was assessed by measuring the amount of $^{45}Ca^{2+}$ uptake, as well as FT-IR analysis of the LUVs, following incubation in SCL. If the Ca^{2+} ionophore, A23187 was added to SCL, rates of $^{45}Ca^{2+}$ uptake occurred that were comparable to those of native MVs (Figure 29A). After incubation of these A23187-activated LUVs for 24 h, sufficient Ca^{2+} uptake occurred to produce substantial amounts of mineral (318). Significantly, the mineral formed had an acid phosphate (HPO_4^{2-}) rich, OCP-like FTIR spectrum essentially identical to that of native MVs (Figure 29B). Thus, this simple LUV model mimicked two key features of MV mineral formation: 1) the soluble Pi-rich luminal fluid was sufficient to drive Ca^{2+} uptake, and 2) entrance of Ca^{2+} into this Pi-rich environment formed an OCP-like mineral just like that seen in native MVs.

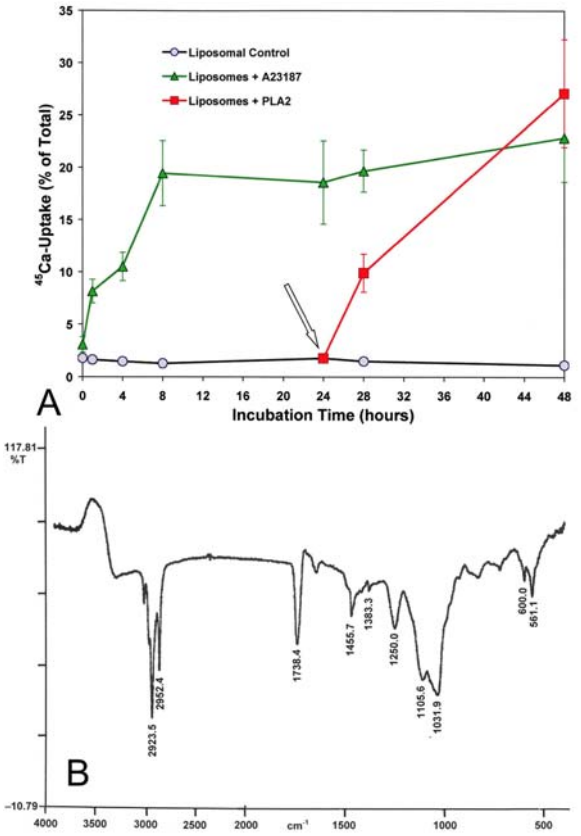

Figure 29. Effect of Ca^{2+} Ionophore A23187 and Phospholipase A_2 (PLA_2) on $^{45}Ca^{2+}$ Uptake by Liposomal Mimics of MVs. **29A** – Time-course of $^{45}Ca^{2+}$ uptake from SCL by large unilamellar vesicles (LUVs) incubated for 24 h, and subsequently treated with PLA_2. The LUV suspensions (50 microliters) containing 100 mM Pi and 150 mM KCl (pH 7.2), were incubated in 1 ml of $^{45}Ca^{2+}$-labeled SCL for the indicated time periods. Negative control – liposomes with no additions (*grey circles*); positive control – liposomes with ionophore A23187 (1.0 micrograms/ml SCL) (*green triangles*). After 24 h incubation, PLA_2 (1 unit/ml) was added to the SCL of the LUVs containing no ionophore (arrow) – (*red squares*), and incubated for the indicated additional times. Note the almost immediate onset of rapid mineral formation after addition of PLA_2. **29B** – FTIR analysis of mineral formation by the liposomes. Shown is the FTIR difference spectrum in which the FTIR spectrum of nonincubated LUVs was computer-subtracted from that of LUVs incubated for 24 h at 37°C in SCL containing A23187 (5.0 micrograms/ml). Note the split 561 and 600 cm^{-1} absorbencies, and the strong absorbencies at 1032 and 1106 cm^{-1} characteristic of HAP formed *via* OCP. These features closely match those of native MV CaPi mineralization. Modified from (318) with permission from Elsevier.

18.2. Minimal effects of annexin A5 on $^{45}Ca^{2+}$ Uptake

Based on the assumption that AnxA5 was functioning as a Ca^{2+} channel in the MV membrane, attempt was made to model MV Ca^{2+} uptake using AnxA5 added to the SCL. Surprisingly, it only weakly supported $^{45}Ca^{2+}$ uptake by the LUVs (319), which was in stark contrast to ionophore A23187 which enabled rapid accumulation of $^{45}Ca^{2+}$. Thinking that the protein perhaps needed to be present within the lumen, we encapsulated the AnxA5 during formation of the LUVs and tested them for their ability to take up $^{45}Ca^{2+}$. Surprisingly, even here AnxA5 also failed to produce significant $^{45}Ca^{2+}$ uptake. At first glance, these findings appear to be at variance with those of Kirsch who reported that AnxA5 stimulated Ca^{2+} flux across liposomal membranes (478). However, in those studies only tiny amounts of Ca^{2+} were accumulated (detectable only by a Ca^{2+}-sensitive fluorescent probe, FURA). There was no encapsulated Pi in those liposomes, and no attempt was made to determine if AnxA5 enabled sufficient Ca^{2+} uptake to induce mineral formation.

18.3. Effects of detergents and phospholipase A_2

There were two other important findings from the Blandford study (318). First, treatment of the Pi-loaded liposomes with the detergent, CHAPS, greatly stimulated $^{45}Ca^{2+}$ uptake. This occurred after a 24 h control incubation of the LUVs in the absence of detergents in which no $^{45}Ca^{2+}$ uptake occurred. Thus, treatment with CHAPS led to rapid and extensive uptake of $^{45}Ca^{2+}$. If the effects of CHAPS were studied sequentially with those of ionophore A23187 in the same LUV preparation, the effects of the two agents were additive. However, from a physiological perspective, the most significant finding of this study was that treatment with phospholipase A_2 caused rapid and extensive $^{45}Ca^{2+}$ accumulation. Again, this occurred after a control 24 h incubation of the liposomes in $^{45}Ca^{2+}$-labled SCL in the absence of either ionophores or strong detergents in which no $^{45}Ca^{2+}$ uptake occurred (Figure 29A). These findings clearly show that disruption of the vesicle membrane is sufficient to trigger rapid Ca^{2+} uptake. At the time these experiments were done, AnxA5 was thought to be an important Ca^{2+} channel in MVs (125, 479). While we were greatly puzzled by its inability to support $^{45}Ca^{2+}$ uptake by the LUVs, we had not yet discovered the extensive breakdown of phospholipids that occurs in native MVs when incubated in SCL (207). It is now apparent that breakdown of membrane phospholipids *via* action of phospholipase activity is an important part of the natural mechanism for allowing Ca^{2+} access to the lumen of the vesicles. However, as noted above (Figure 28), reconstitution of a biomimetic nucleational core clearly reveals that AnxA5 exerts a potent stimulatory effect on its nucleational activity. Its principal effect is to markedly accelerate the onset of mineral formation by enhancing the nucleation of OCP formation within the MV lumen.

18.4. Proteoliposomal MV Models by other groups

As noted above, Kirsch *et al.* (478) produced large unilamellar liposomes for studying the ability of AnxA5 to mediate Ca^{2+} uptake using FURA as an indicator. Very recently, Simao *et al.* reported on the production of proteoliposomes as models of MVs for study of initiation of skeletal mineralization (190, 479). However, in none of these model studies was there any measurement of the kinetics of mineral formation or of the nature of the mineral formed by their MV models. In the Kirsch *et al.* study there was no indication that the level of Ca^{2+} uptake caused by the incorporated AnxA5 was

sufficient to induce mineral formation. In the Simao *et al* studies, although they were able to incorporate specific enzymes (TNAP, NPP1) into the liposomes, and show that these enzymes exhibited appropriate activity when incorporated (190, 479), there was no indication that these enzymes enabled mineral formation by the liposomes. In another recent study, MVs were isolated from cultured osteoblasts derived from wild-type and TNAP-, NPP1- and PHOSPHO1-gene-deleted mice and studied for their ability to hydrolyze putative phosphosubstrates and induce mineral formation (193). However, rather than study the ability of intact MVs to induce mineral formation, these authors first lysed the MVs with deionized water and then added this lysate to a calcification medium that contained at least 3 mM (and most likely 10 mM) AMP, as well as 2.2 mM Ca^{2+} and 1.6 mM Pi. Given these artificial conditions, TNAP would have generated sufficient Pi from the added AMP (plus that from the calcifying medium) to raise the Ca^{2+} x Pi ion product to a level where spontaneous mineral precipitation would occur. Freeze-clamp zonal analysis of growth plate cartilage by Shapiro's group (480) have shown that levels of AMP are only 0.25–0.65 mM, values nearly 10-fold lower than those used in this study.

19. REGULATION OF MV CALCIFICATION

Many factors are involved in the regulation of the nucleation of mineral formation by MVs – and the proliferation and growth of crystals in the extravesicular matrix. Those primarily influencing MV *nucleation* include: a) the inhibitory effects of Mg^{2+}, Zn^{2+}, and PPi, b) the aforementioned synergistic effects of the MV annexins and PS, and c) the inhibitory effects of PE and other lipid components of the MV membrane. Those specifically influencing subsequent *crystal growth* and *proliferation* are: d) PPi – a powerful inhibitor of apatitic crystal growth, e) the proteoglycans that encompass and limit spread of the newly forming mineral in cartilage, and f) the collagens that facilitate and guide crystal growth to form the strong mineral-collagen composite typical of bone. In addition, there are a series of mineral-regulating proteins that bind to apatite and generally inhibit crystal growth. The effects of nearly all of these regulators are complex and to one degree or another affect both nucleation and crystal growth.

19.1. Factors that primarily effect nucleation

The factors that primarily influence the ability of MV to nucleate mineral formation will be discussed first. Experimental studies in which these effects were most clearly delineated were those aimed at reconstituting the native nucleational core present in MVs (116). As a control, ACP was prepared from a Mg^{2+}-containing phosphate buffer modeled after the composition of the cytosol of growth plate chondrocytes (63); it was used as the nucleator to which the various lipid-containing ACP complexes were compared. Parameters studied were: induction time, rate of rapid mineral formation, nucleational potential and amount of final mineral formed. In this Mg^{2+}-containing system, surprisingly, incorporation of PS during formation of the ACP to form the PS-Ca^{2+}-Pi complex significantly impeded mineral formation, decreasing the rate of rapid mineral growth and the final amount of mineral formed (116). However, incorporating AnxA5 along with PS, led to synergistic acceleration of the onset of mineral formation and enhancement of the rate of mineral formation – when compared with the ACP combined with AnxA5 alone (Figure 28). Thus the marked stimulatory effect of incorporating PS in this Mg^{2+}-containing native ACP was dependent on the co-presence of AnxA5.

19.2. Effects of phospholipid composition

As noted earlier, by varying the composition of the lipid mixture used in forming the annexin-containing ACP-based nucleational complex it was documented that pure PS was most effective in stimulating nucleation (443). Dilution with PE, and the other lipids present in MVs progressively reduced the effectiveness of these nucleators. Thus, it is not fortuitous that PS is consistently enriched in all MV preparations, and that *in vivo* mechanisms (*i.e.* PS synthase) are in place to facilitate PS formation – even in the absence of ATP (207, 268). Of physiological importance, the inhibitory effect of incorporating PE into the complex was essentially overcome by the incorporation of AnxA5 (443).

19.3. Stimulatory effect of different annexins on MV nucleation

As was evident above (Figure 28), AnxA5 is important for enhancing the nucleational activity of biomimetic Mg^{2+}-containing nucleational complexes. Although the presence of Mg^{2+} is ignored in many studies, it is the major divalent cation present in all living cells – including growth plate chondrocytes. When the protein composition of nucleationally active MVs was first characterized, annexins A5, A2 and A6 were identified as being quantitatively major proteins (60, 61, 94); subsequent proteomic studies have confirmed this and also revealed the presence of additional annexins – A1, A11 and A4 (78, 87). One of the key features of all of the annexins is their acidic phospholipid-dependent Ca^{2+}-binding affinity. For example, half-maximal binding affinity of Ca^{2+} for AnxA5 in the presence of PS is ~5 x 10^{-7} M (Figure 5) (60). Inorganic P does not interfere with this lipid-dependent Ca^{2+} binding property (Figure 4C). It was thus of major interest to determine the ability of the different MV annexins to stimulate mineral formation when incorporated into synthetic nucleational complexes modeled after those present in native growth plate MVs. In a recent study, the effects of native chicken cartilage annexins A5, A2 and A6 were compared with those of native human placental AnxA5 and avian liver AnxA5 (136). It was found that all of the AnxA5s potently activated the nucleational activity of Mg^{2+}-containing PS-Ca^{2+}-Pi complexes. From a physiological perspective, however, native avian cartilage AnxA5 was the most effective form of the annexins. It is significant that avian cartilage annexin A6 was less active than AnxA5, and that annexin A2 had little or no stimulatory activity.

19.4. Effects of non-apatitic electrolytes

Polyvalent electrolytes that occur as minor

constituents of biological apatites can exert a profound inhibitory influence on formation and growth of calcium phosphate crystals. The three electrolytes that exert the most direct influence on this process are Mg^{2+}, Zn^{2+}, and PPi – although CO_3^{2-} substitution appears to be an almost universal biological "contaminant" that regulates apatitic crystal size (481-484). From a biological perspective, the key issue is the relationship between the levels needed to significantly affect the various mineralization parameters and the levels known to be present in biological fluids. Here it is important to distinguish between the levels present in blood serum (or more specifically, the tissue lymph) and those present within the cells where MVs are formed (*e.g.* growth plate chondrocytes). More relevant still are the levels present in ultrafiltrates of these fluids, eliminating the effects of ions bound to macromolecules like proteins and proteoglycans or anionic phospholipids. Even more relevant are the actual chemical ion *activities* that are modulated by low molecular weight solutes like cellular metabolites. Chemical analysis of MVs, their constituent PS-Ca^{2+}-Pi complexes, and the intracellular and extracellular fluid of growth plate tissue all reveal the presence of substantial levels of Mg^{2+}, Zn^{2+} and PPi. The most relevant comparisons are between the inhibitory IC_{50} values of these ions for different mineralization parameters and the levels present in the bathing fluid.

19.4.1. Effect of Mg^{2+}

MVs are formed by growth plate cells whose cytosolic levels of Mg^{2+} are much higher than those of Ca^{2+} (Table 2) (63). Thus, all PS-Ca^{2+}-Pi complexes formed *in vivo* incorporate both Mg^{2+} and Zn^{2+}; in fact analyses of the complexes present in avian MVs have shown that Mg^{2+} is almost as abundant as Ca^{2+} (64). Our recent studies have revealed that this level of Mg^{2+} is profoundly inhibitory to the nucleational activity of PS-Ca^{2+}-Pi complexes, greatly reducing their rate (Figure 27A) (137). This inhibitory effect is physiologically important because as noted above rapidly growing species like broiler-strain chickens have such fast longitudinal growth that speedy nucleation is essential for mineral formation to keep pace. Thus, delays in the induction time of as little as 1–2 h, or 20% reduction in the rate of mineral formation, if consistent, would lead to the development of rickets in these birds. Mg^{2+} is the predominant intracellular divalent cation in all living cells. Even during the differentiation, maturation and hypertrophy of growth plate chondrocytes the cytosolic levels of ultrafilterable Mg^{2+} are over 10-fold higher than those of Ca^{2+}. This is true at the time of heavy loading and release of mitochondrial Ca^{2+} that triggers the blebbing of Ca^{2+}, Pi, and PS-CPLX-primed MVs. In fact, in MVs that form from these cells, the ratio of soluble Mg^{2+}/Ca^{2+} was ~9/1 (64); this level of Mg^{2+} is sufficient to essentially block the conversion of ACP to HAP. While the molar ratio of Mg^{2+}/Ca^{2+} in the insoluble fraction was much lower (0.15±0.03), this level was still sufficient to delay the conversion of ACP to HAP for a matter of days (444, 463). And as just illustrated, recent studies on synthetic PS-Ca^{2+}-Pi complexes showed that incorporation of low, subphysiological levels of Mg^{2+} led to profound inhibition of their nucleational activity (137). FT-IR analyses showed that Mg^{2+} altered their structure, greatly disordering the 560–600 cm^{-1} region (nu_4 antisymmetric P–O bending modes) characteristic of crystalline phosphate groups (Figure 27C). Mg^{2+} prevented the splitting of this region, indicating destruction of the short-range crystal-like P–O structure normally present in Mg^{2+}-free PS-Ca^{2+}-Pi complexes. FT-IR analyses also showed an increase in the 1062 cm^{-1} disordered nu_3 HPO_4^{2-} groups and a decrease in the 1032 cm^{-1} ordered nu_3 PO_4^{3-} groups of the complex. As noted earlier, packing of clusters of PS-Ca^{2+}-Pi complexes in the MV membrane produces assemblies that form sites for OCP mineral nucleation. Mg^{2+} obviously interferes with the ordering of P–O resonances at these sites; however, as we have just seen, if AnxA5 is also incorporated into the PS-Ca^{2+}-Pi complexes, the effects of Mg^{2+} are largely abrogated (Figure 28) (116, 136). This is because AnxA5 has no affinity for PS in the presence of Mg^{2+}. It is also important to note that when Mg^{2+} was present in the extravesicular lymph its inhibitory effects were far less; supraphysiological levels as high as 2.5 mM cause minimal delay in the onset of mineral formation (137). These findings document that AnxA5 is a key factor that enables Mg^{2+}-rich MVs to form HAP.

19.4.2. Effect of Zn^{2+}

Studies of Sauer *et al.* have shown that levels of *extravesicular* Zn^{2+} as low as 5 microM are sufficient to totally block MV mineral formation (Figure 17A); this Zn^{2+} blockage can be rapidly overcome by subsequent treatment with the Zn^{2+} chelator, *o*-phenanthroline (Figure 17B) (317). Paradoxically, as noted previously, analysis of MVs revealed the presence of surprisingly high levels (1.57±0.17 mM) of total Zn^{2+} within MVs. While most of the Zn^{2+} (~60%) was associated with the insoluble phase, a second phase (~40%) could be lost upon exposure of the MVs to Ca^{2+}-free media. Evidentally, this portion of Zn^{2+} binding within the MVs was Ca^{2+}-dependent (385). However, no Zn^{2+} was detected in expressed growth plate cartilage lymph using highly sensitive atomic emission spectrometry (317). Nonetheless, this intravesicular Zn^{2+} had minimal inhibitory effect on MV mineralization; these vesicles readily induced mineral formation (317). Our recent studies confirm this (137); FT-IR analyses reveal that Zn^{2+} incorporated into PS-CPLX has no disruptive effect on its 560–600 cm^{-1} crystal-like structure (Figure 27C), and had minimal effect on mineral formation (Figure 27B). Normal levels of Zn^{2+} incorporated into the nucleational core of MVs did not interfere with mineral formation. On the other hand, as noted above, the presence of low micromolar levels of Zn^{2+} in *extravesicular* lymph caused profound inhibition of MV mineralization. The key question is how? Blockage of the Ca^{2+} channel activity of AnxA5 at first seemed logical – based on electrophysiological studies by Arispe *et al.* showing Zn^{2+} blockage of AnxA5 Ca^{2+} conductance (125) – presumably because of tight Zn^{2+} binding to Ca^{2+} sites in the ion channel. But there is a more plausible explanation. As noted earlier, in the presence of Ca^{2+}, AnxA5 trimers form planar hexagonal arrays on the surface of PS-rich lipid bilayers (Figures 30A, 31A–B) (129, 130). These planar arrays of AnxA5 trimers appear to be key mineral nucleation sites on the

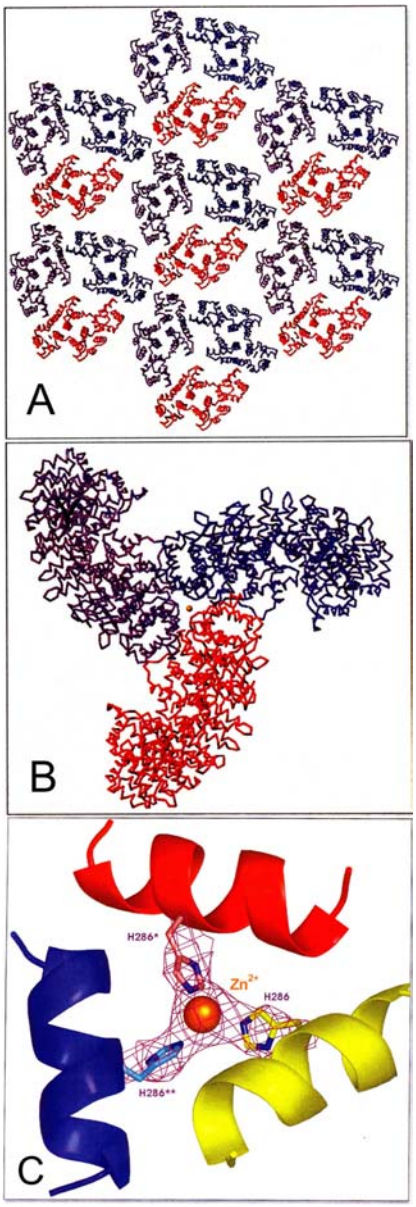

Figure 30. Effect of Incorporation of Zn^{2+} on the Crystal Lattice Structure of Annexin A5. **30A** – Hexagonal array of Zn^{2+}-free AnxA5-Ca^{2+} Trimers. The hexagonal packing closely resembles the arrangement of AnxA5 observed by Oling *et al.* (129) on PS-rich membranes. AnxA5 forms a plane of hexagonally arranged trimers; all Ca^{2+}-binding sites are located on one face of the plane, positioned for interaction with the phospholipid membrane. **30B** – Zn^{2+}-containing AnxA5 trimer. A partial unit cell for the Zn^{2+}-containing trimer is shown. The distorted propeller-like trimers so fomed do not assemble into a planar hexagonal array, even though the 3-D structure of the individual monomers is minimally disturbed. **30C** – Detail of Zn^{2+} binding site in AnxA5-Zn^{2+} trimer. Shown is the coordinated binding of three symmetrically equivalent H286 residues to a Zn^{2+} ion (orange), which resides on a crystallographic three-fold axis. (Reproduced from (485) with permission from Lands Bioscience).

PS-rich MV membrane. Importantly, in studies of the crystal structure of Zn^{2+}-AnxA5 adducts (485), while the 3-D structure of the AnxA5 *monomers* is not altered, Zn^{2+} does bind to a coordination site formed at the interface of those monomers – three His-286 residues (Figure 30C) – distorting the *trimer* structure (Figures 30B, 31C–D). This seriously disrupted the normally planar hexagonal arrays (Figure 31A–B), which would readily explain why addition of *o*-phenanthroline can so rapidly restore mineral formation by Zn^{2+}-inhibited MVs (Figure 17B) (317). Chelation of Zn^{2+} would allow rapid reformation of the planar AnxA5 trimers and the hexagonal nucleation array, because Zn^{2+} does not alter the AnxA5 *monomer* structure.

19.4.3. Effect of pyrophosphate (PPi)

From a metabolic perspective, it is important to realize that PPi is the byproduct of several key activating enzymes in all cells – including growth plate chondrocytes – involved in glycogen, proteoglycan, DNA and RNA synthesis, as well as activation of fatty acid catabolism. Most of these reactions require phosphatase enzymes to cleave PPi, which pull the reactions forward. PPi is also formed *via* NPP1 during chondrocyte and osteoblast activity (165, 193). PPi adsorbs tightly to HAP (486-487) and is capable of blocking crystal growth (488-490). In fact, the concept that PPi is involved in the regulation of skeletal mineral deposition goes back almost 50 years to the hypotheses by Fleisch (194, 491-496). Zonal analysis of PPi and Pi in fetal bovine tissue revealed that during the onset of mineralization in growth plate cartilage the amount of PPi and Pi per unit dry weight both increased, but the ratio of PPi to Pi declined precipitously (497) (Figure 32). While TNAP was already known to hydrolyze PPi (178, 498), it was not established that PPi was actually destroyed *in vivo* by TNAP during growth plate mineralization. In fact, the levels of PPi in growth plate tissue actually increase – but far less rapidly than levels of Pi (497). Further, in hypophosphatasia, a disease of TNAP deficiency, it was known that there was not only defective bone mineralization, but that levels of PPi were elevated in both urine (499) and blood plasma (500). Studies by Ali *et al.* showing that TNAP is highly enriched in MVs (53, 158) were followed by those of Register *et al.* comparing the inhibitory effects of PPi and two non-hydrolyzable bisphosphonates (EHDP and Cl_2MDP) on $^{45}Ca^{2+}$ and ^{32}Pi uptake by TNAP-rich MV-enriched microsomes (501). These studies showed that while inhibition with EHDP and Cl_2MDP persisted for many hours, inhibition by PPi did not; thus revealing that hydrolysis of PPi by MV enzymes was able to overcome its inhibition of apatitic mineral deposition.

However, later it was discovered that MVs isolated from osteoarthritic cartilage or chondrocalcinosis, were capable of depositing Ca^{2+}-PPi dihydrate (CPPD) (502). Thus the conclusion that PPi was a key regulator of cartilage mineralization became problematic. It became even more so when MVs isolated from human osteoarthritic cartilage were found to produce both CPPD and HAP *in vitro* (503). While the formation of CPPD crystals was closely correlated with the presence of

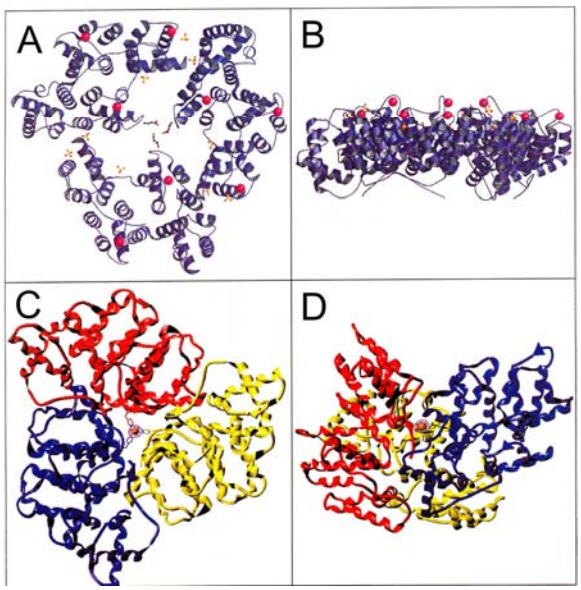

Figure 31. Effect of Incorporation of Zn^{2+} on the Planarity of Annexin A5 Trimers. View of Ca^{2+}-coordinated trimers looking down (**31A**) and perpendicular to (**31B**) the three-fold axis. The protein backbone is shown in blue; Ca^{2+} ions are shown in red and SO_4^{2-} ions are rendered as ball and sticks. This arrangement is observed for membrane-bound annexins, suggesting that their physiological roles depend on trimer formation. View of Zn^{2+}-coordinated trimer arrangement looking down (**31C**) and perpendicular to (**31D**) the three-fold axis. The three (red, gold, blue) subunits form a tight, warped Zn^{2+}-coordinated trimer distinctly different from that of the planar Ca^{2+}-coordinated trimer shown in (31A–B). Rather than forming the open, planar assembly observed with the AnxA5-Ca^{2+} complex, the trimers of AnxA5-Zn^{2+} (31C–D) form a non-planar globular arrangement, even though the structure of the individual monomers is not distorted. (Reproduced from (485) with permission from Lands Bioscience).

nucleoside triphosphate pyrophosphohydrolase (NPP1 – PC1), it became evident that formation of CPPD required the presence of ATP as a substrate (503). The story became even more complex with the discovery that in progressive ankylosis (ANKH) (504-509) the gene expressed was a defective mutant PPi transporter in the chondrocyte plasma membrane. This defect prevented PPi from escaping from the cytosol to the extracellular fluid – where it would have presumably blocked unwanted soft tissue calcification. From gene knockout studies conducted since then it has become progressively clear that TNAP has an important function in hydrolysis of PPi at sites of beginning mineral formation (162, 163). Further studies have shown that co-knockout of PC1 and/or the ANKH gene and TNAP can partially correct the mineralization defects caused by the absence of each alone. While these studies are tantalizing, the findings are not all clear cut. More will be made of this later when several types of gene knockout studies are considered.

19.5. Inhibitory effects of proteoglycans on mineral formation

Early on it was evident that proteoglycans present in the extracellular matrix of growth plate cartilage exerted a powerful inhibitory effect on mineral formation (510-512). Evidence for this role came from the following observations: a) the extracellular fluid collected from the growth plate completely inhibited mineral growth when seeded with mineral isolated from calcifying sites of growth plate mineral formation; b) this inhibitory effect could be abolished by prior treatment with hyaluronidase; and c) the inhibitor reacted positively to antibodies to proteoglycan (511). This work was preceded by a systematic study of the specific interaction between cartilage protein-polysaccharides (proteoglycans) and freshly precipitating calcium phosphate mineral (513). It became evident that certain components of the proteoglycan assembly in cartilage could prevent sedimentation of the precipitating mineral. These studies indicated that proteoglycans confine and limit the spread of mineral formation. They do not bind to specific sites on the developing mineral or prevent crystal growth (*e.g.* like PPi or proteins like osteonectin); they encompass the mineral and present a powerful diffusion barrier. Calcified cartilage exemplifies the effect of proteoglycans; it actually has a higher percentage mineral content than true bone (514-515) – yet half of the proteoglycan is still present in its matrix. Clearly, significant removal of proteoglycans does occur during cartilage calcification. It is largely accomplished by the presence of matrix metalloproteases (516-520) and makes room for apatitic mineral growth. However, extensive degradation of the proteoglycans is not required (521). Calcified cartilage stains strongly with alcian blue, indicating that much of the chondroitin sulfate is still present after calcification is completed.

19.6. Stimulatory effects of collagens on MV mineralization

Early transmission electron microscopy studies showed that the mineral crystallites of bone were in close registration with the periodicity of type I collagen (522), which has been repeatedly confirmed (523). Since it was evident that these two components were intimately related in bone, this supported the earlier hypothesis that type I collagen was the nucleator of HAP during bone formation (524). This compelling hypothesis held sway for at least a decade until 1967 when the first reports were made of MVs being the sites of *de novo* apatite mineralization during growth plate development (1, 3). Subsequent studies revealing that MVs bind tightly to type II and X collagens present in growth plate cartilage (95) enhanced earlier evidence that the C-propeptide of type II collagen was somehow involved in mineral nucleation (525). These studies were in accord with the findings that type II collagen binds to MV proteins like AnxA5 (95, 102, 402-403). Now nearly two decades later, this topic was reinvestigated using AnxA5-, ACP- and the PS-containing complexes as cofactors in the mineralization process (116). From these studies it became evident that neither type II nor type X collagen *accelerated* the onset of mineral formation. In fact, type X collagen tended to slow down the induction of mineral formation. It became

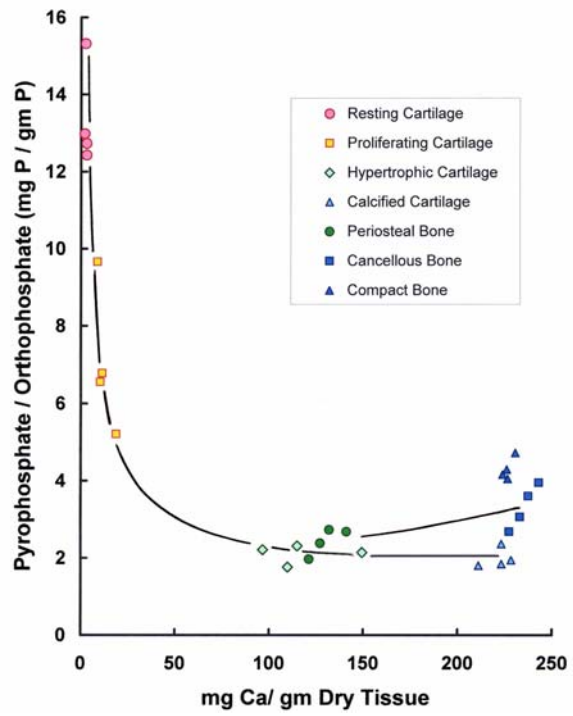

Figure 32. Relationship between Pyrophosphate/-Orthophosphate Ratios and the Degree of Mineralization in Successive Zones of Endochondral and Periosteal Ossification. Leg bones (femora and tibiae) of fetal calves were dissected and tissues from successive zones of calcification harvested (515, 516). Immediately after dissection (with the exception of cancellous bone, which was washed with physiological saline to remove the bulk of the bone marrow), the tissues were left unwashed and immediately freeze-dried. They were then stored at RT in a dessicator over anhydrous silica-gel until analyzed. Pyrophosphate (PPi) was analyzed as described by Bisaz *et al.* (583) using an isotope dilution technique. Shown is the relationship between PPi/Pi ratios and the degree of mineral deposition in successive zones of endochondral and periosteal ossification. Note the precipitous decline in the PPi/Pi ratio during the initial phases of endochondral calcification, and the subsequent increase in PPi/Pi during the maturation of bone. (Adapted in color from (497) with permission from Springer).

apparent that while the cartilage collagens had no ability to *accelerate* the *induction* of mineral formation, they clearly facilitated *mineral growth* once it had been induced by the PS-Ca^{2+}-Pi complexes (116). The effects were dosage-dependent; higher levels of type II collagen enhanced mineral formation in a progressive manner. And, although type X collagen delayed the onset of mineral formation, once it had been initiated, the duration of mineral formation was extended so that in the end it clearly enhanced the amount of total mineral formed. It was further observed that the presence of the non-helical telopeptides were indeed important to the stimulatory effects of type II collagen; pepsin treatment to removal these telopeptides significantly reduced the ability of type II collagen to stimulate mineral formation (116). These observations confirm the long held view of Poole *et al.* (525-528) that the C-propeptide of type II collagen is important to cartilage calcification. Since type I collagen is not significantly present in growth plate cartilage, in the above studies it was not investigated. However, in mineral deposition at other sites where type I collagen is a dominant structural protein, it recently has been found that binding of MV annexins to type I collagen enhanced mineral deposition (144). In this study on pathological calcification in vascular smooth muscle cells, it was evident that calcification was mediated by annexins A2 and A6 and was dependent on type I, not type II collagen (144). Thus, it is now apparent that in different circumstances interaction of different annexins with specific collagen types appears to be required. In this light, it would be of great interest to determine whether annexin A6 is involved in MV-mediated mineralization of turkey leg tendons (529), as well as in osteoblastic mineral deposition where, again, the predominant collagen is type I.

19.7. Effects of non-collagenous bone-related proteins

Many other non-collagenous proteins have been isolated from bone and have been considered to be of potential importance in regulation of HAP formation during bone formation and/or preventing unwanted soft tissue calcifications. While most of these bone-related proteins have not been directly tested for their effects on MV mineralization, most have been studied with regard to regulation of the general mineralization process (530). Since the focus of this review is specifically on MV mineralization, these proteins will not be discussed here; however, because they have obvious importance to overall control of mineralization, they will be mentioned. These proteins include osteonectin (531), osteopontin (532), bone sialoprotein (533-534), chondrocalcin (528, 535-536), and two vitamin K-dependent gamma carboxyglutamate (Gla)-containing proteins – bone Gla protein (BGP) (537-538) and matrix Gla protein (MGP) (539). Most of these proteins appear to act primarily as inhibitors of HAP crystal growth, although bone sialoprotein appears to have the ability to stimulate mineral formation (540). The most recent data indicate that phosphorylation of Ser-136 of BSP is critical for its nucleational properties (541).

20. FURTHER EVALUATION OF THE ROLES OF KEY MATRIX VESICLE PROTEINS

Several MV proteins and enzymes that appear to have important roles in MV mineralization have been subjected to gene knockout in the mouse. Although each was described earlier, their importance to the process of MV mineralization warrants further discussion in the light of these recent gene deletion studies. The proteins in mind are TNAP, AnxA5, PS-synthase, and PHOSPHO-1. Further, because of its newly appreciated role in conjunction with PHOSPHO-1 and phospholipase C; the remarkable stimulation by phospholipase A_2 in liposomal models of MV mineralization also merits further consideration.

20.1. Tissue nonspecific alkaline phosphatase (TNAP)

TNAP has received a great deal of attention over the past ~40 years, particularly since the discovery of its abundance in MVs (53). It has been the subject of numerous reviews, the most recent being a comprehensive and thorough review published in 2010 by Michael Whyte (542). Although the importance of TNAP to skeletal mineralization has been confirmed by gene knockout studies in the mouse, several unexpected issues have surfaced that warrant further discussion.

20.1.1. Role of TNAP in PPi hydrolysis

There is now almost universal acceptance that a major role of TNAP in bone is in the hydrolysis of PPi at sites of mineral formation. This ability of TNAP is important because PPi is such a potent inhibitor of apatitic crystal growth. In pure TNAP knockout in mice there is typically severe osteomalacia; simple reduction of systemic PPi by transgenic over-expression of TNAP using *ApoE-Tnap* completely prevents development of skeletal abnormalities (543). In fact, the concept that TNAP causes local hydrolysis of PPi is supported by studies going back at least 35 years. Even from our group it was shown that isolated pure TNAP had the ability to hydrolyze PPi at physiological pH (54, 177, 544) and that in the growth plate where TNAP is highly expressed, the ratio of PPi/Pi declines precipitously at the site of mineralization (Figure 32) (497). Now, however, with the ability to co-delete genes for TNAP and related PPi-generating or -transporting proteins in mice (165, 543), the key role of TNAP in skeletal mineralization is well established. Yet, although hypophosphatasia often displays increased excretion of PPi accompanying skeletal osteomalacia (542), recent findings by Yadav *et al.* (545) reveal that in PHOSPHO1 deficiency, reduction of circulating PPi does not overcome the mineralization deficit. Similarly, while co-deletion of NPP1 or ANK with TNAP largely prevented the vertebral osteomalacia induced by knockout of TNAP (182, 183, 546), mineralization of the appendicular skeleton was not fully normalized. Sustained osteomalacia of the long bones persisted, despite major improvement in the axial skeleton (162). These studies reveal that TNAP is involved in more than simple removal of PPi from mineralization sites in appendicular long bones.

20.1.2. Additional roles of TNAP

There is another paradox in hypophosphatasia. In TNAP knockout, mineralization of the developing skeleton is typically normal at birth (542). Somehow the maternal support system within the intrauterine environment enables normal mineral formation despite the fetal genetic defect. In these TNAP gene-ablated mice, despite the progressive osteomalacia, ultrastructural analysis reveals that in the growth plate, within MVs there are nevertheless normal amounts of mineral formed (289). However, the mineral fails to propagate from the protective enclave within the MVs. These findings indicate that skeletal mineralization must be a two-step process: 1) the *de novo* induction of mineral formation within the protective enclave of the MV lumen, and 2) the propagation of induced mineral into the extravesicular matrix – a concept expressed by Anderson in his recent review of the role of MV in osteogenesis (547). Thus, TNAP is not required for the induction step, but is essential for propagation of the apatitic mineral. Even in the absence of TNAP, normal mineral formation appears to occur within MVs. While it has been assumed that the lack of TNAP allowed persistent ambient PPi to block mineral crystal growth away from the MV nucleation site, the recent studies of Yadav *et al.* (545) show that this is not an adequate explanation. (From a thermodynamic perspective, once HAP crystals are formed, by a process of secondary nucleation, ordered nanoscale ion clusters are shed from the surface of these crystals and enable rapid spread of mineral formation – provided that crystal growth is not blocked by an inhibitor such as PPi.)

However, here we need to consider an even earlier enigmatic study on the die-off of TNAP during MV mineralization. Over 20 years ago we reported that during MV-induced mineralization there is a concomitant die-off of TNAP activity (76). We have repeatedly observed this phenomenon, but no other group has either confirmed or refuted it; nor has a satisfactory explanation been provided. However, now taken together with the above-stated failure of mineral to spread from the MV lumen, it is evident that TNAP must have yet another role – the extravasation of mineral from within the MV lumen. But in so doing, TNAP loses its enzymatic activity. The most obvious explanation of this phenomenon is that crystal growth from the MV lumen proceeds through and damages the structure of TNAP, leading to its denaturation. When we made this discovery, we attempted revive the activity of TNAP after mineralization had occurred by first removing the mineral using EDTA treatment, followed by restoration of the Zn^{2+} and Mg^{2+} that are known to be crucial to its enzymatic activity (76). We could only partially recover TNAP activity, indicating that mineral formation caused irreversible damage to the TNAP. Exactly how this occurs is currently unclear, but probably involves the Ca^{2+}-binding (174, 175) and Pi- binding (active) sites in the enzyme. This fact points to the need to solve the 3-D structure of skeletal TNAP. With such data in hand, quantum mechanical based molecular modeling should enable the elucidation of how TNAP brings about the extravasation of the mineral crystals from the vesicle lumen.

20.1.3. Improperly assigned roles of TNAP

There is yet one further issue that needs to be discussed here – one where previous and current reports are frequently in error – namely that TNAP is needed to hydrolyze organic phosphate substrates to provide Pi for induction of mineral formation. This error stems from an ignorance of the levels of phosphorylated substrates available in the extracellular fluid where mineralization occurs. Several studies that have addressed this issue and reveal that the levels of organic phosphate esters in the extracellular fluid are in the *micro*molar (not *milli*molar) range (302, 437, 439, 442, 480). Despite this, many investigators continue to use 3–10 mM (grossly excessive amounts) of beta-glycerophosphate (a nonphysiological substrate) to drive mineralization, oblivious of the fact that they are using an abnormal substrate in unwarranted levels when compared to those of extracellular biological substrates. Under these artificial conditions, what is

interpreted as induction of mineralization is simply a manifestation of TNAP activity, which releases sufficient levels of Pi that anomalous mineral deposition is induced. These levels of organic phosphate substrates do not occur normally *in vivo* in the extracellular fluid. Thus, what is thought to be a demonstration of normal induction of mineral formation is in reality a misleading experimental artifact.

20.2. Annexin A5 (AnxA5)

The acidic phospholipid-dependent Ca^{2+}-binding proteins – the annexins – are predominant proteins in MVs. The most physically abundant protein, AnxA5 (60, 94), is present in larger amounts than TNAP or any other MV protein (78). In fact, AnxA5 is the principal protein present in the nucleational core of native MVs (457). As has been demonstrated in this review, it has the remarkable ability to accelerate the onset and rate of mineral formation induced by the nucleational core. Thus, one would logically conclude that AnxA5 must play a major role in MV mineralization. However, there is now major confusion with regard to its physiological role; some regard AnxA5 as being irrelevant – having no biological function at all.

20.2.1. The questionable role of AnxA5 in Ca^{2+} Entrance into MVs

It has been widely assumed that AnxA5 serves as the Ca^{2+} channel in growth plate chondrocytes and MVs (94, 103, 145, 478). This was based on the presence of a hydrophilic channel in the 3-D structure of AnxA5 (and most other annexins) that is presumed to function as a Ca^{2+} channel (121). In fact, AnxA5 has been reported to enable Ca^{2+} acquisition by isolated MVs (330, 478, 548). However, questions are now arising as to whether the principal role of AnxA5 is in fact as a Ca^{2+} channel. *First*, AnxA5 is the principal protein in the nucleational core of native MVs; this core has the ability to induce mineral formation independent of the MV membrane or any Ca^{2+} channel activity (288, 443, 457). *Second*, incorporation of AnxA5 into synthetic nucleational complexes (modeled after those present in native MV) markedly accelerates the rate of mineral formation (Fig. 28) (116, 131, 136). Thus, while AnxA5 clearly enhances mineral formation by MVs, it is doubtful that it does so by acting as a Ca^{2+} ion channel. *Third,* although the studies by Arispe *et al.* showed multiconductance Ca^{2+} channel activity by pure AnxA5 in supported PS-containing phospholipid bilayers (125), there is a problem relating these findings to *in vivo* conditions. This is because the reported Ca^{2+} conductance studies involved use of nonphysiological conditions such as 100 mM CsCl and 70 mM $CaCl_2$ to demonstrate ion channel activity. Further, to cause inhibition of this channel by Zn^{2+} required 2 mM Zn^{2+}– 400-fold higher than what is needed to inhibit MV Ca^{2+} uptake. *Fourth,* more recent studies using large unilamellar liposomes as models of MV mineralization, revealed that encapsulation of AnxA5 within the liposomes, or addition of AnxA5 to the mineralizing fluid, failed to support significant Ca^{2+} acquisition (318). In contrast, ionophores like A12387 enabled rapid Ca^{2+} acquisition by the liposomes and induced definite mineral formation (Fig. 29). In addition, unlike L-type Ca^{2+} channels that have subunits containing multiple transmembrane domains that enable selective transport of Ca^{2+} (321, 324), there are no membrane-spanning domains in the 3-D structure of the annexins (123, 124). Finally, *fifth,* there is quantitatively far more annexin present in MVs than should be required to function as Ca^{2+} channels – if they were active carriers (60, 61, 78, 485). Proteomic analysis shows that the annexins are in far greater abundance than any of the numerous other transporters detected (78). This suggests that if they function as Ca^{2+} transporters, the annexins must be highly inefficient in this role.

20.2.2. Activation of the nucleational core by AnxA5

In contrast, as was described earlier, the most remarkable effect of AnxA5 is its acceleration and enhancement of mineral formation by the reconstituted nucleational core of MVs (Fig. 28) (116, 136, 332). Its ability to overcome the inhibitory effects of the ubiquitous presence of Mg^{2+} and the non-Ca^{2+}-binding MV lipids is nothing less than remarkable (131, 137). Since MVs are able to trigger mineralization in the hostile environment of the proteoglycan-rich extracellular matrix, and contain such abundant amounts of AnxA5, it not surprising that AnxA5 accelerates and enhances rapid mineral formation. In fact, all studies so far performed with respect to the nucleational core of MVs strongly indicate that it has a key role for stimulating mineral formation. As noted previously in the analysis of MV formation, there is also a straight-forward explanation of why AnxA5 becomes incorporated during MV formation, given its Ca^{2+}-dependent PS-binding ability.

20.2.3. Does AnxA5 have a physiological function *in vivo*?

Because of its obvious stimulatory effects on *in vitro* mineral formation – as well as its apparently key role in apoptotic processes – it was widely assumed that deletion of the AnxA5 gene would be lethal. Hence, it was a shock to read the dogmatic assertion that AnxA5 "is not essential for skeletal development" by Brachvogel *et al.* in 2003 (549). Even seven years after that original report, and the recent report that double knockout of AnxA5 and AnxA6 had no discernible effect on the mice (550), these findings still seem implausible. If one is to believe the implications of these reports, both AnxA5 and AnxA6 are irrelevant not only to skeletal mineralization, but to any other physiological function. This is implausible not only because of the their abundant expression in growth plate chondrocytes, but because of their abundance in cells of all phyla so far examined. There have been hundreds of reports indicating biological functions for these and other annexins; many indicate involvement in skeletal formation. Are all these findings invalid? They document activities of proteins whose genes have been expressed and conserved over millions of years of evolution. To date, neither of these annexin gene knockout findings has been confirmed by any other group. However, assuming that they are valid, what rational explanations can be postulated to explain the reported lack of function?

20.2.4. Possible alternative routes to growth plate and skeletal calcification

Knowing of the absolute essentiality of skeletal

mineralization for survival, it is plausible to speculate that backup mechanisms for induction of mineral formation exist and can be called into play if the normal pathway fails. Taking this view, it is plausible that the annexin knockout mice induced mineralization by a MV-independent mechanism. Both annexin knockout reports lacked ultrastructural detail in the histology of the mineralization site; this was particularly true of the initial report (549). While the second report (550) was more comprehensive, it still provided inadequate ultrastructural analysis of how the KO mice induced mineralization. In both studies the authors assumed the presence of of MVs, but provided no clear evidence that they were present at sites of initial mineral formation. Thus, an alternative backup mechanism may explain why apparently normal mineralization occurred in these mice.

20.2.5. Effects of Knockout of anxa5 and anxa6 on expression of other genes

In their most recent report, the Brachvogel group reported that despite having no discernible physiological effect on the mice, co-deletion of both AnxA5 and AnxA6 caused marked up-regulation of three poorly characterized genes: *Depdc6* (+26-fold), *Ptdsr* (+18-fold) and *Pold3* (+14-fold), as well as marked down-regulation of three other little understood genes: *BC045135* (–33-fold), *NAP115274-1* (–30-fold) and *Unc13a* (–11-fold) (550). What is the significance of these findings? The authors provide no clue. The best studied of the upregulated genes is *Ptdsr*, a putative receptor for phosphatidylserine (PS) (551-556). Did the PS receptor (Ptdsr) substitute for AnxA5? Recall that PS is the Ca^{2+}-binding acidic phospholipid previously implicated in binding with AnxA5 in the nucleational core of MVs (64, 457). While it would have been natural to assume that Ptdsr protein would bind PS and thereby provide a substitute for AnxA5, this turns out not to be the case (557-558). While the function of Ptdsr in apoptosis has been studied, the reports have been inconsistent (557, 559-560). It has now been concluded that Ptdsr is a misnomer and that the gene does not produce a receptor for PS. Thus, the putative upregulation of the Ptdsr gene in AnxA5 and AnxA5 knockout mice seems irrelevant. There are currently no clues as to why the expression of the other genes was altered.

20.2.6. What would have been the effects of expression of defective annexin mutants?

Another possibility is that pathology may become evident only if a defective mutant form of AnxA5 is expressed. The Belluoccio report, although comprehensive, did not rigorously exclude the possibility that some other member of this large gene family may have filled in for the two missing members. This story may be akin to what is observed in type X collagen gene deletion (561-565). Deletion of type X collagen caused no apparent growth plate or skeletal pathology (561); however, expression of various defective forms of type X collagen presented with significant skeletal pathology (566-570). Their conclusion was that only in the presence of an abnormal gene product was pathology observed. This may well be the case for the AnxA5 and AnxA6 gene knockout mice. This phenomenon can be envisioned using an analogy of workers in a factory assembly line. If a worker reports that he cannot work, management can bring in a replacement and maintain production. However, if the worker arrives ill, takes his place and is unable do the work, his job will not be performed and production will be blocked. Therefore, would it not be more instructive to over-express defective forms of AnxA5 – *e.g.* those with mutated PS-dependent Ca^{2+}-binding sites or perhaps altered "Ca^{2+} channel" structure – to determine their effects?

20.2.7. Is the need for AnxA5 stress-dependent?

Still another reason for the lack of effect of AnxA5 knockout may be because these highly inbred "wildtype" mice are maintained in a highly protective environment with all of their nutritional and other physical requirements met. If they were exposed to stresses like those of the ancestral wild mouse that affect skeletal development (*e.g.* Ca^{2+} or Pi deficiency, or some developmental stress) then differences between the wildtype and AnxA5-deleted mice may well become evident. A plausible explanation is that skeletal growth in a small rodent does not require the stimulus of AnxA5. The stress of needing very rapid bone growth in much larger, fast growing species like the broiler-strain chicken or long legged mammals like humans may make the requirement for AnxA5 critical. In fact, the principal effect of AnxA5 on mineral nucleation is to markedly accelerate the onset of mineral formation (Figure 28), (136, 332). Thus in a small animal like the mouse, where demands for maximal mineralization are unnecessary, AnxA5 catalytic stimulus may be superfluous. However, this still does not explain why all other bodily processes were unaffected. It seems implausible that the annexins should have been conserved over millions of years of evolution in many genera if they served no useful purpose.

20.3. Phosphatidylserine (PS) synthases

Perhaps the most unusual enzymes involved in MV mineralization are the PS synthases. These enzymee are required for the formation of PS, the key Ca^{2+}-binding acidic phospholipid intimately involved in formation of PS-CPLX.

20.3.1. PS synthases do not require high-energy nucleotides, but requires Ca^{2+}

In contrast to all other biosynthetic enzymes in lipid synthesis, these enzymes do not require high-energy nucleotides to drive PS formation; however the reactions are Ca^{2+}-dependent (571). This fact becomes important in the growth plate at the time of chondrocyte hypertrophy because levels of ATP and other nucleoside triphosphates are very low (442). PS synthases are enzymes that catalyze the Ca^{2+}-dependent exchange of the amino acid, serine, for the base present in the polar head group of either of two neutral membrane phospholipids, phosphatidylethanolamine (PE) or phosphatidylcholine (PC). As noted previously, there are two types of PS synthases (PSS) – PSS1 which exchanges serine for choline in PC, and PSS2 which exchanges serine for ethanolamine in PE (269). PSS2 activity is evident in

growth plate chondrocytes (267) and MVs (268); it must be involved in the increase in PS that occurs during MV mineralization (207). PS is required for synthesis of the PS-CPLXs involved in MV mineral nucleation. Early studies showed that synthesis of PS can occur in isolated MVs, and can be prevented by treatment with EDTA. These findings document the presence of PSS activity in native MVs (268).

20.3.2. PSS1 and PSS2 gene knockouts

Of further interest, recent studies have shown that PSS1-deficient or PSS2-deficient mice are viable, fertile, and have a normal life span; however, crosses of *Pss1*$^{-/-}$ and *Pss2*$^{-/-}$ mice produced no live offspring; this revealed that double knockout mice are not viable (572). However in *Pss1*$^{-/-}$/*Pss2*$^{+/-}$ and *Pss1*$^{+/-}$/*Pss2*$^{-/-}$ mice, where the ability to incorporate serine into PS was reduced by 65–91% with concomitant reduction in both PS and PE levels, the mice were still viable. These findings have bearing on the lack of effects of double knockout of AnxA5 and AnxA6, indicating that the activities of these annexins are not co-dependent. While any effects of PSS1/PSS2 double knockout on skeletal formation were not considered, these studies nevertheless inject a note of caution in the interpretation of negative results in gene knockout studies in mice.

20.4. Phospholipase A and C activities

The remarkable stimulatory effect on induction of mineral formation by simple addition of phospholipase A_2 to reconstituted liposomal models of MVs (Figure 29) (318), as well as the rapid degradation of MV phospholipids during induction of mineral formation (207) point to a heretofore little appreciated consequence of the lipid degradative activity evident in growth plate cartilage (223), in MV formation (73) and in MV mineralization (207).

20.4.1. Membrane lysis and Ca^{2+} access to the nucleational core

Because it was logical to assume that entrance of Ca^{2+} into MVs was mediated by the presence of AnxA5, the lack of ability of this protein to enable Ca^{2+} entrance into synthetic unilamellar liposomal models of MVs was unexpected (318). However in retrospect, it was unlikely that such an abundant protein in MVs as AnxA5 should be required for Ca^{2+} entry. On the other hand, the extraordinary stimulatory effect that simple addition of phospholipase A_2 to reconstituted liposomal models of MVs has on induction of mineral formation (Figure 29) (318) should not have been so surprising. It is apparent that synergistic activation of latent intravesicular phospholipase activity by influx of Ca^{2+}, such as was evident in the rapid breakdown of various phospholipids during MV mineralization, (207), would provide an efficient means for accessing Ca^{2+} and Pi to the nucleational core – once thermodynamically stable OCP crystals were established within the MV lumen.

20.4.2. Role in the egress of mineral from the vesicle lumen

It is highly probable that phospholipase activity is also an important factor in the egress of mineral from within the vesicle lumen; such activity would cause lysis of the membrane barrier. However, nothing is simple with MVs, because as was noted earlier, TNAP associated with lipid rafts in the MV membrane also appears to be involved (76); and it is also evident that Ca^{2+}-activated phospholipid scramblase activity (287) also may get into the act.

20.4.3. Salvage of phospholipid P for mineral formation

But coupled with the breakdown of membrane phospholipids is another little appreciated phenomenon – the catabolism of phospholipids also enables salvage of Pi for MV mineral formation. Phosphate, stored in the linkage of the polar head group of phospholipids of all membranes, including MVs, is made available for enhancing mineral formation by the release of phosphocholine and phosphoethanolamine through the action of phospholipase C on PC and PE, respectively (207). The mechanism by which this occurs will now be discussed.

20.5. PHOSPHO-1

PHOSPHO-1 is another important enzyme present in MVs (202-204, 573). It has the remarkable ability to coordinate breakdown of the MV membrane phospholipids with formation of mineral.

20.5.1. Salvage of Pi and choline$^+$ from phospholipid breakdown

PHOSPHO1 has the ability to hydrolyze phosphoethanolamine and phosphocholine, byproducts of phospholipase C action on PC and PE, to release Pi – as well as the amine bases, choline$^+$ and ethanolamine. What makes the action of PHOSPHO1 especially significant is the finding that Pi transport into hypertrophic chondrocytes and MVs is not strictly Na^+-dependent; in fact Pi uptake was more active with choline$^+$ than with Na^+ (208, 303). Thus, the hydrolytic products of phosphocholine by PHOSPHO1 not only release Pi needed form mineral formation, but choline$^+$ that can enhance Pi uptake by MVs. These are physiologically important functions.

20.5.2. Inhibition of PHOSPHO1 activity

Very recently it has been reported that inhibition of PHOSPHO1 activity resulted in impaired skeletal mineralization during limb development of the chick (205). This plausible conclusion was based on the finding that the inhibitor, Lansoprazole, markedly reduced mineralization of the long bones of the legs and wings. Unfortunately, Lansoprazole is by no means specific for PHOSPHO1 and is in fact a powerful inhibitor of H^+/K^+-ATPase (574-576). Thus, it is equally probable that the drug blocked H^+-transport in the growth plate chondrocytes and interfered with MV Ca^{2+} loading (306). As was discussed previously, H^+ metabolism is notable different in successive zones of the growth plate and appears to be vital for proper MV formation. Thus, although the findings that Lansoprazole inhibits mineralization are tantalizing, they are open to question.

20.5.3. PHOSPHO1 gene knockout

However, very recent findings reveal that knockout of PHOSPHO1 gene causes significant skeletal pathology (545). Deletion of the PHOSPHO1 gene produced numerous physiological effects: generalized mild osteomalacia accompanied by bowing of the long bones with evidence of frequent fractures, as well as growth retardation, and reduced food and water consumption. The specific effects on bone mineralization were not enormous, but led to obvious weakening of the skeletal structures – as evidence by the progressive scoliosis of the spine and the numerous fracture callouses observed. While there were minimal effects on most biochemical parameters in the blood serum, there was a transient increase in Pi levels – perhaps due to reduced mineral formation. One curious side effect was a slight reduction in blood plasma TNAP levels, as well as small increases in blood levels of NPP1 and PPi.

20.5.4. Co-modulation of TNAP and PHOSPHO1 gene expression

While over-expression of TNAP superimposed on the PHOSPHO1 knockout corrected the PPi level in blood, it had no beneficial effect on the osteomalacia. This reveals that the effects of PPi on mineral formation are not simple. From this study it is clear that TNAP and PHOSPHO1, although both acting as phosphoesterases, operate independently. However, superimposing haplo-insufficiency of TNAP (*Akp2*$^{+/-}$) with PHOSPHO1 (*Phospho1*$^{-/-}$) knockout caused a progressive worsening of the skeletal defects. A further finding was that there were differences in the skeletal defects observed with individual *Akp2*$^{-/-}$and *Phospho1*$^{-/-}$ knockout mice: there was a more severe reduction in vertebral mineralization in *Phospho1*$^{-/-}$ than in *Akp2*$^{-/-}$knockouts.

20.5.5. Effect of PHOSPHO1 on MV mineralization

With regard to its effect on MV mineralization, PHOSPHO1 knockout did not block it; in fact ultrastructural studies seem to indicate that, if anything, the mineral formed within the MV was more intense. However, like TNAP knockout, the mineral did not spread from the MVs. In a further study where both PHOSPHO1 and TNAP were concomitantly ablated, there was an almost total block in skeletal mineralization; none of the 272 conceptions continued to live birth. Analysis of the embryonic *Phospho1*$^{-/-}$/ *Akp2*$^{-/-}$ pups showed an almost total lack of skeletal mineralization; there was no evidence of outgrowth of mineral from within the MVs. This effect cannot be due to an excess of PPi. The data clearly indicate that the activities of both TNAP and PHOSPHO1 are concomitantly required for skeletal mineralization in the mouse. However, more detailed biochemical study will be required to definitively establish how the combined activities of these two key enzymes contributes to function of MVs in this complex process.

21. PERSPECTIVES

The processes involved in growth plate mineralization depicted in this review have proven to be remarkably complex and the mechanisms involved have generated frequent controversy. Nevertheless, it is now generally accepted that the entities most responsible for the *de novo* induction of crystalline mineral in most vertebrate hard tissues are MVs. While it is universally recognized that the resident cells are involved, there has been a longstanding question whether they are directly involved in the processing of Ca^{2+} and Pi prior to the production of MVs. Data presented in this review should put that question to rest – at least in avian skeletal development. They document that during growth plate development the chondrocytes initially require Pi for synthesis of DNA, RNA and nucleotides essential for proliferation. Upon termination of cell division, the nucleotides begin to be degraded; ^{31}P-NMR and chemical analyses reveal that Pi builds up in the cytoplasm. Simultaneously, *in situ* confocal imaging reveals that the chondrocytes acquire and process Ca^{2+} at an accelerated pace until in the early hypertrophic zone this climaxes with the cells exfoliating from their plasma membrane the accumulated Ca^{2+} and Pi as ion-loaded vesicles. This mineral phase, present as a nucleational core within the vesicle lumen, is primarily noncrystalline calcium phosphates complexed with both PS and the annexins, which facilitate the induction of crystalline mineral formation.

When MVs are formed by the cells they contain not only Ca^{2+} and Pi, but also other electrolytes that significantly affect the kinetics of mineral formation; these include Mg^{2+}, Zn^{2+}, and PPi, as well as HCO_3^-. How these ions influence mineral formation are discussed, as is the nature of the successive calcium phosphate minerals that form during the mineral induction process. Also discussed are the roles of the plethora of enzymes now known to reside in MVs; however the major focus is on about a half a dozen that have particular importance in mineral induction. What emerges is a remarkably complex and beautifully orchestrated series of cellular events that enable the rapid elongation of bones while maintaining their physical integrity. Production of mineralization-competent MVs enables mineral formation to keep pace with cellular proliferation, preventing development of rickets or osteomalacia. Thus, endochondral bone formatioin involves the provisional calcification of the cartilaginous matrix by chondrocytes – *i.e.* the formation of calcified cartilage – a more heavily calcified, but mechanically weaker temporary scaffolding that maintains mechanical stability until the truly robust type I collagen-hydroxyapatite composite, bone, is generated by osteoblasts.

One of the noteworthy features of this cell-mediated process is that it involves features that are observed pathologically in the ischemia-reperfusion of stroke and cardiac vascular blockage, but are utilized here to induce normal mineral formation in a highly regulated manner during rapid bone growth. This review covers a long period of discovery and involves nearly 50 years of personal participation in elucidation of this remarkable process. It has been a special privilege to have been involved in many of the experimental discoveries that now provide the landscape of understanding. It is important however for workers currently in the bone field to master the fundamentals of the physical chemistry of the mineral forming process, as well of the cellular physiology, biology and biochemistry that are all essential for proper understanding of this highly complex process. Biological mineralization not only involves features characteristic of all living soft tissues cells, but superimposes

on these the need to transform ions in solution into the robust inorganic mineral-collagen composite material (bone) that provides the framework in which our bodies function.

22. ACKNOWLEDGEMENTS

I want to acknowledge first and foremost my incalculable debt to my Lord and Savior, Jesus Christ, for his mercy and grace, and to the Holy Spirit, who has guided and enabled me to have faith in God, our Creator. I thank Him for granting me the privilege of studying and helping to elucidate this remarkable area of vertebrate anatomy, namely the growth plate, and the mechanism by which the cells in this tissue bring about, concomitantly, longitudinal growth and deposition of mineral to maintain mechanical strength as these structures are being formed. It was He who guided me in 1955 to graduate school at the University of Wisconsin, where under the tutelage of my major professor, Paul H. Phillips, Ph.D., I was introduced to hard tissues. Prof. Phillips directed me to study the long-term effects of low dosages of fluoride on both rats and dogs. He also encouraged me to take classes in Histology and Physiology in the School of Medicine in Madison, to be completed with courses in Physical Chemistry and Organic Chemistry laboratory, as part of my basic training. The broad perspective so obtained has been an invaluable asset in approaching the analysis of the complex physico-chemical processes that occur during bone development and mineralization.

Next, I want to express my gratitude for the patience, kindness and wisdom of Prof. James T. Irving, M.D., my postdoctoral mentor at Forsyth Dental Center, who in 1960 revealed to me his remarkable finding of intense Sudanophilia at sites of mineral deposition in the extracellular matrix of hypertrophic chondrocytes of the growth plate in rats. He asked me to determine what this material was and what it was doing there. This was the beginning of a quest that has taken 50 years of study – through the efforts of a small army of students and colleagues to solve – at least to the level of understanding depicted in this review.

That these studies have involved a host of participants is evident from the 583 citations in the reference section. It was through the efforts of this outstanding group of investigators in many institutions and disciplines, who attacked this problem from many different angles that our understanding is what it is today. However, I want to acknowledge the specific contributions of members of my own group – spanning a period from 1960 to the present. Among the earliest was John M. Cotmore, Ph.D., who in 1968 discovered the potentiating effect of inorganic phosphate (Pi) on the binding of Ca^{2+} to phosphatidylserine (PS), a key lipid we had earlier discovered was bound with newly forming bone mineral. The PS-Ca^{2+}-Pi complexes so formed can now be assigned as key components of the nucleational core of MVs. Next was the critical 1970 finding by Eugene Eisenberg, M.D. – from *in vivo* studies on the incorporation of ^{32}Pi into bone lipids of rapidly growing chickens – that the labeling pattern of Ca^{2+}-complexed lipids was distinctly different from that of non-complexed lipids, proving that the association between PS and Ca^{2+} was biological, not an adventitious artifact.

Next, the outstanding contributions of two of my esteemed technical assistants, Paul H. King, in Boston, MA, and Michael S. Giancola, in Burlington, VT must be recognized – Paul for his invaluable assistance in the early lipid chromatography, and Mike for his skill in performing the double-isotope labeling studies that enabled accurate determination of the electrolyte levels within the cells and MVs, as well as those in the extracellular fluid (ECF) from different zones of the growth plate. Added to this list are the many graduate students whose specific contributions cannot be mentioned individually here, but are cited in the list of references.

Next, I must recognize four of my long-term post-doctoral colleagues: Yoshinori Ishikawa (1978–1998), Licia N.Y. Wu (1987–present), Glenn R. Sauer (1987–2000) and Brian R. Genge (1988–present), who each have been major contributors to this story. Yoshi analyzed the levels of free amino acids in the ECF, documenting their stimulatory effect on MV formation, and with Licia, developed primary cultures of growth plate chondrocytes capable of inducing mineralization under physiological conditions. Glenn used FT-IR characterization of the mineral phase and subsequent study of the role of Zn^{2+} in MVs to elucidate key steps in MV function. Licia and Brian, working as a team together, developed definitive techniques for isolation, dissection, characterization, and reconstitution of MV; their subsequent studies on the kinetics of mineral formation, the role of the annexins, the nucleational core, and regulatory effects of Mg^{2+} defined critical aspects of mineral formation by MVs. In particular, their skill, talents, and meticulous attention to details – and their long, hard hours of work – are what made much of this report possible.

Finally, I give special credit and deep appreciation to my dear wife, Shirley Jo Westerfield Wuthier, who for 54 years has been my most loving companion and most insightful critic – one who has enabled me to devote the years of labor described in this fascinating, but complex report. She, more than any other person has encouraged me to invest the effort required to pull together this epic report and had the patience to allow me to do it.

Last, I gratefully acknowledge the 30 years of continuous support of National Institutes of Health, NIH Grant AR18983, for research on the Role of Matrix Vesicles in skeletal mineralization.

23. REFERENCES

1. Anderson, H. C.: Electron microscopic sudies of induced cartilage development and calcification. *J Cell Biol*, 35, 81-101 (1967)

2. Anderson, H. C.: Vesicles associated with calcification in the matrix of epiphyseal cartilage. *J Cell Biol*, 41, 59-72 (1969)

3. Bonucci, E.: Fine structure of early cartilage calcification. *J Ultrastruct Res*, 20, 33-50 (1967)

4. Bonucci, E.: Fine structure and histochemistry of "calcifying globules" in epiphyseal cartilage. *Z. Zellforsch. Mikrosk. Anat.*, 103, 192-217 (1970)

5. Bernard, G. W. & D. C. Pease: An electron microscopic study of initial intramembranous osteogenesis. *Am J Anat*, 125, 274-290 (1969)

6. Ketenjian, A. Y., A. M. Jafri & C. Arsenis: Studies on the mechanism of callus cartilage differentiation and calcification during fracture healing. *Orthop Clin North Am*, 9, 43-65 (1978)

7. Chai, B. F. & X. M. Tang: Ultrastructural investigation on experimental fracture healing. VI. Electron microscopic observation on matrix vesicles. *Chin Med J (Engl)*, 97, 805-12 (1984)

8. Brighton, C. T. & R. M. Hunt: Histochemical localization of calcium in the fracture callus with potassium pyroantimonate. Possible role of chondrocyte mitochondrial calcium in callus calcification. *J Bone Joint Surg Am*, 68, 703-15 (1986)

9. Sisca, R. F. & D. V. Provenza: Initial dentin formation in human deciduous teeth. An electron microscope study. *Calcif Tissue Res*, 9, 1-16 (1972)

10. Sayegh, F. S., G. C. Solomon & R. W. Davis: Ultrastructure of intracellular mineralization in the deer's antler. *Clin Orthop Relat* Res, 99, 267-84 (1974)

11. Kim, K. M.: Calcification of matrix vesicles in human aortic valve and aortic media. *Fed Proc*, 35, 156-62 (1976)

12. Sela, J. & I. A. Bab: The relationship between extracellular matrix vesicles and calcospherities in primary mineralization of neoplastic bone tissue. TEM and SEM studies on osteosarcoma. *Virchows Arch A Pathol Anat Histol*, 382, 1-9 (1979)

13. Fedde, K. N.: Human osteosarcoma cells spontaneously release matrix-vesicle-like structures with the capacity to mineralize. *Bone Miner*, 17, 145-51 (1992)

14. Landis, W. J. & M. J. Song: Early mineral deposition in calcifying tendon characterized by high voltage electron microscopy and three-dimensional graphic imaging. *J Struct Biol*, 107, 116-27 (1991)

15. Arsenault, A. L., B. W. Frankland & F. P. Ottensmeyer: Vectorial sequence of mineralization in the turkey leg tendon determined by electron microscopic imaging. *Calcif Tissue Int*, 48, 46-55 (1991)

16. Irving, J. T.: A histological staining method for sites of calcification in teeth and bone. *Arch Oral Biol*, 1, 89-96 (1959)

17. Irving, J. T. & R. E. Wuthier: Further observations on the Sudan black stain for calcification. *Arch Oral Biol*, 5, 323-324 (1961)

18. Irving, J. T.: The sudanophilic material at sites of calcification. *Arch Oral Biol*, 8, 735-743 (1963)

19. Wuthier, R. E. & J. T. Irving: Lipids in developing calf bone. *J. Dental Res*, 43, 814-815, abstract (1964)

20. Wuthier, R. E.: Lipids of mineralizing epiphyseal tissues in the bovine fetus. *J. Lipid Res*, 9, 68-78 (1968)

21. Shapiro, I. M. & R. E. Wuthier: A study of the phospholipids of bovine dental tissues. II. Developing bovine foetal dental pulp. *Arch Oral Biol*, 11, 513-9 (1966)

22. Shapiro, I. M., R. E. Wuthier & J. T. Irving: A study of the phospholipids of bovine dental tissues. I. Enamel matrix and dentine. *Arch Oral Biol*, 11, 501-12 (1966)

23. Irving, J. T. & R. E. Wuthier: Histochemistry and biochemistry of calcification with special reference to the role of lipids. *Clin Orthop Relat Res*, 56, 237-260 (1968)

24. Abramson, M. B., R. Katzman, C. E. Wilson & H. P. Gregor: Ionic properties of aqueous dispersions of phosphatidic acid. *J Biol Chem*, 239, 4066-72 (1964)

25. Abramson, M. B., R. Katzman & H. P. Gregor: Aqueous dispersions of phosphatidylserine. Ionic properties. *J Biol Chem*, 239, 70-6 (1964)

26. Nash, H. A. & J. M. Tobias: Phospholipids Membrane Model: Importance of phosphatidylserine and its cation exchanger nature. *Proc Natl Acad Sci U S A*, 51, 476-80 (1964)

27. Hendrickson, H. S. & J. G. Fullington: Stabilities of metal complexes of phospholipids: Ca (II), Mg (II), and Ni (II) complexes of phosphatidylserine and triphosphoinositide. *Biochemistry*, 4, 1599-605 (1965)

28. Eisenberg, E., R. E. Wuthier, R. B. Frank, J. T. Irving: Time study of *in vivo* incorporation of 32P-orthophosphate into phospholipids of chicken epiphyseal tissues. *Calcif Tissue Res*, 6, 32-48 (1970)

29. Peress, N. S., H. C. Anderson & S. W. Sajdera: The lipids of matrix vesicles from bovine fetal epiphyseal cartilage. *Calcif Tissue Res*, 14, 275-81 (1974)

30. Wuthier, R. E.: Lipid composition of isolated epiphyseal cartilage cells, membranes and matrix vesicles. *Biochim Biophys Acta*, 409, 128-43 (1975)

31. Wuthier, R. E.: Lipids of matrix vesicles. *Fed Proc*, 35, 117-21 (1976)

32. Morris, D. C. & J. Appleton: The effects of lanthanum on the ultrastructure of hypertrophic chondrocytes and the localization of lanthanum precipitates in condylar cartilages of rats fed on normal

and rachitogenic diets. *J Histochem Cytochem*, 32, 239-47 (1984)

33. Gomez, S., J. M. Lopez-Cepero, G. Silvestrini, P. Mocetti & E. Bonucci: Matrix vesicles and focal proteoglycan aggregates are the nucleation sites revealed by the lanthanum incubation method: a correlated study on the hypertrophic zone of the rat epiphyseal cartilage. *Calcif Tissue Int*, 58, 273-82 (1996)

34. Petersheim, M. & J. Sun: On the coordination of La3+ by phosphatidylserine. *Biophys J*, 55, 631-6 (1989)

35. Bentz, J., D. Alford, J. Cohen & N. Duzgunes: La3+-induced fusion of phosphatidylserine liposomes. Close approach, intermembrane intermediates, and the electrostatic surface potential. *Biophys J*, 53, 593-607 (1988)

36. Aussel, C., R. Marhaba, C. Pelassy & J. P. Breittmayer: Submicromolar La3+ concentrations block the calcium release-activated channel, and impair CD69 and CD25 expression in CD3- or thapsigargin-activated Jurkat cells. *Biochem J*, 313 (Pt 3), 909-13 (1996)

37. Thyberg, J. & U. Friberg: Ultrastructure and acid phosphatase activity of matrix vesicles and cytoplasmic dense bodies in the epiphyseal plate. *J Ultrastruct Res*, 33, 554-73 (1970)

38. Thyberg, J. & U. Friberg: Electron microscopic enzyme histochemical studies on the cellular genesis of matrix vesicles in the epiphyseal plate. *J Ultrastruct Res*, 41, 43-59 (1972)

39. Hunziker, E. B., W. Herrmann, R. K. Schenk, M. Mueller & H. Moor: Cartilage ultrastructure after high pressure freezing, freeze substitution, and low temperature embedding. I. Chondrocyte ultrastructure – implications for the theories of mineralization and vascular invasion. *J Cell Biol*, 98, 267-76 (1984)

40. Arsenault, A. L. & E. B. Hunziker: Electron microscopic analysis of mineral deposits in the calcifying epiphyseal growth plate. *Calcif Tissue Int*, 42, 119-26 (1988)

41. Hunziker, E. B., W. Herrmann, L. M. Cruz-Orive & A. L. Arsenault: Image analysis of electron micrographs relating to mineralization in calcifying cartilage: theoretical considerations. *J Electron Microsc Tech*, 11, 9-15 (1989)

42. Arsenault, A. L., F. P. Ottensmeyer & I. B. Heath: An electron microscopic and spectroscopic study of murine epiphyseal cartilage: analysis of fine structure and matrix vesicles preserved by slam freezing and freeze substitution. *J Ultrastruct Mol Struct Res*, 98, 32-47 (1988)

43. Arsenault, A. L. & D. M. Kohler: Image analysis of the extracellular matrix. *Microsc Res Tech*, 28, 409-21 (1994)

44. Ottensmeyer, F. P. & J. W. Andrew: High-resolution microanalysis of biological specimens by electron energy loss spectroscopy and by electron spectroscopic imaging. *J Ultrastruct Res*, 72, 336-48 (1980)

45. Morris, D. C., H. K. Vaananen & H. C. Anderson: Matrix vesicle calcification in rat epiphyseal growth plate cartilage prepared anhydrously for electron microscopy. *Metab Bone Dis Relat Res*, 5, 131-7 (1983)

46. Akisaka, T., H. Kawaguchi, G. P. Subita, Y. Shigenaga & C. V. Gay: Ultrastructure of matrix vesicles in chick growth plate as revealed by quick freezing and freeze substitution. *Calcif Tissue Int*, 42, 383-93 (1988)

47. Cecil, R. N. A. & H. C. Anderson: Freeze-fracture studies of matrix vesicles in epiphyseal growth plate. *Metab Bone Dis Relat Res*, 1, 89-95 (1978)

48. Borg, T. K., R. B. Runyan & R. E. Wuthier: Correlation of freeze-fracture and scanning electron microscopy of epiphyseal chondrocytes. *Calcif Tissue Res*, 26, 237-41 (1978)

49. Takagi, M., Y. Kasahara, H. Takagi & Y. Toda: Freeze-fracture images of matrix vesicles of epiphyseal cartilage and non-calcified tracheal cartilage. *J Electron Microsc (Tokyo)*, 28, 165-75 (1979)

50. Borg, T. K., R. B. Runyan & R. E. Wuthier: A freeze-fracture study of avian epiphyseal cartilage differentiation. *Anat Rec*, 199, 449-57 (1981)

51. Katchburian, E. & N. J. Severs: Matrix constituents of early developing bone examined by freeze fracture. *Cell Biol Int Rep*, 7, 1063-70 (1983)

52. Ali, S. Y., S. W. Sajdera & H. C. Anderson: Isolation and characterization of calcifying matrix vesicles from epiphyseal cartilage. *Proc Natl Acad Sci U S A*, 67, 1513-20 (1970)

53. Ali, S. Y., H. C. Anderson & S. W. Sajdera: Enzymic and electron-microscopic analysis of extracellular matrix vesicles associated with calcification in cartilage. *Biochem J*, 122, 56P (1971)

54. Majeska, R. J. & R. E. Wuthier: Studies on matrix vesicles isolated from chick epiphyseal cartilage. Association of pyrophosphatase and ATPase activities with alkaline phosphatase. *Biochim Biophys Acta*, 391, 51-60 (1975)

55. Wuthier, R. E., R. E. Linder, G. P. Warner, S. T. Gore & T. K. Borg: Nonenzymatic method for isolation of matrix vesicles: Characterization and initial studies on Ca and P orthophosphate metabolism. *Metab Bone Dis Relat Res*, 1, 125-136 (1978)

56. Watkins, E. L., J. V. Stillo & R. E. Wuthier: Subcellular fractionation of epiphyseal cartilage: Isolation of matrix vesicles and profiles of enzymes, phospholipids, calcium and phosphate. *Biochim Biophys Acta*, 631, 289-304 (1980)

57. Warner, G. P., H. L. Hubbard, G. C. Lloyd & R. E. Wuthier: Pi and Ca metabolism by matrix vesicles prepared from chicken epiphyseal cartilage microsomes by isosmotic

Percoll density-gradient fractionation. *Calcif Tissue Int*, 35, 327-338 (1983)

58. Wuthier, R. E., J. E. Chin, J. E. Hale, T. C. Register, L. V. Hale & Y. Ishikawa: Isolation and characterization of calcium-accumulating matrix vesicles from chondrocytes of chicken epiphyseal growth plate cartilage in primary culture. *J Biol Chem*, 260, 15972-9 (1985)

59. Wu, L. N., W. B. Valhmu, G. C. Lloyd, B. R. Genge & R. E. Wuthier: Isolation of two glycosylated forms of membrane-bound alkaline phosphatase from avian growth plate cartilage matrix vesicle-enriched microsomes. *Bone Miner*, 7, 113-25 (1989)

60. Genge, B. R., L. N. Wu & R. E. Wuthier: Identification of phospholipid-dependent calcium-binding proteins as constituents of matrix vesicles. *J Biol Chem*, 264, 10917-21 (1989)

61. Genge, B. R., L. N. Wu & R. E. Wuthier: Differential fractionation of matrix vesicle proteins. Further characterization of the acidic phospholipid-dependent Ca^{2+}-binding proteins. *J Biol Chem*, 265, 4703-10 (1990)

62. Balcerzak, M., J. Radisson, G. Azzar, D. Farlay, G. Boivin, S. Pikula & R. Buchet: A comparative analysis of strategies for isolation of matrix vesicles. *Anal Biochem*, 361, 176-82 (2007)

63. Wuthier, R. E.: Electrolytes of isolated epiphyseal chondrocytes, matrix vesicles and extracellular fluid. *Calcif Tissue Res*, 23, 125-133 (1977)

64. Wuthier, R. E. & S. T. Gore: Partition of inorganic ions and phospholipids in isolated cell, membrane and matrix vesicle fractions: Evidence for Ca-Pi-acidic phospholipid complexes. *Calcif Tissue Res*, 24, 163-171 (1977)

65. Warner, G. P. & R. E. Wuthier: Metabolism of 32Pi and 45Ca by matrix vesicles isolated from epiphyseal cartilage by nondigestive methods. In: *Third International Conference on Matrix Vesicles*, Eds: Ascenzi, A., E. Bonucci & B. deBernard, Wichtig Editore, Milano, Italy, 47-51 (1981).

66. Register, T. C., F. M. McLean, M. G. Low & R. E. Wuthier: Roles of alkaline phosphatase and labile internal mineral in matrix vesicle-mediated calcification. Effect of selective release of membrane-bound alkaline phosphatase and treatment with isosmotic pH 6 buffer. *J Biol Chem*, 261, 9354-60 (1986)

67. McLean, F. M., P. J. Keller, B. R. Genge, S. A. Walters & R. E. Wuthier: Disposition of preformed mineral in matrix vesicles. Internal localization and association with alkaline phosphatase. *J Biol Chem*, 262, 10481-8 (1987)

68. Hale, J. E., J. E. Chin, Y. Ishikawa, P. R. Paradiso & R. E. Wuthier: Correlation between distribution of cytoskeletal proteins and release of alkaline phosphatase-rich vesicles by epiphyseal chondrocytes in primary culture. *Cell Motil*, 3, 501-12 (1983)

69. Hale, J. E. & R. E. Wuthier: Role of cytoskeletal depolymerization in matrix vesicle formation by primary cultures of epiphyseal growth plate chondrocytes. In: *Cell Mediated Calcification and Matrix Vesicles*, Ed: Ali, S. Y., Elsevier Science Publ., Amsterdam, The Netherlands, 237-240 (1986).

70. Schalk, E. M. & R. E. Wuthier: Effect of trifluoperazine and other drugs on matrix vesicle formation by chicken growth plate chondrocytes in primary cell culture. *Biochem Pharmacol*, 35, 2373-9 (1986)

71. Ishikawa, Y., J. E. Chin, E. M. Schalk & R. E. Wuthier: Effect of amino acid levels on matrix vesicle formation by epiphyseal growth plate chondrocytes in primary culture. *J Cell Physiol*, 126, 399-406 (1986)

72. Garimella, R., X. Bi, N. Camacho, J. B. Sipe & H. C. Anderson: Primary culture of rat growth plate chondrocytes: an *in vitro* model of growth plate histotype, matrix vesicle biogenesis and mineralization. *Bone*, 34, 961-70 (2004)

73. Hale, J. E. & R. E. Wuthier: The mechanism of matrix vesicle formation. Studies on the composition of chondrocyte microvilli and on the effects of microfilament-perturbing agents on cellular vesiculation. *J Biol Chem*, 262, 1916-25 (1987)

74. Boyan, B. D., Z. Schwartz, L. D. Swain, D. L. Carnes, Jr. & T. Zislis: Differential expression of phenotype by resting zone and growth region costochondral chondrocytes *in vitro*. *Bone*, 9, 185-94 (1988)

75. Wu, L. N., G. R. Sauer, B. R. Genge & R. E. Wuthier: Induction of mineral deposition by primary cultures of chicken growth plate chondrocytes in ascorbate-containing media. Evidence of an association between matrix vesicles and collagen. *J Biol Chem*, 264, 21346-55 (1989)

76. Genge, B. R., G. R. Sauer, L. N. Wu, F. M. McLean & R. E. Wuthier: Correlation between loss of alkaline phosphatase activity and accumulation of calcium during matrix vesicle-mediated mineralization. *J Biol Chem*, 263, 18513-9 (1988)

77. Valhmu, W. B., L. N. Wu & R. E. Wuthier: Effects of Ca/Pi ratio, Ca^{2+} x Pi ion product, and pH of incubation fluid on accumulation of $^{45}Ca^{2+}$ by matrix vesicles *in vitro*. *Bone Miner*, 8, 195-209 (1990)

78. Balcerzak, M., A. Malinowska, C. Thouverey, A. Sekrecka, M. Dadlez, R. Buchet & S. Pikula: Proteome analysis of matrix vesicles isolated from femurs of chicken embryo. *Proteomics*, 8, 192-205 (2008)

79. Anderson, H. C., R. Cecil & S. W. Sajdera: Calcification of rachitic rat cartilage *in vitro* by

extracellular matrix vesicles. *Am J Pathol*, 79, 237-54 (1975)

80. Hsu, H. H. & H. C. Anderson: A simple and defined method to study calcification by isolated matrix vesicles. Effect of ATP and vesicle phosphatase. *Biochim Biophys Acta*, 500, 162-72 (1977)

81. Hsu, H. H. & H. C. Anderson: Calcification of isolated matrix vesicles and reconstituted vesicles from fetal bovine cartilage. *Proc Natl Acad Sci U S A*, 75, 3805-8 (1978)

82. Hsu, H. H., N. P. Camacho & H. C. Anderson: Further characterization of ATP-initiated calcification by matrix vesicles isolated from rachitic rat cartilage. Membrane perturbation by detergents and deposition of calcium pyrophosphate by rachitic matrix vesicles. *Biochim Biophys Acta*, 1416, 320-32 (1999)

83 Kakuta, S., D. Malamud, E. E. Golub & I. M. Shapiro: Isolation of matrix vesicles by isoelectric focusing in Pevikon-Sephadex. *Bone*, 6, 187-91 (1985)

84. Vaananen, H. K. & L. K. Korhonen: Matrix vesicles in chicken epiphyseal cartilage. Separation from lysosomes and the distribution of inorganic pyrophosphatase activity. *Calcif Tissue Int*, 28, 65-72 (1979)

85. Slavkin, H. C., R. D. Croissant, P. Bringas, P. Matosian, P. Wilson, W. Mino & H. Guenther: Matrix vesicle heterogeneity: possible morphogenetic functions for matrix vesicles. *Fed Proc*, 35, 127-34 (1976)

86. Deutsch, D., I. Bab, A. Muhlrad & J. Sela: Purification and further characterization of isolated matrix vesicles from rat alveolar bone. *Metab Bone Dis Relat Res*, 3, 209-14 (1981)

87. Xiao, Z., C. E. Camalier, K. Nagashima, K. C. Chan, D. A. Lucas, M. J. de la Cruz, M. Gignac, S. Lockett, H. J. Issaq, T. D. Veenstra, T. P. Conrads & G. R. Beck, Jr.: Analysis of the extracellular matrix vesicle proteome in mineralizing osteoblasts. *J Cell Physiol*, 210, 325-35 (2007)

88. Bab, I. A., A. Muhlrad & J. Sela: Ultrastructural and biochemical study of extracellular matrix vesicles in normal alveolar bone of rats. *Cell Tissue Res*, 202, 1-7 (1979)

89. Sela, J., I. A. Bab & A. Muhlrad: A comparative study on the occurrence and activity of extracellular matrix vesicles in young and adult rat maxillary bone. *Calcif Tissue Int*, 33, 129-34 (1981)

90. Muhlrad, A., A. Setton, J. Sela, I. Bab & D. Deutsch: Biochemical characterization of matrix vesicles from bone and cartilage. *Metab Bone Dis Relat Res*, 5, 93-9 (1983)

91. Chin, J. E., J. E. Hale, Y. Ishikawa, T. C. Register & R. E. Wuthier: Origin of matrix vesicles: Characterization of mineralization-inducing vesicles and their production by primary cultures of chicken growth plate chondrocytes. In: *Endocrine Control of Bone and Calcium Metabolism*, Eds: D. V. Cohn, Potts, J.T., Jr., Fujita, T., Elsevier Science Publ., Amsterdam, The Netherlands, 454-458 (1984).

92. Muhlrad, A., I. A. Bab, D. Deutsch & J. Sela: Occurrence of actin-like protein in extracellular matrix vesicles. *Calcif Tissue Int*, 34, 376-81 (1982)

93. Genge, B. R., L. N. Wu, H. D. Adkisson, IV & R. E. Wuthier: Matrix vesicle annexins exhibit proteolipid-like properties. Selective partitioning into lipophilic solvents under acidic conditions. *J Biol Chem*, 266, 10678-85 (1991)

94. Genge, B. R., X. Cao, L. N. Wu, W. R. Buzzi, R. W. Showman, A. L. Arsenault, Y. Ishikawa & R. E. Wuthier: Establishment of the primary structure of the major lipid-dependent Ca2+ binding proteins of chicken growth plate cartilage matrix vesicles: identity with anchorin CII (annexin V) and annexin II. *J Bone Miner Res*, 7, 807-19 (1992)

95. Wu, L. N., B. R. Genge, G. C. Lloyd & R. E. Wuthier: Collagen-binding proteins in collagenase-released matrix vesicles from cartilage. Interaction between matrix vesicle proteins and different types of collagen. *J Biol Chem*, 266, 1195-203 (1991)

96. Wu, L. N., B. R. Genge & R. E. Wuthier: Association between proteoglycans and matrix vesicles in the extracellular matrix of growth plate cartilage. *J Biol Chem*, 266, 1187-94 (1991)

97. Cao, X., B. R. Genge, L. N. Wu, W. R. Buzzi, R. M. Showman & R. E. Wuthier: Characterization, cloning and expression of the 67-kDA annexin from chicken growth plate cartilage matrix vesicles. *Biochem Biophys Res Commun*, 197, 556-61 (1993)

98. Xiao, Z., T. P. Conrads, G. R. Beck & T. D. Veenstra: Analysis of the extracellular matrix and secreted vesicle proteomes by mass spectrometry. *Methods Mol Biol*, 428, 231-44 (2008)

99. Xiao, Z., J. Blonder, M. Zhou & T. D. Veenstra: Proteomic analysis of extracellular matrix and vesicles. *J Proteomics*, 72, 34-45 (2009)

100. Elias, J. E., W. Haas, B. K. Faherty & S. P. Gygi: Comparative evaluation of mass spectrometry platforms used in large-scale proteomics investigations. *Nat Methods*, 2, 667-75 (2005)

101. Perkins, D. N., D. J. Pappin, D. M. Creasy & J. S. Cottrell: Probability-based protein identification by searching sequence databases using mass spectrometry data. *Electrophoresis*, 20, 3551-67 (1999)

102. Kirsch, T. & M. Pfaffle: Selective binding of anchorin CII (annexin V) to type II and X collagen and to chondrocalcin (C-propeptide of type II collagen).

Implications for anchoring function between matrix vesicles and matrix proteins. *FEBS Lett*, 310, 143-7 (1992)

103. Kirsch, T. & R. E. Wuthier: Stimulation of calcification of growth plate cartilage matrix vesicles by binding to type II and X collagens. *J Biol Chem*, 269, 11462-9 (1994)

104. Poole, C. A., S. Ayad & R. T. Gilbert: Chondrons from articular cartilage. V. Immunohistochemical evaluation of type VI collagen organisation in isolated chondrons by light, confocal and electron microscopy. *J Cell Sci*, 103 (Pt 4), 1101-10 (1992)

105. Jobsis, G. J., H. Keizers, J. P. Vreijling, M. de Visser, M. C. Speer, R. A. Wolterman, F. Baas & P. A. Bolhuis: Type VI collagen mutations in Bethlem myopathy, an autosomal dominant myopathy with contractures. *Nat Genet*, 14, 113-5 (1996)

106. Lamande, S. R., J. F. Bateman, W. Hutchison, R. J. McKinlay Gardner, S. P. Bower, E. Byrne & H. H. Dahl: Reduced collagen VI causes Bethlem myopathy: a heterozygous COL6A1 nonsense mutation results in mRNA decay and functional haploinsufficiency. *Hum Mol Genet*, 7, 981-9 (1998)

107. Camacho Vanegas, O., E. Bertini, R. Z. Zhang, S. Petrini, C. Minosse, P. Sabatelli, B. Giusti, M. L. Chu & G. Pepe: Ullrich scleroatonic muscular dystrophy is caused by recessive mutations in collagen type VI. *Proc Natl Acad Sci U S A*, 98, 7516-21 (2001)

108. Nishino, I. & E. Ozawa: Muscular dystrophies. *Curr Opin Neurol*, 15, 539-44 (2002)

109. Nishiyama, A. & W. B. Stallcup: Expression of NG2 proteoglycan causes retention of type VI collagen on the cell surface. *Mol Biol Cell*, 4, 1097-108 (1993)

110. Burg, M. A., E. Tillet, R. Timpl & W. B. Stallcup: Binding of the NG2 proteoglycan to type VI collagen and other extracellular matrix molecules. *J Biol Chem*, 271, 26110-6 (1996)

111. Bernardi, P. & P. Bonaldo: Dysfunction of mitochondria and sarcoplasmic reticulum in the pathogenesis of collagen VI muscular dystrophies. *Ann N Y Acad Sci*, 1147, 303-11 (2008)

112. Bernardi, P. & A. Rasola: Calcium and cell death: the mitochondrial connection. *Subcell Biochem*, 45, 481-506 (2007)

113. Habuchi, H., H. E. Conrad & J. H. Glaser: Coordinate regulation of collagen and alkaline phosphatase levels in chick embryo chondrocytes. *J Biol Chem*, 260, 13029-34 (1985)

114. Reginato, A. M., I. M. Shapiro, J. W. Lash & S. A. Jimenez: Type X collagen alterations in rachitic chick epiphyseal growth cartilage. *J Biol Chem*, 263, 9938-45 (1988)

115. Salo, L. A., J. Hoyland, S. Ayad, C. M. Kielty, A. Freemont, P. Pirttiniemi, T. Kantomaa, M. E. Grant & J. T. Thomas: The expression of types X and VI collagen and fibrillin in rat mandibular condylar cartilage. Response to mastication forces. *Acta Odontol Scand*, 54, 295-302 (1996)

116. Genge, B. R., L. N. Wu & R. E. Wuthier: Mineralization of annexin-5-containing lipid-calcium-phosphate complexes: modulation by varying lipid composition and incubation with cartilage collagens. *J Biol Chem*, 283, 9737-48 (2008)

117. Ruggiero, F., B. Petit, M. C. Ronziere, J. Farjanel, D. J. Hartmann & D. Herbage: Composition and organization of the collagen network produced by fetal bovine chondrocytes cultured at high density. *J Histochem Cytochem*, 41, 867-75 (1993)

118. Keene, D. R., C. D. Jordan, D. P. Reinhardt, C. C. Ridgway, R. N. Ono, G. M. Corson, M. Fairhurst, M. D. Sussman, V. A. Memoli & L. Y. Sakai: Fibrillin-1 in human cartilage: developmental expression and formation of special banded fibers. *J Histochem Cytochem*, 45, 1069-82 (1997)

119. Trask, B. C., T. M. Trask, T. Broekelmann & R. P. Mecham: The microfibrillar proteins MAGP-1 and fibrillin-1 form a ternary complex with the chondroitin sulfate proteoglycan decorin. *Mol Biol Cell*, 11, 1499-507 (2000)

120. Francke, U. & H. Furthmayr: Genes and gene products involved in Marfan syndrome. *Semin Thorac Cardiovasc Surg*, 5, 3-10 (1993)

121. Huber, R., M. Schneider, I. Mayr, J. Romisch & E. P. Paques: The calcium binding sites in human annexin V by crystal structure analysis at 2.0 A resolution. Implications for membrane binding and calcium channel activity. *FEBS Lett*, 275, 15-21 (1990)

122. Huber, R., J. Romisch & E. P. Paques: The crystal and molecular structure of human annexin V, an anticoagulant protein that binds to calcium and membranes. *Embo J*, 9, 3867-74 (1990)

123. Huber, R., R. Berendes, A. Burger, H. Luecke & A. Karshikov: Annexin V-crystal structure and its implications on function. *Behring Inst Mitt*, 91, 107-25 (1992)

124. Voges, D., R. Berendes, A. Burger, P. Demange, W. Baumeister & R. Huber: Three-dimensional structure of membrane-bound annexin V. A correlative electron microscopy-X-ray crystallography study. *J Mol Biol*, 238, 199-213 (1994)

125. Arispe, N., E. Rojas, B. R. Genge, L. N. Wu & R. E. Wuthier: Similarity in calcium channel activity of annexin

V and matrix vesicles in planar lipid bilayers. *Biophys J*, 71, 1764-75 (1996)

126. Reviakine, I. I., W. Bergsma-Schutter & A. Brisson: Growth of protein 2-D crystals on supported planar lipid bilayers imaged *in situ* by AFM. *J Struct Biol*, 121, 356-61 (1998)

127. Sopkova, J., M. Vincent, M. Takahashi, A. Lewit-Bentley & J. Gallay: Conformational flexibility of domain III of annexin V at membrane/water interfaces. *Biochemistry*, 38, 5447-58 (1999)

128. Reviakine, I., W. Bergsma-Schutter, C. Mazeres-Dubut, N. Govorukhina & A. Brisson: Surface topography of the p3 and p6 annexin V crystal forms determined by atomic force microscopy. *J Struct Biol*, 131, 234-9 (2000)

129. Oling, F., J. S. Santos, N. Govorukhina, C. Mazeres-Dubut, W. Bergsma-Schutter, G. Oostergetel, W. Keegstra, O. Lambert, A. Lewit-Bentley & A. Brisson: Structure of membrane-bound annexin A5 trimers: a hybrid cryo-EM - X-ray crystallography study. *J Mol Biol*, 304, 561-73 (2000)

130. Oling, F., W. Bergsma-Schutter & A. Brisson: Trimers, dimers of trimers, and trimers of trimers are common building blocks of annexin a5 two-dimensional crystals. *J Struct Biol*, 133, 55-63 (2001)

131. Wu, L. N., B. R. Genge & R. E. Wuthier: Analysis and molecular modeling of the formation, structure, and activity of the phosphatidylserine-calcium-phosphate complex associated with biomineralization. *J Biol Chem*, 283, 3827-38 (2008)

132. Martin, S. J., C. P. Reutelingsperger, A. J. McGahon, J. A. Rader, R. C. van Schie, D. M. LaFace & D. R. Green: Early redistribution of plasma membrane phosphatidylserine is a general feature of apoptosis regardless of the initiating stimulus: inhibition by overexpression of Bcl-2 and Abl. *J Exp Med*, 182, 1545-56 (1995)

133. Fabisiak, J. P., V. E. Kagan, V. B. Ritov, D. E. Johnson & J. S. Lazo: Bcl-2 inhibits selective oxidation and externalization of phosphatidylserine during paraquat-induced apoptosis. *Am J Physiol*, 272, C675-84 (1997)

134. Zhang, G., V. Gurtu, S. R. Kain & G. Yan: Early detection of apoptosis using a fluorescent conjugate of annexin V. *Biotechniques*, 23, 525-31 (1997)

135. Johnson, K., K. Pritzker, J. Goding & R. Terkeltaub: The nucleoside triphosphate pyrophosphohydrolase isozyme PC-1 directly promotes cartilage calcification through chondrocyte apoptosis and increased calcium precipitation by mineralizing vesicles. *J Rheumatol*, 28, 2681-91 (2001)

136. Genge, B. R., L. N. Wu & R. E. Wuthier: *In vitro* modeling of matrix vesicle nucleation: synergistic stimulation of mineral formation by annexin A5 and phosphatidylserine. *J Biol Chem*, 282, 26035-45 (2007)

137. Wu, L. N., B. R. Genge & R. E. Wuthier: Differential effects of zinc and magnesium ions on mineralization activity of phosphatidylserine calcium phosphate complexes. *J Inorg Biochem*, 103, 948-62 (2009)

138. Smith, P. D. & S. E. Moss: Structural evolution of the annexin supergene family. *Trends Genet*, 10, 241-6 (1994)

139. Smith, P. D., A. Davies, M. J. Crumpton & S. E. Moss: Structure of the human annexin VI gene. *Proc Natl Acad Sci U S A*, 91, 2713-7 (1994)

140. Avila-Sakar, A. J., C. E. Creutz & R. H. Kretsinger: Crystal structure of bovine annexin VI in a calcium-bound state. *Biochim Biophys Acta*, 1387, 103-16 (1998)

141. Crompton, M. R., R. J. Owens, N. F. Totty, S. E. Moss, M. D. Waterfield & M. J. Crumpton: Primary structure of the human, membrane-associated Ca^{2+}-binding protein p68 a novel member of a protein family. *Embo J*, 7, 21-7 (1988)

142. Bandorowicz-Pikula, J. & S. Pikula: Modulation of annexin VI-driven aggregation of phosphatidylserine liposomes by ATP.*Biochimie*, 80, 613-20 (1998)

143. Theobald, J., P. D. Smith, S. M. Jacob & S. E. Moss: Expression of annexin VI in A431 carcinoma cells suppresses proliferation: a possible role for annexin VI in cell growth regulation. *Biochim Biophys Acta*, 1223, 383-90 (1994)

144. Chen, N. X., K. D. O'Neill, X. Chen & S. M. Moe: Annexin-mediated matrix vesicle calcification in vascular smooth muscle cells. *J Bone Miner Res*, 23, 1798-805 (2008)

145. Kirsch, T., G. Harrison, E. E. Golub & H. D. Nah: The roles of annexins and types II and X collagen in matrix vesicle-mediated mineralization of growth plate cartilage. *J Biol Chem*, 275, 35577-83 (2000)

146. Merrifield, C. J., U. Rescher, W. Almers, J. Proust, V. Gerke, A. S. Sechi & S. E. Moss: Annexin 2 has an essential role in actin-based macropinocytic rocketing. *Curr Biol*, 11, 1136-41 (2001)

147. Senda, T.: Mechanisms of secretory granule transport and exocytosis in anterior pituitary cells. *Ital J Anat Embryol*, 100 Suppl 1, 219-29 (1995)

148. Chasserot-Golaz, S., N. Vitale, E. Umbrecht-Jenck, D. Knight, V. Gerke & M. F. Bader: Annexin 2 promotes the formation of lipid microdomains required for calcium-regulated exocytosis of dense-core vesicles. *Mol Biol Cell*, 16, 1108-19 (2005)

149. Christian, H. C., A. D. Taylor, R. J. Flower, J. F. Morris & J. C. Buckingham: Characterization and

localization of lipocortin 1-binding sites on rat anterior pituitary cells by fluorescence-activated cell analysis/sorting and electron microscopy. *Endocrinology*, 138, 5341-51 (1997)

150. Serres, M., C. Comera & D. Schmitt: Annexin 1 regulation in human epidermal cells. *Cell Mol Biol (Noisy-le-grand)*, 40, 701-6 (1994)

151. Kim, K. M., D. K. Kim, Y. M. Park, C. K. Kim & D. S. Na: Annexin-I inhibits phospholipase A2 by specific interaction, not by substrate depletion. *FEBS Lett*, 343, 251-5 (1994)

152. Bastian, B. C., C. Sellert, A. Seekamp, J. Romisch, E. P. Paques & E. B. Brocker: Inhibition of human skin phospholipase A2 by "lipocortins" is an indirect effect of substrate/lipocortin interaction. *J Invest Dermatol*, 101, 359-63 (1993)

153. Solito, E., R. De Caterina, D. Giannessi, P. L. Paggiaro, R. Sicari & L. Parente: Studies on the induction of lipocortin-1 by glucocorticoids. *Ann Ist Super Sanita*, 29, 391-4 (1993)

154. Northington, F. K., T. D. Oglesby, Y. Ishikawa & R. E. Wuthier: Localization of prostaglandin synthetase in chicken epiphyseal cartilage. *Calcif Tissue Res*, 26, 227-36 (1978)

155. Teixeira, M. M., A. M. Das, J. M. Miotla, M. Perretti & P. G. Hellewell: The role of lipocortin-1 in the inhibitory action of dexamethasone on eosinophil trafficking in cutaneous inflammatory reactions in the mouse. *Br J Pharmacol*, 123, 538-44 (1998)

156. Yi, M. & J. E. Schnitzer: Impaired tumor growth, metastasis, angiogenesis and wound healing in annexin A1-null mice. *Proc Natl Acad Sci U S A*, 106, 17886-91 (2009)

157. Ruan, G. R., H. S. Zhao, Y. Chang, J. L. Li, Y. Z. Qin, Y. R. Liu, S. S. Chen & X. J. Huang: Adenovirus-mediated PDCD5 gene transfer sensitizes K562 cells to apoptosis induced by idarubicin *in vitro* and *in vivo*. *Apoptosis*, 13, 641-8 (2008)

158. Ali, S. Y.: Analysis of matrix vesicles and their role in the calcification of epiphyseal cartilage. *Fed Proc*, 35, 135-42 (1976)

159. Hosokawa, R., Y. Uchida, S. Fujiwara & T. Noguchi: Lactate dehydrogenase isoenzymes are present in matrix vesicles. *J Biol Chem*, 263, 10045-7 (1988)

160. Sauer, G. R., B. R. Genge, L. N. Wu & J. E. Donachy: A facilitative role for carbonic anhydrase activity in matrix vesicle mineralization. *Bone Miner*, 26, 69-79 (1994)

161. Robison, R.: The possible significance of hexosephosphoric esters in ossification. *Biochem J*, 17, 286-93 (1923)

162. Anderson, H. C., D. Harmey, N. P. Camacho, R. Garimella, J. B. Sipe, S. Tague, X. Bi, K. Johnson, R. Terkeltaub & J. L. Millan: Sustained osteomalacia of long bones despite major improvement in other hypophosphatasia-related mineral deficits in tissue nonspecific alkaline phosphatase/nucleotide pyrophosphatase phosphodiesterase 1 double-deficient mice. *Am J Pathol*, 166, 1711-20 (2005)

163. Anderson, H. C., J. B. Sipe, L. Hessle, R. Dhanyamraju, E. Atti, N. P. Camacho & J. L. Millan: Impaired calcification around matrix vesicles of growth plate and bone in alkaline phosphatase-deficient mice. *Am J Pathol*, 164, 841-7 (2004)

164. Hessle, L., K. A. Johnson, H. C. Anderson, S. Narisawa, A. Sali, J. W. Goding, R. Terkeltaub & J. L. Millan: Tissue-nonspecific alkaline phosphatase and plasma cell membrane glycoprotein-1 are central antagonistic regulators of bone mineralization. *Proc Natl Acad Sci U S A*, 99, 9445-9 (2002)

165. Harmey, D., L. Hessle, S. Narisawa, K. A. Johnson, R. Terkeltaub & J. L. Millan: Concerted regulation of inorganic pyrophosphate and osteopontin by akp2, enpp1, and ank: an integrated model of the pathogenesis of mineralization disorders. *Am J Pathol*, 164, 1199-209 (2004)

166. Weiss, M. J., P. S. Henthorn, M. A. Lafferty, C. Slaughter, M. Raducha & H. Harris: Isolation and characterization of a cDNA encoding a human liver/bone/kidney-type alkaline phosphatase. *Proc Natl Acad Sci U S A*, 83, 7182-6 (1986)

167. Low, M. G. & D. B. Zilversmit: Role of phosphatidylinositol in attachment of alkaline phosphatase to membranes. *Biochemistry*, 19, 3913-8 (1980)

168. Hsu, D. S. & S. S. Chen: Heterogeneity of alkaline phosphatase observed by high-performance liquid chromatography. *J Chromatogr*, 328, 409-12 (1985)

169. Hsu, H. H., P. A. Munoz, J. Barr, I. Oppliger, D. C. Morris, H. K. Vaananen, N. Tarkenton & H. C. Anderson: Purification and partial characterization of alkaline phosphatase of matrix vesicles from fetal bovine epiphyseal cartilage. Purification by monoclonal antibody affinity chromatography. *J Biol Chem*, 260, 1826-31 (1985)

170. Sowadski, J. M., M. D. Handschumacher, H. M. Murthy, B. A. Foster & H. W. Wyckoff: Refined structure of alkaline phosphatase from Escherichia coli at 2.8 A resolution. *J Mol Biol*, 186, 417-33 (1985)

171. Kim, E. E. & H. W. Wyckoff: Reaction mechanism of alkaline phosphatase based on crystal structures. Two-metal ion catalysis. *J Mol Biol*, 218, 449-64 (1991)

172. Llinas, P., E. A. Stura, A. Menez, Z. Kiss, T. Stigbrand, J. L. Millan & M. H. Le Du: Structural studies

of human placental alkaline phosphatase in complex with functional ligands. *J Mol Biol*, 350, 441-51 (2005)

173. Llinas, P., M. Masella, T. Stigbrand, A. Menez, E. A. Stura & M. H. Le Du: Structural studies of human alkaline phosphatase in complex with strontium: implication for its secondary effect in bones. *Protein Sci*, 15, 1691-700 (2006)

174. Stagni, N., G. Furlan, F. Vittur, M. Zanetti & B. de Bernard: Enzymatic properties of the Ca2+-binding glycoprotein isolated from preosseous cartilage. *Calcif Tissue Int*, 29, 27-32 (1979)

175. de Bernard, B., M. Gherardini, G. C.Lunazzi, C. Modricky, L. Moro, E. Panfili, P. Pollesello, N. Stagni & F. Vittur: Role of the Ca^{++}-binding alkaline phosphatase in the mechanism of cartilage calcification. In: *Cell Mediated Calcification and Matrix Vesicles*.Ed: Y. Ali, Elsevier Science Publishers B.V., Amsterdam, The Netherlands, 95-100 (1986).

176. Harrison, G., I. M. Shapiro & E. E. Golub: The phosphatidylinositol-glycolipid anchor on alkaline phosphatase facilitates mineralization initiation *in vitro*. *J Bone Miner Res*, 10, 568-73 (1995)

177. Cyboron, G. W. & R. E. Wuthier: Purification and initial characterization of intrinsic membrane-bound alkaline phosphatase from chicken epiphyseal cartilage. *J Biol Chem*, 256, 7262-7268 (1981)

178. Eaton, R. H. & D. W. Moss: Organic pyrophosphates as substrates for human alkaline phosphatases. *Biochem J*, 105, 1307-1312 (1967)

179. Moss, D. W., R. H. Eaton, J. K. Smith & L. G. Whitby: Association of inorganic-pyrophosphatase activity with human alkaline-phosphatase preparations. *Biochem J*, 102, 53-7 (1967)

180. Anderson, H. C.: Matrix vesicles and calcification. *Curr Rheumatol Rep*, 5, 222-6 (2003)

181. Whyte, M. P.: Hypophosphatasia and the role of alkaline phosphatase in skeletal mineralization. *Endocr Rev*, 15, 439-61 (1994)

182. Narisawa, S., N. Frohlander & J. L. Millan: Inactivation of two mouse alkaline phosphatase genes and establishment of a model of infantile hypophosphatasia. *Dev Dyn*, 208, 432-46 (1997)

183. Fedde, K. N., L. Blair, J. Silverstein, S. P. Coburn, L. M. Ryan, R. S. Weinstein, K. Waymire, S. Narisawa, J. L. Millan, G. R. MacGregor & M. P. Whyte: Alkaline phosphatase knock-out mice recapitulate the metabolic and skeletal defects of infantile hypophosphatasia. *J Bone Miner Res*, 14, 2015-26 (1999)

184. Vittur, F., N. Stagni, L. Moro & B. de Bernard: Alkaline phosphatase binds to collagen; a hypothesis on the mechanism of extravesicular mineralization in epiphyseal cartilage. *Experientia*, 40, 836-7 (1984)

185. Crawford, K., H. Weissig, F. Binette, J. L. Millan & P. F. Goetinck: Tissue-nonspecific alkaline phosphatase participates in the establishment and growth of feather germs in embryonic chick skin cultures. *Dev Dyn*, 204, 48-56 (1995)

186. Murphree, S., H. H. Hsu & H. C. Anderson: *In vitro* formation of crystalline apatite by matrix vesicles isolated from rachitic rat epiphyseal cartilage. *Calcif Tissue Int*, 34 Suppl 2, S62-8 (1982)

187. Siegel, S. A., C. F. Hummel & R. P. Carty: The role of nucleoside triphosphate pyrophosphohydrolase in *in vitro* nucleoside triphosphate-dependent matrix vesicle calcification. *J Biol Chem*, 258, 8601-7 (1983)

188. Kanabe, S., H. H. Hsu, R. N. Cecil & H. C. Anderson: Electron microscopic localization of adenosine triphosphate (ATP)-hydrolyzing activity in isolated matrix vesicles and reconstituted vesicles from calf cartilage. *J Histochem Cytochem*, 31, 462-70 (1983)

189. Caswell, A. M. & R. G. Russell: Identification of ecto-nucleoside triphosphate pyrophosphatase in human articular chondrocytes in monolayer culture. *Biochim Biophys Acta*, 847, 40-7 (1985)

190. Simao, A. M., M. C. Yadav, S. Narisawa, M. Bolean, J. M. Pizauro, M. F. Hoylaerts, P. Ciancaglini & J. L. Millan: Proteoliposomes harboring alkaline phosphatase and nucleotide pyrophosphatase as matrix vesicle biomimetics. *J Biol Chem*, 285, 7598-609 (2010)

191. Vaingankar, S. M., T. A. Fitzpatrick, K. Johnson, J. W. Goding, M. Maurice & R. Terkeltaub: Subcellular targeting and function of osteoblast nucleotide pyrophosphatase phosphodiesterase 1.*Am J Physiol Cell Physiol*, 286, C1177-87 (2004)

192. Garimella, R., X. Bi, H. C. Anderson & N. P. Camacho: Nature of phosphate substrate as a major determinant of mineral type formed in matrix vesicle-mediated *in vitro* mineralization: An FTIR imaging study. *Bone*, 38, 811-7 (2006)

193. Ciancaglini, P., M. C. Yadav, A. M. Simao, S. Narisawa, J. M. Pizauro, C. Farquharson, M. F. Hoylaerts & J. L. Millan: Kinetic analysis of substrate utilization by native and TNAP-, NPP1-, or PHOSPHO1-deficient matrix vesicles. *J Bone Miner Res*, 25, 716-23

194. Fleisch, H. & S. Bisaz: Mechanism of calcification: inhibitory role of pyrophosphate. *Nature*, 195, 911 (1962)

195. Terkeltaub, R., M. Rosenbach, F. Fong & J. Goding: Causal link between nucleotide pyrophosphohydrolase overactivity and increased intracellular inorganic pyrophosphate generation demonstrated by transfection of cultured fibroblasts and osteoblasts with plasma cell membrane glycoprotein-1. Relevance to calcium pyrophosphate dihydrate deposition disease. *Arthritis Rheum*, 37, 934-41 (1994)

196. Rehemtulla, A. & R. J. Kaufman: Protein processing within the secretory pathway. *Curr Opin Biotechnol*, 3, 560-5(1992)

197. Goding, J. W. & F. W. Shen: Structure of the murine plasma cell alloantigen PC-1: comparison with the receptor for transferrin. *J Immunol*, 129, 2636-40 (1982)Goding, J. W. & F. W. Shen: Structure of the murine plasma cell alloantigen PC-1: comparison with the receptor for transferrin. *J Immunol*, 129, 2636-40(1982)

198. van Driel, I. R. & J. W. Goding: Plasma cell membrane glycoprotein PC-1. Primary structure deduced from cDNA clones. *J Biol Chem*, 262, 4882-7 (1987)

199. Gijsbers, R., H. Ceulemans, W. Stalmans & M. Bollen: Structural and catalytic similarities between nucleotide pyrophosphatases/phosphodiesterases and alkaline phosphatases. *J Biol Chem*, 276, 1361-8 (2001)

200. Fridrich, D., M. Kern, J. Fritz, G. Pahlke, N. Kohler, P. Winterhalter & D. Marko: The epidermal growth factor receptor and human topoisomerases represent potential cellular targets of oligomeric procyanidins. *Mol Nutr Food Res*, 51, 192-200 (2007)

201. Muller, G. & W. Frick: Signalling via caveolin: involvement in the cross-talk between phosphoinositolglycans and insulin. *Cell Mol Life Sci*, 56, 945-70 (1999)

202. Roberts, S., S. Narisawa, D. Harmey, J. L. Millan & C. Farquharson: Functional involvement of PHOSPHO1 in matrix vesicle-mediated skeletal mineralization. *J Bone Miner Res*, 22, 617-27 (2007)

203. Stewart, A. J., R. Schmid, C. A. Blindauer, S. J. Paisey & C. Farquharson: Comparative modelling of human PHOSPHO1 reveals a new group of phosphatases within the haloacid dehalogenase superfamily. *Protein Eng*, 16, 889-95 (2003)

204. Houston, B., E. Seawright, D. Jefferies, E. Hoogland, D. Lester, C. Whitehead & C. Farquharson: Identification and cloning of a novel phosphatase expressed at high levels in differentiating growth plate chondrocytes. *Biochim Biophys Acta*, 1448, 500-6 (1999)

205. Macrae, V. E., M. G. Davey, L. McTeir, S. Narisawa, M. C. Yadav, J. L. Millan & C. Farquharson: Inhibition of PHOSPHO1 activity results in impaired skeletal mineralization during limb development of the chick. *Bone*, 46, 1146-55 (2010)

206. Roberts, S. J., A. J. Stewart, R. Schmid, C. A. Blindauer, S. R. Bond, P. J. Sadler & C. Farquharson: Probing the substrate specificities of human PHOSPHO1 and PHOSPHO2. *Biochim Biophys Acta*, 1752, 73-82 (2005)

207. Wu, L. N., B. R. Genge, M. W. Kang, A. L. Arsenault & R. E. Wuthier: Changes in phospholipid extractability and composition accompany mineralization of chicken growth plate cartilage matrix vesicles. *J Biol Chem*, 277, 5126-33 (2002)

208. Wu, L. N., G. R. Sauer, B. R. Genge, W. B. Valhmu & R. E. Wuthier: Effects of analogues of inorganic phosphate and sodium ion on mineralization of matrix vesicles isolated from growth plate cartilage of normal rapidly growing chickens. *J Inorg Biochem*, 94, 221-35 (2003)

209. Anderson, H. C.: Molecular biology of matrix vesicles. *Clin Orthop Relat Res*266-80 (1995)

210. Hirschman, A., D. Deutsch, M. Hirschman, I. A. Bab, J. Sela & A. Muhlrad: Neutral peptidase activities in matrix vesicles from bovine fetal alveolar bone and dog osteosarcoma. *Calcif Tissue Int*, 35, 791-7 (1983)

211. Katsura, N. & K. Yamada: Isolation and characterization of a metalloprotease associated with chicken epiphyseal cartilage matrix vesicles. *Bone*, 7, 137-43 (1986)

212. Hirschman, A. & D. D. Dziewiatkowski: Protein-polysaccharide loss during endochondral ossification: immunochemical evidence. *Science*, 154, 393-5 (1966)

213. Jibril, A. O.: Proteolytic degradation of ossifying cartilage matrix and the removal of acid mucopolysaccharides prior to bone formation. *Biochim Biophys Acta*, 136, 162-5 (1967)

214. Hirschman, A. & M. Hirschman: Aminopeptidase profile and protease activity in rat cartilage at physiological pH. *Isr J MedSci*, 7, 403-5 (1971)

215. Hosokawa, R., H. Ohashi-Takeuchi, N. Yamada, Y. Uchida, S. Fujiwara & T. Noguchi: Lactate dehydrogenase isoenzymes in matrix vesicles (review). *Bone Miner*, 17, 177-81 (1992)

216. Rajpurohit, R., C. J. Koch, Z. Tao, C. M. Teixeira & I. M. Shapiro: Adaptation of chondrocytes to low oxygen tension: relationship between hypoxia and cellular metabolism. *J Cell Physiol*, 168, 424-32 (1996)

217. Cuervo, L. A., J. C. Pita & D. S. Howell: Ultramicroanalysis of pH, pCO_2 and carbonic anhydrase activity at calcifying sites in cartilage. *Calcif Tissue Res*, 7, 220-31 (1971)

218. Vaananen, H. K.: Immunohistochemical localization of carbonic anhydrase isoenzymes I and II in human bone, cartilage and giant cell tumor. *Histochemistry*, 81, 485-7 (1984)

219. Anderson, R. E., H. Schraer & C. V. Gay: Ultrastructural immunocytochemical localization of carbonic anhydrase in normal and calcitonin-treated chick osteoclasts. *Anat Rec*, 204, 9-20 (1982)

220. Gay, C. V., R. E. Anderson, H. Schraer & D. S. Howell: Identification of carbonic anhydrase in chick

growth-plate cartilage. *J Histochem Cytochem*, 30, 391-4 (1982)

221. Wuthier, R. E.: Effect of phospholipids on the transformation of amorphous calcium phosphate to hydroxapatite *in vitro*. *Calcif Tissue Res*, 19, 197-210 (1975)

222. Genge, B. R., L. N. Wu & R. E. Wuthier: Separation and quantification of chicken and bovine growth plate cartilage matrix vesicle lipids by high-performance liquid chromatography using evaporative light scattering detection. *Anal Biochem*, 322, 104-15 (2003)

223. Wuthier, R. E.: The role of phospholipids in biological calcification: distribution of phospholipase activity in calcifying epiphyseal cartilage. *Clin Orthop Relat Res,* 90, 191-200 (1973)

224. Balcerzak, M., S. Pikula & R. Buchet: Phosphorylation-dependent phospholipase D activity of matrix vesicles. *FEBS Lett*, 580, 5676-80 (2006)

225. Kramer, R. M., C. Hession, B. Johansen, G. Hayes, P. McGray, E. P. Chow, R. Tizard & R. B. Pepinsky: Structure and properties of a human non-pancreatic phospholipase A_2. *J Biol Chem*, 264, 5768-75 (1989)

226. Komada, M., I. Kudo, H. Mizushima, N. Kitamura & K. Inoue: Structure of cDNA coding for rat platelet phospholipase A2. *J Biochem*, 106, 545-7 (1989)

227. Stillo, J. V.: Characterization and metabolism of phospholipids in chicken epiphyseal cartilage: Studies on phospholipase A activity. *Department of Chemistry and Biochemistry*, University of South Carolina, Columbia (1980).

228. Nevalainen, T. J., F. Marki, P. T. Kortesuo, M. G. Grutter, S. Di Marco & A. Schmitz: Synovial type (group II) phospholipase A_2 in cartilage. *J Rheumatol*, 20, 325-30 (1993)

229. Pruzanski, W., K. Scott, G. Smith, I. Rajkovic, E. Stefanski & P. Vadas: Enzymatic activity and immunoreactivity of extracellular phospholipase A_2 in inflammatory synovial fluids. *Inflammation*, 16, 451-7 (1992)

230. Vignon, E., J. C. Balblanc, P. Mathieu, P. Louisot & M. Richard: Metalloprotease activity, phospholipase A_2 activity and cytokine concentration in osteoarthritis synovial fluids. *Osteoarthritis Cartilage*, 1, 115-20 (1993)

231. Schwartz, Z. & B. Boyan: The effects of vitamin D metabolites on phospholipase A_2 activity of growth zone and resting zone cartilage cells *in vitro*. *Endocrinology*, 122, 2191-8 (1988)

232. Schwartz, Z., D. L. Schlader, L. D. Swain & B. D. Boyan: Direct effects of 1,25-dihydroxyvitamin D3 and 24,25-dihydroxyvitamin D3 on growth zone and resting zone chondrocyte membrane alkaline phosphatase and phospholipase A_2 specific activities. *Endocrinology*, 123, 2878-84 (1988)

233. Kristensen, T., C. J. Saris, T. Hunter, L. J. Hicks, D. J. Noonan, J. R. Glenney, Jr. & B. F. Tack: Primary structure of bovine calpactin I heavy chain (p36), a major cellular substrate for retroviral protein-tyrosine kinases: homology with the human phospholipase A_2 inhibitor lipocortin. *Biochemistry*, 25, 4497-503 (1986)

234. Berridge, M. J.: The Albert Lasker Medical Awards. Inositol trisphosphate, calcium, lithium, and cell signaling. *Jama*, 262, 1834-41 (1989)

235. Berridge, M. J. & R. F. Irvine: Inositol trisphosphate, a novel second messenger in cellular signal transduction. *Nature*, 312, 315-21 (1984)

236. Nishizuka, Y.: Intracellular signaling by hydrolysis of phospholipids and activation of protein kinase C. *Science*, 258, 607-14 (1992)

237. Frey, R. S., X. Gao, K. Javaid, S. S. Siddiqui, A. Rahman & A. B. Malik: Phosphatidylinositol 3-kinase gamma signaling through protein kinase Czeta induces NADPH oxidase-mediated oxidant generation and NF-kappaB activation in endothelial cells. *J Biol Chem*, 281, 16128-38 (2006)

238. O'Rourke, F. A., S. P. Halenda, G. B. Zavoico & M. B. Feinstein: Inositol 1,4,5-trisphosphate releases Ca^{2+} from a Ca^{2+}-transporting membrane vesicle fraction derived from human platelets. *J Biol Chem*, 260, 956-62 (1985)

239. Ekstein, J., E. Nasatzky, B. D. Boyan, A. Ornoy & Z. Schwartz: Growth-plate chondrocytes respond to 17beta-estradiol with sex-specific increases in IP_3 and intracellular calcium ion signalling via a capacitative entry mechanism. *Steroids*, 70, 775-86 (2005)

240. Sjoholm, A., Q. Zhang, N. Welsh, A. Hansson, O. Larsson, M. Tally & P. O. Berggren: Rapid Ca^{2+} influx and diacylglycerol synthesis in growth hormone-mediated islet beta-cell mitogenesis. *J Biol Chem*, 275, 21033-40 (2000)

241. Du, C., Q. Zhao, S. Araki, S. Zhang & J. Miao: Apoptosis mediated by phosphatidylcholine-specific phospholipase C is associated with cAMP, p53 level, and cell-cycle distribution in vascular endothelial cells. *Endothelium*, 10, 141-7 (2003)

242. Liu, X., Q. Zhao, S. Araki, S. Zhang & J. Miao: Contrasting effects of phosphatidylinositol- and phosphatidylcholine-specific phospholipase C on apoptosis in cultured endothelial cells. *Endothelium*, 13, 205-11 (2006)

243. Szumilo, M. & I. Rahden-Staron: (Biological role of phosphatidylcholine-specific phospholipase C in mammalian cells). *Postepy Hig Med Dosw (Online)*, 62, 593-8 (2008)

244. Fu, D., Y. Ma, W. Wu, X. Zhu, C. Jia, Q. Zhao, C. Zhang & X. Z. Wu: Cell-cycle-dependent PC-PLC regulation by APC/C (Cdc20)-mediated ubiquitin-proteasome pathway. *J Cell Biochem*, 107, 686-96 (2009)

245. Sun, C., N. Wang, J. Huang, J. Xin, F. Peng, Y. Ren, S. Zhang & J. Miao: Inhibition of phosphatidylcholine-specific phospholipase C prevents bone marrow stromal cell senescence *in vitro*. *J Cell Biochem*, 108, 519-28 (2009)

246. van Dijk, M. C., F. J. Muriana, J. de Widt, H. Hilkmann & W. J. van Blitterswijk: Involvement of phosphatidylcholine-specific phospholipase C in platelet-derived growth factor-induced activation of the mitogen-activated protein kinase pathway in Rat-1 fibroblasts. *J Biol Chem*, 272, 11011-6 (1997)

247. Ramoni, C., F. Spadaro, B. Barletta, M. L. Dupuis & F. Podo: Phosphatidylcholine-specific phospholipase C in mitogen-stimulated fibroblasts. *Exp Cell Res*, 299, 370-82 (2004)

248. Boyan, B. D., L. Wang, K. L. Wong, H. Jo & Z. Schwartz: Plasma membrane requirements for 1alpha,25 $(OH)_2D_3$ dependent PKC signaling in chondrocytes and osteoblasts. *Steroids*, 71, 286-90 (2006)

249. Murphy, E. J., K. M. Brindle, C. J. Rorison, R. M. Dixon, B. Rajagopalan & G. K. Radda: Changes in phosphatidylethanolamine metabolism in regenerating rat liver as measured by ^{31}P-NMR. *Biochim Biophys Acta*, 1135, 27-34 (1992)

250. Hafez, M. M. & M. E. Costlow: Phosphatidylethanolamine turnover is an early event in the response of NB2 lymphoma cells to prolactin. *Exp Cell Res*, 184, 37-43 (1989)

251. Sakagami, H., J. Aoki, Y. Natori, K. Nishikawa, Y. Kakehi, Y. Natori & H. Arai: Biochemical and molecular characterization of a novel choline-specific glycerophosphodiester phosphodiesterase belonging to the nucleotide pyrophosphatase/phosphodiesterase family. *J Biol Chem*, 280, 23084-93 (2005)

252. Liu, B. & Y. A. Hannun: Inhibition of the neutral magnesium-dependent sphingomyelinase by glutathione. *J Biol Chem*, 272, 16281-7 (1997)

253. Zhang, P., B. Liu, G. M. Jenkins, Y. A. Hannun & L. M. Obeid: Expression of neutral sphingomyelinase identifies a distinct pool of sphingomyelin involved in apoptosis. *J Biol Chem*, 272, 9609-12 (1997)

254. Clarke, C. J. & Y. A. Hannun: Neutral sphingomyelinases and nSMase2: bridging the gaps. *Biochim Biophys Acta*, 1758, 1893-901 (2006)

255. Clarke, C. J., C. F. Snook, M. Tani, N. Matmati, N. Marchesini & Y. A. Hannun: The extended family of neutral sphingomyelinases. *Biochemistry*, 45, 11247-56 (2006)

256. Clarke, C. J., B. X. Wu & Y. A. Hannun: The neutral sphingomyelinase family: Identifying biochemical connections. *Adv Enzyme Regul (In press)*

257. Wu, B. X., C. J. Clarke & Y. A. Hannun: Mammalian Neutral Sphingomyelinases: Regulation and roles in cell signaling responses. *Neuromolecular Med*, 12, 320-330

258. Marchesini, N., C. Luberto & Y. A. Hannun: Biochemical properties of mammalian neutral sphingomyelinase 2 and its role in sphingolipid metabolism. *J Biol Chem*, 278, 13775-83 (2003)

259. Majeska, R. J., D. L. Holwerda & R. E. Wuthier: Localization of phosphatidylserine in isolated chick epiphyseal cartilage matrix vesicles with trinitrobenzenesulfonate. *Calcif Tissue Int*, 27, 41-6 (1979)

260. Tani, M. & Y. A. Hannun: Analysis of membrane topology of neutral sphingomyelinase 2. *FEBS Lett*, 581, 1323-8 (2007)

261. Tani, M. & Y. A. Hannun: Neutral sphingomyelinase 2 is palmitoylated on multiple cysteine residues. Role of palmitoylation in subcellular localization. *J Biol Chem*, 282, 10047-56 (2007)

262. Marchesini, N., W. Osta, J. Bielawski, C. Luberto, L. M. Obeid & Y. A. Hannun: Role for mammalian neutral sphingomyelinase 2 in confluence-induced growth arrest of MCF7 cells. *J Biol Chem*, 279, 25101-11 (2004)

263. Mikati, M. A., M. Zeinieh, R. A. Habib, J. El Hokayem, A. Rahmeh, M. El Sabban, J. Usta & G. Dbaibo: Changes in sphingomyelinases, ceramide, Bax, Bcl (2), and caspase-3 during and after experimental status epilepticus. *Epilepsy Res*, 81, 161-6 (2008)

264. Stoffel, W., B. Jenke, B. Holz, E. Binczek, R. H. Gunter, J. Knifka, J. Koebke & A. Niehoff: Neutral sphingomyelinase (SMPD3) deficiency causes a novel form of chondrodysplasia and dwarfism that is rescued by Col2A1-driven smpd3 transgene expression. *Am J Pathol*, 171, 153-61 (2007)

265. Aubin, I., C. P. Adams, S. Opsahl, D. Septier, C. E. Bishop, N. Auge, R. Salvayre, A. Negre-Salvayre, M. Goldberg, J. L. Guenet & C. Poirier: A deletion in the gene encoding sphingomyelin phosphodiesterase 3 (Smpd3) results in osteogenesis and dentinogenesis imperfecta in the mouse. *Nat Genet*, 37, 803-5 (2005)

266. Cotmore, J. M., G. Nichols, Jr. & R. E. Wuthier: Phospholipid-calcium phosphate complex: enhanced calcium migration in the presence of phosphate. *Science*, 172, 1339-41 (1971)

267. Wuthier, R. E. & J. W. Cummins: *In vitro* incorporation of (^{3}H)serine into phospholipids of

proliferating and calcifying epiphyseal cartilage and liver. *Biochim Biophys Acta*, 337, 50-9 (1974)

268. Wuthier, R. E., F. H. Wians, Jr., M. S. Giancola & S. S. Dragic: *In vitro* biosynthesis of phospholipids by chondrocytes and matrix vesicles of epiphyseal cartilage. *Biochemistry*, 17, 1431-6 (1978)

269. Vance, J. E.: Phosphatidylserine and phosphatidylethanolamine in mammalian cells: two metabolically related aminophospholipids. *J Lipid Res*, 49, 1377-87 (2008)

270. Vance, J. E.: Molecular and cell biology of phosphatidylserine and phosphatidylethanolamine metabolism. *Prog Nucleic Acid Res Mol Biol*, 75, 69-111 (2003)

271. Matthews, J. L., J. H. Martin, H. W. Sampson, A. S. Kunin & J. H. Roan: Mitochondrial granules in the normal and rachitic rat epiphysis. *Calcif Tissue Res*, 5, 91-9 (1970)

272. Martin, J. H. & J. L. Matthews: Mitochondrial granules in chondrocytes. *Calcif Tissue Res*, 3, 184-93 (1969)

273. Matthews, J. L., J. H. Martin & E. J. Collins: Metabolism of radioactive calcium by cartilage. *Clin Orthop Relat Res*, 58, 213-23 (1968)

274. Matthews, J. L. & J. H. Martin: Intracellular transport of calcium and its relationship to homeostasis and mineralization. An electron microscope study. *Am J Med*, 50, 589-97 (1971)

275. Matthews, J. L., J. H. Martin, J. A. Lynn & E. J. Collins: Calcium incorporation in the developing cartilaginous epiphysis. *Calcif Tissue Res*, 1, 330-6 (1968)

276. Stone, S. J., Z. Cui & J. E. Vance: Cloning and expression of mouse liver phosphatidylserine synthase-1 cDNA. Overexpression in rat hepatoma cells inhibits the CDP-ethanolamine pathway for phosphatidylethanolamine biosynthesis. *J Biol Chem*, 273, 7293-302 (1998)

277. Stone, S. J. & J. E. Vance: Cloning and expression of murine liver phosphatidylserine synthase (PSS)-2: differential regulation of phospholipid metabolism by PSS1 and PSS2. *Biochem J*, 342 (Pt 1), 57-64 (1999)

278. Kuge, O., K. Hasegawa, T. Ohsawa, K. Saito & M. Nishijima: Purification and characterization of Chinese hamster phosphatidylserine synthase 2. *J Biol Chem*, 278, 42692-8 (2003)

279. Saito, K., M. Nishijima & O. Kuge: Genetic evidence that phosphatidylserine synthase II catalyzes the conversion of phosphatidylethanolamine to phosphatidylserine in Chinese hamster ovary cells. *J Biol Chem*, 273, 17199-205 (1998)

280. Voelker, D. R.: Interorganelle transport of aminoglycerophospholipids. *Biochim Biophys Acta*, 1486, 97-107 (2000)

281. Daleke, D. L.: Phospholipid flippases. *J Biol Chem*, 282, 821-5 (2007)

282. Sahu, S. K., S. N. Gummadi, N. Manoj & G. K. Aradhyam: Phospholipid scramblases: an overview. *Arch Biochem Biophys*, 462, 103-14 (2007)

283. Wolfs, J. L., P. Comfurius, J. T. Rasmussen, J. F. Keuren, T. Lindhout, R. F. Zwaal & E. M. Bevers: Activated scramblase and inhibited aminophospholipid translocase cause phosphatidylserine exposure in a distinct platelet fraction. *Cell Mol Life Sci*, 62, 1514-25 (2005)

284. Zwaal, R. F., P. Comfurius & E. M. Bevers: Surface exposure of phosphatidylserine in pathological cells. *Cell Mol Life Sci*, 62, 971-88 (2005)

285. Zhou, Q., J. Zhao, J. G. Stout, R. A. Luhm, T. Wiedmer & P. J. Sims: Molecular cloning of human plasma membrane phospholipid scramblase. A protein mediating transbilayer movement of plasma membrane phospholipids. *J Biol Chem*, 272, 18240-4 (1997)

286. Contreras, F. X., L. Sanchez-Magraner, A. Alonso & F. M. Goni: Transbilayer (flip-flop) lipid motion and lipid scrambling in membranes. *FEBS Lett* (2009)

287. Damek-Poprawa, M., E. Golub, L. Otis, G. Harrison, C. Phillips & K. Boesze-Battaglia: Chondrocytes utilize a cholesterol-dependent lipid translocator to externalize phosphatidylserine. *Biochemistry*, 45, 3325-36 (2006)

288. Wu, L. N., T. Yoshimori, B. R. Genge, G. R. Sauer, T. Kirsch, Y. Ishikawa & R. E. Wuthier: Characterization of the nucleational core complex responsible for mineral induction by growth plate cartilage matrix vesicles. *J Biol Chem*, 268, 25084-94 (1993)

289. Anderson, H. C., H. H. Hsu, D. C. Morris, K. N. Fedde & M. P. Whyte: Matrix vesicles in osteomalacic hypophosphatasia bone contain apatite-like mineral crystals. *Am J Pathol*, 151, 1555-61 (1997)

290. Cotter, G., S. Verhaegen, M. Clynes & K. Kavanagh: Membrane changes associated with the early stages of apoptosis in HEp-2 cells decrease susceptibility to adherence by Candida albicans. *J Med Vet Mycol*, 35, 219-24 (1997)

291. Jefferies, D., B. Houston, D. Lester, C. C. Whitehead, B. H. Thorp, M. Botman & C. Farquharson: Expression patterns of chondrocyte genes cloned by differential display in tibial dyschondroplasia. *Biochim Biophys Acta*, 1501, 180-8 (2000)

292. Seulberger, H., F. Lottspeich & W. Risau: The inducible blood-brain barrier specific molecule HT7 is a novel immunoglobulin-like cell surface glycoprotein. *Embo J*, 9, 2151-8 (1990)

293. Kang, J. S., M. Gao, J. L. Feinleib, P. D. Cotter, S. N. Guadagno & R. S. Krauss: CDO: an oncogene-, serum-, and anchorage-regulated member of the Ig/fibronectin type III repeat family. *J Cell Biol*, 138, 203-13 (1997)

294. Wegorzewska, M., R. S. Krauss & J. S. Kang: Overexpression of the immunoglobulin superfamily members CDO and BOC enhances differentiation of the human rhabdomyosarcoma cell line RD. *Mol Carcinog*, 37, 1-4 (2003)

295. Durr, J., S. Goodman, A. Potocnik, H. von der Mark & K. von der Mark: Localization of beta 1-integrins in human cartilage and their role in chondrocyte adhesion to collagen and fibronectin. *Exp Cell Res*, 207, 235-44 (1993)

296. Enomoto, M., P. S. Leboy, A. S. Menko & D. Boettiger: Beta 1 integrins mediate chondrocyte interaction with type I collagen, type II collagen, and fibronectin. *Exp Cell Res*, 205, 276-85 (1993)

297. Loeser, R. F.: Chondrocyte integrin expression and function. *Biorheology*, 37, 109-16 (2000)

298. Shakibaei, M.: Integrin expression on epiphyseal mouse chondrocytes in monolayer culture. *Histol Histopathol*, 10, 339-49 (1995)

299. Shakibaei, M., B. Zimmermann & H. J. Merker: Changes in integrin expression during chondrogenesis *in vitro*: an immunomorphological study. *J Histochem Cytochem*, 43, 1061-9 (1995)

300. Wang, Y., F. Middleton, J. A. Horton, L. Reichel, C. E. Farnum & T. A. Damron: Microarray analysis of proliferative and hypertrophic growth plate zones identifies differentiation markers and signal pathways. *Bone*, 35, 1273-93 (2004)

301. Cecil, D. L., C. T. Appleton, M. D. Polewski, J. S. Mort, A. M. Schmidt, A. Bendele, F. Beier & R. Terkeltaub: The pattern recognition receptor CD36 is a chondrocyte hypertrophy marker associated with suppression of catabolic responses and promotion of repair responses to inflammatory stimuli. *J Immunol*, 182, 5024-31 (2009)

302. Hubbard, H. L.: Characterization of the extracellular fluid of chicken epiphyseal growth plate cartilage: Studies on metabolites and electrolytes. *Department of Chemistry & Biochemistry*, University of South Carolina, 1-125 (1984).

303. Wu, L. N., Y. Guo, B. R. Genge, Y. Ishikawa & R. E. Wuthier: Transport of inorganic phosphate in primary cultures of chondrocytes isolated from the tibial growth plate of normal adolescent chickens. *J Cell Biochem*, 86, 475-89 (2002)

304. Cameron, T. L., D. Belluoccio, P. G. Farlie, B. Brachvogel & J. F. Bateman: Global comparative transcriptome analysis of cartilage formation *in vivo*. *BMC Dev Biol*, 9, 20 (2009)

305. Phan, M. N., H. A. Leddy, B. J. Votta, S. Kumar, D. S. Levy, D. B. Lipshutz, S. H. Lee, W. Liedtke & F. Guilak: Functional characterization of TRPV4 as an osmotically sensitive ion channel in porcine articular chondrocytes. *Arthritis Rheum*, 60, 3028-37 (2009)

306. Wu, L. N., M. G. Wuthier, B. R. Genge & R. E. Wuthier: *In situ* levels of intracellular Ca^{2+} and pH in avian growth plate cartilage. *Clin Orthop Relat Res*310-24 (1997)

307. Chalothorn, D., H. Zhang, J. E. Smith, J. C. Edwards & J. E. Faber: Chloride intracellular channel-4 is a determinant of native collateral formation in skeletal muscle and brain. *Circ Res*, 105, 89-98 (2009)

308. Tung, J. J., O. Hobert, M. Berryman & J. Kitajewski: Chloride intracellular channel 4 is involved in endothelial proliferation and morphogenesis *in vitro*. *Angiogenesis*, 12, 209-20 (2009)

309. Suh, K. S., M. Mutoh, K. Nagashima, E. Fernandez-Salas, L. E. Edwards, D. D. Hayes, J. M. Crutchley, K. G. Marin, R. A. Dumont, J. M. Levy, C. Cheng, S. Garfield & S. H. Yuspa: The organellular chloride channel protein CLIC4/mtCLIC translocates to the nucleus in response to cellular stress and accelerates apoptosis. *J Biol Chem*, 279, 4632-41 (2004)

310. Kopito, R. R. & H. F. Lodish: Primary structure and transmembrane orientation of the murine anion exchange protein. *Nature*, 316, 234-8 (1985)

311. Kopito, R. R. & H. F. Lodish: Structure of the murine anion exchange protein. *J Cell Biochem*, 29, 1-17 (1985)
Chandra, D., G. Choy, P. T. Daniel & D. G. Tang: Bax-dependent regulation of Bak by voltage-dependent anion channel 2. *J Biol Chem*, 280, 19051-61 (2005)

312. Chandra, D., G. Choy, P. T. Daniel & D. G. Tang: Bax-dependent regulation of Bak by voltage-dependent anion channel 2. *J Biol Chem*, 280, 19051-61 (2005)

313. Premkumar, A. & R. Simantov: Mitochondrial voltage-dependent anion channel is involved in dopamine-induced apoptosis. *J Neurochem*, 82, 345-52 (2002)

314. Rajpurohit, R., K. Mansfield, K. Ohyama, D. Ewert & I. M. Shapiro: Chondrocyte death is linked to development of a mitochondrial membrane permeability transition in the growth plate. *J Cell Physiol*, 179, 287-96 (1999)

315. Jansen, S., M. Pantaleon & P. L. Kaye: Characterization and regulation of monocarboxylate

cotransporters Slc16a7 and Slc16a3 in preimplantation mouse embryos. *Biol Reprod*, 79, 84-92 (2008)

316. Graham, C., I. Gatherar, I. Haslam, M. Glanville & N. L. Simmons: Expression and localization of monocarboxylate transporters and sodium/proton exchangers in bovine rumen epithelium. *Am J Physiol Regul Integr Comp Physiol*, 292, R997-1007 (2007)

317. Sauer, G. R., H. D. Adkisson, B. R. Genge & R. E. Wuthier: Regulatory effect of endogenous zinc and inhibitory action of toxic metal ions on calcium accumulation by matrix vesicles *in vitro*. *Bone Miner*, 7, 233-44 (1989)

318. Blandford, N. R., G. R. Sauer, B. R. Genge, L. N. Wu & R. E. Wuthier: Modeling of matrix vesicle biomineralization using large unilamellar vesicles. *J Inorg Biochem*, 94, 14-27 (2003)

319. Messler, H. H., W. Koch & K. J. Munzenberg: Analogous effects of organic calcium antagonists and magnesium on the epiphyseal growth plate. *Clin Orthop Relat Res*135-41 (1990)

320. Duriez, J., B. Flautre, M. C. Blary & P. Hardouin: Effects of the calcium channel blocker nifedipine on epiphyseal growth plate and bone turnover: a study in rabbit. *Calcif Tissue Int*, 52, 120-4 (1993)

321. Mancilla, E. E., M. Galindo, B. Fertilio, M. Herrera, K. Salas, H. Gatica & A. Goecke: L-type calcium channels in growth plate chondrocytes participate in endochondral ossification. *J Cell Biochem*, 101, 389-98 (2007)

322. Adams, B. A., T. Tanabe & K. G. Beam: Ca^{2+} current activation rate correlates with alpha 1 subunit density. *Biophys J*, 71, 156-62 (1996)

323. Yamada, Y., K. Masuda, Q. Li, Y. Ihara, A. Kubota, T. Miura, K. Nakamura, Y. Fujii, S. Seino & Y. Seino: The structures of the human calcium channel alpha 1 subunit (CACNL1A2) and beta subunit (CACNLB3) genes. *Genomics*, 27, 312-9 (1995)

324. Fallon, J. L., M. R. Baker, L. Xiong, R. E. Loy, G. Yang, R. T. Dirksen, S. L. Hamilton & F. A. Quiocho: Crystal structure of dimeric cardiac L-type calcium channel regulatory domains bridged by Ca^{2+}* calmodulins. *Proc Natl Acad Sci U S A*, 106, 5135-40 (2009)

325. Kwok, T. C., K. Hui, W. Kostelecki, N. Ricker, G. Selman, Z. P. Feng & P. J. Roy: A genetic screen for dihydropyridine (DHP)-resistant worms reveals new residues required for DHP-blockage of mammalian calcium channels. *PLoS Genet*, 4, e1000067 (2008)

326. Dolphin, A. C.: A short history of voltage-gated calcium channels. *Br J Pharmacol*, 147 Suppl 1, S56-62 (2006)

327. Zanetti, M., R. Camerotto, D. Romeo & B. De Bernard: Active extrusion of Ca^{2+} from epiphysial chondrocytes of normal and rachitic chickens. *Biochem J*, 202, 303-7 (1982)

328. Akisaka, T. & C. V. Gay: Ultrastructural localization of calcium-activated adenosine triphosphatase (Ca^{2+}-ATPase) in growth-plate cartilage. *J Histochem Cytochem*, 33, 925-32 (1985)

329. Gunter, T. E., M. J. Zuscik, J. E. Puzas, K. K. Gunter & R. N. Rosier: Cytosolic free calcium concentrations in avian growth plate chondrocytes. *Cell Calcium*, 11, 445-57 (1990)

330. Kirsch, T., B. Swoboda & H. Nah: Activation of annexin II and V expression, terminal differentiation, mineralization and apoptosis in human osteoarthritic cartilage. *Osteoarthritis Cartilage*, 8, 294-302 (2000)

331. Wang, W., J. Xu & T. Kirsch: Annexin-mediated Ca^{2+} influx regulates growth plate chondrocyte maturation and apoptosis. *J Biol Chem*, 278, 3762-9 (2003)

332. Genge, B. R., L. N. Wu & R. E. Wuthier: Kinetic analysis of mineral formation during *in vitro* modeling of matrix vesicle mineralization: effect of annexin A5, phosphatidylserine, and type II collagen. *Anal Biochem*, 367, 159-66 (2007)

333. Virkki, L. V., J. Biber, H. Murer & I. C. Forster: Phosphate transporters: a tale of two solute carrier families. *Am J Physiol Renal Physiol*, 293, F643-54 (2007)

334. Montessuit, C., J. Caverzasio & J. P. Bonjour: Characterization of a Pi transport system in cartilage matrix vesicles. Potential role in the calcification process. *J Biol Chem*, 266, 17791-7 (1991)

335. Montessuit, C., J. P. Bonjour & J. Caverzasio: Pi transport regulation by chicken growth plate chondrocytes. *Am J Physiol*, 267, E24-31 (1994)

336. Guo, Y.: Characterization of phosphate transport, and isolation of cDNAs encoding the mitochondrial Pi transporter and pyrophosphate transporter from chicken growth plate chondrocytes. *Department of Chemistry and Biochemistry*, University of South Carolina, 1-188 (2002).

337. Kavanaugh, M. P., D. G. Miller, W. Zhang, W. Law, S. L. Kozak, D. Kabat & A. D. Miller: Cell-surface receptors for gibbon ape leukemia virus and amphotropic murine retrovirus are inducible sodium-dependent phosphate symporters. *Proc Natl Acad Sci U S A*, 91, 7071-5 (1994)

338. Giral, H., Y. Caldas, E. Sutherland, P. Wilson, S. Breusegem, N. Barry, J. Blaine, T. Jiang, X. X. Wang & M. Levi: Regulation of rat intestinal Na-dependent phosphate transporters by dietary phosphate. *Am J Physiol Renal Physiol*, 297, F1466-75 (2009)

339. Howell, D. S., J. C. Pita, J. F. Marquez & J. E. Madruga: Partition of calcium, phosphate, and protein in the fluid phase aspirated at calcifying sites in epiphyseal cartilage. *J Clin Invest*, 47, 1121-32 (1968)

340. Grootjans, J. J., P. Zimmermann, G. Reekmans, A. Smets, G. Degeest, J. Durr & G. David: Syntenin, a PDZ

protein that binds syndecan cytoplasmic domains. *Proc Natl Acad Sci U S A*, 94, 13683-8 (1997)

341. Zimmermann, P., D. Tomatis, M. Rosas, J. Grootjans, I. Leenaerts, G. Degeest, G. Reekmans, C. Coomans & G. David: Characterization of syntenin, a syndecan-binding PDZ protein, as a component of cell adhesion sites and microfilaments. *Mol Biol Cell*, 12, 339-50 (2001)

342. Stier, S., G. Totzke, E. Grunewald, T. Neuhaus, S. Fronhoffs, A. Sachinidis, H. Vetter, K. Schulze-Osthoff & Y. Ko: Identification of syntenin and other TNF-inducible genes in human umbilical arterial endothelial cells by suppression subtractive hybridization. *FEBS Lett*, 467, 299-304 (2000)

343. Yuan, K., T. M. Hong, J. J. Chen, W. H. Tsai & M. T. Lin: Syndecan-1 up-regulated by ephrinB2/EphB4 plays dual roles in inflammatory angiogenesis. *Blood*, 104, 1025-33 (2004)

344. Kirsch, T., E. Koyama, M. Liu, E. E. Golub & M. Pacifici: Syndecan-3 is a selective regulator of chondrocyte proliferation. *J Biol Chem*, 277, 42171-7 (2002)

345. Pacifici, M., T. Shimo, C. Gentili, T. Kirsch, T. A. Freeman, M. Enomoto-Iwamoto, M. Iwamoto & E. Koyama: Syndecan-3: a cell-surface heparan sulfate proteoglycan important for chondrocyte proliferation and function during limb skeletogenesis. *J Bone Miner Metab*, 23, 191-9 (2005)

346. Beekman, J. M. & P. J. Coffer: The ins and outs of syntenin, a multifunctional intracellular adaptor protein. *J Cell Sci*, 121, 1349-55 (2008)

347. Grootjans, J. J., G. Reekmans, H. Ceulemans & G. David: Syntenin-syndecan binding requires syndecan-synteny and the co-operation of both PDZ domains of syntenin. *J Biol Chem*, 275, 19933-41 (2000)

348. San Antonio, J. D., M. J. Karnovsky, S. Gay, R. D. Sanderson & A. D. Lander: Interactions of syndecan-1 and heparin with human collagens. *Glycobiology*, 4, 327-32 (1994)

349. Sulka, B., H. Lortat-Jacob, R. Terreux, F. Letourneur & P. Rousselle: Tyrosine dephosphorylation of the syndecan-1 PDZ binding domain regulates syntenin-1 recruitment. *J Biol Chem*, 284, 10659-71 (2009)

350. Hagiwara, H., A. Inoue, S. Nakajo, K. Nakaya, S. Kojima & S. Hirose: Inhibition of proliferation of chondrocytes by specific receptors in response to retinoids. *Biochem Biophys Res Commun*, 222, 220-4 (1996)

351. Pouyssegur, J., J. C. Chambard, G. L'Allemain, I. Magnaldo & K. Seuwen: Transmembrane signalling pathways initiating cell growth in fibroblasts. *Philos Trans R Soc Lond B Biol Sci*, 320, 427-36 (1988)

352. Roche, S., J. McGlade, M. Jones, G. D. Gish, T. Pawson & S. A. Courtneidge: Requirement of phospholipase C gamma, the tyrosine phosphatase Syp and the adaptor proteins Shc and Nck for PDGF-induced DNA synthesis: evidence for the existence of Ras-dependent and Ras-independent pathways. *Embo J*, 15, 4940-8 (1996)

353. Dunn, M. J.: Red blood cell calcium and magnesium: effects upon sodium and potassium transport and cellular morphology. *Biochim Biophys Acta*, 352, 97-116 (1974)

354. Prentki, M., C. Chaponnier, B. Jeanrenaud & G. Gabbiani: Actin microfilaments, cell shape, and secretory processes in isolated rat hepatocytes. Effect of phalloidin and cytochalasin D. *J Cell Biol*, 81, 592-607 (1979)

355. Burgess, D. R.: Reactivation of intestinal epithelial cell brush border motility: ATP-dependent contraction via a terminal web contractile ring. *J Cell Biol*, 95, 853-63 (1982)

356. Lu, J., G. Lian, R. Lenkinski, A. De Grand, R. R. Vaid, T. Bryce, M. Stasenko, A. Boskey, C. Walsh & V. Sheen: Filamin B mutations cause chondrocyte defects in skeletal development. *Hum Mol Genet*, 16, 1661-75 (2007)

357. Bicknell, L. S., T. Morgan, L. Bonafe, M. W. Wessels, M. G. Bialer, P. J. Willems, D. H. Cohn, D. Krakow & S. P. Robertson: Mutations in FLNB cause boomerang dysplasia. *J Med Genet*, 42, e43 (2005)

358. Williams, R. C., Jr., C. Shah & D. Sackett: Separation of tubulin isoforms by isoelectric focusing in immobilized pH gradient gels. *Anal Biochem*, 275, 265-7 (1999)

359. Nogales, E., K. H. Downing, L. A. Amos & J. Lowe: Tubulin and FtsZ form a distinct family of GTPases. *Nat Struct Biol*, 5, 451-8 (1998)

360. Heald, R. & E. Nogales: Microtubule dynamics. *J Cell Sci*, 115, 3-4 (2002)

361. Howard, J. & A. A. Hyman: Dynamics and mechanics of the microtubule plus end. *Nature*, 422, 753-8 (2003)

362. Hoeflich, K. P. & M. Ikura: Radixin: cytoskeletal adopter and signaling protein. *Int J Biochem Cell Biol*, 36, 2131-6 (2004)

363. Sun, H. Q., M. Yamamoto, M. Mejillano & H. L. Yin: Gelsolin, a multifunctional actin regulatory protein. *J Biol Chem*, 274, 33179-82 (1999)

364. Kiselar, J. G., P. A. Janmey, S. C. Almo & M. R. Chance: Visualizing the Ca^{2+}-dependent activation of gelsolin by using synchrotron footprinting. *Proc Natl Acad Sci U S A*, 100, 3942-7 (2003)

365. Hai, C. M. & Z. Gu: Caldesmon phosphorylation in actin cytoskeletal remodeling. *Eur J Cell Biol*, 85, 305-9 (2006)

366. Spinardi, L. & P. C. Marchisio: Podosomes as smart regulators of cellular adhesion. *Eur J Cell Biol*, 85, 191-4 (2006)

367. Koya, R. C., H. Fujita, S. Shimizu, M. Ohtsu, M. Takimoto, Y. Tsujimoto & N. Kuzumaki: Gelsolin inhibits

apoptosis by blocking mitochondrial membrane potential loss and cytochrome c release. *J Biol Chem*, 275, 15343-9 (2000)

368. Lin, C. S., T. Park, Z. P. Chen & J. Leavitt: Human plastin genes. Comparative gene structure, chromosome location, and differential expression in normal and neoplastic cells. *J Biol Chem*, 268, 2781-92 (1993)

369. Wuthier, R. E.: Purification of lipids from nonlipid contaminants on Sephadex bead columns. *J Lipid Res*, 7, 558-61 (1966)

370. Wuthier, R. E.: Two-dimensional chromatography on silica gel-loaded paper for the microanalysis of polar lipids. *J Lipid Res*, 7, 544-50 (1966)

371. Wuthier, R. E.: Zonal analysis of phospholipids in the epiphyseal cartilage and bone of normal and rachitic chickens and pigs. *Calcif Tissue Res*, 8, 36-53 (1971)

372. Boskey, A. L. & A. S. Posner: *In vitro* nucleation of hydroxyapatite by a bone calcium-phospholipid-phosphate complex. *Calcif Tissue Res*, 22 Suppl, 197-201 (1977)

373. Holwerda, D. L., P. D. Ellis & R. E. Wuthier: Carbon-13 and phosphorus-31 nuclear magnetic resonance studies on interaction of calcium with phosphatidylserine. *Biochemistry*, 20, 418-23 (1981)

374. Gordesky, S. E. & G. V. Marinetti: The asymetric arrangement of phospholipids in the human erythrocyte membrane. *Biochem Biophys Res Commun*, 50, 1027-31 (1973)

375. Rawyler, A., P. H. van der Schaft, B. Roelofsen & J. A. Op den Kamp: Phospholipid localization in the plasma membrane of Friend erythroleukemic cells and mouse erythrocytes. *Biochemistry*, 24, 1777-83 (1985)

376. Hullin, F., M. J. Bossant & N. Salem, Jr.: Aminophospholipid molecular species asymmetry in the human erythrocyte plasma membrane. *Biochim Biophys Acta*, 1061, 15-25 (1991)

377. Boskey, A. L., W. Ullrich, L. Spevak & H. Gilder: Persistence of complexed acidic phospholipids in rapidly mineralizing tissues is due to affinity for mineral and resistance to hydrolytic attack: *in vitro* data. *Calcif Tissue Int*, 58, 45-51 (1996)

378. Gerke, V. & K. Weber: Calcium-dependent conformational changes in the 36-kDa subunit of intestinal protein I related to the cellular 36-kDa target of Rous sarcoma virus tyrosine kinase. *J Biol Chem*, 260, 1688-95 (1985)

379. Glenney, J. R., Jr.: Phosphorylation of p36 *in vitro* with pp60src. Regulation by Ca^{2+} and phospholipid. *FEBS Lett*, 192, 79-82 (1985)

380. Hargest, T. E., C. V. Gay, H. Schraer & A. J. Wasserman: Vertical distribution of elements in cells and matrix of epiphyseal growth plate cartilage determined by quantitative electron probe analysis. *J Histochem Cytochem*, 33, 275-86 (1985)

381. Long, K. J. & K. B. Walsh: A calcium-activated potassium channel in growth plate chondrocytes: regulation by protein kinase A. *Biochem Biophys Res Commun*, 201, 776-81 (1994)

382. Brighton, C. T. & R. M. Hunt: Mitochondrial calcium and its role in calcification. Histochemical localization of calcium in electron micrographs of the epiphyseal growth plate with K-pyroantimonate. *Clin Orthop Relat Res*, 100, 406-16 (1974)

383. Brighton, C. T. & R. M. Hunt: Histochemical localization of calcium in growth plate mitochondria and matrix vesicles. *Fed Proc*, 35, 143-7 (1976)

384. Brighton, C. T. & R. M. Hunt: The role of mitochondria in growth plate calcification as demonstrated in a rachitic model. *J Bone Joint Surg Am*, 60, 630-9 (1978)

385. Sauer, G. R., L. N. Wu, M. Iijima & R. E. Wuthier: The influence of trace elements on calcium phosphate formation by matrix vesicles. *J Inorg Biochem*, 65, 57-65 (1997)

386. Eanes, E. D.: Thermochemical studies on amorphous calcium phosphate. *Calcif Tissue Res*, 5, 133-45 (1970)

387. Sauer, G. R. & R. E. Wuthier: Fourier transform infrared characterization of mineral phases formed during induction of mineralization by collagenase-released matrix vesicles *in vitro*. *J Biol Chem*, 263, 13718-24 (1988)

388. Sauer, G. R., W. B. Zunic, J. R. Durig & R. E. Wuthier: Fourier transform Raman spectroscopy of synthetic and biological calcium phosphates. *Calcif Tissue Int*, 54, 414-20 (1994)

389. Adkisson, H. D. t., F. S. Risener, Jr., P. P. Zarrinkar, M. D. Walla, W. W. Christie & R. E. Wuthier: Unique fatty acid composition of normal cartilage: discovery of high levels of n-9 eicosatrienoic acid and low levels of n-6 polyunsaturated fatty acids. *Faseb J*, 5, 344-53 (1991)

390. Brighton, C. T. & R. B. Heppenstall: Oxygen tension in zones of the epiphyseal plate, the metaphysis and diaphysis. An *in vitro* and *in vivo* study in rats and rabbits. *J Bone Joint Surg Am*, 53, 719-28 (1971)

391. Haselgrove, J. C., I. M. Shapiro & S. F. Silverton: Computer modeling of the oxygen supply and demand of cells of the avian growth cartilage. *Am J Physiol*, 265, C497-506 (1993)

392. Meyer, W. L. & A. S. Kunin: The inductive effect of rickets on glycolytic enzymes of rat epiphyseal cartilage

and its reversal by vitamin D and phosphate. *Arch Biochem Biophys*, 129, 438-46 (1969)

393. Sampson, H. W. & M. S. Cannon: Zonal analysis of metabolic profiles of articular-epiphyseal cartilage chondrocytes: a histochemical study. *Histochem J*, 18, 233-8 (1986)

394. Kim, J. K., J. C. Haselgrove & I. M. Shapiro: Measurement of metabolic events in the avian epiphyseal growth cartilage using a bioluminescence technique. *J Histochem Cytochem*, 41, 693-702 (1993)

395. Shapiro, I. M., E. E. Golub, B. Chance, C. Piddington, O. Oshima, O. C. Tuncay, P. Frasca & J. C. Haselgrove: Linkage between energy status of perivascular cells and mineralization of the chick growth cartilage. *Dev Biol*, 129, 372-9 (1988)

396. Teixeira, C. C., K. Mansfield, C. Hertkorn, H. Ischiropoulos & I. M. Shapiro: Phosphate-induced chondrocyte apoptosis is linked to nitric oxide generation. *Am J Physiol Cell Physiol*, 281, C833-9 (2001)

397. Teixeira, C. C., H. Ischiropoulos, P. S. Leboy, S. L. Adams & I. M. Shapiro: Nitric oxide-nitric oxide synthase regulates key maturational events during chondrocyte terminal differentiation. *Bone*, 37, 37-45 (2005)

398. Wuthier, R. E., R. J. Majeska & G. M. Collins: Biosynthesis of matrix vesicles in epiphyseal cartilage. I. *In vivo* incorporation of ^{32}P orthophosphate into phospholipids of chondroxyte, membrane, and matrix vesicle fractions. *Calcif Tissue Res*, 23, 135-9 (1977)

399. Wu, L. N., Y. Ishikawa, G. R. Sauer, B. R. Genge, F. Mwale, H. Mishima & R. E. Wuthier: Morphological and biochemical characterization of mineralizing primary cultures of avian growth plate chondrocytes: evidence for cellular processing of Ca^{2+} and Pi prior to matrix mineralization. *J Cell Biochem*, 57, 218-37 (1995)

400. Shapiro, I. M., P. S. Leboy, T. Tokuoka, E. Forbes, K. DeBolt, S. L. Adams & M. Pacifici: Ascorbic acid regulates multiple metabolic activities of cartilage cells. *Am J Clin Nutr*, 54, 1209S-1213S (1991)

401. Boskey, A. L., D. Stiner, S. B. Doty & I. Binderman: Requirement of vitamin C for cartilage calcification in a differentiating chick limb-bud mesenchymal cell culture. *Bone*, 12, 277-82 (1991)

402. von der Mark, K., J. Mollenhauer, P. K. Muller & M. Pfaffle: Anchorin CII, a type II collagen-binding glycoprotein from chondrocyte membranes. *Ann N Y Acad Sci*, 460, 214-23 (1985)

403. Mollenhauer, J., J. A. Bee, M. A. Lizarbe & K. von der Mark: Role of anchorin CII, a 31,000-mol-wt membrane protein, in the interaction of chondrocytes with type II collagen. *J Cell Biol*, 98, 1572-9 (1984)

404. Wuthier, R. E.: Involvement of cellular metabolism of calcium and phosphate in calcification of avian growth plate cartilage. *J Nutr*, 123, 301-9 (1993)

405. von der Mark, K. & J. Mollenhauer: Annexin V interactions with collagen. *Cell Mol Life Sci*, 53, 539-45 (1997)

406. Lehninger, A. L., C. S. Rossi & J. W. Greenawalt: Respiration-dependent accumulation of inorganic phosphate and Ca ions by rat liver mitochondria. *Biochem Biophys Res Commun*, 10, 444-8 (1963)

407. Carafoli, E., C. S. Rossi & A. L. Lehninger: Cation and anion balance during active accumulation of Ca^{++} and Mg^{++} by isolated mitochondria. *J Biol Chem*, 239, 3055-61 (1964)

408. Shapiro, I. M. & N. H. Lee: Effects of Ca^{2+} on the respiratory activity of chondrocyte mitochondria. *Arch Biochem Biophys*, 170, 627-33 (1975)

409. Shapiro, I. M. & N. H. Lee: Calcium accumulation by chondrocyte mitochondria. *Clin Orthop Relat Res*323-9 (1975)

410. Simmons, D. J., C. Arsenis, S. W. Whitson, S. E. Kahn, A. L. Boskey & N. Gollub: Mineralization of rat epiphyseal cartilage: a circadian rhythm. *Miner Electrolyte Metab*, 9, 28-37 (1983)

411. Matthews, J. L.: Role of Mitochondria in Calcification. In: *Cell Mediated Calcification and Matrix Vesicles*, Ed: S. Y. Ali, Elsevier Science Publishers B. V., Amsterdam, The Netherlands.115-118 (1986).

412. Lee, N. H. & I. M. Shapiro: A method for isolating respiring mitochondria from epiphyseal cartilage. *Anal Biochem*, 58, 117-22 (1974)

413. Lee, N. H. & I. M. Shapiro: Oxidative phosphorylation by chondrocyte mitochondria. *Calcif Tissue Res*, 16, 277-82 (1974)

414. Shapiro, L. M., A. Burke & N. H. Lee: Heterogeneity of chondrocyte mitochondria. A study of the Ca^{2+} concentration and density banding characteristics of normal and rachitic cartilage. *Biochim Biophys Acta*, 451, 583-91 (1976)

415. Lehninger, A. L.: Role of phosphate and other proton-donating anions in respiration-coupled transport of Ca^{2+} by mitochondria. *Proc Natl Acad Sci U S A*, 71, 1520-4 (1974)

416. Gunter, T. E. & D. R. Pfeiffer: Mechanisms by which mitochondria transport calcium. *Am J Physiol*, 258, C755-86 (1990)

417. Pfeiffer, D. R., T. E. Gunter, R. Eliseev, K. M. Broekemeier & K. K. Gunter: Release of Ca^{2+} from mitochondria via the saturable mechanisms and the permeability transition. *IUBMB Life*, 52, 205-12 (2001)

418. Lee, N. H. & I. M. Shapiro: Ca^{2+} transport by chondrocyte mitochondria of the epiphyseal growth plate. *J Membr Biol*, 41, 349-60 (1978)

419. Beatrice, M. C., J. W. Palmer & D. R. Pfeiffer: The relationship between mitochondrial membrane permeability, membrane potential, and the retention of Ca^{2+} by mitochondria. *J Biol Chem*, 255, 8663-71 (1980)

420. Beatrice, M. C., D. L. Stiers & D. R. Pfeiffer: Increased permeability of mitochondria during Ca^{2+} release induced by t-butyl hydroperoxide or oxalacetate.The effect of ruthenium red. *J Biol Chem*, 257, 7161-71 (1982)

421. Bernardi, P., L. Scorrano, R. Colonna, V. Petronilli & F. Di Lisa: Mitochondria and cell death. Mechanistic aspects and methodological issues. *Eur J Biochem*, 264, 687-701 (1999)

422. Hirsch, T., I. Marzo & G. Kroemer: Role of the mitochondrial permeability transition pore in apoptosis. *Biosci Rep*, 17, 67-76 (1997)

423. Lemasters, J. J., A. L. Nieminen, T. Qian, L. C. Trost, S. P. Elmore, Y. Nishimura, R. A. Crowe, W. E. Cascio, C. A. Bradham, D. A. Brenner & B. Herman: The mitochondrial permeability transition in cell death: A common mechanism in necrosis, apoptosis and autophagy. *Biochim Biophys Acta*, 1366, 177-96 (1998)

424. Zamzami, N., T. Hirsch, B. Dallaporta, P. X. Petit & G. Kroemer: Mitochondrial implication in accidental and programmed cell death: apoptosis and necrosis. *J Bioenerg Biomembr*, 29, 185-93 (1997)

425. Mansfield, K., R. Rajpurohit & I. M. Shapiro: Extracellular phosphate ions cause apoptosis of terminally differentiated epiphyseal chondrocytes. *J Cell Physiol*, 179, 276-86 (1999)

426. Mansfield, K., C. C. Teixeira, C. S. Adams & I. M. Shapiro: Phosphate ions mediate chondrocyte apoptosis through a plasma membrane transporter mechanism. *Bone*, 28, 1-8 (2001)

427. Bowser, D. N., S. Petrou, R. G. Panchal, M. L. Smart & D. A. Williams: Release of mitochondrial Ca^{2+} via the permeability transition activates endoplasmic reticulum Ca^{2+} uptake. *Faseb J*, 16, 1105-7 (2002)

428. Ferreira, G. C., R. D. Pratt & P. L. Pedersen: Energy-linked anion transport. Cloning, sequencing, and characterization of a full length cDNA encoding the rat liver mitochondrial proton/phosphate symporter. *J Biol Chem*, 264, 15628-33 (1989)

429. Pratt, R. D., G. C. Ferreira & P. L. Pedersen: Mitochondrial phosphate transport. Import of the H^+/Pi symporter and role of the presequence. *J Biol Chem*, 266, 1276-80 (1991)

430. Ferreira, G. C. & P. L. Pedersen: Phosphate transport in mitochondria: past accomplishments, present problems, and future challenges. *J Bioenerg Biomembr*, 25, 483-92 (1993)

431. Caverzasio, J., C. Montessuit & J. P. Bonjour: Stimulatory effect of insulin-like growth factor-1 on renal Pi transport and plasma 1,25-dihydroxyvitamin D3. *Endocrinology*, 127, 453-9 (1990)

432. Halestrap, A. P., C. P. Connern, E. J. Griffiths & P. M. Kerr: Cyclosporin A binding to mitochondrial cyclophilin inhibits the permeability transition pore and protects hearts from ischaemia/reperfusion injury. *Mol Cell Biochem*, 174, 167-72 (1997)

433. Halestrap, A. P., P. M. Kerr, S. Javadov & K. Y. Woodfield: Elucidating the molecular mechanism of the permeability transition pore and its role in reperfusion injury of the heart. *Biochim Biophys Acta*, 1366, 79-94 (1998)

434. Halestrap, A. P., K. Y. Woodfield & C. P. Connern: Oxidative stress, thiol reagents, and membrane potential modulate the mitochondrial permeability transition by affecting nucleotide binding to the adenine nucleotide translocase. *J Biol Chem*, 272, 3346-54 (1997)

435. Leung, A. W., P. Varanyuwatana & A. P. Halestrap: The mitochondrial phosphate carrier interacts with cyclophilin D and may play a key role in the permeability transition. *J Biol Chem*, 283, 26312-23 (2008)

436. Halestrap, A. P.: What is the mitochondrial permeability transition pore? *J Mol Cell Cardiol*, 46, 821-31 (2009)

437. Matsumoto, H., K. DeBolt & I. M. Shapiro: Adenine, guanine, and inosine nucleotides of chick growth cartilage: relationship between energy status and the mineralization process. *J Bone Miner Res*, 3, 347-52 (1988)

438. Pollesello, P., B. de Bernard, M. Grandolfo, S. Paoletti, F. Vittur & B. J. Kvam: Energy state of chondrocytes assessed by ^{31}P-NMR studies of preosseous cartilage. *Biochem Biophys Res Commun*, 180, 216-22 (1991)

439. Hatori, M., C. C. Teixeira, K. Debolt, M. Pacifici & I. M. Shapiro: Adenine nucleotide metabolism by chondrocytes *in vitro*: Role of ATP in chondrocyte maturation and matrix mineralization. *J Cell Physiol*, 165, 468-74 (1995)

440. Wu, L. N., B. R. Genge, Y. Ishikawa & R. E. Wuthier: Modulation of cultured chicken growth plate chondrocytes by transforming growth factor-beta 1 and basic fibroblast growth factor. *J Cell Biochem*, 49, 181-98 (1992)

441. Shapiro, I. M. & A. Boyde: Mineralization of normal and rachitic chick growth cartilage: vascular canals, cartilage calcification and osteogenesis. *Scanning Microsc*, 1, 599-606 (1987)

442. Shapiro, I. M., E. E. Golub, M. May & J. L. Rabinowitz: Studies of nucleotides of growth-plate cartilage: evidence linking changes in cellular metabolism with cartilage calcification. *Biosci Rep*, 3, 345-51 (1983)

443. Wu, L. N., B. R. Genge, G. R. Sauer & R. E. Wuthier: Characterization and reconstitution of the nucleational complex responsible for mineral formation by growth plate cartilage matrix vesicles. *Connect Tissue Res*, 35, 309-15 (1996)

444. Termine, J. D., R. A. Peckauskas & A. S. Posner: Calcium phosphate formation *in vitro*. II. Effects of environment on amorphous-crystalline transformation. *Arch Biochem Biophys*, 140, 318-25 (1970)

445. Wu, L. N., Y. Ishikawa, B. R. Genge, T. K. Sampath & R. E. Wuthier: Effect of osteogenic protein-1 on the development and mineralization of primary cultures of avian growth plate chondrocytes: Modulation by retinoic acid. *J Cell Biochem*, 67, 498-513 (1997)

446. Wu, L. N., Y. Ishikawa, D. Nie, B. R. Genge & R. E. Wuthier: Retinoic acid stimulates matrix calcification and initiates type I collagen synthesis in primary cultures of avian weight-bearing growth plate chondrocytes. *J Cell Biochem*, 65, 209-30 (1997)

447. Shapiro, I. M., C. S. Adams, T. Freeman & V. Srinivas: Fate of the hypertrophic chondrocyte: microenvironmental perspectives on apoptosis and survival in the epiphyseal growth plate. *Birth Defects Res C Embryo Today*, 75, 330-9 (2005)

448. Hsu, H. H. & H. C. Anderson: Evidence of the presence of a specific ATPase responsible for ATP-initiated calcification by matrix vesicles isolated from cartilage and bone. *J Biol Chem*, 271, 26383-8 (1996)

449. Register, T. C., G. P. Warner & R. E. Wuthier: Effect of L- and D-tetramisole on ^{32}Pi and ^{45}Ca uptake and mineralization by matrix vesicle-enriched fractions from chicken epiphyseal cartilage. *J Biol Chem*, 259, 922-8 (1984)

450. Hsu, H. H. & H. C. Anderson: Effects of zinc and divalent cation chelators on ATP hydrolysis and Ca deposition by rachitic rat matrix vesicles. *Bone*, 17, 473-7 (1995)

451. Ali, S. Y., A. Wisby, L. Evans & J. Craig-Gray: The sequence of calcium and phosphorus accumulation by matrix vesicles. *Calcif Tissue Res*, 22 Suppl, 490-3 (1977)

452. Anderson, H. C.: Mineralization by matrix vesicles. *Scan Electron Microsc*953-64 (1984)

453. Balcerzak, M., E. Hamade, L. Zhang, S. Pikula, G. Azzar, J. Radisson, J. Bandorowicz-Pikula & R. Buchet: The roles of annexins and alkaline phosphatase in mineralization process. *Acta Biochim Pol*, 50, 1019-38 (2003)

454. Hsu, H. H. & H. C. Anderson: The deposition of calcium pyrophosphate and phosphate by matrix vesicles isolated from fetal bovine epiphyseal cartilage. *Calcif Tissue Int*, 36, 615-21 (1984)

455. Wuthier, R. E.: Mechanism of matrix vesicle-mediated mineralization in cartilage. *ISI Atlas of Science: Biochemistry*, 1, 231-241 (1988)

456. Register, T. C. & R. E. Wuthier: Effect of vanadate, a potent alkaline phosphatase inhibitor, on ^{45}Ca and ^{32}Pi uptake by matrix vesicle-enriched fractions from chicken epiphyseal cartilage. *J Biol Chem*, 259, 3511-8 (1984)

457. Wu, L. N., B. R. Genge, D. G. Dunkelberger, R. Z. LeGeros, B. Concannon & R. E. Wuthier: Physicochemical characterization of the nucleational core of matrix vesicles. *J Biol Chem*, 272, 4404-11 (1997)

458. Betts, F., N. C. Blumenthal, A. S. Posner, G. L. Becker & A. L. Lehninger: Atomic structure of intracellular amorphous calcium phosphate deposits. *Proc Natl Acad Sci U S A*, 72, 2088-90 (1975)

459. Aue, W. P., A. H. Roufosse, M. J. Glimcher & R. G. Griffin: Solid-state phosphorus-31 nuclear magnetic resonance studies of synthetic solid phases of calcium phosphate: potential models of bone mineral. *Biochemistry*, 23, 6110-4 (1984)

460. Roufosse, A. H., W. P. Aue, J. E. Roberts, M. J. Glimcher & R. G. Griffin: Investigation of the mineral phases of bone by solid-state phosphorus-31 magic angle sample spinning nuclear magnetic resonance. *Biochemistry*, 23, 6115-20 (1984)

461. Brecevic, L. & H. Furedi-Milhofer: Precipitation of calcium phosphates from electrolyte solutions. II. The formation and transformation of the precipitates. *Calcif Tissue Res*, 10, 82-90 (1972)

462. Boskey, A. L. & A. S. Posner: Optimal conditions for Ca-acidic phospholipid-PO4 formation. *Calcif Tissue Int*, 34 Suppl 2, S1-7 (1982)

463. Boskey, A. L., Posner, A.S.: Magnesium stabilization of amorphous calcium phosphate: A kinetic study. *Materials Research Bulletin*, 9, 907-916 (1974)

464. Posner, A. S., F. Betts & N. C. Blumenthal: Role of ATP and Mg in the stabilization of biological and synthetic amorphous calcium phosphates. *Calcif Tissue Res*, 22 Suppl, 208-12 (1977)

465. Termine, J. D., R. E. Wuthier & A. S. Posner: Amorphous-crystalline mineral changes during endochondral and periosteal bone formation. *Proc Soc Exp Biol Med*, 125, 4-9 (1967)

466. Lyster, R. L., S. Mann, S. B. Parker & R. J. Williams: Nature of micellar calcium phosphate in cows' milk as studied by high-resolution electron microscopy. *Biochim Biophys Acta*, 801, 315-7 (1984)

467. McGann, T. C., R. D. Kearney, W. Buchheim, A. S. Posner, F. Betts & N. C. Blumenthal: Amorphous calcium phosphate in casein micelles of bovine milk. *Calcif Tissue Int*, 35, 821-3 (1983)

468. Taylor, M. G., K. Simkiss, J. Simmons, L. N. Wu & R. E. Wuthier: Structural studies of a phosphatidylserine-amorphous calcium phosphate complex. *Cell Mol Life Sci*, 54, 196-202 (1998)

469. Andersson, M., A. Malmendal, S. Linse, I. Ivarsson, S. Forsen & L. A. Svensson: Structural basis for the negative allostery between Ca (2+)- and Mg (2+)-binding in the intracellular Ca (2+)-receptor calbindin D9k. *Protein Sci*, 6, 1139-47 (1997)

470. Babu, A., H. Su, Y. Ryu & J. Gulati: Determination of residue specificity in the EF-hand of troponin C for Ca^{2+} coordination, by genetic engineering. *J Biol Chem*, 267, 15469-74 (1992)

471. Fahie, K., R. Pitts, K. Elkins & D. J. Nelson: Molecular dynamics study of Ca (2+) binding loop variants of silver hake parvalbumin with aspartic acid at the "gateway" position. *J Biomol Struct Dyn*, 19, 821-37 (2002)

472. Buchbinder, J. L., J. Baraniak, P. A. Frey & G. H. Reed: Stereochemistry of metal ion coordination to the terminal thiophosphoryl group of adenosine 5'-O- (3-thiotriphosphate) at the active site of pyruvate kinase. *Biochemistry*, 32, 14111-6 (1993)

473. Soultanas, P., M. S. Dillingham, S. S. Velankar & D. B. Wigley: DNA binding mediates conformational changes and metal ion coordination in the active site of PcrA helicase. *J Mol Biol*, 290, 137-48 (1999)

474. Iijima, M., Y. Moriwaki & Y. Kuboki: Effect of some physico-chemical properties of matrix on lengthwise and oriented growth of octacalcium phosphate crystal. *Connect Tissue Res*, 38, 171-9; discussion 201-5 (1998)

475. Nelson, D. G. & J. D. McLean: High-resolution electron microscopy of octacalcium phosphate and its hydrolysis products. *Calcif Tissue Int*, 36, 219-32 (1984)

476. Suzuki, O., H. Yagishita, T. Amano & T. Aoba: Reversible structural changes of octacalcium phosphate and labile acid phosphate. *J Dent Res*, 74, 1764-9 (1995)

477. Wu, Y., M. J. Glimcher, C. Rey & J. L. Ackerman: A unique protonated phosphate group in bone mineral not present in synthetic calcium phosphates. Identification by phosphorus-31 solid state NMR spectroscopy. *J Mol Biol*, 244, 423-35 (1994)

478. Kirsch, T., H. D. Nah, D. R. Demuth, G. Harrison, E. E. Golub, S. L. Adams & M. Pacifici: Annexin V-mediated calcium flux across membranes is dependent on the lipid composition: implications for cartilage mineralization. *Biochemistry*, 36, 3359-67 (1997)

479. Simao, A. M., M. C. Yadav, P. Ciancaglini & J. L. Millan: Proteoliposomes as matrix vesicle biomimetics to study the initiation of skeletal mineralization. *Braz J Med Biol Res*, 43, 234-41

480. Matsumoto, H., Golub, E.E., Shapiro. I.M.: Superoxide required for matrix vesicle formation. In: *Cell Mediated Calcification and Matrix Vesicles*, Ed: S. Y. Ali, Elsevier Science Publishers D.V., Amsterdam, The Netherlands, 241-245 (1985).

481. McConnell, D.: The problem of the carbonate apatites. *Science*, 119, 913-914 (1954)

482. McConnell, D. & A. S. Posner: Carbonate in apatites. *Science*, 134, 213-215 (1961)

483. Bachra, B. N., O. R. Trautz, D. McConnell, W. J. Frajola & D. W. Deamer: Carbonic anhydrase and the precipitation of apatite. *Science*, 137, 337-8 (1962)

484. McConnell, D., J. D. Termine & A. S. Posner: Infrared Absorption of Carbonate Apatite. *Science*, 155, 607-608 (1967)

485. Ortlund, E., Chai, G., Genge, B., Wuthier, R..E., Lebioda, L.: Crystal structure of chicken annexin A5 in complex with functional modifiers Ca^{2+} and Zn^{2+} reveal Zn^{2+}-induced formation of non-planar assemblies. *Annexins*, 1, 183-190 (2004)

486. Burton, F. G., M. W. Neuman & W. F. Neuman: On the possible role of crystals in the origins of life. I. The adsorption of nucleosides, nucleotides and pyrophosphate by apatite crystals. *Curr Mod Biol*, 3, 20-6 (1969)

487. Neuman, M. W., W. F. Neuman & K. Lane: On the possible role of crystals in the origins of life. 3. The phosphorylation of adenosine to AMP by apatite. *Curr Mod Biol*, 3, 253-9 (1970)

488. Jung, A., S. Bisaz & H. Fleisch: The binding of pyrophosphate and two diphosphonates by hydroxyapatite crystals. *Calcif Tissue Res*, 11, 269-80 (1973)

489. Bisaz, S., R. Felix, N. M. Hansen & H. Fleisch: Disaggregation of hydroxyapatite crystals. *Biochim Biophys Acta*, 451, 560-6 (1976)

490. McGaughey, C. & E. C. Stowell: Effects of polyphosphates on the solubility and mineralization of HA: Relevance to a rationale for anticaries activity. *J Dent Res*, 56, 579-87 (1977)

491. Fleisch, H. & S. Bisaz: Isolation from urine of pyrophosphate, a calcification inhibitor. *Am J Physiol*, 203, 671-5 (1962)

492. Fleisch, H., D. Schibler, J. Maerki & I. Frossard: Inhibition of aortic calcification by means of pyrophosphate and polyphosphates. *Nature*, 207, 1300-1 (1965)

493. Fleisch, H., J. Maerki & R. G. Russell: Effect of pyrophosphate on dissolution of hydroxyapatite and its possible importance in calcium homeostasis. *Proc Soc Exp Biol Med*, 122, 317-20 (1966)

494. Fleisch, H., R. G. Russell & F. Straumann: Effect of pyrophosphate on hydroxyapatite and its implications in calcium homeostasis. *Nature*, 212, 901-3 (1966)

495. Fleisch, H., R. G. Russell, S. Bisaz, P. A. Casey & R. C. Muhlbauer: The influence of pyrophosphate analogues (diphosphonates) on the precipitation and dissolution. *Calcif Tissue Res* Suppl:10-10a (1968)

496. Francis, M. D., R. G. Russell & H. Fleisch: Diphosphonates inhibit formation of calcium phosphate crystals *in vitro* and pathological calcification *in vivo*. *Science*, 165, 1264-6 (1969)

497. Wuthier, R. E., S. Bisaz, R. G. Russell & H. Fleisch: Relationship between pyrophosphate, amorphous calcium phosphate and other factors in the sequence of calcification *in vivo*. *Calcif Tissue Res*, 10, 198-206 (1972)

498. Eaton, R. H. & D. W. Moss: Inhibition of the orthophosphatase and pyrophosphatase activities of human alkaline-phosphatase preparations. *Biochem J*, 102, 917-921 (1967)

499. Russell, R. G.: Excretion of inorganic pyrophosphate in hypophosphatasia. *Lancet*, 2, 461-4 (1965)

500. Russell, R. G., S. Bisaz, A. Donath, D. B. Morgan & H. Fleisch: Inorganic pyrophosphate in plasma in normal persons and in patients with hypophosphatasia, osteogenesis imperfecta, and other disorders of bone. *J Clin Invest*, 50, 961-9 (1971)

501. Register, T. C. & R. E. Wuthier: Effect of pyrophosphate and two diphosphonates on ^{45}Ca and ^{32}Pi uptake and mineralization by matrix vesicle-enriched fractions and by hydroxyapatite. *Bone*, 6, 307-12 (1985)

502. Derfus, B. A., J. W. Rachow, N. S. Mandel, A. L. Boskey, M. Buday, V. M. Kushnaryov & L. M. Ryan: Articular cartilage vesicles generate calcium pyrophosphate dihydrate-like crystals *in vitro*. *Arthritis Rheum*, 35, 231-40 (1992)

503. Derfus, B., S. Kranendonk, N. Camacho, N. Mandel, V. Kushnaryov, K. Lynch & L. Ryan: Human osteoarthritic cartilage matrix vesicles generate both calcium pyrophosphate dihydrate and apatite *in vitro*. *Calcif Tissue Int*, 63, 258-62 (1998)

504. Ho, A. M., M. D. Johnson & D. M. Kingsley: Role of the mouse *ank* gene in control of tissue calcification and arthritis. *Science*, 289, 265-70 (2000)

505. Nurnberg, P., H. Thiele, D. Chandler, W. Hohne, M. L. Cunningham, H. Ritter, G. Leschik, K. Uhlmann, C. Mischung, K. Harrop, J. Goldblatt, Z. U. Borochowitz, D. Kotzot, F. Westermann, S. Mundlos, H. S. Braun, N. Laing & S. Tinschert: Heterozygous mutations in ANKH, the human ortholog of the mouse progressive ankylosis gene, result in craniometaphyseal dysplasia. *Nat Genet*, 28, 37-41 (2001)

506. Pendleton, A., M. D. Johnson, A. Hughes, K. A. Gurley, A. M. Ho, M. Doherty, J. Dixey, P. Gillet, D. Loeuille, R. McGrath, A. Reginato, R. Shiang, G. Wright, P. Netter, C. Williams & D. M. Kingsley: Mutations in ANKH cause chondrocalcinosis. *Am J Hum Genet*, 71, 933-40 (2002)

507. Williams, C. J.: Familial calcium pyrophosphate dihydrate deposition disease and the ANKH gene. *Curr Opin Rheumatol*, 15, 326-31 (2003)

508. Zaka, R. & C. J. Williams: Role of the progressive ankylosis gene in cartilage mineralization. *Curr Opin Rheumatol*, 18, 181-6 (2006)

509. Gurley, K. A., H. Chen, C. Guenther, E. T. Nguyen, R. B. Rountree, M. Schoor & D. M. Kingsley: Mineral formation in joints caused by complete or joint-specific loss of ANK function. *J Bone Miner Res*, 21, 1238-47 (2006)

510. Howell, D. S., J. C. Pita, J. F. Marquez & R. A. Gatter: Demonstration of macromolecular inhibitors of calcification and nucleational factors in fluid from calcifying sites in cartilage. *J Clin Invest*, 48, 630-41 (1969)

511. Pita, J. C., L. A. Cuervo, J. E. Madruga, F. J. Muller & D. S. Howell: Evidence for a role of proteinpolysaccharides in regulation of mineral phase separation in calcifying cartilage. *J Clin Invest*, 49, 2188-97 (1970)

512. Howell, D. S. & J. C. Pita: Role of proteoglycans in calcification of cartilage. *Ups J Med Sci*, 82, 97-8 (1977)

513. Di Salvo, J. & M. Schubert: Specific interaction of some cartilage proteinpolysaccharides with freshly precipitating calcium phosphate. *J Biol Chem*, 242, 705-10 (1967)

514. Wuthier, R. E.: A zonal analysis of inorganic and organic constituents of the epiphysis during endochondral calcification. *Calcif Tissue Res*, 4, 20-38 (1969)

515. Wuthier, R. E.: Zonal analysis of electrolytes in epiphyseal cartilage and bone of normal and rachitic chickens and pigs. *Calcif Tissue Res*, 8, 24-35 (1971)

516. Ehrlich, M. G., A. L. Armstrong & H. J. Mankin: Partial purification and characterization of a proteoglycan-degrading neutral protease from bovine epiphyseal cartilage. *J Orthop Res*, 2, 126-33 (1984)

517. Dean, D. D., Z. Schwartz, O. E. Muniz, R. Gomez, L. D. Swain, D. S. Howell & B. D. Boyan: Matrix vesicles are enriched in metalloproteinases that degrade proteoglycans. *Calcif Tissue Int*, 50, 342-9 (1992)

518. Dean, D. D., Z. V. Schwartz, O. E. Muniz, R. Gomez, L. D. Swain, D. S. Howell & B. D. Boyan: Matrix vesicles contain metalloproteinases that degrade proteoglycans. *Bone Miner*, 17, 172-6 (1992)

519. Boskey, A. L., D. Stiner, I. Binderman & S. B. Doty: Effects of proteoglycan modification on mineral formation

in a differentiating chick limb-bud mesenchymal cell culture system. *J Cell Biochem*, 64, 632-43 (1997)

520. D'Angelo, M., Z. Yan, M. Nooreyazdan, M. Pacifici, D. S. Sarment, P. C. Billings & P. S. Leboy: MMP-13 is induced during chondrocyte hypertrophy. *J Cell Biochem*, 77, 678-93 (2000)

521. Howell, D. S., J. C. Pita, J. F. Marquez, J. E. Madruga & F. J. Muller: Evidence for altered proteinpolysaccharide complexes (PPC) in fresh osteoarthritic cartilage in human hips. *Calcif Tissue Res* Suppl:127 (1970)

522. Glimcher, M. J.: A basic architectural principle in the organization of mineralized tissues. *Clin Orthop Relat Res*, 61, 16-36 (1968)

523. Landis, W. J., K. J. Hodgens, J. Arena, M. J. Song & B. F. McEwen: Structural relations between collagen and mineral in bone as determined by high voltage electron microscopic tomography. *Microsc Res Tech*, 33, 192-202 (1996)

524. Glimcher, M. J., Hodge, A.J., Schmitt, F.O.: Molecular aggregation states in relation to mineralization: The collagen-hydroxyapatite system studied *in vitro*. *Proc Natl Acad Sci U S A*, 43, 860-867 (1957)

525. Poole, A. R., Y. Matsui, A. Hinek & E. R. Lee: Cartilage macromolecules and the calcification of cartilage matrix. *Anat Rec*, 224, 167-79 (1989)

526. Hinek, A., A. Reiner & A. R. Poole: The calcification of cartilage matrix in chondrocyte culture: studies of the C-propeptide of type II collagen (chondrocalcin). *J Cell Biol*, 104, 1435-41 (1987)

527. Kujawa, M. J., M. Weitzhandler, A. R. Poole, L. Rosenberg & A. I. Caplan: Association of the C-propeptide of type II collagen with mineralization of embryonic chick long bone and sternal development. *Connect Tissue Res*, 23, 179-99 (1989)

528. Van der Rest, M., L. C. Rosenberg, B. R. Olsen & A. R. Poole: Chondrocalcin is identical with the C-propeptide of type II procollagen. *Biochem J*, 237, 923-5 (1986)

529. Landis, W. J., K. J. Hodgens, M. D. McKee, A. Nanci, M. J. Song, S. Kiyonaga, J. Arena & B. McEwen: Extracellular vesicles of calcifying turkey leg tendon characterized by immunocytochemistry and high voltage electron microscopic tomography and 3-D graphic image reconstruction. *Bone Miner*, 17, 237-41 (1992)

530. Hunter, G. K., P. V. Hauschka, A. R. Poole, L. C. Rosenberg & H. A. Goldberg: Nucleation and inhibition of hydroxyapatite formation by mineralized tissue proteins. *Biochem J*, 317 (Pt 1), 59-64 (1996)

531. Termine, J. D., H. K. Kleinman, S. W. Whitson, K. M. Conn, M. L. McGarvey & G. R. Martin: Osteonectin, a bone-specific protein linking mineral to collagen. *Cell*, 26, 99-105 (1981)

532. Termine, J. D.: Non-collagen proteins in bone. *Ciba Found Symp*, 136, 178-202 (1988)

533. Herring, G. M.: Comparison of Bovine Bone Sialoprotein and Serum Orosomucoid. *Nature*, 201, 709 (1964)

534. Williams, P. A. & A. R. Peacocke: The physical properties of a glycoprotein from bovine cortical bone (bone sialoprotein). *Biochim Biophys Acta*, 101, 327-35 (1965)

535. Poole, A. R., I. Pidoux, A. Reiner, H. Choi & L. C. Rosenberg: Association of an extracellular protein (chondrocalcin) with the calcification of cartilage in endochondral bone formation. *J Cell Biol*, 98, 54-65 (1984)

536. Poole, A. R., I. Pidoux, A. Reiner, H. Choi & L. C. Rosenberg: The association of a newly discovered protein, called chondrocalcin, with cartilage calcification. *Acta Biol Hung*, 35, 143-9 (1984)

537. Price, P. A., A. A. Otsuka, J. W. Poser, J. Kristaponis & N. Raman: Characterization of a gamma-carboxyglutamic acid-containing protein from bone. *Proc Natl Acad Sci U S A*, 73, 1447-51 (1976)

538. Price, P. A., J. W. Poser & N. Raman: Primary structure of the gamma-carboxyglutamic acid-containing protein from bovine bone. *Proc Natl Acad Sci U S A*, 73, 3374-5 (1976)

539. Price, P. A., M. R. Urist & Y. Otawara: Matrix Gla protein, a new gamma-carboxyglutamic acid-containing protein which is associated with the organic matrix of bone. *Biochem Biophys Res Commun*, 117, 765-71 (1983)

540. Goldberg, H. A., K. J. Warner, M. J. Stillman & G. K. Hunter: Determination of the hydroxyapatite-nucleating region of bone sialoprotein. *Connect Tissue Res*, 35, 385-92 (1996)

541. Baht, G. S., J. O'Yong, A. Borovina, H. Chen, C. E. Tye, M. Karttunen, G. A. Lajoie, G. K. Hunter & H. A. Goldberg: Phosphorylation of Ser136 is critical for potent bone sialoprotein-mediated nucleation of hydroxyapatite crystals. *Biochem J*, 428, 385-395 (2010)

542. Whyte, M. P.: Physiological role of alkaline phosphatase explored in hypophosphatasia. *Ann N Y Acad Sci*, 1192, 190-200 (2010)

543. Murshed, M., D. Harmey, J. L. Millan, M. D. McKee & G. Karsenty: Unique coexpression in osteoblasts of broadly expressed genes accounts for the spatial restriction of ECM mineralization to bone. *Genes Dev*, 19, 1093-104 (2005)

544. Cyboron, G. W., M. S. Vejins & R. E. Wuthier: Activity of epiphyseal cartilage membrane alkaline

phosphatase and the effects of its inhibitors at physiological pH. *J Biol Chem*, 257, 4141-4146 (1982)

545. Yadav, M. C., Simao, A.M.S., Narisawa, S., Huesa, C., McKee, M.D., Farquharson, C. and Millan, J.L.: Loss of skeletal mineralization by the simultaneous ablation of PHOSPHO1 and alkaline phosphatase function – A unified model of the mechanisms of initiation of skeletal calcification. *J Bone Miner Res*, (In Press), (2010)

546. Waymire, K. G., J. D. Mahuren, J. M. Jaje, T. R. Guilarte, S. P. Coburn & G. R. MacGregor: Mice lacking tissue non-specific alkaline phosphatase die from seizures due to defective metabolism of vitamin B-6. *Nat Genet*, 11, 45-51 (1995)

547. Anderson, H. C., R. Garimella & S. E. Tague: The role of matrix vesicles in growth plate development and biomineralization. *Front Biosci*, 10, 822-37 (2005)

548. Kirsch, T.: Annexins - their role in cartilage mineralization. *Front Biosci*, 10, 576-81 (2005)

549. Brachvogel, B., J. Dikschas, H. Moch, H. Welzel, K. von der Mark, C. Hofmann & E. Poschl: Annexin A5 is not essential for skeletal development. *Mol Cell Biol*, 23, 2907-13 (2003)

550. Belluoccio, D., I. Grskovic, A. Niehoff, U. Schlotzer-Schrehardt, S. Rosenbaum, J. Etich, C. Frie, F. Pausch, S. E. Moss, E. Poschl, J. F. Bateman & B. Brachvogel: Deficiency of annexins A5 and A6 induces complex changes in the transcriptome of growth plate cartilage but does not inhibit the induction of mineralization. *J Bone Miner Res*, 25, 141-53 (2010)

551. De, S. R., M. A. Ajmone-Cat, A. Nicolini & L. Minghetti: Expression of phosphatidylserine receptor and down-regulation of pro-inflammatory molecule production by its natural ligand in rat microglial cultures. *J Neuropathol Exp Neurol*, 61, 237-44 (2002)

552. Fadok, V. A., D. L. Bratton, D. M. Rose, A. Pearson, R. A. Ezekewitz & P. M. Henson: A receptor for phosphatidylserine-specific clearance of apoptotic cells. *Nature*, 405, 85-90 (2000)

553. Hoffmann, P. R., A. M. deCathelineau, C. A. Ogden, Y. Leverrier, D. L. Bratton, D. L. Daleke, A. J. Ridley, V. A. Fadok & P. M. Henson: Phosphatidylserine (PS) induces PS receptor-mediated macropinocytosis and promotes clearance of apoptotic cells. *J Cell Biol*, 155, 649-59 (2001)

554. Hoffmann, P. R., J. A. Kench, A. Vondracek, E. Kruk, D. L. Daleke, M. Jordan, P. Marrack, P. M. Henson & V. A. Fadok: Interaction between phosphatidylserine and the phosphatidylserine receptor inhibits immune responses *in vivo*. *J Immunol*, 174, 1393-404 (2005)

555. Li, M. O., M. R. Sarkisian, W. Z. Mehal, P. Rakic & R. A. Flavell: Phosphatidylserine receptor is required for clearance of apoptotic cells. *Science*, 302, 1560-3 (2003)

556. Otsuka, M., K. Goto, S. Tsuchiya & Y. Aramaki: Phosphatidylserine-specific receptor contributes to TGF-beta production in macrophages through a MAP kinase, ERK. *Biol Pharm Bull*, 28, 1707-10 (2005)

557. Bose, J., A. D. Gruber, L. Helming, S. Schiebe, I. Wegener, M. Hafner, M. Beales, F. Kontgen & A. Lengeling: The phosphatidylserine receptor has essential functions during embryogenesis but not in apoptotic cell removal. *J Biol*, 3, 15 (2004)

558. Hahn, P., J. Bose, S. Edler & A. Lengeling: Genomic structure and expression of Jmjd6 and evolutionary analysis in the context of related JmjC domain containing proteins. *BMC Genomics*, 9, 293 (2008)

559. Williamson, P. & R. A. Schlegel: Hide and seek: the secret identity of the phosphatidylserine receptor. *J Biol*, 3, 14 (2004)

560. Kunisaki, Y., S. Masuko, M. Noda, A. Inayoshi, T. Sanui, M. Harada, T. Sasazuki & Y. Fukui: Defective fetal liver erythropoiesis and T lymphopoiesis in mice lacking the phosphatidylserine receptor. *Blood*, 103, 3362-4 (2004)

561. Rosati, R., G. S. Horan, G. J. Pinero, S. Garofalo, D. R. Keene, W. A. Horton, E. Vuorio, B. de Crombrugghe & R. R. Behringer: Normal long bone growth and development in type X collagen-null mice. *Nat Genet*, 8, 129-35 (1994)

562. Warman, M. L., M. Abbott, S. S. Apte, T. Hefferon, I. McIntosh, D. H. Cohn, J. T. Hecht, B. R. Olsen & C. A. Francomano: A type X collagen mutation causes Schmid metaphyseal chondrodysplasia. *Nat Genet*, 5, 79-82 (1993)

563. Chan, D., Y. M. Weng, A. M. Hocking, S. Golub, D. J. McQuillan & J. F. Bateman: Site-directed mutagenesis of human type X collagen. Expression of alpha1 (X) NC1, NC2, and helical mutations *in vitro* and in transfected cells. *J Biol Chem*, 271, 13566-72 (1996)

564. McIntosh, I., M. H. Abbott, M. L. Warman, B. R. Olsen & C. A. Francomano: Additional mutations of type X collagen confirm COL10A1 as the Schmid metaphyseal chondrodysplasia locus. *Hum Mol Genet*, 3, 303-7 (1994)

565. Nielsen, V. H., C. Bendixen, J. Arnbjerg, C. M. Sorensen, H. E. Jensen, N. M. Shukri & B. Thomsen: Abnormal growth plate function in pigs carrying a dominant mutation in type X collagen. *Mamm Genome*, 11, 1087-92 (2000)

566. Jacenko, O., P. LuValle, K. Solum & B. R. Olsen: A dominant negative mutation in the alpha 1 (X) collagen gene produces spondylometaphyseal defects in mice. *Prog Clin Biol Res*, 383B, 427-36 (1993)

567. Jacenko, O., P. A. LuValle & B. R. Olsen: Spondylometaphyseal dysplasia in mice carrying a dominant negative mutation in a matrix protein specific for cartilage-to-bone transition. *Nature*, 365, 56-61 (1993)

568. Jacenko, O. & B. R. Olsen: Transgenic mouse models in studies of skeletal disorders. *J Rheumatol Suppl*, 43, 39-41 (1995)

569. Olsen, B. R.: Mutations in collagen genes resulting in metaphyseal and epiphyseal dysplasias. *Bone*, 17, 45S-49S (1995)

570. Jacenko, O., D. Chan, A. Franklin, S. Ito, C. B. Underhill, J. F. Bateman & M. R. Campbell: A dominant interference collagen X mutation disrupts hypertrophic chondrocyte pericellular matrix and glycosaminoglycan and proteoglycan distribution in transgenic mice. *Am J Pathol*, 159, 2257-69 (2001)

571. Vance, J. E. & D. E. Vance: Phospholipid biosynthesis in mammalian cells. *Biochem Cell Biol*, 82, 113-28 (2004)

572. Arikketh, D., R. Nelson & J. E. Vance: Defining the importance of phosphatidylserine synthase-1 (PSS1): unexpected viability of PSS1-deficient mice. *J Biol Chem*, 283, 12888-97 (2008)

573. Stewart, A. J., S. J. Roberts, E. Seawright, M. G. Davey, R. H. Fleming & C. Farquharson: The presence of PHOSPHO1 in matrix vesicles and its developmental expression prior to skeletal mineralization. *Bone*, 39, 1000-7 (2006)

574. Barradell, L. B., D. Faulds & D. McTavish: Lansoprazole. A review of its pharmacodynamic and pharmacokinetic properties and its therapeutic efficacy in acid-related disorders. *Drugs*, 44, 225-50 (1992)

575. Iwahi, T., H. Satoh, M. Nakao, T. Iwasaki, T. Yamazaki, K. Kubo, T. Tamura & A. Imada: Lansoprazole, a novel benzimidazole proton pump inhibitor, and its related compounds have selective activity against Helicobacter pylori. *Antimicrob Agents Chemother*, 35, 490-6 (1991)

576. Nagaya, H., H. Satoh, K. Kubo & Y. Maki: Possible mechanism for the inhibition of gastric (H+ + K+)-adenosine triphosphatase by the proton pump inhibitor AG-1749. *J Pharmacol Exp Ther*, 248, 799-805 (1989)

577. Morse, A.: Formic acid-sodium citrate decalcifiecation and butyl alcohol dehydration of teeth and bones for sectioning in paraffin. *J Dent Res*, 24, 143 (1945)

578. Arsenault, A. L.: Fine structure and elemental maps of the calcifying epiphysis preserved by slam freezing and freeze substitution. In: *The Chemistry and Biology of Mineralized Tissues*, Ed: William T. Butler, Ebsco Media, Inc., Birmingham, AL, 364-367 (1984).

579. Carraway, K. L., 3rd, Y. Liu, D. Puett, K. L. Carraway & C. A. Carraway: Phenothiazine binding by a homolog of calpactin, the pp60src tyrosine kinase substrate. *Faseb J*, 1, 46-50 (1987)

580. Grynkiewicz, G., M. Poenie & R. Y. Tsien: A new generation of Ca^{2+} indicators with greatly improved fluorescence properties. *J Biol Chem*, 260, 3440-50 (1985)

581. Concannon, B.: Nuclear magnetic resonance investigations of 1. Early stages of biomineralization, and 2. Rat mammary healthy and tumorous cells and tissues. *Department of Chemistry and Biochemistry*, University of South Carolina, 1-79 (1996).

582. Pleshko, N., A. Boskey & R. Mendelsohn: Novel infrared spectroscopic method for the determination of crystallinity of hydroxyapatite minerals. *Biophys J*, 60, 786-93 (1991)

583. Bisaz, S., R. G. Russell & H. Fleisch: Isolation of inorganic pyrophosphate from bovine and human teeth. *Arch Oral Biol*, 13, 683-96 (1968)

Key Words: Matrix Vesicles, Ca^{2+}, cellular Ca^{2+}, Ca^{2+} Channels, Inorganic Phosphate, Pi, Pi Transporters, Matrix Vesicle Formation, Mitochondria, Annexins, Annexin A5, Calcification, Mg^{2+}, Zn^{2+}, Pyrophosphate, PPi, Alkaline Phosphatase, Collagen, types VI, X, and II, Liposomal Models, Phospholipases A_2, Phospholipases C, phosphatidylserine, PS, PS-Ca^{2+}-Pi Complexes, Nucleation, Nucleational Core, Molecular Simulation, Amorphous Calcium Phosphate, Octacalcium Phosphate, Hydroxyapatite

Send correspondence to: Roy E. Wuthier, Department of Chemistry and Biochemistry, University of South Carolina, Columbia, SC 29208, Tel: 803-798-2176, Fax: 803-777-9521, E-mail: wuthierr@bellsouth.net

http://www.bioscience.org/current/vol16.htm